

**PREDICTING THE INFLUENCE OF DRUG SOLUBILIZING AGENTS ON
COCRYSTAL SOLUBILITY, STABILITY, AND TRANSITION POINTS**

by

Maya Pandit Lipert

A dissertation submitted in partial fulfillment
of the requirements for the degree of
Doctor of Philosophy
(Pharmaceutical Sciences)
in the University of Michigan
2015

Doctoral Committee:

Associate Professor Naír Rodríguez-Hornedo, Chair
Professor Gordon L. Amidon
Research Professor Gregory E. Amidon
Associate Professor Anne J. McNeil
Professor Gustavo Rosania

© Maya Pandit Lipert 2015

ACKNOWLEDGEMENTS

I would like to acknowledge the support of all the people who have encouraged and championed me during my time in graduate school. First, I must thank my graduate advisor, Dr. Naír Rodríguez-Hornedo. She is an excellent scientist and problem-solver and I would not have matured into a Ph.D. scientist without her guidance and training. My ability to critically think and answer difficult scientific questions has improved exponentially under her tutelage. I would also like to acknowledge the other members of my dissertation committee, Dr. Gordon Amidon, Dr. Greg Amidon, Dr. Gus Rosania, and Dr. Anne McNeil for their critical review of my work and helpful suggestions for improvement. Dr. Greg Amidon, in particular, has been a tremendous mentor to me and provided me with support on numerous occasions.

My parents must be acknowledged for their endless support during my graduate studies. They have always been my biggest advocates, and I know without a doubt that I would not be earning a Ph.D. without their love and encouragement. Both my mom and dad are Ph.D. scientists, and having parents who are familiar with the challenges of graduate school has been extremely helpful during my time at Michigan. They have flown all over the country to support me during my poster presentations at national meetings and have taken it upon themselves to become familiar with my work and show an interest in my projects and career development. They always give me sound advice and prevent me from wandering too far off-track when I get overwhelmed and discouraged. I also want to acknowledge my boyfriend, John for his unending

support and love during the last year and a half of my graduate career. The last months of graduate school can be very stressful, and John has been a calm, nurturing force in my life during this hectic time.

This research has been made possible by financial support from many sources including the Gordon and Pamela Amidon Fellowship in Pharmaceuticals, the American Foundation for Pharmaceutical Education (AFPE) Pre-doctoral Fellowship in Pharmaceutical Sciences, the Chhotubhai and Savitaben Patel Fellowship, the Everett Hiestand Scholarship Fund, the Fred Lyons Jr. Fellowship, and the Graduate Student Instructor (GSI) program. I would also like to acknowledge Dr. Scott Childs, who was a collaborator on some of the work found in Chapters 2 and 5.

Lastly, I want to thank the people who supported me on a day-to-day basis. My fellow Rodríguez lab members Neal Huang, Chinmay Maheshwari, Lilly Roy, Yitian Chen, Fengjuan Cao, and Nick Waltz deserve special thanks. The environment in our laboratory has always been one of collaboration and support, and discussions with my peers were a valuable part of my graduate school experience. I also want to thank former Rodríguez lab member Sarah Bethune. Though our time at Michigan did not overlap, Sarah has been an important mentor to me and I have relied on her advice to help me make many tough decisions. Finally, I'd like to thank my fellow graduate students, especially Amy Doty and Maria Posada who were my roommates for much of my graduate career. I feel lucky to have professional peers that are also close friends and look forward to being connected to these people throughout my career.

TABLE OF CONTENTS

Acknowledgements	ii
List of Figures	ix
List of Tables	xv
Abstract	xvii
Chapter 1 Introduction	1
Pharmaceutical Cocrystal Formation and Design.....	4
Cocrystal Solubility and Stability	6
Modeling Cocrystal Solubility	7
The cocrystal eutectic point	11
The critical stabilization concentration (CSC).....	13
Additives for Solubility and Dissolution Enhancement.....	14
Physiologically relevant surfactants	15
Nonionic Surfactants.....	18
Relationships between hydrophobicity and micellar solubilization	20
Effect of Temperature, pH and Ionic Strength on Micellar Solubilization.....	23
Modeling Solubilization in Mixed Surfactants	25
Drug Solubilization in Ideal Surfactant Mixtures	25
Statement of dissertation research	27
References.....	30
Chapter 2 Quantitative prediction of cocrystal solubilization by biorelevant media	36
Introduction.....	36
Theoretical	40
Estimation of cocrystal solubilization ratio from drug solubilization ratio	40
Cocrystal solubility in the presence of physiologically relevant surfactants	44
Materials and Methods.....	47
Materials	47
Cocrystal constituents	47

Solvents and buffer components	48
Methods.....	49
FeSSIF and acetate buffer preparation.....	49
Cocrystal synthesis.....	49
Solubility measurements of cocrystal constituents	50
Cocrystal solubility measurements	51
X-ray powder diffraction	52
Thermal analysis	52
High performance liquid chromatography.....	53
Results.....	54
Cocrystal solubilization in FeSSIF	54
Predicting cocrystal solubility in FeSSIF and buffer from relevant equilibrium constants..	60
Drug and cofomer solubilization in FeSSIF	65
Cocrystal solubility measurements at eutectic points	69
Conclusions.....	69
References.....	71
Appendix.....	74
Cocrystal and drug solubility at the eutectic point.....	74
Derivation of K_s^T equations.....	78
Solubility derivations	80
K_{sp} Measurements	88
Chapter 3 Cocrystal supersaturation during dissolution in physiologically relevant surfactants	91
Introduction.....	91
Theoretical	93
Calculation of cocrystal solubility and thermodynamic stability from eutectic point measurements.....	93
Materials and Methods.....	96
Materials	96
Cocrystal constituents	96
Solvents and buffer components.....	97
Methods.....	98
FeSSIF and acetate buffer preparation.....	98

Cocrystal synthesis.....	98
Solubility measurements of cocrystal constituents	99
Cocrystal solubility measurements	99
Calculation of $S_{\text{cocrystal}}/S_{\text{drug}}$	100
Cocrystal dissolution studies.....	100
X-ray powder diffraction	101
Thermal analysis	101
High performance liquid chromatography.....	101
Results.....	102
Drug solubility	102
Cocrystal solubility	105
Cocrystal thermodynamic stability	107
Cocrystal dissolution and supersaturation	116
Conclusions.....	122
References.....	123
Chapter 4 Understanding the relationship between cocrystal solubilization ratio and drug hydrophobicity	125
Introduction.....	125
Theoretical	127
Estimation of cocrystal solubilization ratio from drug solubilization ratio.....	127
Building log SR-log D relationships.....	128
Materials and Methods.....	131
Materials	131
Cocrystal constituents	131
Solvents and buffer components.....	131
Methods.....	132
FeSSIF and acetate buffer preparation.....	132
Cocrystal synthesis.....	132
Solubility measurements of cocrystal constituents	133
Cocrystal solubility measurements	134
X-ray powder diffraction	135
Thermal analysis	135
High performance liquid chromatography.....	135

Results.....	136
Log D is a better predictor of SR than log P for ionizable drugs.....	136
Predicting log SR_{cocystal} from log SR_{drug} -log D correlations.....	141
Conclusions.....	146
References.....	146
Chapter 5 Cocystal solubilization in the presence of multiple solubilizing agents	149
Introduction.....	149
Theoretical	151
Cocystal solubility in multiple surfactants	151
Cocystal solution stability in multiple surfactants.....	155
Materials and Methods.....	159
Materials	159
Cocystal constituents	159
Solvents and buffer components.....	159
Methods.....	160
FeSSIF, acetate buffer, and Tween 80 solution preparation.....	160
Cocystal synthesis.....	160
Solubility measurements of cocystal constituents	161
Cocystal solubility measurements	161
X-ray powder diffraction	162
Thermal analysis	162
High performance liquid chromatography.....	162
Results.....	163
Cocystal component solubilization in multiple surfactants.....	163
Cocystal solubility prediction in multiple surfactants	168
Drug solubility in the presence of and in the absence of cofomer	176
$S_{\text{cocystal}}/S_{\text{drug}}$ and cocystal dissolution in the presence of multiple surfactants	178
Conclusions.....	182
References.....	182
Chapter 6 Cocystal transition points: Role of cocystal solubility, drug solubility, and solubilizing agents	185
Introduction.....	185
Theoretical	187

Calculation of cocrystal solubilization from drug solubilization.....	187
Cocrystal transition points	191
Implications of coformer solubilization on $SR_{\text{cocrystal}}$ and S^*	196
Materials and Methods.....	198
Materials	198
Cocrystal components.....	198
Solvents and buffer components.....	198
Methods.....	199
FeSSIF, acetate buffer, and Tween 80 solution preparation.....	199
Cocrystal synthesis.....	200
Drug solubility measurements	200
Cocrystal solubility measurements	201
X-ray powder diffraction	202
Thermal analysis	202
High performance liquid chromatography.....	202
Results.....	203
Solubilization ratios of cocrystals and drugs	203
Prediction of cocrystal solubility ($S_{\text{cocrystal,T}}$) in the presence of drug solubilizing agents..	206
Cocrystal transition points	209
Solubilization ratio and cocrystal transition points.....	213
Influence of coformer solubilization.....	217
Conclusions.....	221
References.....	222
Chapter 7 Conclusions and future work.....	225

LIST OF FIGURES

Figure 1.1. Common supramolecular synthons formed between carboxylic acid and amide groups ³⁸	5
Figure 1.2. Cocrystal solution phase interactions and associated equilibria for a cocrystal RHA of a nonionizable drug I and weakly acidic coformer (HA) in a micellar solution ⁶	7
Figure 1.3. Dependence of cocrystal solubility or drug concentration $[R]_T$, on coformer concentration $[A]_T$, and pH for a 1:1 RHA cocrystal; calculated from equation (1.13) with $K_{sp} = 1 \text{ mM}^2$ and coformer $pK_a = 3.0$. Solubility of the drug, S_R is represented by the yellow surface ($S_R = 2 \text{ mM}$) and cocrystal by the blue/green surface ^{6, 23}	9
Figure 1.4. Phase solubility diagram of cocrystal AB (solid red line) and drug A (dashed blue line). B_{tr} is the coformer transition concentration, also called eutectic concentration $[B]_{eu}$ where $S_{cocrystal} = S_A$. Adapted from reference 36	13
Figure 1.5. Differential solubilization of cocrystal components represented by the relative values of K_s^{HA} and K_s^R leads to nonlinear cocrystal solubility dependence and to intersection of the cocrystal and drug solubility curves at the CSC. CSC refers to the critical stabilization concentration, at which both cocrystal and drug are thermodynamically stable ²¹	14
Figure 1.6. Proposed structures of primary and secondary bile salt micelles ⁶¹	17
Figure 1.7. Solubility of carbamazepine (mM) as a function of sodium deoxycholate concentration (M) at 37°C ⁶³	17
Figure 1.8. Log Polysorbate 80 molar micelle–water partition coefficient ($\log K_M^N$) versus $\log P$ of several drugs ⁷⁷	20
Figure 1.9. Log SR in aqueous NaTC as a function of $\log P$ for 6 steroidal and 6 non-steroidal compounds ⁵⁵	21
Figure 1.10. The solubilization capacity (SR) versus $\log P_{oct}$ of FaSSIF (●) and FeSSIF (○) for a data set of nonionizable and ionizable drugs; an R^2 of 0.32 was obtained ⁷⁸	22
Figure 1.11. The solubilization capacity (SR) versus $\log D_{oct}$ of FaSSIF (●) and FeSSIF (○) for a data set of nonionizable and ionizable drugs; an R^2 of 0.74 was obtained ⁷⁸	23
Figure 2.1. Transition point (S^* and CSC) for a 1:1 cocrystal (—) and its constituent drug (—) in the presence of a solubilizing agent. The curves represent the theoretical cocrystal and drug solubility dependence on solubilizing agent concentration ⁷ . $S^* = (S_{cocrystal,aq})^2 / (S_{drug,aq})$	37

Figure 2.2. Solubility values for a drug and three 1:1 cocrystals of that drug in aqueous buffer (■) and in the presence of a solubilizing agent (■). Cocrystal solubility enhancement over drug in aqueous buffer is not maintained in the presence of solubilizing agent. All cocrystals are more soluble than the drug in buffer, but not in the solubilizing agent. 43

Figure 2.3. Solubilization ratios for cocrystals (■) and constituent drugs (□) in FeSSIF at experimental pH values indicated in Table 2.4 and Table 2.5 at 25°C. Error bars represent standard errors of measurements..... 55

Figure 2.4. Drug and cocrystal solubility measured in FeSSIF (■) and buffer (■) at 25°C for IND, IND-SAC, DNZ, DNZ-VAN, and DNZ-HBA. SR in FeSSIF calculated from solubility values is also shown (■). The initial pH was 5.00 in both buffer and FeSSIF. The final pH of each solubility measurement in FeSSIF and buffer, respectively, are as follows: IND (4.98±0.06 and 4.96±0.03), IND-SAC (3.65±0.05 and 3.66±0.02), DNZ (5.01±0.05 and 4.96±0.01), DNZ-VAN (5.00±0.01 and 4.96±0.01), and DNZ-HBA (4.46±0.06 and 4.47±0.01)..... 56

Figure 2.5. Drug and cocrystal solubility measured in FeSSIF (■) and buffer (■) at 25°C for CBZ (H), CBZ-4ABA (H), CBZ-SLC, CBZ-SAC, PXC (H), and PXC-SAC. SR in FeSSIF calculated from solubility values is also shown (■). The final pH of each solubility measurement in FeSSIF and buffer, respectively, are as follows: CBZ (H) (4.86±0.05 and 4.95±0.01), CBZ-4ABA (H) (4.94±0.02 and 4.84±0.03), CBZ-SLC (4.29±0.02 and 4.37±0.02), CBZ-SAC (3.11±0.02 and 3.08±0.03), PXC (H) (5.03±0.02 and 4.98±0.01), and PXC-SAC (3.79±0.02 and 3.64±0.02). 56

Figure 2.6. $SR_{cocrystal}$ dependence on $\sqrt{SR_{drug}}$ for 1:1 cocrystals in FeSSIF at 25°C. Line represents the theoretical relationship according to equation (2.3). Symbols represent experimentally determined SR values in equilibrium conditions for IND-SAC (▶), CBZ-SAC (■), CBZ-SLC (▼), , PXC-SAC (▲), DNZ-HBA (■), and DNZ-VAN (◆).. 58

Figure 2.7. Comparison of predicted and observed cocrystal solubility in FeSSIF (filled symbols) and buffer (open symbols) at 25°C for IND-SAC (▶), CBZ-SAC (■), CBZ-SLC (▼), , PXC-SAC (▲), DNZ-HBA (■), and DNZ-VAN (◆). Line indicates the function $y = x$, where the predicted and observed solubilities are equivalent. Errors fit within the size of each symbol. Solubilities were predicted according to the equations in Table 2.2 according to the equilibrium constants in Table 2.3 and Table 2.5..... 65

Figure 2.8. Drug solubility measured in FeSSIF (■) and buffer (■) at 25°C. SR_{drug} in FeSSIF calculated from solubility values is also shown (■). The final pH of each drug solubility measurement in FeSSIF and buffer, respectively, are as follows: DNZ (5.01±0.05 and 4.96±0.01), IND (4.98±0.06 and 4.96±0.03), PXC (H) (5.03±0.02 and 4.98±0.01), and CBZ (H) (4.86±0.05 and 4.95±0.01). PXC (H) represents the monohydrate form of PXC and CBZ (H) represents the dihydrate form of CBZ, which are the stable forms in aqueous solution..... 66

Figure 2.9. Cofomer solubility measured in FeSSIF (■) and buffer (■) at 25°C. $SR_{coformer}$ in FeSSIF calculated from solubility values is also shown (■). The final pH of each cofomer

solubility measurement in FeSSIF and buffer, respectively, are as follows: 4ABA (4.72±0.02 and 4.57±0.04), VAN (4.99±0.01 and 4.94±0.01), HBA (H) (4.45±0.02 and 4.41±0.02), SLC (3.78±0.03 and 3.58±0.06), and SAC (2.60±0.02 and 2.58±0.02). HBA (H) represents the monohydrate form of HBA which is the stable form in aqueous solution.

- 67
- Figure 3.1. K_{eu} dependence on cocrystal solubility advantage ($S_{cocrystal}/S_{drug}$) in FeSSIF (filled symbols) and buffer (open symbols) at 25°C for 1:1 cocrystals IND-SAC (▶), CBZ-SAC (■), CBZ-SLC (▼), PXC-SAC (▲), DNZ-HBA (◻), and DNZ-VAN (◆). Experimental errors fit within the size of each symbol. The line represents $K_{eu} = (S_{cocrystal}/S_{drug})^2$. K_{eu} values are experimentally determined at the eutectic point according to equation (3.3) (Method 1) and $S_{cocrystal}/S_{drug}$ values are predicted using equations (3.5)-(3.7). 108
- Figure 3.2. $S_{cocrystal}/S_{drug}$ values measured at pH_{eu} at 25°C in FeSSIF (■) and buffer (□). Values were calculated by Method 1 as described in the Theoretical and Methods sections using equation (3.9) for 1:1 cocrystals and equation (3.10) for 2:1 cocrystals. pH values for each measurement are in Table 3.2. 112
- Figure 3.3. IND-SAC dissolution in FeSSIF (■) and buffer (◆) at 25°C. (a) $[IND]_T$ vs time profile for dissolution and (b) supersaturation generated by IND-SAC during dissolution ($[IND]_T/S_T^{IND}$). 117
- Figure 3.4. pH during cocrystal dissolution for (a) IND-SAC and (b) PXC-SAC in (■) FeSSIF and (◆) buffer at 25°C. 118
- Figure 3.5. Concentration-time profile for $[IND]_T$ (◆) and $[SAC]_T$ (●) during dissolution of IND-SAC in (a) buffer and (b) FeSSIF. 119
- Figure 3.6. PXC-SAC dissolution in FeSSIF (■) and buffer (◆) at 25°C. (a) $[PXC]_T$ vs time profile for dissolution from neat cocrystal and (b) supersaturation generated by PXC-SAC during dissolution ($[PXC]_T/S_{PXC,T}$). 120
- Figure 3.7. Concentration-time profile for $[PXC]_T$ (◆) and $[SAC]_T$ (●) during dissolution of PXC-SAC in (a) buffer and (b) FeSSIF. 121
- Figure 4.1. Log SR_{drug} correlation with (a) log P and (b) log D. Symbols (Δ) represent experimentally measured data and the lines are a result of linear regression of the data (a) $y = (0.76±0.08)x - 1.3±0.3$ and (b) $y = (1.02±0.09)x - 1.9±0.3$ where errors on regression parameters represent the 95% confidence interval. Log P values are from the literature and log D values calculated at experimentally measured pH values in Table 4.1 using the ADMET Predictor Module in Gastro-Plus. For nonionizable drugs DNZ and CBZ (H), the measured log P was used in lieu of a calculated log D since the log D is not predicted to change with pH. 137
- Figure 4.2. Log $SR_{cocrystal}$ correlation with (a) log P and (b) log D. Symbols (◆) represent experimentally measured data and the lines are a result of linear regression of the data (a) $y = (0.45±0.07)x - 0.9±0.3$ and (b) $y = (0.50±0.05)x - 1.0±0.2$ where errors on regression parameters represent the 95% confidence interval. Log P values are from literature and log

D values calculated using the ADMET Predictor Module in Gastro-Plus. For nonionizable drugs DNZ and CBZ (H), the measured log P was used in lieu of a calculated log D since the log D is not predicted to change with pH..... 139

Figure 4.3. Log $SR_{\text{cococrystal}}$ -log D for 1:1 cococrystals and log SR_{drug} -log D correlations. Symbols for drugs (Δ) and cococrystals (\blacklozenge) represent experimentally measured data and the lines are a result of linear regression of the data ($y = (1.02 \pm 0.09)x - 1.9 \pm 0.3$) for drugs and ($y = (0.50 \pm 0.05)x - 1.0 \pm 0.2$) for cococrystals. Errors on regression parameters indicate the 95% confidence interval. log D values calculated using the ADMET Predictor Module in Gastro-Plus. For nonionizable drugs DNZ and CBZ (H), the measured log P was used in lieu of a calculated log D since the log D is not predicted to change with pH. 141

Figure 4.4. Log $SR_{\text{cococrystal}}$ correlation with log D. Symbols represent experimentally measured values for 1:1 cococrystals (\blacklozenge) and 2:1 (\blacklozenge) cococrystals. The lines represent predicted linear regression equations in Table X, $y = 0.51(\log D) - 1.03$ for 1:1 cococrystals and $y = 0.68(\log D) - 1.38$ for 2:1 cococrystals. Log D values are calculated using the ADMET Predictor Module in Gastro-Plus. For nonionizable drugs DNZ and CBZ (H), the measured log P was used in lieu of a calculated log D since the log D is not predicted to change with pH..... 144

Figure 5.1. $S_{\text{cococrystal}}/S_{\text{drug}}$ for two 1:1 cococrystals predicted from equation (5.24) for 1 surfactant (formulation only) and (5.25) for 2 surfactants (formulation + physiologically relevant) in increasing concentrations of a formulation surfactant. Dotted lines represent cococrystal A with $(S_{\text{cococrystal}}/S_{\text{drug}})_{\text{aq}} = 500$ and solid lines represent cococrystal B with $(S_{\text{cococrystal}}/S_{\text{drug}})_{\text{aq}} = 100$. Conditions with only one solubilizing agent (formulation) are shown in orange and those with two solubilizing agents (formulation + physiologically relevant) are shown in green. Values used for predictions are: $K_{\text{sp}} = 2.5 \text{ mM}^2$ for cococrystal A and 62.5 mM^2 for cococrystal B, $S_{\text{drug, aq}}^0 = 0.5 \text{ mM}$, $K_{\text{s, formulation surfactant}} = 150 \text{ mM}^{-1}$, $K_{\text{s, physiologically relevant}} = 50 \text{ mM}^{-1}$, $[M]$ of the physiologically relevant surfactant = 147 mM (that of FeSSIF)..... 157

Figure 5.2. Influence of Tween 80 on the solubility of DNZ in pH 5.00 buffer and in FeSSIF. Symbols represent experimentally measured solubility values in Tween 80 in pH 5.00 buffer (\blacklozenge) and in Tween 80 + FeSSIF (\blacktriangle). Lines are drawn according to equations obtained from linear regression of the data: $y = (2.00 \pm 0.03)x + 0.008 \pm 0.003$ for Tween 80 in buffer (blue) and $y = (1.87 \pm 0.01)x + 0.008 \pm 0.001$ for Tween 80 + FeSSIF (red). Errors on regression parameters represent the 95% confidence interval. 164

Figure 5.3. Influence of Tween 80 on the solubility of HBA (H) (a) and VAN (b) in pH 5.00 buffer and in FeSSIF. Symbols represent experimentally measured solubility values in Tween 80 in pH 5.00 buffer (\blacklozenge) and Tween 80 + FeSSIF (\blacktriangle). Lines are drawn according to equations obtained from linear regression of the data: for (a) $y = (1.38 \pm 0.02)x + 82 \pm 2$ for Tween 80 in buffer (blue) and $y = (1.45 \pm 0.06)x + 87 \pm 5$ for Tween 80 + FeSSIF (red), for (b) $y = (1.53 \pm 0.03)x + 57 \pm 2$ in Tween 80 in buffer (blue) and $y = (1.52 \pm 0.03)x + 55 \pm 3$ in Tween 80 in FeSSIF (red). Errors on regression parameters represent the 95% confidence interval. HBA (H) represents the monohydrate form of HBA which is the stable form in aqueous solution..... 165

- Figure 5.4. Comparison of predicted and observed DNZ-HBA (\blacktriangle) and DNZ-VAN (\blacksquare) in (a) buffer (blue symbols), FeSSIF (red symbols), and Tween 80 (green symbols) separately and (b) Tween 80 and FeSSIF (purple symbols) at 25°C. Predictions were made using equation (5.33) in aqueous buffer, (5.34) in a single surfactant, and (5.22) in two surfactants. Line indicates the function $y=x$, where the predicted and observed solubilities are equivalent. Experimental errors fit within the size of each symbol. 171
- Figure 5.5. $S_{\text{cococrystal}}/S_{\text{drug}}$ for DNZ-HBA (—) and DNZ-VAN (----) predicted using equation (5.24) for increasing concentrations of Tween 80 in pH 5.00 buffer (blue lines) and equation (5.25) for increasing concentrations of Tween 80 in FeSSIF (red lines). Values used for predictions are K_{sp} values from Table 5.4, K_{s}^{T} and pK_{a} values from Table 2.5, and measured value of $S_{\text{DNZ, aq}}^0 = 1.6 \times 10^{-4}$ mM. Symbols represent experimentally measured values for DNZ-HBA in buffer (\blacktriangle) DNZ-HBA in FeSSIF (\blacktriangle), DNZ-VAN in buffer (\blacksquare) and DNZ-VAN in FeSSIF (\blacksquare) at 0, 25, 50, and 150 mM Tween 80. 178
- Figure 5.6. DNZ-VAN dissolution in FeSSIF (\blacksquare) and FeSSIF + 150 mM Tween 80 (\square) at 25°C. (a) $[\text{DNZ}]_{\text{T}}$ vs time profile and (b) supersaturation generated by DNZ-VAN during dissolution ($[\text{DNZ}]_{\text{T}}/S_{\text{DNZ, T}}$). The pH of both media had an initial and final pH of 5.00.... 179
- Figure 5.7. Concentrations of DNZ (\blacksquare) and VAN (\blacklozenge) during DNZ-VAN dissolution in FeSSIF (a) and FeSSIF + 150 mM Tween 80 (b) at 25°C. The pH of both media had an initial and final pH of 5.00. 180
- Figure 6.1. Dependence of $\text{SR}_{\text{cococrystal}}$ on SR_{drug} for cococrystal stoichiometries 1:1 (—) and 2:1 (----) predicted from equations (6.1) and (6.7) using a typical range of SR_{drug} values. 191
- Figure 6.2. Transition points (S^* and CSC) for a cococrystal (—) and its constituent drug (—) in two different solubilizing agents, a and b . S^* is constant and CSC varies with the extent of drug solubilization by the solubilizing agent. Drug is solubilized to a greater extent by a than by b and thus $\text{CSC}_a < \text{CSC}_b$. The curves were generated from equations (6.4) and (6.9) under nonionizing conditions and the parameter values $S_{\text{drug, aq}}^0 = 0.5$ mM, $S_{\text{cococrystal, aq}} = 2.4$ mM ($K_{\text{sp}} = 5.76$ mM²), $K_{\text{s}}^{\text{drug}} = 1.5$ mM and 0.5 mM⁻¹ for solubilizing agents a and b , respectively. 193
- Figure 6.3. Graphical representation of S^* as a function of cococrystal and drug aqueous solubilities for a 1:1 cococrystal, according to equation (6.12). S^* is reached at the cococrystal/drug transition point. 195
- Figure 6.4. $\text{SR}_{\text{cococrystal}}$ dependence on SR_{drug} for (a) 1:1 cococrystals and (b) 2:1 cococrystals. Lines represent theoretical relationships between $\text{SR}_{\text{cococrystal}}$ and SR_{drug} according to equation (6.1) for 1:1 cococrystals and (6.7) for 2:1 cococrystals. 1:1 cococrystals have a slope of $1/2$. 2:1 cococrystals have a slope of $2/3$. Symbols represent experimentally determined SR values in equilibrium conditions. 204
- Figure 6.5. Transition points for CBZ cococrystals induced by solubilizing CBZ with SLS for (a) CBZ-SAC, (b) CBZ-4ABA-HYD, and (c) (CBZ-SUC) from reference 13. Transition points are characterized by a solubility (S^*) and a solubilizing agent concentration (CSC).

Both S^* and CSC vary with cocrystal aqueous solubility and stoichiometry. Symbols represent experimentally measured cocrystal (○) and drug (△) solubility values¹². 210

Figure 6.6. Transition points for CBZ and CBZ-SLC induced by solubilizing CBZ with SLS from reference 13. Transition points are characterized by a solubility (S^*) and a solubilizing agent concentration (CSC). Both S^* and CSC vary with cocrystal aqueous solubility and stoichiometry. SLC was found to influence the CMC of SLS, raising it from 6 mM (a) to 9 mM, (b) which had a minor impact on the CSC (20-23 mM) and no impact on S^* . Symbols represent experimentally measured cocrystal (○) and drug (△) solubility values¹². 211

Figure 6.7. Measured solubilities for DNZ and PTB and their cocrystals in solubilizing agents: Tween 80 aqueous solution (150 mM, pH 5.0) for DNZ and lipid mixture for PTB. How to determine where a cocrystal stands with respect to its transition point in a given formulation or in the presence of solubilizing agents from knowledge of SR_{drug} and without having to measure $SR_{cocrystal}$ is described in the text. Numbers in parentheses represent SR values, and numbers within the lines represent SA_{aq} . Transition point solubilities, S^* , were calculated from equations (6.12) and (6.13) for 1:1 DNZ and PTB cocrystals and the 2:1 PTB-PIP cocrystal with the measured values of $S_{drug,aq}$ and $S_{cocrystal,aq}$ presented in the plot. PTB data obtained from references²⁶⁻²⁸. 216

Figure 6.8. The influence of ε in SLS on S^* at varying $S_{cocrystal,aq}$ for CBZ-SLC (△), CBZ-SAC (○), CBZ-4ABA-HYD (□), CBZ-SUC (◇). S^* is simulated using equation (6.19) for 1:1 (—) and (6.13) for 2:1 (---) cocrystals and $S_{drug,aq} = 0.53$ mM, solubilizing agent is SLS. ε values are 0, 1.10, and 1.44 (calculated values for CBZ-SAC and CBZ-SLC in Table 6.4), and 0 for 2:1 cocrystals since neither SUC or 4ABA were reported to be solubilized in SLS¹². 220

LIST OF TABLES

Table 1.1. Chemical structure, CMC, and use of common nonionic and anionic surfactants.	19
Table 2.1. Comparison of experimentally measured and predicted $SR_{\text{cocrystral}}$ values.	59
Table 2.2. Cocrystral solubility equations in aqueous buffer and FeSSIF.	61
Table 2.3. K_{sp} and pK_{sp} values for the cocrystrals studied.	62
Table 2.4. Comparison between predicted and experimentally measured cocrystral solubility values.	64
Table 2.5. Drug and cofomer solubility measurements in FeSSIF and buffer and calculated K_s^T	68
Table 2.6. Measured eutectic concentrations and calculated stoichiometric solubility in FeSSIF and buffer.	74
Table 2.7 Comparison of drug solubilities in FeSSIF buffer measured in the absence of and in the presence of cofomer and calculated K_s^T values.	76
Table 2.8. Comparison of experimentally measured cocrystral solubility and predicted solubility from K_s^T determined independently and at the eutectic point.	77
Table 2.9. Comparison of K_{sp} values obtained by linear regression and single point calculations for DNZ-HBA.	89
Table 2.10. Eutectic concentrations of DNZ and VAN used to calculate K_{sp} of DNZ-VAN.	89
Table 2.11. Eutectic concentrations of PXC and SAC used to calculate the K_{sp} of PXC-SAC. ..	90
Table 3.1. Comparison of drug solubility values measured at the eutectic point (in the presence of cofomer in solution) and in the absence of cofomer.	103
Table 3.2. Cocrystral constituent eutectic concentrations and stoichiometric solubility at the eutectic point compared to solubility at pH 5.00.	106
Table 3.3. Experimentally determined K_{eu} and $S_{\text{cocrystral}}/S_{\text{drug}}$ calculated from Methods 1 and 2 compared to predicted $S_{\text{cocrystral}}/S_{\text{drug}}$ using equations (3.5)-(3.8) at the eutectic point pH. .	110
Table 3.4. Log P, K_s^{drug} and $S_{\text{cocrystral}}/S_{\text{drug}}$ decrease in FeSSIF compared to buffer calculated using Method 1.	113
Table 3.5. $S_{\text{cocrystral}}/S_{\text{drug}}$ calculated using Method 1 at the eutectic pH compared to $S_{\text{cocrystral}}/S_{\text{drug}}$ predicted at pH 5.00.	115

Table 4.1. Log P, log D, and SR values used to correlate log SR _{drug} with drug hydrophobicity.	138
Table 4.2. Log P, log D, and SR values used to correlate log SR _{cocrystal} of 1:1 cocrystals with drug hydrophobicity.....	140
Table 4.3. Comparison of fitted and predicted linear relationships between log SR _{cocrystal} of 1:1 cocrystals and log D of the constituent drug.....	143
Table 4.4. Predicted logSR _{cocrystal} -log D linear regression equations for 1:1 and 2:1 cocrystals.	144
Table 4.5. Comparison of predicted and measured logSR _{cocrystal} for 1:1 and 2:1 cocrystals.....	145
Table 5.1. Influence of Tween 80 on the solubility of DNZ in pH 5.00 buffer and FeSSIF.	164
Table 5.2. Influence of Tween 80 on the solubility of HBA (H) and VAN in pH 5.00 buffer and FeSSIF.....	165
Table 5.3. K _s ^T in Tween 80 calculated from linear regression analysis of measured solubility values of DNZ, HBA (H), and VAN in increasing concentrations of Tween 80 in buffer and FeSSIF.....	167
Table 5.4. Cocrystal K _{sp} and coformer pK _a values at 25°C.....	168
Table 5.5. K _s ^T values for DNZ, HBA, and VAN in FeSSIF and Tween 80.	168
Table 5.6. Comparison between predicted and experimentally measured cocrystal solubility values.	170
Table 5.7. Measured DNZ and HBA eutectic concentrations used to calculate stoichiometric cocrystal solubility (S _{cocrystal}), K _{eu} , and S _{cocrystal} /S _{drug}	173
Table 5.8. Measured DNZ and VAN eutectic concentrations used to calculate stoichiometric cocrystal solubility (S _{cocrystal}), K _{eu} , and S _{cocrystal} /S _{drug}	175
Table 5.9. Comparison of DNZ solubilities in increasing concentrations of Tween 80 in buffer or FeSSIF measured in the absence of and in the presence of coformer at the eutectic point (either DNZ-HBA or DNZ-VAN eutectic point).....	177
Table 6.1. Comparison of experimental and predicted PTB cocrystal solubilities in lipid-based formulations.	207
Table 6.2. Predicted and observed S* values for CBZ cocrystals in aqueous solutions of SLS.	212
Table 6.3. SR _{cocrystal} deviations due to coformer solubilization.	218
Table 6.4. S* deviations due to coformer solubilization for CBZ-SLC and CBZ-SAC.....	219

ABSTRACT

PREDICTING THE INFLUENCE OF DRUG SOLUBILIZING AGENTS ON COCRYSTAL SOLUBILITY, STABILITY, AND TRANSITION POINTS

by

Maya Pandit Lipert

Chair: Naír Rodríguez-Hornedo

Pharmaceutical cocrystals have emerged as a useful strategy to improve the aqueous solubility of inherently poorly soluble drugs to improve their oral absorption and bioavailability. Aqueous cocrystal solubility can be orders of magnitude higher than that of the constituent drug. Chemical interactions between cocrystal constituents and dissolution media additives are critically important for cocrystals to achieve a wide range of solubility and stability ($S_{\text{cocrystal}}/S_{\text{drug}}$) behaviors. In the presence of drug solubilizing agents, a cocrystal with high aqueous $S_{\text{cocrystal}}/S_{\text{drug}}$ can display higher, equal, or lower solubility than the drug, depending on the nature and concentration of the additive. This dissertation explores the mechanisms of cocrystal solubilization by solubilizing agents and the impact on cocrystal solubility, $S_{\text{cocrystal}}/S_{\text{drug}}$, and transition points.

The objectives of this work are to (1) understand the effect of solubilization by physiologically relevant solubilizing agents on cocrystal solubility, solubilization ratio ($SR_{\text{cocrystal}}$), and $S_{\text{cocrystal}}/S_{\text{drug}}$ (2) develop models to describe cocrystal solubility, $SR_{\text{cocrystal}}$, and

$S_{\text{cocystal}}/S_{\text{drug}}$ based on cocystal dissociation and constituent ionization and micellar solubilization solution equilibria, (3) expand these models to consider the effect of multiple solubilizing agents, and (4) develop simplified models for the facile estimation of cocystal transition points from commonly reported drug solubility descriptors.

Cocystal solubility, SR_{cocystal} , and $S_{\text{cocystal}}/S_{\text{drug}}$, were investigated in fed state simulated intestinal fluid (FeSSIF) for seven cocystals comprised of constituents with a range of ionization and micellar solubilization properties. Mathematical models that predicted cocystal solubility and $S_{\text{cocystal}}/S_{\text{drug}}$ based on cocystal dissociation and constituent ionization and micellar solubilization were derived and expanded to consider two ideally mixing solubilizing agents (FeSSIF and Tween 80). The models were found to be in excellent agreement with the experimentally measured values. SR_{cocystal} was found to be correlated with the log octanol-water distribution coefficient (log D) and models derived to predict SR_{cocystal} from log D. Cocystal solubility at the transition point (S^*) was found to be independent of solubilizing agent and solely depend on drug and cocystal aqueous solubility and models derived to predict this behavior. The influence of solubilizing agents on the position of cocystal solubility relative to the transition point was predicted by comparing SR_{drug} with S^* .

CHAPTER 1

INTRODUCTION

The absorption of an orally administered drug depends on its permeability through the gut wall and its ability to dissolve in gastrointestinal fluids¹. Oral absorption can be described according to the biopharmaceutics classification system (BCS) which groups drugs based on their aqueous solubility and permeability². For BCS Class II drugs (poorly soluble, highly permeable), absorption is dissolution rate-limited, and solubility is a critical physicochemical property than can be altered to improve absorption³. A large percentage of newly discovered drug candidates have inadequate solubility and consequently limited absorption and bioavailability after oral administration^{4,5}. To improve the solubility and dissolution of a drug molecule without changing its chemical structure, and therefore pharmacological effect, a number of strategies can be employed. Various solid forms can be generated such as polymorphs, amorphous materials, salts, and cocrystals; additionally, the solution environment can be modulated by changing the pH, surfactants, or complexing agents present in solution³.

Cocrystals are of increasing interest to the pharmaceutical industry because of their ability to fine-tune the aqueous solubility of inherently insoluble drugs that are otherwise difficult to develop. Cocrystals have several advantages in that (1) they apply to a large number of drug molecules since not all drugs are acidic or basic enough to form salts, (2) are crystalline in nature, giving them a stability advantage over most amorphous materials, (3) their stoichiometry and composition can be designed using crystal engineering principles rather than

empirical approaches, and (4) drug delivery can be fine-tuned because of the cocrystal sensitivity to molecular interactions in solution⁶⁻⁸.

Cocrystals are supersaturating drug delivery systems (SDDS) and one of the main barriers to their development is rapid conversion to the original drug due to thermodynamic instability⁷. While there are numerous examples of cocrystals that exhibit enhanced aqueous solubility and dissolution rate compared to their drug component⁹⁻¹⁶, this improved dissolution behavior does not always result in improved bioavailability^{17, 18}, which has been attributed to rapid conversion to parent drug *in vivo*¹⁸. Additives such as polymers and surfactants have been shown to improve the dissolution behavior of cocrystals in aqueous media by inhibiting conversion to parent drug^{11, 19, 20}. Cocrystal solubility and stability dependence on micellar solubilization is established in the literature, but only confirmed for cocrystals of a nonionizable drug in a single surfactant²⁰⁻²². The influence of solution conditions such as pH and surfactant concentration on the solubility of a given drug is different from the influence on the solubility of a cocrystal of that drug²⁰⁻²⁸. This difference in solution behavior underlines the need for informed additive selection to capture a cocrystal's solubility advantage^{19, 21, 22}. In addition, physiologically relevant surfactants composed of bile salts and phospholipids greatly influence the solubility of poorly soluble drugs²⁹⁻³³; however their effect on the solubility of cocrystals of poorly soluble drugs remains to be established. Knowledge of cocrystal solution behavior in physiologically relevant surfactants will aid in understanding cocrystal performance *in vivo* and guide additive selection to meet target solubilities in biorelevant environments.

The solubility and dissolution of several cocrystals have been evaluated in physiologically relevant solubilizing agents^{18, 34}. These preliminary studies show dissolution enhancement compared to parent drug, but a fundamental understanding of how the media

affects cocrystal solution interactions is lacking³⁴. Since cocrystal solubility dependence in the presence of a single micellar surfactant is profoundly different from the linear dependence of a drug^{21, 22, 24, 26}, it is not unreasonable to assume that cocrystals may exhibit distinct behavior in physiologically relevant surfactants; however, this remains to be established. In addition, oral drug products usually contain at least one additive, if not many³⁵, and solubility evaluation of formulated cocrystals in physiologically relevant surfactants may be more meaningful to predict *in vivo* performance. Understanding cocrystal-additive solution interactions in these conditions is complicated by competing factors such as the nature of additives, diversity of associations of cocrystal components in solubilizing agents, and different ionization states⁶. The ability to predict how cocrystal solubility and stability are influenced by formulation additives and biorelevant conditions would provide a useful development tool.

The solubility of cocrystals in aqueous solution has been described by the solubility product (K_{sp}), in addition to equilibrium constants that describe cocrystal component complexation (K_{11}), ionization (K_a), and micellar solubilization (K_s), depending on the interactions taking place in solution^{13, 21, 23, 36-41}. Additionally, the critical stabilization concentration (CSC), the surfactant concentration above which cocrystal is thermodynamically stable and no transformation to parent drug is possible has been described^{21, 22}. Since solution conditions influence drug and cocrystal solubility differently^{21, 23}, it is essential to extend the cocrystal solubility model to biorelevant environments since it is unlikely cocrystals will behave similarly to drugs.

This chapter introduces cocrystals and concepts relevant to micellar solubilization in the context of cocrystal design, the current understanding of cocrystal solution chemistry and

solubility properties, and fundamentals of micellar solubilization. This chapter will conclude with a statement of research objectives.

Pharmaceutical Cocrystal Formation and Design

A pharmaceutical cocrystal is a multicomponent crystal composed of two or more different molecules (one of which is a drug molecule) in a defined stoichiometric ratio which are solids at room temperature^{9, 38, 41-43}. Molecular recognition events lead to the supramolecular self-assembly of cocrystal formers to form molecular complexes in either the solid state through noncovalent interactions with energetically favorable geometries⁴². Both single component and multicomponent (cocrystalline) solid complexes can be formed. The noncovalent interactions responsible for cocrystal formation include Van der Waals forces, π - π interactions, and most commonly, hydrogen bonds^{38, 43, 44}.

Molecular recognition through hydrogen bonding imparts directional interactions between cocrystal components. Based on characterized molecular structures containing multiple functional groups capable of hydrogen bonding, three guidelines to predict which hydrogen bond interactions lead to molecular assembly have been established⁴⁵:

1. All acidic hydrogens will be used in hydrogen bonding in the crystal structure of a compound.
2. All good acceptors will be used in hydrogen bonding if there are sufficient hydrogen bond donors.
3. Hydrogen bonds will preferentially form between the best hydrogen bond donor and best hydrogen bond acceptor.

Common noncovalent intermolecular interactions of specified geometries and bonding motifs are referred to as synthons. Supramolecular synthons are useful in the design and

synthesis of cocrystals of a given drug as they predict successful coformers based on structural properties⁴⁶. Examples of common hydrogen-bonded synthons are shown in Figure 1.1^{38,44}.

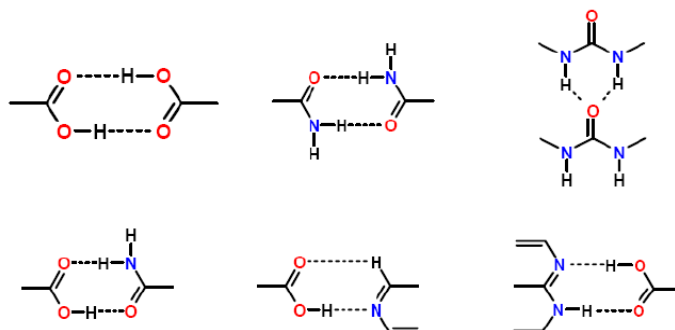


Figure 1.1. Common supramolecular synthons formed between carboxylic acid and amide groups³⁸.

Synthons are classified as homosynthons when identical functional moieties interact and as heterosynthons when different functional groups interact³⁸. Cocrystal structures can form through both hetero and homosynthons, depending on the functional groups interacting. Using synthon design strategies, it is possible to generate many cocrystals of a given drug. Selection of a particular cocrystal to optimize a particular property of the drug, such as solubility or dissolution, requires an understanding of cocrystal solution phase interactions.

Solid form modification is an effective means to change the physicochemical properties of a drug substance without changing its chemical structure and therefore pharmacological effect. Additionally, knowledge of the different possible solid forms of a drug is essential to ensure quality control and prevent unwanted solid form transformations during processing. Once the thermodynamically stable polymorph has been identified, other single and multicomponent solid forms can be explored. To increase solubility, single component solid forms like higher energy (metastable) polymorphs or amorphous phases can be utilized. However, polymorphs

exist in limited chemical space and cannot be rationally designed, and amorphous phases often lack the required stability for solid dosage forms³⁸.

Multicomponent options include solvates, salts, and cocrystals. Solvates are very similar to cocrystals, but are composed of the drug molecule and one component that is a liquid at room temperature, rather than two solid components. Salts are formed through an acid-base reaction between components, creating an ionic interaction⁴⁷. Successful salt formation generally requires a ΔpK_a of 2 or greater between the two salt components⁴¹. Cocrystallization does not have this requirement, and can occur with both nonionizable and weakly ionizable drugs. Additionally, there are many more possible cocrystal cofomers than salt counter ions, resulting in an increased ability to fine-tune properties of the drug molecule^{6, 38}.

Cocrystal Solubility and Stability

The ability of cocrystals to fine-tune drug solubility arises from not only their range of lattice properties, but also from their solution phase interactions as a result of their diverse molecular properties⁶. Understanding the effect of solution chemistry on cocrystal components is essential to control cocrystal solubility and stability. Since cocrystals are composed of multiple components molecular associations in the solution phase are an important contribution to the solubility, as shown in Figure 1.2⁶. Some of these processes include dissociation, complexation, ionization, and micellar solubilization.

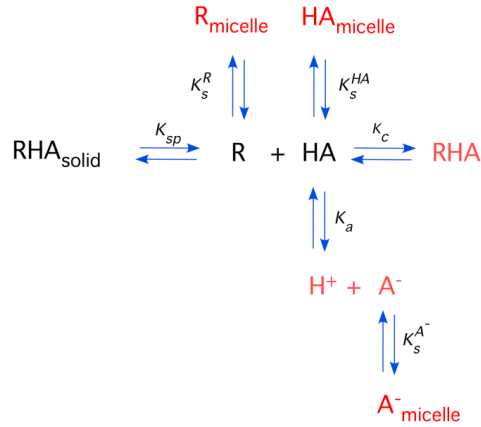


Figure 1.2. Cocystal solution phase interactions and associated equilibria for a cocystal RHA of a nonionizable drug I and weakly acidic coformer (HA) in a micellar solution⁶.

Modeling Cocystal Solubility

Cocystal dissociation, complexation, ionization, and micellar solubilization can be described by the following equilibrium reactions and associated constants for a cocystal RHA of a nonionizable drug R monoprotic and weakly acidic coformer HA^{13, 21, 23, 36, 48}:



And the associated equilibrium constants are:

The cocystal solubility product K_{sp}

$$K_{sp} = [R][HA] \quad (1.6)$$

The ionization constant K_a for the monoprotic weakly acidic coformer HA

$$K_a = \frac{[A^-]_{aq}[H^+]_{aq}}{[HA]_{aq}} \quad (1.7)$$

The micellar solubilization constant K_s^R for nonionizable drug R

$$K_s^R = \frac{[R]_m}{[R]_{aq}[M]} \quad (1.8)$$

The micellar solubilization constants K_s^{HA} , and K_s^A for weakly acidic coformer HA

$$K_s^{HA} = \frac{[HA]_m}{[HA]_{aq}[M]} \quad (1.9)$$

$$K_s^A = \frac{[A^-]_m}{[A^-]_{aq}[M]} \quad (1.10)$$

where the subscripts aq and m refer to aqueous and micellar pseudophases, respectively. M is the micellar surfactant, or the total surfactant minus the critical micellar concentration (CMC). Activities are replaced by concentrations assuming dilute solution conditions. Equations (1.8), (1.9), and (1.10) assume the partitioning of R, HA, and A^- into micelles is independent²¹. [M] is the micellar surfactant concentration given by total surfactant concentration minus the critical micellar concentration (CMC). Generally, the partitioning of the ionized coformer into micelles (equation (1.10)) is negligible and can be ignored²¹. After the appropriate equilibrium reactions are identified for a cocrystal, they can be used to model the cocrystal solubility. For a 1:1 cocrystal of nonionizable drug R and weakly acidic coformer HA, the mass balances for each component in aqueous solution (no micellar solubilization) are²³:

$$[R]_T = [R]_{aq} + [R]_m \quad (1.11)$$

$$[A]_T = [HA]_{aq} + [HA]_m + [A^-]_{aq} + [A^-]_m \quad (1.12)$$

By combining equations (1.11), (1.12), and (1.6), and substituting appropriate equilibrium constants, an expression for total drug concentration as a function of total coformer concentration can be derived:

$$[R]_T = \frac{K_{sp}}{[A]_T} \left(1 + \frac{K_a}{[H^+]} \right) \quad (1.13)$$

Cocrystal solubility is predicted to increase with pH and decrease as coformer solution concentration increases, as shown in Figure 1.3²³.

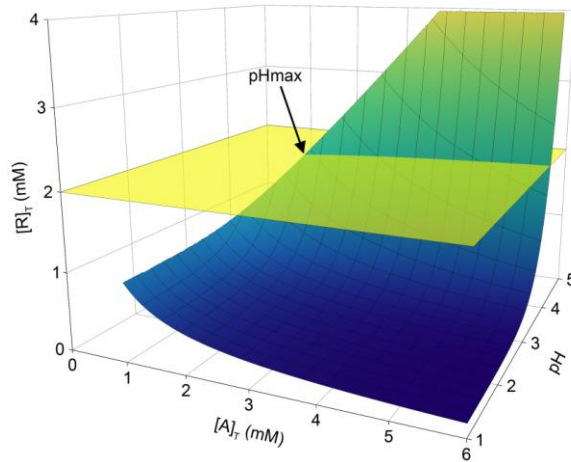


Figure 1.3. Dependence of cocrystal solubility or drug concentration $[R]_T$, on coformer concentration $[A]_T$, and pH for a 1:1 RHA cocrystal; calculated from equation (1.13) with $K_{sp} = 1 \text{ mM}^2$ and coformer $pK_a = 3.0$. Solubility of the drug, S_R is represented by the yellow surface ($S_R = 2 \text{ mM}$) and cocrystal by the blue/green surface^{6, 23}.

The cocrystal and drug solubility surfaces intersect at a given pH value and solution concentrations of R and A. At this point, cocrystal and drug are in equilibrium with solution at a particular pH, and it is regarded as a pH_{max} ⁶.

Under stoichiometric conditions, when cocrystal is in equilibrium with a solution of cocrystal components in stoichiometry equal to that of the cocrystal, the cocrystal solubility will equal the total drug or total coformer concentration. That is, for a 1:1 cocrystal:

$$S_{\text{RHA,T}} = [\text{R}]_{\text{T}} = [\text{A}]_{\text{T}} \quad (1.14)$$

By substituting $S_{\text{cocrystal}}$ into equation (1.13), the following equation for the solubility of a 1:1 cocrystal with a nonionizable drug and a weakly acidic coformer can be derived:

$$S_{\text{RHA,T}} = \sqrt{K_{\text{sp}} \left(1 + \frac{K_{\text{a}}}{[\text{H}^+]} \right)} \quad (1.15)$$

The cocrystal solubility-pH dependence has been derived for cocrystals of varying stoichiometries and ionization properties²³.

When cocrystal is in the presence of a micellar surfactant, equations (1.3)-(1.5) must be considered^{21, 23}. Under stoichiometric conditions, the solubility of RHA is given by:

$$S_{\text{RHA,T}} = \sqrt{K_{\text{sp}} \left(1 + K_{\text{s}}^{\text{R}} [\text{M}] \right) \left(1 + \frac{K_{\text{a}}}{[\text{H}^+]} + K_{\text{s}}^{\text{HA}} [\text{M}] + \frac{K_{\text{a}}}{[\text{H}^+]} K_{\text{s}}^{\text{A}^-} [\text{M}] \right)} \quad (1.16)$$

where $[\text{M}]$ is the micellar surfactant concentration given by total surfactant concentration minus the critical micellar concentration (CMC). Equation (1.16) assumes that the micellar partitioning of drug and coformer is independent and can be used to describe the solubility of a 1:1 cocrystal RHA as a function of surfactant concentration. It is important to note that the nonlinear cocrystal solubility dependence on surfactant concentration can lead to an intersection point with the drug solubility curve, which is called the critical solubilization concentration (CSC). The CSC defines important stability regions and will be discussed in the stability region.

Determining the solubility of a cocrystal can be difficult if the cocrystal is more soluble than the drug. In these instances, the cocrystal can undergo solution-mediated transformation to the less soluble drug. Equilibrium eutectic points can be used to describe the cocrystal solubility and stability and are described in the next section.

The cocrystal eutectic point

The eutectic point is a three-phase equilibrium point between two solid phases (cocrystal and drug or coformer) and solution^{13, 48}. At this point, two solid phases, usually cocrystal and drug, coexist in equilibrium with solution⁶. The solution composition of cocrystal components ($[\text{drug}]_{\text{eu}}$ and $[\text{coformer}]_{\text{eu}}$) is fixed at a given temperature and pH at this equilibrium point. The eutectic constant, K_{eu} , has been introduced for racemic chiral systems and has been applied to describe the stability of cocrystals^{6, 13, 49, 50}. K_{eu} is an experimentally accessible parameter for both stable and metastable cocrystals that has been shown to be a function of the cocrystal to drug solubility ratio and indicate cocrystal stability relative to the drug⁴⁸. It can also be used to estimate stoichiometric cocrystal solubility¹³. K_{eu} is defined as the activity ratio of coformer to drug at the eutectic point, and in dilute conditions, can be calculated from the total cocrystal component solution concentrations at the eutectic point where solid cocrystal and solid drug coexist in are in equilibrium with solution⁶:

$$K_{\text{eu}} \equiv \frac{a_{\text{coformer,eu}}}{a_{\text{drug,eu}}} \approx \frac{[\text{coformer}]_{\text{eu}}}{[\text{drug}]_{\text{eu}}} \quad (1.17)$$

To understand how K_{eu} reflects cocrystal stability, consider the following equilibrium reactions and constants for 1:1 cocrystal of drug A and coformer B, neglecting any solution phase interactions such as ionization, complexation, and micellar solubilization:



$$K_{sp} = [A][B] \quad (1.19)$$

The cocrystal solubility and eutectic constant are given by:

$$K_{eu} = \frac{[B]_{eu}}{[A]_{eu}} \quad (1.20)$$

$$S_{cocrystal} = K_{sp} \quad (1.21)$$

For drug component A:



$$S_A = [A]_T = [A] \quad (1.23)$$

By substituting equations (1.19), (1.21), and (1.23) into (1.20), K_{eu} can be described as a function of the cocrystal to drug solubility ratio:

$$K_{eu} = \frac{[B]_{eu}}{[A]_{eu}} = \frac{K_{sp}}{S_A} = \left(\frac{S_{cocrystal}}{S_{drug}} \right)^2 \quad (1.24)$$

This derivation for K_{eu} is greatly simplified; K_{eu} has been determined to depend on solvent, cocrystal stoichiometry, and solution interactions such as complexation, ionization, and micellar solubilization^{22, 48}.

A phase solubility diagram (PSD) that describes the solubility of cocrystal AB and drug A can be generated by plotting equations (1.23) and (1.19)³⁷. The drug solubility curve will intersect the cocrystal solubility curve when drug A is less soluble than coformer B and the cocrystal AB³⁷. An example PSD is shown in Figure 1.4

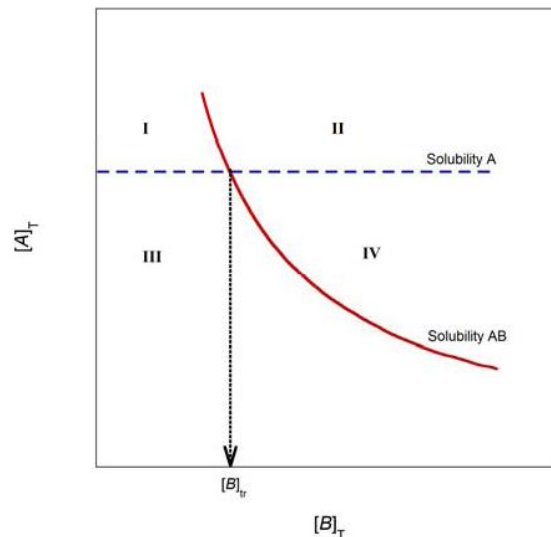


Figure 1.4. Phase solubility diagram of cocrystal AB (solid red line) and drug A (dashed blue line). B_{tr} is the coformer transition concentration, also called eutectic concentration $[B]_{eu}$ where $S_{cocrystal} = S_A$. Adapted from reference 36.

The eutectic point establishes the thermodynamic stability regions I-IV of the cocrystal as shown in Figure 1.4. At $[B] < [B]_{eu}$, cocrystal AB is unstable in solution and can transform to less soluble drug A. At $[B] > [B]_{eu}$, cocrystal is stable in solution. At the eutectic point, $S_A = S_{cc}$, and both solid drug A and solid cocrystal AB will be present in solution.

The critical stabilization concentration (CSC)

The critical stabilization concentration (CSC) is the surfactant concentration at which cocrystal solubility is equal to drug solubility²¹. At the CSC, solid cocrystal and drug phases are in equilibrium with solution; thus, it is a eutectic point by definition⁶. As in the cases of K_{eu} and pH_{max} described above, the CSC marks cocrystal thermodynamic stability regions in solution.

The ability of a surfactant to stabilize a cocrystal (reduce the cocrystal to drug solubility ratio to achieve a critical stabilization concentration, CSC) is dependent on the differential solubilization of drug versus coformer. That is, the greater the drug micellar solubilization K_s^R relative to that of the coformer, K_s^{HA} , the lower the CSC value as shown in Figure 1.5^{6, 21}.

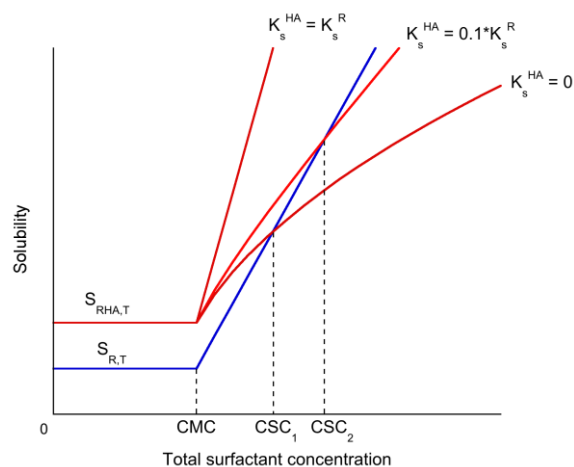


Figure 1.5. Differential solubilization of cocrystal components represented by the relative values of K_s^{HA} and K_s^R leads to nonlinear cocrystal solubility dependence and to intersection of the cocrystal and drug solubility curves at the CSC. CSC refers to the critical stabilization concentration, at which both cocrystal and drug are thermodynamically stable²¹.

In this way, the ability of a cocrystal to be stabilized by a surfactant can be judged. As coformer micellar solubilization approaches that of the drug, the ability of the surfactant to stabilize the cocrystal by achieving a CSC is diminished²¹. At surfactant concentrations $> CSC$, cocrystal is thermodynamically stable relative to the drug. Below the CSC, drug is the thermodynamically stable solid phase. The dependence of CSC on relevant parameters such as pH, cocrystal stoichiometry, cocrystal solubility, and cocrystal ionization properties has been derived and has important implications for cocrystal solution phase solubility and stability in the presence of surfactants^{22, 27}.

Additives for Solubility and Dissolution Enhancement

Important additives to examine with regards to cocrystal solubility and dissolution include those that are physiologically relevant and have been used to model *in vivo* conditions. Biorelevant media to model the fasted and fed states in the GI tract is composed of bile salts alone or in combination with phospholipids, usually lecithin⁵¹. Understanding cocrystal solution phase behavior in the presence of these physiologically relevant surfactants will give greater

understanding and aid in the prediction of cocrystal *in vivo* performance. Additionally, additives that enhance dissolution through wetting, solubilization, or stabilization are important to enable high solubility cocrystals in solution^{6, 11}. Nonionic, and anionic surfactants are often used to solubilize or wet poorly soluble drugs^{3, 40}, and understanding their impact on cocrystal solubility and dissolution is important to optimize these critical properties. Since a cocrystal of a poorly soluble drug formulated with a formulation surfactant will also encounter physiologically relevant surfactants *in vivo*, it is also necessary to understand cocrystal solubility and stability in these mixed systems.

Physiologically relevant surfactants

Biorelevant media containing physiologically relevant surfactants were first developed and standardized in composition in the late 1990's^{30, 52}. Since their introduction, the use of simulated gastric and intestinal fluids has increased tremendously as an integral part of the development and optimization of oral dosage forms⁵³. Updated compositions have since been introduced to more accurately mimic *in vivo* conditions⁵⁴; however, the main components remain the same. The bile salt sodium taurocholate (NaTC) is used in varying concentrations, usually in combination with the phospholipid lecithin, to simulate *in vivo* solution conditions in the fasted and fed states^{52, 55}. In some cases, these natural solubilizing components have been replaced with sodium lauryl sulfate (SLS) or Triton X synthetic surfactants, but in most cases, NaTC and lecithin are used^{32, 52, 56}.

Bile salts are natural surfactants present in the GI tract that have been shown to greatly affect the bioavailability of poorly soluble drugs in fed state conditions^{31, 32, 51, 52, 55}. It has been suggested that the increased bioavailability is either due to increased solubility of drugs in this media compared to aqueous buffer due to micellar solubilization or enhanced dissolution rate

due to wetting effects^{32, 57}. It has been observed that more hydrophobic drugs exhibit improved dissolution behavior due to micellar solubilization in bile salt/lecithin mixed micelles while more hydrophilic drugs exhibit improvement due to wetting phenomena^{29, 33}. Poorly soluble and highly permeable drugs are more susceptible to variation in dissolution medium during *in vitro* dissolution testing to be meaningfully evaluated^{2, 3, 58}. Lecithin, a naturally occurring phospholipid, forms mixed micelles with NaTC, resulting in an enhanced solubilization capacity for NaTC^{51, 52, 59}. Physiologically relevant concentrations of bile salts range between 10-30 mM in the fed state and 3-8 mM in the fasted state^{51, 54}. Lecithin is usually present in a 1:2.5 – 1:5 ratio with NaTC, depending on bile output⁵². Examples of other bile salts include sodium cholate, sodium glycocholate and sodium deoxycholate⁴⁰.

The mechanism of solubilization is different for bile salts and bile salt/lecithin mixed micelles compared to traditional surfactants. Due to their complex mechanism of aggregation where they self-associate noncritically, bile salts do not exhibit a distinct CMC⁶⁰. A range of CMC values for these systems is reported in the literature due to variation in experimental parameters such as ionic strength, temperature, etc⁵². At 25°C, 0.1M NaCl, the CMC of NaTC was reported to drop from 4.7 to 0.25 mM with addition of lecithin in a 4:1 NaTC/lecithin ratio^{30, 52}. NaTC/lecithin mixtures which are rich in NaTC (like most biorelevant media) first form small aggregates of 2-10 NaTC monomers via hydrophobic interactions^{61, 62}. These small “primary micelles” can then interact via hydrogen bonding to form large planar “secondary micelles” at higher NaTC concentration⁶¹ and are characterized by a gradual increase in solubilization^{60, 63}. Figure 1.6 shows the structures of bile salt micelles⁶¹.

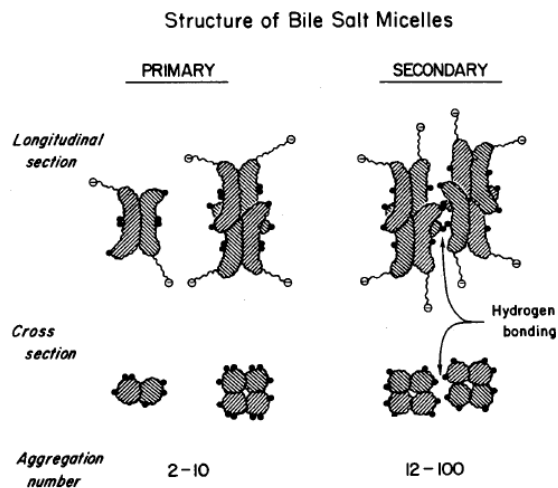


Figure 1.6. Proposed structures of primary and secondary bile salt micelles⁶¹.

The solubilization achieved by bile salts and bile salt/lecithin mixed micelles can be analyzed based on the narrow concentration ranges that exhibit linear solubilization of a particular drug^{30, 55}. Figure 1.7 shows carbamazepine solubility as a function of bile salt (sodium deoxycholate) concentration⁶³.

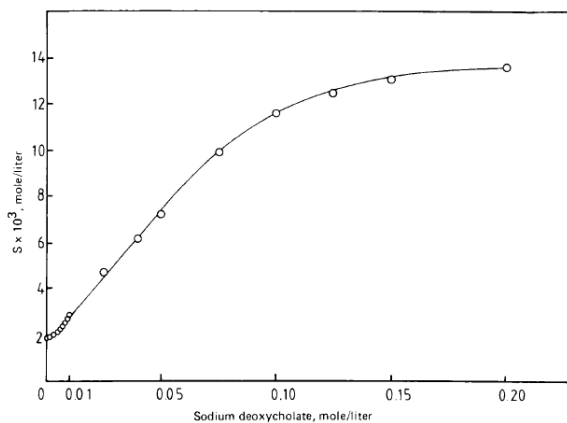


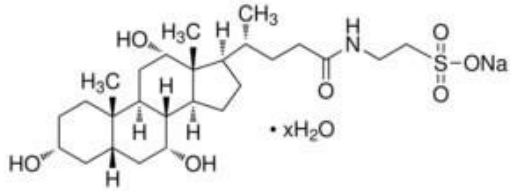
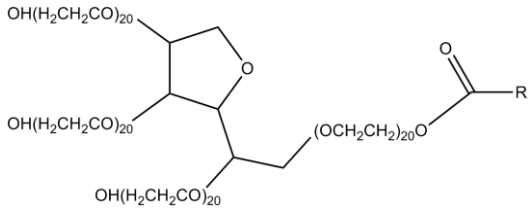
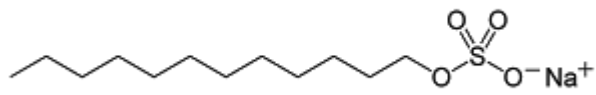
Figure 1.7. Solubility of carbamazepine (mM) as a function of sodium deoxycholate concentration (M) at 37°C⁶³.

Solubility increases linearly with bile salt concentration in the range from 0.01 to 0.10 M, and a solubilization constant for carbamazepine can be calculated from the slope of the plot in this region.

Nonionic Surfactants

Nonionic surfactants are commonly used in pharmaceutical formulations due to their relatively low toxicity, stability, and ability to interact favorably with other common formulation additives^{3, 40, 62, 64}. Polysorbate surfactants (common brand name Tween®) are used to wet, solubilize, stabilize drugs in oral, topical, ocular and parenteral formulations due to their ability to solubilize and emulsify water insoluble substances^{40, 64, 65}. Since they are well-tolerated physiologically, polysorbate 20 and 80 can be used up to 10% in oral and topical formulations. Other commonly used nonionic formulation surfactants include Myrj®, and Brij®. Table 1.1 shows the chemical structures of some commonly used nonionic surfactants.

Table 1.1. Chemical structure, CMC, and use of common nonionic and anionic surfactants.

Surfactant	CMC (M) ^a	Type	Use
<p>NaTC</p> 	^a 2.5 x 10 ⁻⁵	anionic	dissolution media
<p>Tween 80</p> 	^b 1 x 10 ⁻⁵	nonionic	formulation
<p>SLS</p> 	^c 8.2 x 10 ⁻³	anionic	formulation dissolution media

(a) From reference⁵⁵.

(b) From reference⁶⁶.

(c) From reference⁶⁷.

Information regarding the solubilization of poorly soluble drugs by nonionic surfactants is widely available in the literature. The solubilization of carbamazepine, indomethacin, and piroxicam has been studied in polysorbates and Brij, and Myrj surfactants⁶⁸⁻⁷⁵. In addition, the effect of polysorbate 80, Myrj 52, and Brij 99 on the solubility and stability of IND-SAC and CBZ-SAC has been investigated in our laboratory^{21, 76}. Results indicate that IND-SAC is

stabilized to a greater extent than CBZ-SAC in these surfactants, and that a critical stabilization constant (CSC) exists for IND-SAC in these surfactants.

Relationships between hydrophobicity and micellar solubilization

The micellar partitioning of several drugs in different types of surfactants is observed to increase with the hydrophobicity (as determined by octanol-water partition coefficient, $\log P$) of the drug^{55, 77, 78}. The log micellar equilibrium partition coefficient ($\log K_M^N$) is observed to increase linearly with the $\log P$ of the drug for several drugs including barbiturates, steroids, and benzoic acid derivatives for polysorbate (Tween®) 80 as shown in Figure 1.8⁷⁷.

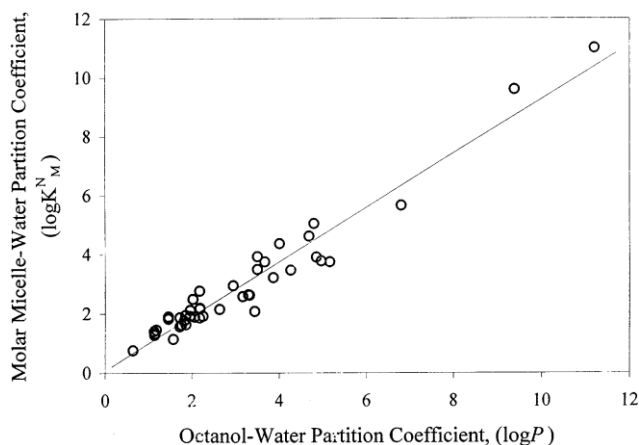


Figure 1.8. Log Polysorbate 80 molar micelle–water partition coefficient ($\log K_M^N$) versus $\log P$ of several drugs⁷⁷.

In this example, K_M^N is equivalent to K_s as defined in equation 10. Based on this data set, equation (1.25) can be used to calculate the K_s in units of M^{-1} of a drug in polysorbate 80 based on its $\log P$ ⁷⁷:

$$\log K_s = 0.9201(\log P) + 0.0690 \quad (1.25)$$

Linear relationships between the solubilization of drugs in the bile salt sodium taurocholate (NaTC), and in bile salt/phospholipid mixed micelles (NaTC/lecithin) and their log P have also been observed^{55, 78}. In NaTC, a linear relationship was established between the log P and the log solubilization ratio (log SR) of nonionizable nonsteroidal and steroidal drugs, shown in Figure 1.9⁵⁵.

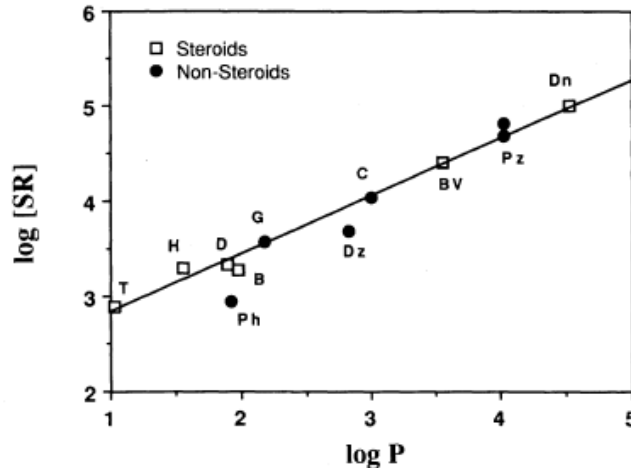


Figure 1.9. Log SR in aqueous NaTC as a function of log P for 6 steroidal and 6 non-steroidal compounds⁵⁵.

SR is defined as:

$$SR = \frac{SC_{\text{bile salt}}}{SC_{\text{aqueous}}} \quad (1.26)$$

where $SC_{\text{bile salt}}$ is the solubilization capacity of the bile salt for drug and SC_{aqueous} the solubilization capacity of water for the drug⁵⁵. SC is defined as the number of moles of solubilize per mole of micellized surfactant (in case of bile salt) or per mole of water (aqueous). Based on the definition of the solubilization capacities^{40, 55}, SR can be related to K_s (in units of M^{-1}):

$$K_s = SR(1.8 \times 10^{-2}) \quad (1.27)$$

The relationship between hydrophobicity and SR of several nonionizable and ionizable drugs in the biorelevant media FaSSIF and FeSSIF which contain NaTC/lecithin mixed micelles was recently investigated⁷⁸. In this study, SR was defined as:

$$SR = \frac{SC_{\text{biorelevant media}}}{SC_{\text{aqueous buffer}}} \quad (1.28)$$

where biorelevant media was either FeSSIF or FaSSIF and aqueous buffer was at the pH of the media (6.5 for FaSSIF, 5.0 for FeSSIF). The log SR was plotted against log P, as shown in Figure 1.10, and a weak linear correlation was observed with $R^2 = 0.32$ ⁷⁸.

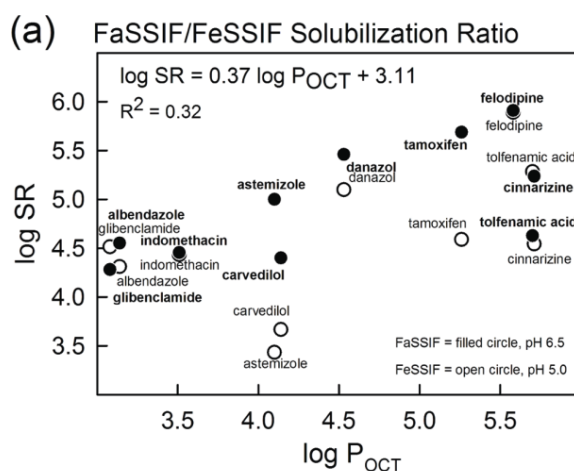


Figure 1.10. The solubilization capacity (SR) versus log P_{oct} of FaSSIF (●) and FeSSIF (○) for a data set of nonionizable and ionizable drugs; an R² of 0.32 was obtained⁷⁸.

This weak correlation was expected, as the majority of compounds in the sample set carry a net charge at the pHs of FaSSIF (pH=6.5) and FeSSIF (pH=5.0)⁷⁸. When the log P was exchanged for log D_{pH 6.5} for FaSSIF and log D_{pH 5.0} for FeSSIF, a stronger linear relationship was observed (R² = 0.74), as shown in Figure 1.11.

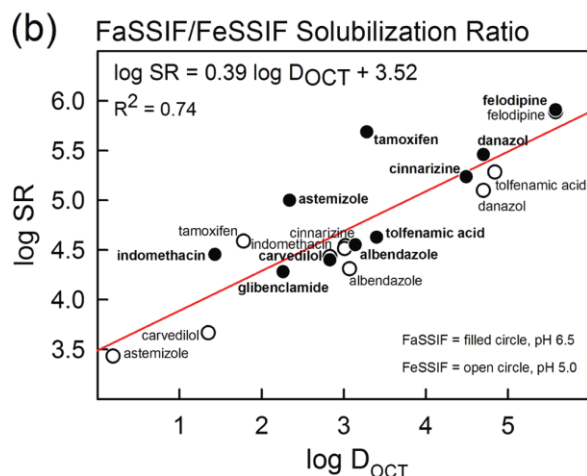


Figure 1.11. The solubilization capacity (SR) versus log D_{oct} of FaSSIF (●) and FeSSIF (○) for a data set of nonionizable and ionizable drugs; an R² of 0.74 was obtained⁷⁸.

Since log D (distribution coefficient) values give apparent log P (partition coefficient) values at a given pH, they account for both ionized and unionized species in aqueous solution⁷⁸. This type of relationship can be used to investigate whether the differential solubilization of cocrystal components can be explained by hydrophobicity differences (either log P for nonionizable components, or log D for ionizable components).

Effect of Temperature, pH and Ionic Strength on Micellar Solubilization

Micellar solubilization is affected by temperature, pH and ionic strength⁶²; therefore, the equilibrium solubilization constants (K_s) will vary with these parameters as well. For nonionic surfactants, the extent of solubilization increases with temperature due to the changes in the aqueous solubility properties of the solubilizate and changes in the properties of the micelles⁶². This trend has been verified for solubilization of poorly soluble drugs by polysorbate 80⁷⁹. The micelle size of nonionic surfactants has been observed to increase and the CMC has been reported to decrease with increasing temperature resulting in an overall increase in micellar solubilization^{3, 40, 62, 80}. In contrast, ionic surfactants often show reduced solubilization with temperature increase^{3, 40}. The CMCs of the ionic surfactants sodium lauryl sulfate (SLS) and

ctroimondium bromide (CTAB) have been observed to both increase and decrease slightly with temperature^{3, 40}. For SLS, the CMC initially decreases as temperature increases due to dehydration of monomers, followed by a sharp increase in CMC due to disruption of water around the hydrophobic groups, which opposes micellization⁶². In addition, it is not uncommon for both nonionic and ionic micelles to go from spherically shaped to more asymmetrical at higher temperatures and for the size distribution of micelles to become more polydisperse⁶². The CMC of the bile salts sodium taurocholate and sodium taurodeoxycholate are observed to increase with increasing temperature above 40°C with little change at lower temperatures⁴⁰.

The effect of pH on the micellar solubilization of a nonionic surfactant depends solely on the ionization properties of the solubilize^{3, 62}. Unionized solubilizes are expected to partition into micelles more favorably than ionized solubilizes^{3, 40}. The effect of pH on the micellar solubilization by an ionic surfactant will depend on the pKa of the surfactant and the ionization properties of the solubilize^{3, 40}. As the pH decreases towards the pKa of an ionic surfactant, it becomes less soluble resulting in a lowering of its CMC⁴⁰. At low pH, bile acids are precipitated from solution, initially being incorporated or solubilized in existing micelles⁶². The pH at which precipitation/saturation occurs is generally one pH unit higher than the pKa of the bile acid (pKa of NaTC = 1.84)⁶².

Strong electrolytes have been observed to decrease in the CMC of both nonionic and ionic surfactants^{3, 40, 62}. For nonionic surfactants, this leads to increased solubilization capacity^{3, 40}. However, for ionic surfactants, at concentrations in great excess of the CMC, this is not the case⁶². The location of solubilize in the micelle is important factor in determining the effect of electrolyte on solubilization by ionic surfactants. Addition of electrolyte to an ionic surfactant decreases the repulsion between polar head groups, stabilizing the micelle and allowing for

denser packing of the surfactant monomers, increasing micelle size^{40, 62}. Addition of a strong electrolyte can also influence micelle morphology by changing spherical micelles to more asymmetrical forms⁶². SLS micelles are observed to change from spherical to spherocylindrical (rods) with added NaCl⁶².

Modeling Solubilization in Mixed Surfactants

Surfactant mixtures are commonly encountered in pharmaceutical applications³⁵. For poorly soluble oral drugs, several formulation surfactants are often used to improve solubility and dissolution behavior³. Additionally, formulated oral drugs encounter physiological surfactants, such bile salt/lecithin mixed micelles *in vivo*. In order to better predict and optimize cocrystal *in vivo* performance, an understanding of cocrystal solubility and stability in the presence of physiologically relevant surfactants and formulation surfactants is necessary. These mixed surfactant systems can be theoretically modeled for two cases⁸¹. In one case, the two surfactants are assumed to either act independently or interact to form micelles identical to those of the constituent surfactants; in the other case, the two surfactants interact to some extent to form mixed micelles⁸¹.

Drug Solubilization in Ideal Surfactant Mixtures

If micelle formation is ideal in a binary surfactant mixture, the two surfactants are assumed to either form micelles independently of each other^{35, 81}, or form mixed micelles identical to those of the constituent surfactants. In this simplified case of non-interacting surfactants, the CMC, K_s , or other relevant property of the mixture can be determined from the properties of the pure surfactants comprising the mixture and knowledge of the mixture composition³⁵. A similar approach has been used to calculate the hydrophile-lipophile balance (HLB) numbers of mixed surfactant systems in emulsion literature⁶². With regards to

solubilization, ideal interaction means that the environment of the solubilize (incorporation site in the micelle) is identical among the mixed surfactants (either a mixture of pure micelles or mixed micelles) and the pure micelles of the constituent surfactants. Clearly, this is an ideal case that may not apply to many real-life scenarios. Binary mixtures of structurally similar nonionic surfactants can approach this behavior; however, in most cases, there is some degree of nonideality⁸². The equilibrium partition coefficient of a solubilize in an ideal mixture of A and B can be modeled as:

$$\ln K_s^{AB} = X_A \ln K_s^A + X_B \ln K_s^B \quad (1.29)$$

where K_s^{AB} is the partition coefficient of the mixture, K_s^A and K_s^B are the partition coefficients of the pure surfactants A and B, and X_A and X_B are the mole fraction of A and B present in the mixture⁸¹. Equation (1.29) ignores nonideal surfactant-surfactant and surfactant-solubilize interactions^{35, 81, 83, 84}. While equation 44 for nonsynergistic solubilization represents an ideal case, it can still be applied to cocrystal systems as a simplified situation from which to start modeling nonideal mixed surfactant systems.

Mixtures of the anionic surfactant sodium lauryl sulfate (SLS) and the bile salt sodium taurodeoxycholate (NaTDC) have been studied assuming ideal mixing. The CMC of the ideal mixture was calculated according to^{85, 86}:

$$\frac{1}{\text{CMC}_{\text{mix,ideal}}} = \frac{X_{\text{SLS}}}{\text{CMC}_{\text{SLS}}} + \frac{X_{\text{NaTDC}}}{\text{CMC}_{\text{NaTDC}}} \quad (1.30)$$

where X_{SLS} and X_{NaTDC} are the mole fraction of SLS and NaTDC in the mixture. Experimentally measured CMC_{mix} values at for compositions ranging from 1:9 to 1:1 SLS/NaTDC were greater than the $\text{CMC}_{\text{mix,ideal}}$ while compositions ranging from 2:1 to 4:1 SLS/NaTDC were less than the

calculated $CMC_{mix, ideal}^{85}$. This was attributed to a noncompatibility of the bile salt and SLS with regard to charge interaction, head group type, and structure of hydrophobic moieties below 50 mol % SLS⁸⁵. While the authors were not able to quantitatively predict the CMC of the mixture due to nonidealities, the ideal calculations did allow them to draw conclusions about the nature of bile salt-anionic surfactant interactions.

Statement of dissertation research

The purpose of this dissertation is to explore the mechanisms of cocrystal solubilization by solubilizing agents and their impact on cocrystal solubility, $S_{cocrystal}/S_{drug}$, and transition points. Cocrystals have been shown to profoundly increase aqueous solubility of poorly soluble drugs. However, there remains a significant lack of understanding of the factors that influence the solution behavior of cocrystals such as differential solubilization of cocrystal components by physiologically relevant and synthetic formulation solubilizing agents. There is a critical need to develop mechanism-based strategies to understand and predict cocrystal solution behavior in these environments to guide cocrystal development leading to optimized oral delivery. The objective of this work is to develop a theoretical framework that explains cocrystal solution behavior in the presence of drug solubilizing agents in terms of experimentally accessible thermodynamic parameters. The following chapters model and explain cocrystal solubility, solubilization ratio, and thermodynamic stability by considering appropriate solution phase equilibria.

Chapter 2 investigates the mechanisms of cocrystal solubilization in the presence of physiologically relevant surfactants. Previous work has shown the influence of synthetic surfactants on cocrystal solubility in nonionizing conditions, and mechanism based models have been derived to predict this behavior. In physiological environments, drugs are often in ionizing

conditions and in solution with physiologically relevant surfactants, such as bile salts and phospholipid mixed micelles. Mathematical models that predict cocrystal solubility and cocrystal solubilization ratio ($SR_{\text{cocrystal}}$) are derived based on solution equilibria that consider cocrystal dissociation and constituent ionization and micellar solubilization. $SR_{\text{cocrystal}}$ is shown to be orders of magnitude less than SR_{drug} when the drug constituent is preferentially solubilized. This chapter discusses and challenges the model's predictions of $SR_{\text{cocrystal}}$ and cocrystal solubility with a series of seven cocrystals of diverse properties in fed state simulated intestinal fluid (FeSSIF). Predicted the $SR_{\text{cocrystal}}$ and solubility values are in excellent agreement with the predictions.

Chapter 3 investigates the impact of preferential solubilization of drug constituents on $S_{\text{cocrystal}}/S_{\text{drug}}$ in the presence of physiologically relevant surfactants. The objective of this chapter is to study the reduction in $S_{\text{cocrystal}}/S_{\text{drug}}$ in physiologically relevant surfactants due to preferential solubilization and assess the impact on supersaturation during dissolution in this media. Mechanism-based mathematical models to predict $S_{\text{cocrystal}}/S_{\text{drug}}$ are in good agreement with the experimentally measured $S_{\text{cocrystal}}/S_{\text{drug}}$ values for a diverse series of cocrystals in FeSSIF and blank aqueous buffer. Cocrystals are demonstrated to exhibit significantly lower $S_{\text{cocrystal}}/S_{\text{drug}}$ in the solubilizing agent compared to aqueous buffer due to preferential solubilization of the drug constituent, with cocrystals of more hydrophobic and highly solubilized drugs exhibiting the largest decreases in $S_{\text{cocrystal}}/S_{\text{drug}}$. The decreased $S_{\text{cocrystal}}/S_{\text{drug}}$ results in sustained supersaturated drug concentrations and slower transformation to drug during cocrystal dissolution in physiologically relevant surfactants compared to aqueous buffer.

Chapter 4 develops models that describe the relationship between $\log SR_{\text{cocrystal}}$ and $\log SR_{\text{drug}}$ in the presence of drug solubilizing agents for the purpose of comparing the correlation

between log SR and drug hydrophobicity for drugs and cocrystals were derived. The octanol-water distribution coefficient (log D) is found to be a good predictor of log SR for drug and cocrystals. The log $SR_{\text{cocrystal}}$ is shown to exhibit a weaker dependence on drug log D compared to log SR_{drug} , which is predicted from the derived models. Log $SR_{\text{cocrystal}}$ can be calculated simply from knowledge of drug log D if a robust log SR_{drug} -log D linear regression correlation is calculated from experimentally measured SR_{drug} values. These models are valuable since SR_{drug} and log P and/or log D are commonly measured and reported drug properties.

Chapter 5 investigates cocrystal solubilization in the presence of multiple drug solubilizing agents. This chapter expands on the theoretical framework developed in Chapter 2 to consider cocrystal solubilization in the presence of two ideally mixing surfactants, where the solubilization contributions of the surfactants are assumed to be additive. Additional mathematical equations that predict cocrystal solubility and $S_{\text{cocrystal}}/S_{\text{drug}}$ in two surfactants based on cocrystal dissociation and constituent ionization and micellar solubilization are derived for the first time. The solubility and $S_{\text{cocrystal}}/S_{\text{drug}}$ in the presence of FeSSIF and Tween 80 of two cocrystals of danazol (DNZ) was quantitatively predicted from relevant equilibrium constants based on the presented models. Preferential solubilization of DNZ is shown to result in a dramatic decrease in $S_{\text{cocrystal}}/S_{\text{drug}}$ as Tween 80 concentration increases, but this effect is dampened in the presence of FeSSIF, particularly at low Tween 80 concentrations.

Chapter 6 brings together concepts that are relevant to the solubilization and thermodynamic stability in the presence of drug solubilizing agents. Simple equations are derived that allow for the facile calculation of $SR_{\text{cocrystal}}$ and transition point solubility. Analysis of 10 cocrystals in 6 different solubilizing agents shows that $SR_{\text{cocrystal}}$ is quantitatively predicted from knowledge of SR_{drug} . Drug solubilizing agents are shown to induce cocrystal transition

points, where drug and cocrystal solubilities are equal and above which the cocrystal solubility advantage over drug is eliminated. This chapter demonstrates for the first time that cocrystal solubility at the transition point can be predicted from the aqueous solubilities of drug and cocrystal and is independent of the nature and concentration of the solubilizing agent. Based on the derived models, the concept of a critical transition point solubility S^* is developed, where drug and cocrystal have equal solubilities in the presence of a solubilizing agent. Predicted S^* values are in good agreement with experimentally determined values for cocrystals of carbamazepine (CBZ). Simple equations that relate the cocrystal $S_{\text{cocrystal}}/S_{\text{drug}}$ in aqueous solution to SR_{drug} are derived to predict a cocrystal's position on a phase diagram relative to its transition point. Predicted transition points are shown to be in good agreement with experimentally measured values for cocrystals of pterostilbene (PTB) and DNZ.

The conclusions of this dissertation and future directions of this research are discussed in Chapter 7. Several of these chapters are currently in preparation for submission for publication. Chapter 2 is a manuscript currently under review in the *Journal of Pharmaceutical Sciences* 2015. Chapter 6 is a manuscript currently under review in *Molecular Pharmaceutics* 2015.

References

1. Lobenberg, R., Amidon, Gordon L, and Viera, Michael, Solubility as a Limiting Factor to Drug Absorption. In *Oral Drug Absorption: Prediction and Assessment*, Jennifer B Dressman, H. L., Ed. Marcel Dekker Inc.: New York, New York, 2000; Vol. 106, pp 137-154.
2. Amidon, G. L.; Lennernas, H.; Shah, V. P.; Crison, J. R. A Theoretical Basis for a Biopharmaceutic Drug Classification - the Correlation of in-Vitro Drug Product Dissolution and in-Vivo Bioavailability. *Pharm. Res.* **1995**, *12*, (3), 413-420.
3. Liu, R., *Water Insoluble Drug Formulation*. 2nd ed.; CRC Press: Newark, New Jersey, 2008.
4. Lipinski, C. A. Drug-like properties and the causes of poor solubility and poor permeability. *J. Pharmacol. Toxicol. Methods* **2000**, *44*, (1), 235-249.
5. Gursoy, R. N.; Benita, S. Self-emulsifying drug delivery systems (SEDDS) for improved oral delivery of lipophilic drugs. *Biomed. Pharmacother.* **2004**, *58*, (3), 173-182.
6. Roy, L., Lipert, Maya and Rodriguez-Hornedo, Nair, Cocrystal Solubility and Thermodynamic Stability. In *Handbook of Pharmaceutical Salts and Cocrystals*, Submitted,

Quere, J. W. a. L., Ed. Royal Society of Chemistry: London, United Kingdom, 2011; Vol. 16, pp 247-279.

7. Roy, L.; Lipert, M. P.; Rodriguez-Hornedo, N., Co-crystal Solubility and Thermodynamic Stability. In *Pharmaceutical Salts and Co-Crystals*, Wouters, J.; Quere, L., Eds. 2011; pp 247-279.

8. Thakuria, R.; Delori, A.; Jones, W.; Lipert, M. P.; Roy, L.; Rodriguez-Hornedo, N. Pharmaceutical cocrystals and poorly soluble drugs. *Int. J. Pharm.* **2013**, *453*, (1), 101-125.

9. Childs, S. L.; Chyall, L. J.; Dunlap, J. T.; Smolenskaya, V. N.; Stahly, B. C.; Stahly, G. P. Crystal engineering approach to forming cocrystals of amine hydrochlorides with organic acids. Molecular complexes of fluoxetine hydrochloride with benzoic, succinic, and fumaric acids. *J. Am. Chem. Soc.* **2004**, *126*, (41), 13335-13342.

10. McNamara, D. P.; Childs, S. L.; Giordano, J.; Iarriccio, A.; Cassidy, J.; Shet, M. S.; Mannion, R.; O'Donnell, E.; Park, A. Use of a glutaric acid cocrystal to improve oral bioavailability of a low solubility API. *Pharm. Res.* **2006**, *23*, (8), 1888-1897.

11. Remenar, J. F.; Peterson, M. L.; Stephens, P. W.; Zhang, Z.; Zimenkov, Y.; Hickey, M. B. Celecoxib : Nicotinamide dissociation: Using excipients to capture the cocrystal's potential. *Mol. Pharm.* **2007**, *4*, (3), 386-400.

12. Basavoju, S.; Bostrom, D.; Velaga, S. P. Indomethacin-saccharin cocrystal: Design, synthesis and preliminary pharmaceutical characterization. *Pharm. Res.* **2008**, *25*, (3), 530-541.

13. Good, D. J.; Rodriguez-Hornedo, N. Solubility Advantage of Pharmaceutical Cocrystals. *Cryst. Growth Des.* **2009**, *9*, (5), 2252-2264.

14. Remenar, J. F.; Morissette, S. L.; Peterson, M. L.; Moulton, B.; MacPhee, J. M.; Guzman, H. R.; Almarsson, O. Crystal engineering of novel cocrystals of a triazole drug with 1,4-dicarboxylic acids. *J. Am. Chem. Soc.* **2003**, *125*, (28), 8456-8457.

15. Cheney, M. L.; Weyna, D. R.; Shan, N.; Hanna, M.; Wojtas, L.; Zaworotko, M. J. Cofomer Selection in Pharmaceutical Cocrystal Development: a Case Study of a Meloxicam Aspirin Cocrystal That Exhibits Enhanced Solubility and Pharmacokinetics. *J. Pharm. Sci.* **2011**, *100*, (6), 2172-2181.

16. Smith, A. J.; Kavuru, P.; Wojtas, L.; Zaworotko, M. J.; Shytle, R. D. Cocrystals of Quercetin with Improved Solubility and Oral Bioavailability. *Mol. Pharm.* **2011**, *8*, (5), 1867-1876.

17. Hickey, M. B.; Peterson, M. L.; Scoppettuolo, L. A.; Morissette, S. L.; Vetter, A.; Guzman, H.; Remenar, J. F.; Zhang, Z.; Tawa, M. D.; Haley, S.; Zaworotko, M. J.; Almarsson, O. Performance comparison of a co-crystal of carbamazepine with marketed product. *Eur. J. Pharm. Biopharm.* **2007**, *67*, (1), 112-119.

18. Stanton, M. K.; Bak, A. Physicochemical properties of pharmaceutical co-crystals: A case study of ten AMG 517 co-crystals. *Cryst. Growth Des.* **2008**, *8*, (10), 3856-3862.

19. Childs, S. L.; Kandi, P.; Lingireddy, S. R. Formulation of a Danazol Cocrystal with Controlled Supersaturation Plays an Essential Role in Improving Bioavailability. *Mol. Pharm.* **2013**, *10*, (8), 3112-3127.

20. Roy, L. Engineering Cocrystal and Cocrystalline Salt Solubility by Modulation of Solution Phase Chemistry. *University of Michigan (Doctoral Dissertation)* **2013**, Retrieved from Deep Blue. (<http://hdl.handle.net/2027.42/98067>).

21. Huang, N.; Rodriguez-Hornedo, N. Effect of Micellar Solubilization on Cocrystal Solubility and Stability. *Cryst. Growth Des.* **2010**, *10*, (5), 2050-2053.

22. Huang, N. a. R.-H., Nair. Engineering cocrystal thermodynamic stability and eutectic points by micellar solubilization and ionization. *Crystal Engineering Communications* **2011**, *13*, 5409-5422.
23. Bethune, S. J.; Huang, N.; Jayasankar, A.; Rodriguez-Hornedo, N. Understanding and Predicting the Effect of Cocrystal Components and pH on Cocrystal Solubility. *Cryst. Growth Des.* **2009**, *9*, (9), 3976-3988.
24. Huang, N.; Rodriguez-Hornedo, N. Engineering Cocrystal Solubility, Stability, and pH(max) by Micellar Solubilization. *J. Pharm. Sci.* **2011**, *100*, (12), 5219-5234.
25. Huang, N.; Rodriguez-Hornedo, N. Engineering cocrystal thermodynamic stability and eutectic points by micellar solubilization and ionization. *Crystengcomm* **2011**, *13*, (17), 5409-5422.
26. Huang, N.; Rodriguez-Hornedo, N. Effect of Micelliar Solubilization on Cocrystal Solubility and Stability. *Cryst. Growth Des.* **2010**, *10*, (5), 2050-2053.
27. Huang, N. a. R.-H., Nair. Engineering cocrystal solubility, stability, and pHmax by micellar solubilization, *manuscript accepted. J. Pharm. Sci.* **2011**.
28. Roy, L.; Rodriguez-Hornedo, N. A Rational Approach for Surfactant Selection to Modulate Cocrystal Solubility and Stability. *Poster presentation at the 2010 AAPS Annual Meeting and Exposition 2010, New Orleans, LA*, (November 14-18, 2010), Poster R6072.
29. Galia, E.; Nicolaidis, E.; Horter, D.; Lobenberg, R.; Reppas, C.; Dressman, J. B. Evaluation of various dissolution media for predicting in vivo performance of class I and II drugs. *Pharm. Res.* **1998**, *15*, (5), 698-705.
30. Naylor, L. J.; Bakatselou, V.; RodriguezHornedo, N.; Weiner, N. D.; Dressman, J. B. Dissolution of steroids in bile salt solutions is modified by the presence of lecithin. *Eur. J. Pharm. Biopharm.* **1995**, *41*, (6), 346-353.
31. Charman, W. N.; Porter, C. J. H.; Mithani, S.; Dressman, J. B. Physicochemical and physiological mechanisms for the effects of food on drug absorption: The role of lipids and pH. *J. Pharm. Sci.* **1997**, *86*, (3), 269-282.
32. Bakatselou, V.; Oppenheim, R. C.; Dressman, J. B. Solubilization and Wetting Effects of Bile-Salts on the Dissolution of Steroids. *Pharm. Res.* **1991**, *8*, (12), 1461-1469.
33. Miyazaki, S.; Yamahira, T.; Morimoto, Y.; Nadai, T. Micellar Interaction of Indomethacin and Phenylbutazone with Bile-Salts. *Int. J. Pharm.* **1981**, *8*, (4), 303-310.
34. Yadav, A. V.; Dabke, A. P.; Shete, A. S. Crystal engineering to improve physicochemical properties of mefloquine hydrochloride. *Drug Dev. Ind. Pharm.* *36*, (9), 1036-1045.
35. Shiloach, A.; Blankschtein, D. Predicting micellar solution properties of binary surfactant mixtures. *Langmuir* **1998**, *14*, (7), 1618-1636.
36. Nehm, S. J.; Rodriguez-Spong, B.; Rodriguez-Hornedo, N. Phase solubility diagrams of cocrystals are explained by solubility product and solution complexation. *Cryst. Growth Des.* **2006**, *6*, (2), 592-600.
37. Rodriguez-Hornedo, N.; Nehru, S. J.; Seefeldt, K. F.; Pagan-Torres, Y.; Falkiewicz, C. J. Reaction crystallization of pharmaceutical molecular complexes. *Mol. Pharm.* **2006**, *3*, (3), 362-367.
38. Rodriguez-Hornedo, N., Nehm, Sarah J, and Jayasankar, Adivaraha, Cocrystals: Design, Properties, and Formation Mechanisms. In *Encyclopedia of Pharmaceutical Technology*, 3rd ed.; Francis and Taylor: London, United Kingdom, 2007; pp 615-635.

39. Jayasankar, A.; Reddy, L. S.; Bethune, S. J.; Rodriguez-Hornedo, N. Role of Cocrystal and Solution Chemistry on the Formation and Stability of Cocrystals with Different Stoichiometry. *Cryst. Growth Des.* **2009**, *9*, (2), 889-897.
40. Yalkowsky, S. H., *Solubility and Solubilization in Aqueous Media*. Oxford University Press: New York, New York, 1999.
41. Childs, S. L.; Stahly, G. P.; Park, A. The salt-cocrystal continuum: The influence of crystal structure on ionization state. *Mol. Pharm.* **2007**, *4*, (3), 323-338.
42. Aakeroy, C. B.; Salmon, D. J. Building co-crystals with molecular sense and supramolecular sensibility. *Crystengcomm* **2005**, *7*, 439-448.
43. Childs, S. L.; Hardcastle, K. I. Cocrystals of piroxicam with carboxylic acids. *Cryst. Growth Des.* **2007**, *7*, (7), 1291-1304.
44. Desiraju, G. R. Supramolecular Synthons in Crystal Engineering - a New Organic-Synthesis. *Angew. Chem.-Int. Edit. Engl.* **1995**, *34*, (21), 2311-2327.
45. Etter, M. C. Hydrogen-Bonds as Design Elements in Organic-Chemistry. *J. Phys. Chem.* **1991**, *95*, (12), 4601-4610.
46. Friscic, T.; Trask, A. V.; Jones, W.; Motherwell, W. D. S. Screening for inclusion compounds and systematic construction of three-component solids by liquid-assisted grinding. *Angew. Chem.-Int. Edit.* **2006**, *45*, (45), 7546-7550.
47. Stahl, P. H., and Nakano Masahiro, Pharmaceutical Aspects of the Drug Salt Form. In *Handbook of Pharmaceutical Salts: Properties, Selection, and Use*, P Heinrich Stahl, C. G. W., Ed. Verlag Helvetica Chimica Acta: Zurich, Switzerland, 2002; pp 83-100.
48. Good, D. J.; Rodriguez-Hornedo, N. Cocrystal Eutectic Constants and Prediction of Solubility Behavior. *Cryst. Growth Des.* **2010**, *10*, (3), 1028-1032.
49. Wang, Y. L.; LoBrutto, R.; Wenslow, R. W.; Santos, I. Eutectic composition of a chiral mixture containing a racemic compound. *Org. Process Res. Dev.* **2005**, *9*, (5), 670-676.
50. Klussmann, M.; White, A. J. R.; Armstrong, A.; Blackmond, D. G. Rationalization and prediction of solution enantiomeric excess in ternary phase systems. *Angew. Chem.-Int. Edit.* **2006**, *45*, (47), 7985-7989.
51. Horter, D.; Dressman, J. B. Influence of physicochemical properties on dissolution of drugs in the gastrointestinal tract. *Adv. Drug Deliv. Rev.* **2001**, *46*, (1-3), 75-87.
52. Naylor, L. J.; Bakatselou, V.; Dressman, J. B. Comparison of the Mechanism of Dissolution of Hydrocortisone in Simple and Mixed Micelle Systems. *Pharm. Res.* **1993**, *10*, (6), 865-870.
53. Schwebel, H. J.; van Hoogevest, P.; Leigh, M. L. S.; Kuentz, M. The apparent solubilizing capacity of simulated intestinal fluids for poorly water-soluble drugs. *Pharm. Dev. Technol.* **16**, (3), 278-286.
54. Jantratid, E.; Janssen, N.; Reppas, C.; Dressman, J. B. Dissolution media simulating conditions in the proximal human gastrointestinal tract: An update. *Pharm. Res.* **2008**, *25*, (7), 1663-1676.
55. Mithani, S. D.; Bakatselou, V.; TenHoor, C. N.; Dressman, J. B. Estimation of the increase in solubility of drugs as a function of bile salt concentration. *Pharm. Res.* **1996**, *13*, (1), 163-167.
56. Kostewicz, E. S.; Brauns, U.; Becker, R.; Dressman, J. B. Forecasting the oral absorption behavior of poorly soluble weak bases using solubility and dissolution studies in biorelevant media. *Pharm. Res.* **2002**, *19*, (3), 345-349.

57. Ottaviani, G.; Gosling, D. J.; Patissier, C.; Rodde, S.; Zhou, L. P.; Faller, B. What is modulating solubility in simulated intestinal fluids? *Eur. J. Pharm. Sci.* **41**, (3-4), 452-457.
58. Shah, V. P.; Konecny, J. J.; Everett, R. L.; McCullough, B.; Noorizadeh, A. C.; Skelly, J. P. In vitro Dissolution Profile of Water-Insoluble Drug-Dosage Forms in the Presence of Surfactants. *Pharm. Res.* **1989**, *6*, (7), 612-618.
59. Tian, F.; Zeitler, J. A.; Strachan, C. J.; Saville, D. J.; Gordon, K. C.; Rades, T. Characterizing the conversion kinetics of carbamazepine polymorphs to the dihydrate in aqueous suspension using Raman spectroscopy. *J. Pharm. Biomed. Anal.* **2006**, *40*, (2), 271-280.
60. Ninomiya, R.; Matsuoka, K.; Moroi, Y. Micelle formation of sodium chenodeoxycholate and solubilization into the micelles: comparison with other unconjugated bile salts. *Biochim. Biophys. Acta Mol. Cell Biol. Lipids* **2003**, *1634*, (3), 116-125.
61. Carey, M. C.; Small, D. M. Micelle Formation by Bile-Salts - Physical-Chemical and Thermodynamic Considerations. *Arch. Intern. Med.* **1972**, *130*, (4), 506-&.
62. Attwood, D. a. F. A. T., *Surfactant Systems: Their chemistry, pharmacy, and biology*. Chapman and Hall Ltd: London, Great Britain, 1983.
63. Samaha, M. W.; Cadalla, M. A. F. Solubilization of Carbamazepin by Different Classes of Nonionic Surfactants and a Bile-Salt. *Drug Dev. Ind. Pharm.* **1987**, *13*, (1), 93-112.
64. Strickley, R. G. Solubilizing excipients in oral and injectable formulations. *Pharm. Res.* **2004**, *21*, (2), 201-230.
65. Li, P.; Ghosh, A.; Wagner, R. F.; Krill, S.; Joshi, Y. M.; Serajuddin, A. T. M. Effect of combined use of nonionic surfactant on formation of oil-in-water microemulsions. *Int. J. Pharm.* **2005**, *288*, (1), 27-34.
66. Chatterjee, A.; Moulik, S. P.; Sanyal, S. K.; Mishra, B. K.; Puri, P. M. Thermodynamics of micelle formation of ionic surfactants: A critical assessment for sodium dodecyl sulfate, cetyl pyridinium chloride and dioctyl sulfosuccinate (Na salt) by microcalorimetric, conductometric, and tensiometric measurements. *Journal of Physical Chemistry B* **2001**, *105*, (51), 12823-12831.
67. Williams, R. J.; Phillips, J. N.; Mysels, K. J. The Critical Micelle Concentration of Sodium Lauryl Sulphate at 25-Degrees-C. *Transactions of the Faraday Society* **1955**, *51*, (5), 728-737.
68. Valizadeh, H.; Nokhodchi, A.; Qarakhani, N.; Zakeri-Milani, P.; Azarmi, S.; Hassanzadeh, D.; Lobenberg, R. Physicochemical characterization of solid dispersions of indomethacin with PEG 6000, Myrj 52, lactose, sorbitol, dextrin, and Eudragit (R) E100. *Drug Dev. Ind. Pharm.* **2004**, *30*, (3), 303-317.
69. Attwood, D.; Ktistis, G.; McCormick, Y.; Story, M. J. Solubilization of Indomethacin by Polysorbate-80 in Mixed Water-Sorbitol Solvents. *J. Pharm. Pharmacol.* **1989**, *41*, (2), 83-86.
70. Najib, N. M.; Suleiman, M. S. The Effect of Hydrophilic Polymers and Surface-Active Agents on the Solubility of Indomethacin. *Int. J. Pharm.* **1985**, *24*, (2-3), 165-171.
71. Javadzadeh, Y.; Jafari-Navimipour, B.; Nokhodchi, A. Liquefied technique for dissolution rate enhancement of a high dose water-insoluble drug (carbamazepine). *Int. J. Pharm.* **2007**, *341*, (1-2), 26-34.
72. Fontan, J. E.; Arnaud, P.; Chaumeil, J. C. Enhancing Properties of Surfactants on the Release of Carbamazepine from Suppositories. *Int. J. Pharm.* **1991**, *73*, (1), 17-21.
73. Valizadeh, H.; Zakeri-Milani, P.; Barzegar-Jalali, M.; Mohammadi, G.; Danesh-Bahreini, M. A.; Adibkia, K.; Nokhodchi, A. Preparation and characterization of solid dispersions of piroxicam with hydrophilic carriers. *Drug Dev. Ind. Pharm.* **2007**, *33*, (1), 45-56.

74. Nokhodchi, A.; Javadzadeh, Y.; Siah-Shadbad, M. R.; Barzegar-Jalali, M. The effect of type and concentration of vehicles on the dissolution rate of a poorly soluble drug (indomethacin) from liquisolid compacts. *J. Pharm. Pharm. Sci.* **2005**, *8*, (1), 18-25.
75. Acuna, J. A.; Delafuente, C.; Vazquez, M. D.; Tascon, M. L.; Sanchezbatanero, P. Voltammetric Determination of Piroxicam in Micellar Media by Using Conventional and Surfactant Chemically-Modified Carbon-Paste Electrodes. *Talanta* **1993**, *40*, (11), 1637-1642.
76. Roy, L., Rodriguez-Hornedo, Nair. Rational surfactant selection to modulate cocrystal solubility and stability, *manuscript in preparation*. **2011**.
77. Alvarez-Nunez, F. A.; Yalkowsky, S. H. Relationship between Polysorbate 80 solubilization descriptors and octanol-water partition coefficients of drugs. *Int. J. Pharm.* **2000**, *200*, (2), 217-222.
78. Fagerberg, J. H.; Tsinman, O.; Sun, N.; Tsinman, K.; Avdeef, A.; Bergstrom, C. A. S. Dissolution Rate and Apparent Solubility of Poorly Soluble Drugs in Biorelevant Dissolution Media. *Mol. Pharm.* **2010**, *7*, (5), 1419-1430.
79. Hamid, I. A.; Parrott, E. L. Effect of Temperature on Solubilization and Hydrolytic Degradation of Solubilized Benzocaine and Homatropine. *J. Pharm. Sci.* **1971**, *60*, (6), 901-&.
80. Kadam, Y.; Yerramilli, U.; Bahadur, A. Solubilization of poorly water-soluble drug carbamezapine in Pluronic (R) micelles: Effect of molecular characteristics, temperature and added salt on the solubilizing capacity. *Colloid Surf. B-Biointerfaces* **2009**, *72*, (1), 141-147.
81. Nishikido, N., Solubilization in Mixed Micelles. In *Solubilization in Surfactant Aggregates*, Sherril D Christian, J. F. S., Ed. Marcel Dekker Inc: New York, New York, 1995; Vol. 55, pp 143-189.
82. Abe, M. a. O., Keizo, *Mixed Surfactant Systems*. Marcel Dekker: New York, New York, 1992; Vol. 46.
83. Treiner, C. Micellar Solubilization and Related Phenomena in Weakly Interacting Binary Cationic Surfactant Solutions. *Abstr. Pap. Am. Chem. Soc.* **1992**, *204*, 128-COLL.
84. Treiner, C. The Thermodynamics of Micellar Solubilization of Neutral Solutes in Aqueous Binary Surfactant Systems. *Chem. Soc. Rev.* **1994**, *23*, (5), 349-356.
85. Jana, P. K.; Moulik, S. P. Interaction of Bile-Salts with Hexadecyltrimethylammonium Bromide and Sodium Dodecyl-Sulfate. *J. Phys. Chem.* **1991**, *95*, (23), 9525-9532.
86. Clint, J. H. Micellization of Mixed Nonionic Surface-Active Agents. *Journal of the Chemical Society-Faraday Transactions I* **1975**, *71*, (6), 1327-1334.

CHAPTER 2

QUANTITATIVE PREDICTION OF COCRYSTAL SOLUBILIZATION BY BIORELEVANT MEDIA

Equation Chapter (Next) Section 1

Introduction

Pharmaceutical cocrystals have emerged as a useful strategy to improve the aqueous solubility of inherently poorly soluble drugs to improve their oral absorption and bioavailability¹⁻⁶. Cocrystal solubility can be orders of magnitude higher than that of the constituent drug in aqueous solutions. In the presence of a solubilizing agent, however, a cocrystal can display higher, equal, or lower solubility than the constituent drug, depending on the concentration of the additive⁷⁻⁹. The solubility advantage of several carbamazepine cocrystals in buffer was eliminated by the presence of sodium lauryl sulfate (SLS)⁷⁻⁹. SLS concentrations of 0.5% and 1% induced a turning point in the cocrystal solubility enhancement over drug for CBZ-SLC (pH 3.0) and CBZ-SAC (pH 2.2), respectively. These cocrystals were 2.5 and 4.5 times more soluble than the stable form of carbamazepine (dihydrate) under the aqueous conditions studied and low levels of surfactants reduced the cocrystal solubility enhancement to zero ($S_{\text{cocrystal}} = S_{\text{drug}}$) and/or to negative values ($S_{\text{cocrystal}} < S_{\text{drug}}$)^{7,8}.

The underlying mechanism for this behavior is the preferential solubilization of the drug constituent over the coformer⁷⁻⁹. Generally, coformers are much more hydrophilic than the constituent drugs and therefore preferential drug solubilization is often observed with solubilizing agents in aqueous media⁷⁻¹¹. This behavior leads to a nonlinear dependence of

cocrystal solubilization on solubilizing agent concentration. The characteristic behavior for 1:1 cocrystal and its constituent drug is illustrated in Figure 2.1.

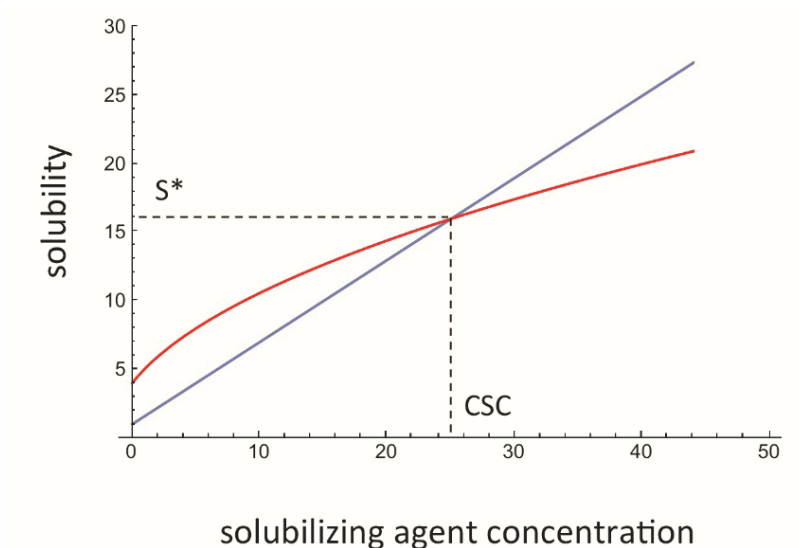


Figure 2.1. Transition point (S^* and CSC) for a 1:1 cocrystal (—) and its constituent drug (—) in the presence of a solubilizing agent. The curves represent the theoretical cocrystal and drug solubility dependence on solubilizing agent concentration⁷. $S^* = (S_{\text{cocrystal,aq}})^2 / (S_{\text{drug,aq}})$.

Cocrystals have a square-root dependence on solubilizing agent concentration, whereas the drug has a linear dependence. The cocrystal solubility can therefore reach a point at which it is equal to the drug solubility, and above which the cocrystal solubility is lower than the drug solubility. The cocrystal transition point is described by a solubilizing agent concentration (CSC, or critical stabilization concentration) and a solubility at which both drug and cocrystal are in equilibrium (S^*)¹². Not knowing such behavior will lead to variability in cocrystal performance and associated risks for cocrystal selection and formulation.

Cocrystal solubility is therefore more than just "one number" that describes how soluble the cocrystal is compared to the constituent drug. There is a multi-dimensional set of variables and solution conditions that all work in concert to change/tune cocrystal solubility and thus its performance. Solubilizing agents and pH, for instance, can impart order of magnitude changes

to cocrystal solubility and its relationship to parent drug solubility. The central hypothesis of the research presented here is that physiological surfactants such as those encountered in intestinal fluids will solubilize cocrystals to a lesser extent than drugs when the drug (not the coformer) is preferentially solubilized in biorelevant media. This has huge implications as cocrystals may mitigate food effects and could in concert with formulation additives become less soluble than the drug.

Mechanism-based models that describe cocrystal solubility dependence on solubilizing agent have been established in the literature, but only confirmed for cocrystals of carbamazepine and indomethacin in synthetic surfactants⁷⁻¹¹. These models consider cocrystal dissociation, cocrystal constituent ionization, and constituent solubilization by solubilizing agents. Physiologically relevant surfactants composed of bile salts and phospholipids have been shown to greatly influence the solubility and bioavailability of poorly soluble drugs¹³⁻¹⁷. Administration of danazol with a lipid-rich meal results in a four-fold increase in absolute bioavailability due to increased solubilization and absorption in the presence of high concentrations of bile salts^{18, 19}. The effect of physiologically relevant surfactants on the solubility of cocrystals of poorly soluble drugs remains to be established. While there are examples of cocrystal solubility and dissolution studies in biorelevant media containing physiologically relevant surfactants to simulate *in vivo* conditions^{5, 20}, relationships between observed results and solution phase interactions of cocrystal constituents have not been published.

The complexity of cocrystal interactions with solubilizing agents has been documented in the literature. For the case of a sorbic acid cocrystal of the weakly basic drug AMG 517, the cocrystal was discovered when it precipitated in a suspending vehicle which contained a relatively high concentration (10% w/v) of Pluronic F108, a nonionic surfactant⁵. However, a

dissolution study in fasted simulated intestinal fluid (FaSSIF) containing physiologically relevant mixed micelles of sodium taurocholate and lecithin showed that the cocrystal achieved 10-fold higher drug concentrations after 1 hour relative to the crystalline drug⁵. The authors noted the contradictory nature of observing lower cocrystal solubility relative to the drug leading to its precipitation in the Pluronic F108 surfactant, but observing improved solubility and dissolution characteristics relative to the drug in FaSSIF. An understanding of the specific interactions of cocrystals with physiologically relevant surfactants would allow for the prediction of cocrystal solubility in the presence of these surfactants and aid *in-vitro* evaluation and formulation.

The aim of this work is to understand the mechanisms of cocrystal solubilization in biorelevant media and derive models to predict this behavior. The solubilities of seven cocrystals comprised of hydrophobic drugs, several of which are reported to exhibit food effects^{18, 19, 21} were measured in fed state simulated intestinal fluid (FeSSIF) and pH 5 acetate buffer. FeSSIF was chosen due to its relatively high concentration of sodium taurocholate (NaTC) and the phospholipid lecithin which are known to form mixed micelles in solution and significantly solubilize poorly soluble drugs¹⁷. The cocrystals studied include: 1:1 carbamazepine-saccharin (CBZ-SAC), 1:1 carbamazepine-salicylic acid (CBZ-SLC), 2:1 carbamazepine 4-aminobenzoic acid hydrate, (CBZ-4ABA-HYD), 1:1 piroxicam-saccharin (PXC-SAC), 1:1 indomethacin-saccharin (IND-SAC), 1:1 danazol-hydroxybenzoic acid (DNZ-HBA), and 1:1 danazol-vanillin (DNZ-VAN). The work with the CBZ and IND cocrystals has been previously published¹⁰. The selected cocrystals include both 1:1 and 2:1 cocrystal stoichiometries and cover a range of ionization behaviors for both drug and cofomers. PXC is a zwitterionic drug with pK_a values of 1.86 and 5.46²², and IND is a monoprotic weakly acidic drug with a pK_a of 4.2²³. SAC is a monoprotic weak acid with pK_a values reported between 1.6-

2.2^{24, 25}, SLC is a monoprotic weak acid with a reported pK_a value of 3.0²⁴, 4ABA is amphoteric with pK_a values 2.6 and 4.8²⁶, HBA is a monoprotic weak acid with a reported pK_a value of 4.48²⁷ and VAN is a monoprotic weak acid with a pK_a of 7.4²⁸.

Theoretical

Estimation of cocrystal solubilization ratio from drug solubilization ratio

The relationship between cocrystal and drug solubilization ratios ($SR_{\text{cocrystal}}$) and (SR_{drug}) has been previously described^{7, 29}. $SR_{\text{cocrystal}}$ in a drug solubilizing agent such as a surfactant, complexing agent, or lipid can be estimated once SR_{drug} is known under the same conditions (solubilizing agent concentration, pH, and temperature). The general form of the equation for a cocrystal with stoichiometry A_xB_y , where A and B are the cocrystal constituents, drug and cofomer respectively; and x and y are the stoichiometric coefficients or molar ratios, is⁷

$$SR_{\text{cocrystal}} = \left(SR_{\text{drug}} \right)^{\frac{x}{x+y}} \quad (2.1)$$

where

$$SR = \left(\frac{S_T}{S_{\text{aq}}} \right) \quad (2.2)$$

for either cocrystal or drug. S_T is defined as the sum of the concentrations of all species dissolved ($S_T = S_{\text{aq}} + S_s$). S_{aq} represents the cocrystal aqueous solubility at a particular pH in the absence of solubilizing agent ($S_{\text{aq}} = S_{\text{nonionized, aq}} + S_{\text{ionized, aq}}$) and is the sum of the nonionized and ionized contributions to the aqueous solubility. S_s represents the cocrystal solubilized by solubilizing agents ($S_s = S_{\text{nonionized, s}} + S_{\text{ionized, s}}$) and contributions from the ionized species as appropriate.

Equation (2.1) allows for the facile estimation of $SR_{\text{cocrystal}}$ in a particular solubilizing agent at a specific pH for a cocrystal of a given drug. From the general form of the relationship

between SR_{cocystal} and SR_{drug} in equation (2.1), the following equations can be derived for cocystals of 1:1 and 2:1 stoichiometry (systems studied in this work):

For a 1:1 cocystal:

$$SR_{\text{cocystal}} = \sqrt{SR_{\text{drug}}} \quad (2.3)$$

For 2:1 cocystal:

$$SR_{\text{cocystal}} = SR_{\text{drug}}^{\frac{2}{3}} \quad (2.4)$$

These equations assume that cofomer solubilization by solubilizing agents is negligible, and that drug solubilization is not affected by the presence of cofomer. The assumption that cofomer solubilization is negligible is often justified as cocystals are generally composed of poorly water-soluble, hydrophobic drugs and soluble, hydrophilic cofomers. Cofomers, therefore, interact to a far lesser extent with solubilizing agents than the drug constituents.

The above relationships are derived from the full solubility equations for drug and cocystal in solubilizing agents assuming that $K_s^{\text{coformer}} = 0$ and that the pH of the solubilizing agent and buffer for both cocystal and drug are equal¹². For the first case considered here, of a 1:1 cocystal of a nonionizable drug and an ionizable (monoprotic) acidic cofomer, the cocystal solubility in a solubilizing agent is

$$S_{\text{cocystal,T}} = \sqrt{K_{\text{sp}} \left(1 + K_s^{\text{drug}} [M]\right) \left(1 + 10^{\text{pH} - \text{pKa,coformer}} + K_s^{\text{coformer}} [M]\right)} \quad (2.5)$$

K_{sp} is the cocystal solubility product, K_s stands for solubilization constants of cocystal constituents, and $[M]$ is solubilizing agent concentration. For the case of a micellar surfactant, $[M]$ is the total surfactant concentration minus the critical micellar concentration (CMC). K_a

represents the dissociation constant of a monoprotic acidic coformer. When the solubilizing agent enhances drug solubility and not coformer solubility, ($K_s^{\text{coformer}} = 0$), the cocrystal total solubility equation becomes

$$S_{\text{cocrystal,T}} = \sqrt{K_{\text{sp}} (1 + K_s^{\text{drug}} [M]) (1 + 10^{\text{pH} - \text{pKa,coformer}})} \quad (2.6)$$

The above equation can also be expressed in terms of cocrystal and drug aqueous solubilities, and drug total solubility, $S_{\text{drug,T}}$ by considering that

$$S_{\text{cocrystal,aq}} = \sqrt{K_{\text{sp}} (1 + 10^{\text{pH} - \text{pKa,coformer}})} \quad (2.7)$$

and that

$$\left(\frac{S_{\text{T}}}{S_{\text{aq}}}_{\text{drug}} \right) = (1 + K_s^{\text{drug}} [M]) \quad (2.8)$$

to yield the relationship between cocrystal solubilization ratio and drug solubilization ratio presented in equation (2.3). Equation (2.4) for 2:1 cocrystals is similarly derived⁷ from the equation that describes cocrystal total solubility.

Cocrystal and drug solubilities have different dependence on solubilizing agent concentration: (1:1) cocrystals have a *square-root* dependence whereas drugs have a *linear* dependence on solubilizing agent concentration. Cocrystal solubility measurements will not be the same in buffer alone and in the presence of drug solubilizing agents. As indicated by the equations above, drug solubilizing agents will increase cocrystal solubility and solubilization ratio to a lesser extent than the drug.

Figure 2.2 illustrates the influence of a drug solubilizing agent on the solubility and solubilization of a hypothetical drug and 3 different (1:1) cocrystals of the drug. All cocrystals are shown to be more soluble than the drug in aqueous media ($S_{\text{cocrystal, aq}}$ are 2, 3, and 4-fold times higher than $S_{\text{drug, aq}}$), but this is not the case in the presence of a drug solubilizing agent. The solubilizing agent increases the drug solubility by a factor of 9 ($SR_{\text{drug}} = 9$) and the cocrystal solubility by a factor of 3. According to equation (3), $SR_{\text{cocrystal}} = \sqrt{SR_{\text{drug}}}$ thus $SR_{\text{cocrystal}} = \sqrt{9} = 3$. Under the assumptions to derive the simple square root relationship, the cocrystal solubilization ratio is only dependent on drug solubilization ratio.

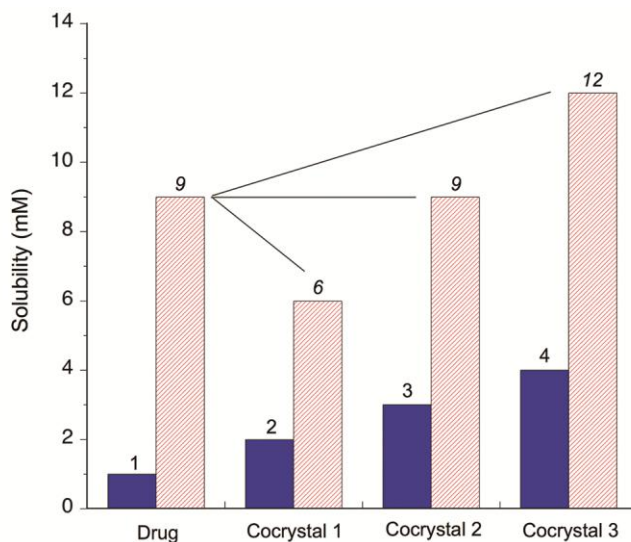


Figure 2.2. Solubility values for a drug and three 1:1 cocrystals of that drug in aqueous buffer (■) and in the presence of a solubilizing agent (▨). Cocrystal solubility enhancement over drug in aqueous buffer is not maintained in the presence of solubilizing agent. All cocrystals are more soluble than the drug in buffer, but not in the solubilizing agent.

Another important observation from Figure 2.2 is that not all cocrystals exhibit enhanced solubility over the drug in the presence of the drug solubilizing agent: $S_{\text{cocrystal1, T}} < S_{\text{drug, T}}$, $S_{\text{cocrystal2, T}} = S_{\text{drug, T}}$, and $S_{\text{cocrystal3, T}} > S_{\text{drug, T}}$. Preferential drug solubilization in the presence of a drug solubilizing agent can lead to a cocrystal transition point at which $S_{\text{cocrystal, T}} = S_{\text{drug, T}}$. Above

the transition point in the presence of a solubilizing agent, a cocrystal that is more soluble than the drug in aqueous buffer becomes less soluble. Thus, cocrystal 2 is at the transition point, whereas cocrystals 1 and 3 are above and below the transition point, respectively. We have investigated the nature of cocrystal transition points for a series of drugs and cocrystals in the presence of synthetic surfactants and lipids⁷⁻¹². Excellent correlations were observed between the drug solubilization provided by the solubilizing agents and the transition points. Large decreases in both cocrystal solubility enhancement compared to drug solubility ($S_{\text{cocrystal}}$ compared to S_{drug}) and $SR_{\text{cocrystal}}$ compared to SR_{drug} were associated with increased drug solubilization by the additives.

SR_{drug} can reach values in the order of 100 to 1000 in physiologically relevant surfactants and one would expect cocrystals of these drugs to have solubilization ratios that are at least an order of magnitude lower than the drug ($\sqrt{100}$ and $\sqrt{1000}$). These predictions will be compared with experimental observations for several cocrystals in physiologically relevant surfactants in the results section.

Cocrystal solubility in the presence of physiologically relevant surfactants

In addition to estimating $SR_{\text{cocrystal}}$ from SR_{drug} , cocrystal total solubility in physiologically relevant surfactants can be derived from cocrystal constituent dissociation, ionization, and micellar solubilization^{7-11, 30-33}. Cocrystal solubility in synthetic surfactants has been thoroughly described in the literature for cocrystals of nonionizing drugs⁷⁻⁹. Here, we similarly derive expressions for cocrystal solubility in physiologically relevant surfactants for cocrystals of ionizable drugs and cofomers.

For cocrystal RHA of nonionizable drug (R) and a monoprotic weakly acidic cofomer (HA), the relevant solution equilibria are:



and the associated equilibrium constants are given by

$$K_{\text{sp}} = [\text{R}]_{\text{aq}} [\text{HA}]_{\text{aq}} \quad (2.14)$$

the cocrystal solubility product K_{sp} ,

$$K_{\text{a}} = \frac{[\text{A}^{-}]_{\text{aq}} [\text{H}^{+}]_{\text{aq}}}{[\text{HA}]_{\text{aq}}} \quad (2.15)$$

the ionization constant K_{a} for the monoprotic weakly acidic cofomer HA,

$$K_{\text{s}}^{\text{R}} = \frac{[\text{R}]_{\text{m}}}{[\text{R}]_{\text{aq}} [\text{M}]} \quad (2.16)$$

the micellar solubilization constant K_{s}^{R} for nonionizable drug R, and the micellar solubilization constants K_{s}^{HA} , and K_{s}^{A} for weakly acidic cofomer HA

$$K_s^{HA} = \frac{[HA]_m}{[HA]_{aq}[M]} \quad (2.17)$$

$$K_s^{A^-} = \frac{[A^-]_m}{[A^-]_{aq}[M]} \quad (2.18)$$

where the subscripts aq and m refer to aqueous and micellar pseudophases, respectively. M is the micellar surfactant concentration, or the total surfactant minus the CMC. Activities are replaced by concentrations assuming dilute solution conditions.

The total stoichiometric solubility of RHA, $S_{RHA,T}$, is equal to the total concentration of each cocystal constituent in equilibrium with solution $S_{RHA,T} = [R]_T = [A]_T$ for this 1:1 cocystal. An expression for $S_{RHA,T}$ in terms of experimentally accessible equilibrium constants and solution properties is derived by considering the mass balances of R and A:

$$[R]_T = [R]_{aq} + [R]_m \quad (2.19)$$

$$[A]_T = [HA]_{aq} + [HA]_m + [A^-]_{aq} + [A^-]_m \quad (2.20)$$

and by substituting the equilibrium constants above to yield

$$S_{RHA,T} = \sqrt{K_{sp} \left(1 + K_s^R [M]\right) \left(1 + 10^{\text{pH} - \text{pKa,coformer}} + K_s^{HA} [M] + 10^{\text{pH} - \text{pKa,coformer}} K_s^{A^-} [M]\right)} \quad (2.21)$$

Biorelevant media containing physiologically relevant surfactants are often defined by a particular [M] and pH. While the solubilization constant of the nonionized (K_s^{HA}) and ionized ($K_s^{A^-}$) coformer can be determined experimentally at multiple pH values³⁴, to quantify solubilization at a single pH, total solubilization constants (K_s^T) can be calculated. To simplify

equation (2.21), total solubilization constants in specified pH conditions (K_s^T) can be substituted to yield

$$S_{\text{cocystal}} = \sqrt{K_{\text{sp}} \left(1 + K_s^{R,T} [M]\right) \left(1 + 10^{\text{pH} - \text{p}K_{\text{a,coformer}}} + K_s^{\text{HA},T} [M]\right)} \quad (2.22)$$

For nonionizable drug R, $K_s^{R,T}$ is simply the solubilization constant for the nonionized constituent (K_s^R). For ionizable constituents, the total solubilization constant takes into account the equilibrium solubilization constants in a given media for both the ionized and unionized species. For example, for weakly acidic component HA, the total solubility in a surfactant as a function of intrinsic aqueous solubility S_{aq} , ionization constant K_a , and micellar solubilization is given by:

$$S_T^{\text{HA}} = S_{\text{aq}}^{\text{HA}} \left(1 + 10^{\text{pH} - \text{p}K_{\text{a,acid}}} + \underbrace{\left(K_s^{\text{HA}} + 10^{\text{pH} - \text{p}K_{\text{a,acid}}} K_s^{\text{A}^-}\right)}_{K_s^{\text{A},T}} [M]\right) \quad (2.23)$$

where the solubilization constants of the ionized and nonionized constituents are represented by the term $K_s^{\text{A},T}$. In this work, K_s^T values were calculated from solubility measurements in biorelevant media as explained in the Methods section.

Materials and Methods

Materials

Cocrystal constituents

Anhydrous carbamazepine form III (CBZ), anhydrous indomethacin form γ (IND) were purchased from Sigma Chemical Company (St. Louis, MO) and used as received. Anhydrous piroxicam form I was received as a gift from Pfizer (Groton, CT) and used as received.

Anhydrous danazol was received as a gift from Renovo Research (Atlanta, GA) and used as received.

Anhydrous saccharin (SAC), 4-aminobenzoic acid (4ABA), and salicylic acid (SLC), were purchased from Sigma Chemical Company (St. Louis, MO) and used as received.

Anhydrous hydroxybenzoic acid was purchased from Acros Organics (Pittsburgh, PA) and used as received. Anhydrous vanillin was purchased from Fisher Scientific (Fair Lawn, NJ) and used as received. Carbamazepine dihydrate (CBZ (H)), piroxicam monohydrate (PXC (H)), and hydroxybenzoic acid monohydrate (HBA (H)) were prepared by slurring CBZ, PXC, and HBA in deionized water for at least 24 hours. All crystalline drugs and cofomers were characterized by X-ray power diffraction (XRPD) and differential scanning calorimetry (DSC) before carrying out experiments.

Solvents and buffer components

Ethyl acetate and ethanol were purchased from Acros Organics (Pittsburgh, PA) and used as received, and HPLC grade methanol and acetonitrile were purchased from Fisher Scientific (Pittsburgh, PA). Trifluoroacetic acid spectrophometric grade 99% was purchased from Aldrich Company (Milwaukee, WI) and phosphoric acid ACS reagent 85% was purchased from Sigma Chemical Company (St. Louis, MO). Water used in this study was filtered through a double deionized purification system (Milli Q Plus Water System) from Millipore Co. (Bedford, MA).

FeSSIF and acetate buffer were prepared using sodium taurocholate (NaTC) purchased from Sigma Chemical Company (St. Louis, MO), lecithin purchased from Fisher Scientific (Pittsburgh, PA), sodium hydroxide pellets (NaOH) purchased from J.T. Baker (Philipsburg, NJ), and acetic acid and potassium chloride (KCl) purchased from Acros Organics (Pittsburgh, PA).

Methods

FeSSIF and acetate buffer preparation

FeSSIF and acetate buffer were prepared according to the protocol of Galia and coworkers³⁵. Acetate buffer was prepared as a stock solution at room temperature by dissolving 8.08 g NaOH (pellets), 17.3 g glacial acetic acid and 23.748 g NaCl in 2 L of purified water. The pH was adjusted to 5.00 with 1 N NaOH and 1N HCl. FeSSIF was prepared by dissolving 0.41 g sodium taurocholate in 12.5 mL of pH 5.00 acetate buffer. 0.148 g lecithin was added with magnetic stirring at 37 °C until dissolved. The volume was adjusted to exactly 50 mL with acetate buffer.

Cocrystal synthesis

Cocrystals were prepared by the reaction crystallization method³⁶ at 25°C. The 1:1 indomethacin-saccharin cocrystal (IND-SAC) was synthesized by adding stoichiometric amounts of cocrystal constituents (IND and SAC) to nearly saturated SAC solution in ethyl acetate. The 1:1 carbamazepine saccharin cocrystal (CBZ-SAC) was prepared by adding stoichiometric amounts of cocrystal constituents (CBZ and SAC) to nearly saturated SAC solution in ethanol. The 1:1 carbamazepine-salicylic acid cocrystal (CBZ-SLC) was prepared by adding stoichiometric amounts of cocrystal constituents (CBZ and SLC) to nearly saturated SLC solution in acetonitrile. The 2:1 carbamazepine-4-aminobenzoic acid monohydrate cocrystal (CBZ-4ABA (H)) was prepared by suspending stoichiometric amounts of cocrystal constituents (CBZ and 4ABA) in a 0.01M 4ABA aqueous solution at pH 3.9. The 1:1 piroxicam-saccharin cocrystal (PXC-SAC) was prepared by adding stoichiometric amounts of cocrystal constituents (PXC and SAC) to nearly saturated SAC in acetonitrile. The 1:1 danazol-hydroxybenzoic acid cocrystal (DNZ-HBA) was prepared by adding stoichiometric amounts of cocrystal constituents

(DNZ and HBA) to nearly saturated HBA solution in ethyl acetate. The 1:1 danazol-vanillin cocrystal (DNZ-VAN) was prepared by adding stoichiometric amounts of cocrystal constituents (DNZ and VAN) to nearly saturated VAN solution in ethyl acetate. Prior to carrying out any solubility experiments, solid phases were characterized by XRPD and DSC and stoichiometry verified by HPLC. Full conversion to cocrystal was observed in 24 hours.

Solubility measurements of cocrystal constituents

Cocrystal constituent solubilities were measured in FeSSIF and pH 5.00 acetate buffer (FeSSIF without NaTC and lecithin). Solubilities of cocrystal constituents were determined by adding excess solid (drug or coformer) to 3 mL of media (FeSSIF or buffer). Solutions were magnetically stirred and maintained at $25 \pm 0.1^\circ\text{C}$ using a water bath for up to 96 h. At 24 hr intervals, 0.30 mL of samples were collected, pH of solutions measured, and filtered through a $0.45 \mu\text{m}$ pore membrane. After dilution with mobile phase, solution concentrations of drug or coformer were analyzed by HPLC. The equilibrium solid phases were characterized by XRPD and DSC.

Total solubilization constants, K_s^T , were evaluated from solubility measurements of drug and coformer in FeSSIF and buffer. For weakly acidic constituent HA, the total solubility in FeSSIF is given by

$$S_T^{\text{HA}} = S_{\text{aq}}^{\text{HA}} \left(1 + 10^{\text{pH} - \text{pK}_{\text{a,acid}}} + K_s^{\text{A,T}} [\text{M}] \right) \quad (2.24)$$

Solving for $K_s^{\text{A,T}}$:

$$K_s^{\text{A,T}} = \frac{\frac{S_T^{\text{HA}}}{S_{\text{aq}}^{\text{HA}}} - 1 - 10^{\text{pH} - \text{pK}_{\text{a,acid}}}}{[\text{M}]} \quad (2.25)$$

Derivations of equations to calculate K_s^T for other ionizable constituents are included in the Appendix. For an amphoteric component like 4ABA, K_s^T was calculated from

$$K_s^{ABH,T} = \frac{\frac{S_T^{ABH}}{S_{aq}^{ABH}} - 1 - 10^{\text{pH} - \text{pKa}_{1,\text{amphoteric}}} - 10^{\text{pKa}_{2,\text{amphoteric}} - \text{pH}}}{[M]} \quad (2.26)$$

For a zwitterionic component like PXC, K_s^T was obtained from

$$K_s^{ABH^+,T} = \frac{\frac{S_T^{ABH^+}}{S_{aq}^{ABH^+}} - 1 - 10^{\text{pH} - \text{pKa}_{1,\text{zwitterionic}}} - 10^{\text{pKa}_{2,\text{zwitterionic}} - \text{pH}}}{[M]} \quad (2.27)$$

Cocrystal solubility measurements

Cocrystal equilibrium solubilities were measured in FeSSIF and pH 5.00 acetate buffer (FeSSIF without NaTC and lecithin) at the eutectic point, where drug and cocrystal solid phases are in equilibrium with solution^{37, 38}. The eutectic point between cocrystal and drug was approached by cocrystal dissolution (suspending solid cocrystal (~100 mg) and drug (~50 mg) in 3 mL of media (FeSSIF or buffer)) and by cocrystal precipitation (suspending solid cocrystal (~50 mg) and drug (~100 mg) in 3 mL of media (FeSSIF or buffer) nearly saturated with cofomer). Solutions were magnetically stirred and maintained at $25 \pm 0.1^\circ\text{C}$ using a water bath for up to 96 h. At 24 hr intervals, 0.30 mL aliquots of suspension were collected, pH was measured, before filtration through a $0.45 \mu\text{m}$ pore membrane. Solid phases were also collected at 24 hr intervals to ensure the sample was at the eutectic point (confirmed by presence of both drug and cocrystal solid phases and constant [coformer] and [drug] solution concentrations). After dilution of filtered solutions with mobile phase, drug and coformer concentrations were analyzed by HPLC. The equilibrium solid phases were characterized by XRPD and DSC.

The cocrystal stoichiometric solubility was calculated from measured total eutectic concentrations of drug and coformer ($[\text{drug}]_{T,\text{eu}}$ and $[\text{coformer}]_{T,\text{eu}}$) according to the following equations for 1:1 and 2:1 cocrystals³⁷:

$$S_T^{1:1 \text{ cocrystal}} = \sqrt{[\text{drug}]_{T,\text{eu}} [\text{coformer}]_{T,\text{eu}}} \quad (2.28)$$

$$S_T^{2:1 \text{ cocrystal}} = 2 \left(\sqrt[3]{\frac{[\text{drug}]_{T,\text{eu}}^2 [\text{coformer}]_{T,\text{eu}}}{4}} \right) \quad (2.29)$$

This method of calculating the stoichiometric solubility of cocrystals from equilibrium solubility measurements in nonstoichiometric conditions is well established in the literature^{7-10, 37-39}.

X-ray powder diffraction

X-ray powder diffraction diffractograms of solid phases were collected on a benchtop Rigaku Miniflex X-ray diffractometer (Rigaku, Danverse, MA) using Cu K α radiation ($\lambda = 1.54 \text{ \AA}$), a tube voltage of 30 kV, and a tube current of 15 mA. Data were collected from 5 to 40° at a continuous scan rate of 2.5°/min.

Thermal analysis

Solid phases collected during solubility studies were dried at room temperature and analyzed by differential scanning calorimetry (DSC) using a TA instrument (Newark, DE) 2910MDSC system equipped with a refrigerated cooling unit. DSC experiments were performed by heating the samples at a rate of 10 °C/min under a dry nitrogen atmosphere. A high purity indium standard was used for temperature and enthalpy calibration. Standard aluminum sample pans were used for all measurements.

High performance liquid chromatography

Solution concentrations were analyzed by a Waters HPLC (Milford, MA) equipped with an ultraviolet-visible spectrometer detector. For the IND-SAC and CBZ-SAC, CBZ-SLC, CBZ-4ABA-HYD cocrystals and their components, a C18 Thermo Electron Corporation (Quebec, Canada) column (5 μ m, 250 x 4.6 mm) at ambient temperature was used. For the IND-SAC cocrystal, the injection volume was 20 μ l and analysis conducted using an isocratic method with a mobile phase composed of 70% acetonitrile and 30% water with 0.1% trifluoroacetic acid and a flow rate of 1 ml/min. Absorbance of IND and SAC were monitored at 265 nm. For the CBZ cocrystals, the injection volume was 20 μ l and analysis conducted using an isocratic method with a mobile phase composed of 55% methanol and 45% water with 0.1% trifluoroacetic acid and a flow rate of 1 mL/min. Absorbance was monitored as follows:

CBZ and 4ABA at 284 nm, SAC at 265 nm, and SLC at 303 nm. For the PXC-SAC, DNZ-HBA, and DNZ-VAN cocrystals and their components, a C18 Waters Atlantis (Milford, MA) column (5 μ M 250 x 6 mm) at ambient temperature was used. For PXC-SAC, the injection volume was 20 μ L and analysis was conducted using an isocratic method with a mobile phase composed of 70% methanol and 30% water with 0.3% phosphoric acid and a flow rate of 1 mL/min. Absorbance of PXC was monitored at 340 nm and SAC at 240 nm. For the DNZ cocrystals, the injection volume was 20 μ L in FeSSIF experiments, and 100 μ L in buffer experiments due to the extremely low solubility of DNZ in aqueous solutions. Analysis was conducted using an isocratic method composed of 80% methanol and 20% water with 0.1% trifluoroacetic acid and a flow rate of 1 mL/min. Absorbance of DNZ was monitored at 285 nm, HBA at 242 nm, and VAN at 300 nm. For all cocrystals, the Waters' operation software Empower 2 was used to collect and process data.

Results

Cocrystal solubilization in FeSSIF

The influence of FeSSIF on drug and cocrystal solubilization is shown in Figure 2.3. Results indicate that cocrystals and drugs are solubilized to different extents in FeSSIF. Drugs are solubilized to a greater extent than cocrystals, as indicated by SR_{drug} values that are higher than $SR_{\text{cocrystal}}$ as predicted by equations (2.3) and (2.4). Such behavior is due to preferential solubilization of drug over coformer. DNZ was found to be 720 times more soluble in FeSSIF compared to aqueous buffer, whereas its cocrystals, DNZ-HBA and DNZ-VAN, were only 23 and 24 times more soluble in FeSSIF than in buffer. This highlights the order of magnitude reduction in cocrystal solubilization that is possible compared to their highly solubilized constituent drugs. DNZ showed the largest solubilization by FeSSIF and most extreme difference in constituent drug and cocrystal solubilization among the cocrystals studied. IND-SAC also exhibited a large decrease in solubilization compared to IND. IND was 16 times more soluble in FeSSIF compared to buffer while the 1:1 IND-SAC cocrystal was only solubilized 4.5 times.

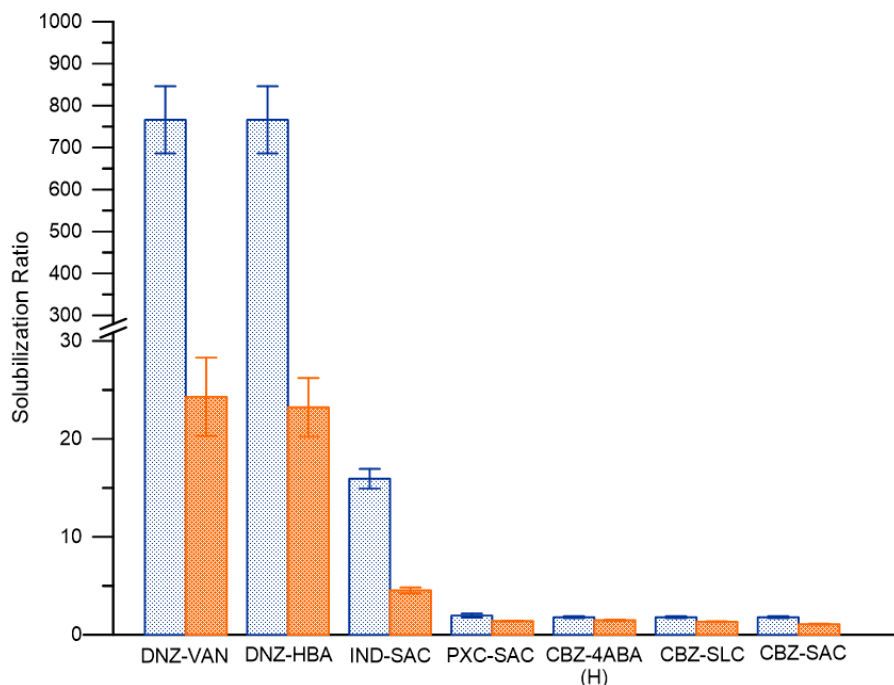


Figure 2.3. Solubilization ratios for cocrystals (■) and constituent drugs (□) in FeSSIF at experimental pH values indicated in Table 2.4 and Table 2.5 at 25°C. Error bars represent standard errors of measurements.

PXC and CBZ exhibit a less pronounced decrease in $SR_{\text{cocrystal}}$ compared to SR_{drug} since these drugs are solubilized to a lower extent in FeSSIF. PXC (H) was moderately solubilized (2.0 times more soluble in FeSSIF compared to buffer), and the 1:1 PXC-SAC cocrystal was only 1.40 times more soluble. CBZ (H) was 1.8 times more soluble in FeSSIF than in buffer, and its cocrystals ranged from 1.03-1.33 times more soluble in FeSSIF for the 1:1 cocrystals CBZ-SAC and CBZ-SLC and 1.49 times more soluble in FeSSIF for the 2:1 cocrystal CBZ-4ABA-HYD.

Cocrystal and drug solubilities measured in FeSSIF and buffer are presented in Figure 2.4 and Figure 2.5 together with the cocrystal and drug solubilization ratios in FeSSIF.

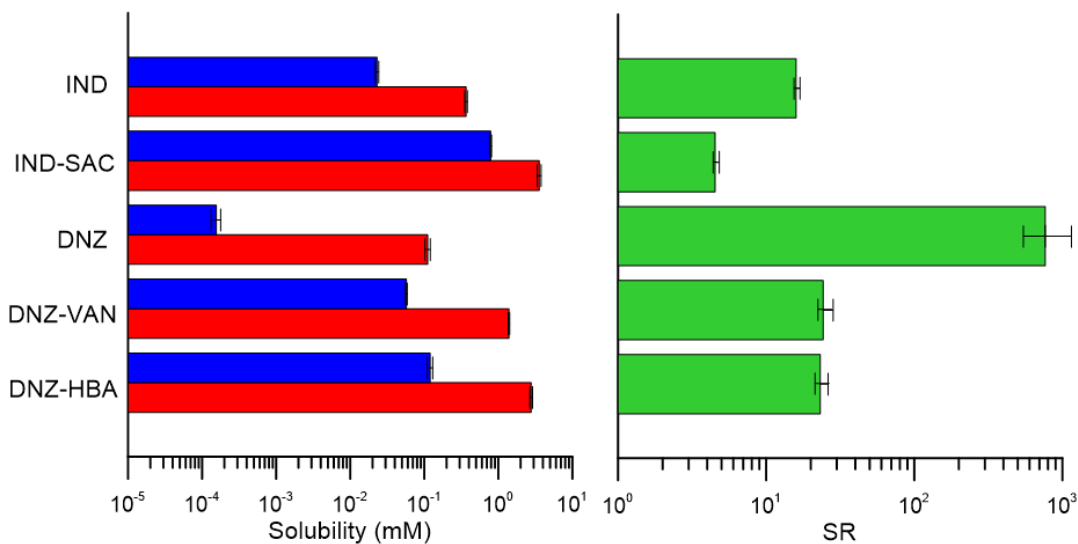


Figure 2.4. Drug and cocrystal solubility measured in FeSSIF (■) and buffer (■) at 25°C for IND, IND-SAC, DNZ, DNZ-VAN, and DNZ-HBA. SR in FeSSIF calculated from solubility values is also shown (■). The initial pH was 5.00 in both buffer and FeSSIF. The final pH of each solubility measurement in FeSSIF and buffer, respectively, are as follows: IND (4.98±0.06 and 4.96±0.03), IND-SAC (3.65±0.05 and 3.66±0.02), DNZ (5.01±0.05 and 4.96±0.01), DNZ-VAN (5.00±0.01 and 4.96±0.01), and DNZ-HBA (4.46±0.06 and 4.47±0.01).

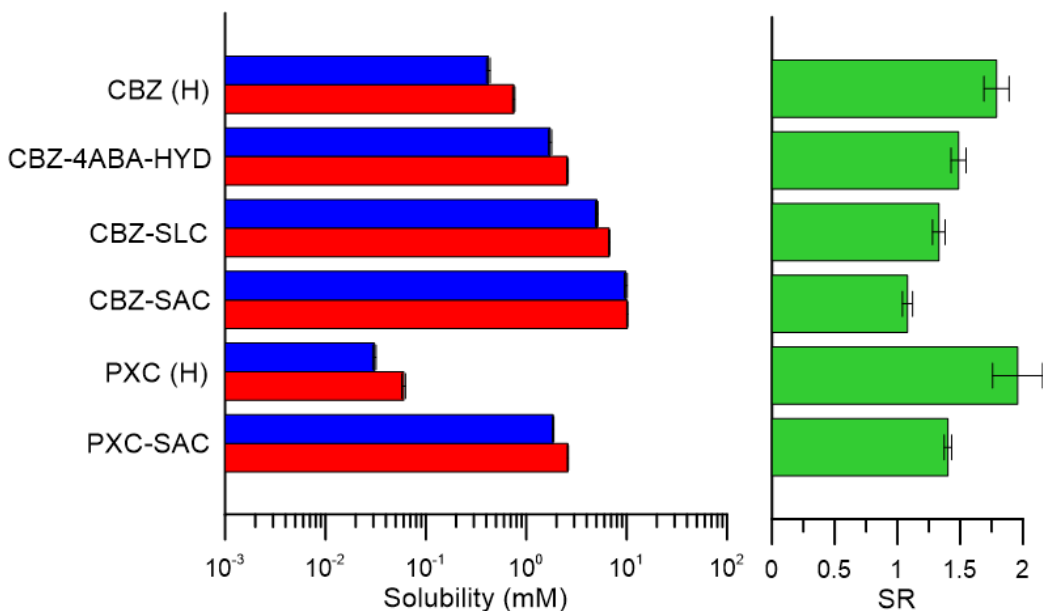


Figure 2.5. Drug and cocrystal solubility measured in FeSSIF (■) and buffer (■) at 25°C for CBZ (H), CBZ-4ABA (H), CBZ-SLC, CBZ-SAC, PXC (H), and PXC-SAC. SR in FeSSIF calculated from solubility values is also shown (■). The final pH of each solubility

measurement in FeSSIF and buffer, respectively, are as follows: CBZ (H) (4.86 ± 0.05 and 4.95 ± 0.01), CBZ-4ABA (H) (4.94 ± 0.02 and 4.84 ± 0.03), CBZ-SLC (4.29 ± 0.02 and 4.37 ± 0.02), CBZ-SAC (3.11 ± 0.02 and 3.08 ± 0.03), PXC (H) (5.03 ± 0.02 and 4.98 ± 0.01), and PXC-SAC (3.79 ± 0.02 and 3.64 ± 0.02).

Results for the more hydrophobic drugs IND and DNZ and their cocrystals (Figure 2.4) indicate that cocrystals are more soluble than drugs in buffer and that this cocrystal solubility enhancement is maintained in FeSSIF but to a lower extent than in buffer. Similar behavior is observed for cocrystals of the less hydrophobic drugs CBZ and PXC (Figure 2.5).

We have recently shown that cocrystal solubility at the transition point (S^*) can be calculated from the aqueous cocrystal and drug solubilities according to $S^* = (S_{\text{cocrystal,aq}})^2 / S_{\text{drug,aq}}$ for a 1:1 cocrystal¹². For the series of cocrystals studied in the present work, S^* values are much higher than the measured cocrystal solubilities in FeSSIF, therefore all cocrystals are below their transition point under the conditions studied. These findings are in agreement with the observed cocrystal solubility enhancement over drug in FeSSIF.

The predicted and measured $SR_{\text{cocrystal}}$ values in FeSSIF are shown in Figure 2.6 and Table 2.1. $SR_{\text{cocrystal}}$ was predicted from measured SR_{drug} values from the simple SR equations (2.3) and (2.4).

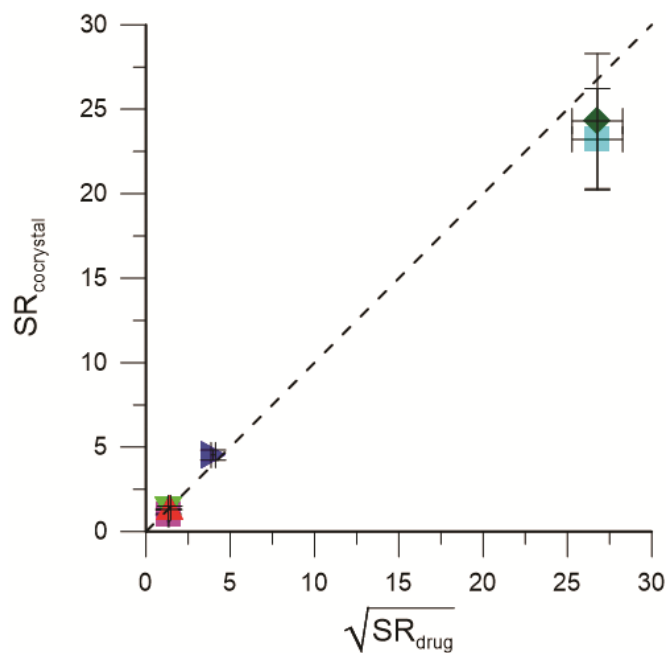


Figure 2.6. $SR_{cocrystal}$ dependence on $\sqrt{SR_{drug}}$ for 1:1 cocrystals in FeSSIF at 25°C. Line represents the theoretical relationship according to equation (2.3). Symbols represent experimentally determined SR values in equilibrium conditions for IND-SAC (▶), CBZ-SAC (■), CBZ-SLC (▼), PXC-SAC (▲), DNZ-HBA (◻), and DNZ-VAN (◆).

Table 2.1. Comparison of experimentally measured and predicted $SR_{\text{cococrystal}}$ values.

Cocrystal	SR_{drug} ,	pH	pH	$SR_{\text{cococrystal}}$,	$SR_{\text{cococrystal}}$	pH	pH
	exp ^a	FeSSIF	buffer	pred ^b	exp ^c	FeSSIF	buffer
CBZ-SAC (1:1)	1.8 ± 0.1	4.86 ± 0.05	4.95 ± 0.01	1.3	1.03 ± 0.04	3.11 ± 0.02	3.08 ± 0.03
CBZ-SLC (1:1)	1.8 ± 0.1	4.86 ± 0.05	4.95 ± 0.01	1.3	1.33 ± 0.05	4.29 ± 0.02	4.37 ± 0.02
CBZ-4ABA (H) (2:1)	1.8 ± 0.1	4.86 ± 0.05	4.95 ± 0.01	1.5	1.49 ± 0.06	4.94 ± 0.02	4.84 ± 0.03
PXC-SAC (1:1)	2.0 ± 0.2	5.02 ± 0.02	4.98 ± 0.01	1.4	1.40 ± 0.03	3.79 ± 0.02	3.64 ± 0.02
IND-SAC (1:1)	16 ± 1	4.98 ± 0.06	4.96 ± 0.03	4.0	4.5 ± 0.3	3.65 ± 0.05	3.66 ± 0.02
DNZ-HBA (1:1)	720 ± 80	5.01 ± 0.05	4.96 ± 0.01	27	23 ± 3	4.46 ± 0.06	4.47 ± 0.04
DNZ-VAN (1:1)	720 ± 80	5.01 ± 0.05	4.96 ± 0.01	27	24 ± 4	5.00 ± 0.01	4.96 ± 0.01

a) Experimentally measured in absence of coformer.

b) Predicted from experimental SR_{drug} values using equation (2.3) for 1:1 cocrystals and (2.4) for 2:1 cocrystals.

c) Determined from $S_{\text{cococrystal}}$ measurement at eutectic points.

Results demonstrate excellent agreement between the predicted and measured $SR_{\text{cococrystal}}$ values.

As predicted by the models, $SR_{\text{cococrystal}}$ for a given drug did not significantly vary for the systems studied (DNZ cocrystals 23 and 24 and CBZ 1:1 cocrystals 1.03 and 1.3). The simple relationships used in these calculations were derived from the more rigorous solubility equations for cocrystal and drug that consider cocrystal K_{sp} and the pK_{a} and K_{s}^{T} values of cocrystal constituents under the assumption that coformer K_{s}^{T} is negligible. Prediction of cocrystal solubility in FeSSIF using the more rigorous equations is presented in the next section.

Predicting cocrystal solubility in FeSSIF and buffer from relevant equilibrium constants

Table 2.2 shows the cocrystal solubility equations in buffer and FeSSIF for the systems studied. The derivation for equation (2.22) for a 1:1 cocrystal of a nonionizable drug R and a weakly acidic coformer HA is shown in the theoretical section. Full derivations for cocrystals of other constituents can be found in the Appendix.

Table 2.2. Cocrystal solubility equations in aqueous buffer and FeSSIF.

Cocrystal	Solubility in buffer	Solubility in FeSSIF
RHA (CBZ-SAC, CBZ-SLC, DNZ-HBA, DNZ-VAN)	$S_T^{RHA} = \sqrt{K_{sp}^{RHA} (1 + 10^{\text{pH} - \text{pKa,coformer}})}$	$S_T^{RHA} = \sqrt{K_{sp}^{RHA} (1 + K_s^{R,T} [M]) (1 + 10^{\text{pH} - \text{pKa,coformer}} + K_s^{HA,T} [M])}$
R ₂ ABH (CBZ-4ABA- HYD)	$S_T^{R_2ABH} = 2\sqrt[3]{\frac{K_{sp}^{R_2ABH}}{4} (1 + 10^{\text{pH} - \text{pKa1,coformer}} + 10^{\text{pKa2,coformer} - \text{pH}})}$	$S_T^{R_2ABH} = 2\sqrt[3]{\frac{K_{sp}^{R_2ABH}}{4} (1 + K_s^{R,T} [M])^2 (1 + 10^{\text{pH} - \text{pKa1,coformer}} + 10^{\text{pKa2,coformer} - \text{pH}} + K_s^{ABH,T} [M])}$
HDHA (IND-SAC)	$S_T^{HDHA} = \sqrt{K_{sp}^{HDHA} (1 + 10^{\text{pH} - \text{pKa,drug}}) (1 + 10^{\text{pH} - \text{pKa,coformer}})}$	$S_T^{HDHA} = \sqrt{K_{sp}^{HDHA} (1 + 10^{\text{pH} - \text{pKa,drug}} + K_s^{HD,T} [M]) (1 + 10^{\text{pH} - \text{pKa,coformer}} + K_s^{HA,T} [M])}$
⁻ ABH ⁺ HA (PXC-SAC)	$S_T^{\text{-ABH}^+\text{HA}} = \sqrt{K_{sp}^{\text{-ABH}^+\text{HA}} (1 + 10^{\text{pH} - \text{pKa1,drug}} + 10^{\text{pKa2,drug} - \text{pH}}) (1 + 10^{\text{pH} - \text{pKa,coformer}})}$	$S_T^{\text{-ABH}^+\text{HA}} = \sqrt{K_{sp}^{\text{-ABH}^+\text{HA}} (1 + 10^{\text{pH} - \text{pKa1,drug}} + 10^{\text{pKa2,drug} - \text{pH}} + K_s^{\text{-ABH}^+,T} [M]) (1 + 10^{\text{pH} - \text{pKa,coformer}} + K_s^{HA,T} [M])}$

The parameter values used in cocrystal solubility predictions are summarized in Table 2.3 and Table 2.5. K_{sp} values used in solubility predictions (Table 2.3) were either obtained from the literature or experimentally determined in our laboratory. The K_s^T values were determined from drug and solubility measurements in FeSSIF and buffer (Table 2.5). pK_a values (Table 2.5) were obtained from the literature.

Table 2.3. K_{sp} and pK_{sp} values for the cocrystals studied.

Cocrystal	K_{sp}	pK_{sp}
CBZ-SLC	$1.13 \pm 0.05 \text{ mM}^2$ ^a	5.95 ± 0.02
CBZ-SAC	$1.00 \pm 0.05 \text{ mM}^2$ ^b	6.00 ± 0.02
CBZ-4ABA (H)	$1.2 \pm 0.2 \text{ mM}^3$ ^a	8.92 ± 0.07
PXC-SAC	$(7.6 \pm 0.3) \times 10^{-2} \text{ mM}^2$ ^c	7.11 ± 0.02
IND-SAC	$(1.38 \pm 0.09) \times 10^{-3} \text{ mM}^2$ ^b	8.86 ± 0.07
DNZ-HBA	$(1.1 \pm 0.4) \times 10^{-2} \text{ mM}^2$ ^c	8.0 ± 0.2
DNZ-VAN	$(3.5 \pm 0.5) \times 10^{-3} \text{ mM}^2$ ^c	8.46 ± 0.06

a) From reference⁴⁰.

b) From reference²⁵.

c) Experimentally determined at 25°C.

Results of cocrystal solubility measurements at the eutectic point and K_{sp} evaluation for PXC and the DNZ cocrystals can be found in the Appendix.

The predicted and experimentally measured cocrystal solubilities in FeSSIF and buffer are presented in Table 2.4 and Figure 2.7. The predicted cocrystal solubilities are in good

agreement with the experimentally observed values in both FeSSIF and buffer, with all predictions falling within a factor of two of the measured values. Cocrystal solubilities ranged from 10.1 mM for CBZ-SAC to 1.39 mM for DNZ-VAN in FeSSIF and from 9.8 mM for CBZ-SAC to 0.057 mM for DNZ-VAN in buffer. Some cocrystals, such as PXC-SAC in FeSSIF and CBZ-SAC in buffer, showed deviations between experimental and predicted values, which may be due to a number of factors such as reduced drug solubilization in the presence of coformer and interactions between constituents in solution that are assumed to be negligible by the models presented in this work. The models, however, provide valuable insights into why and how biorelevant media influence cocrystal solubilization from knowledge of drug solubilization characteristics.

Table 2.4. Comparison between predicted and experimentally measured cocrystal solubility values.

Cocrystal	$S_{\text{cocrystal}}$ FeSSIF(mM)			$S_{\text{cocrystal}}$ buffer (mM)		
	Pred ^a	Exp ^b	pH ^c	Pred ^a	Exp ^b	pH ^c
CBZ-SAC	7.7	10.1±0.1	3.11 ± 0.02	5.6	9.8±0.3	3.08 ± 0.03
CBZ-SLC	6.6	6.71±0.09	4.29 ± 0.02	5.2	5.1±0.1	4.37 ± 0.02
PXC-SAC	4.2	2.60±0.03	3.79 ± 0.02	2.8	1.85±0.03	3.64 ± 0.02
DNZ-HBA	4.2	2.8±0.1	4.46±0.06	0.15	0.12±0.01	4.47±0.04
IND-SAC	4.4	3.6±0.2	3.65 ± 0.05	0.42	0.79±0.03	3.66 ± 0.02
CBZ-4ABA (H)	2.7	2.57±0.05	4.94 ± 0.02	0.17	1.73±0.06	4.84 ± 0.03
DNZ-VAN	1.7	1.39±0.03	5.00 ± 0.01	5.9×10^{-2}	$(5.7±0.2) \times 10^{-2}$	4.96 ± 0.01

- (a) Predicted from equations in Table 2.2 and parameter values in Table 2.3 and Table 2.5.
 (b) Calculated from experimentally measured eutectic concentrations using equation (2.28) for 1:1 cocrystals and equation (2.29) for 2:1 cocrystals.

Since many of the cocrystals contain acidic components, the pH at the eutectic point was often lower than 5.00 (the pH of FeSSIF and the aqueous buffer), especially for cocrystals of SAC. The pH at the eutectic point ranged from 3.79-3.08 for PXC-SAC, IND-SAC, and CBZ-SAC. Cocrystal solubility has been shown to vary with pH³⁹, making it imperative to consider its influence when comparing predictions with measurements. The cocrystal solubility in FeSSIF and buffer was predicted at the pH of the experimental conditions in Table 2.4.

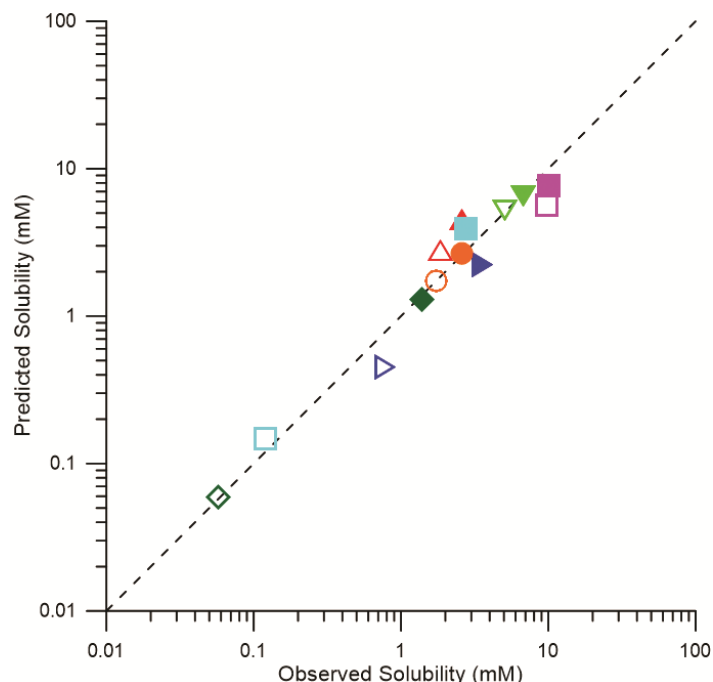


Figure 2.7. Comparison of predicted and observed cocrystal solubility in FeSSIF (filled symbols) and buffer (open symbols) at 25°C for IND-SAC (▶), CBZ-SAC (■), CBZ-SLC (▼), CBZ-4ABA (H) (●), PXC-SAC (▲), DNZ-HBA (◻), and DNZ-VAN (◆). Line indicates the function $y = x$, where the predicted and observed solubilities are equivalent. Errors fit within the size of each symbol. Solubilities were predicted according to the equations in Table 2.2 according to the equilibrium constants in Table 2.3 and Table 2.5.

Cocrystal solubility can be predicted over orders of magnitude using the equations in Table 2.2. These mathematical models allow for the prediction of cocrystal solubility in the presence of solubilizing agents from knowledge of K_{sp} , as well as the K_a and K_s values of the drug and coformer. K_{sp} can be obtained from a single solubility measurement in aqueous buffer, and these models are particularly useful to predict the influence of solubilizing agents on cocrystal solution behavior without doing experiments when limited quantities of cocrystal are available.

Drug and coformer solubilization in FeSSIF

Drug and coformer solubilities were measured in FeSSIF and in buffer. Drugs were significantly solubilized by FeSSIF and SR_{drug} ranged from 1.8 to 720 as shown in Figure 2.8.

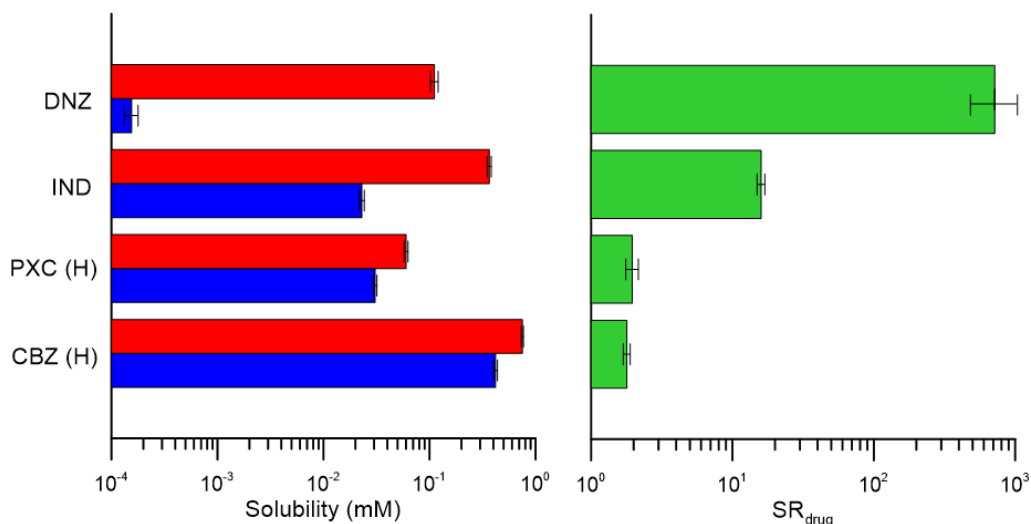


Figure 2.8. Drug solubility measured in FeSSIF (■) and buffer (■) at 25°C. SR_{drug} in FeSSIF calculated from solubility values is also shown (■). The final pH of each drug solubility measurement in FeSSIF and buffer, respectively, are as follows: DNZ (5.01 ± 0.05 and 4.96 ± 0.01), IND (4.98 ± 0.06 and 4.96 ± 0.03), PXC (H) (5.03 ± 0.02 and 4.98 ± 0.01), and CBZ (H) (4.86 ± 0.05 and 4.95 ± 0.01). PXC (H) represents the monohydrate form of PXC and CBZ (H) represents the dihydrate form of CBZ, which are the stable forms in aqueous solution.

Solubilization by physiologically relevant surfactants similar to those in FeSSIF has been shown to be directly proportional to the hydrophobicity of a compound as measured by the octanol/water partition coefficient ($\log P$)^{17, 41, 42}. More hydrophobic drugs (DNZ, $\log P$ 4.53⁴³ and IND, $\log P$ 4.27⁴⁴) were solubilized to a higher extent than less hydrophobic drugs (CBZ, $\log P$ 2.32⁴⁵ and PXC, $\log P$ 1.80⁴⁶). The most hydrophobic drug studied, DNZ, was remarkably 720 times more soluble in FeSSIF compared to aqueous buffer, showing extremely high solubilization by the bile salt/lecithin mixed micelles.

One of the underlying assumptions of equations (2.3) and (2.4) is that the cofomer solubilization by FeSSIF is negligible. Figure 2.9 shows measured cofomer solubilities in FeSSIF and buffer and solubilization ratios ($SR_{coformer}$).

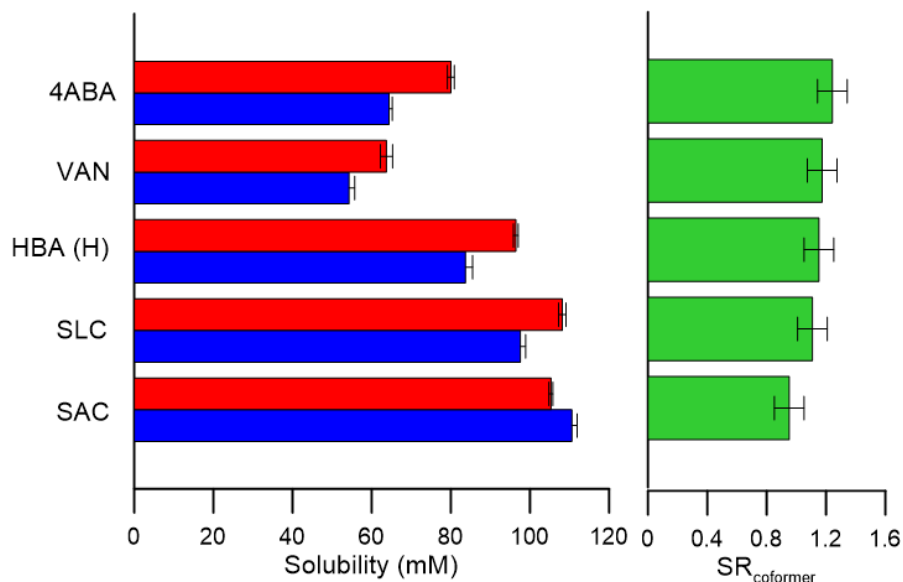


Figure 2.9. Coformer solubility measured in FeSSIF (■) and buffer (■) at 25°C. SR_{coformer} in FeSSIF calculated from solubility values is also shown (■). The final pH of each coformer solubility measurement in FeSSIF and buffer, respectively, are as follows: 4ABA (4.72 ± 0.02 and 4.57 ± 0.04), VAN (4.99 ± 0.01 and 4.94 ± 0.01), HBA (H) (4.45 ± 0.02 and 4.41 ± 0.02), SLC (3.78 ± 0.03 and 3.58 ± 0.06), and SAC (2.60 ± 0.02 and 2.58 ± 0.02). HBA (H) represents the monohydrate form of HBA which is the stable form in aqueous solution.

All coformers had slightly higher solubilities in FeSSIF compared to buffer with the exception of SAC. Coformers showed negligible solubilization by FeSSIF, and SR_{coformer} ranged from 1.0-1.2. Log P values range from 0.77 for 4ABA to 2.26 for SLC^{47, 48} and the low observed SR values of the coformers are expected due to their hydrophilic nature. Since the assumption that coformer solubilization is negligible is justified for this set of cocrystals in FeSSIF, equations (2.3) and (2.4) can be used to predict $SR_{\text{cocrystal}}$ from SR_{drug} .

Values of total equilibrium solubilization constants (K_s^T) were calculated for cocrystal components at the pH of the solubility measurements from measured drug and coformer solubilities in FeSSIF and buffer, (Table 2.5) using equations (2.25) - (2.27).

Table 2.5. Drug and coformer solubility measurements in FeSSIF and buffer and calculated K_s^T .

Component	S_{FeSSIF} (mM)	$\text{pH}_{\text{FeSSIF}}$	S_{buffer} (mM)	$\text{pH}_{\text{buffer}}$	pKa	K_s^T (mM^{-1}) ^f	
Drugs	CBZ (H)	$(7.5 \pm 0.2) \times 10^{-1}$	4.86 ± 0.05	$(4.2 \pm 0.2) \times 10^{-1}$	4.95 ± 0.01	---	0.054 ± 0.003
	PXC (H)	$(6.0 \pm 0.3) \times 10^{-2}$	5.03 ± 0.02	$(3.1 \pm 0.1) \times 10^{-2}$	4.98 ± 0.01	1.86, 5.45 ^a	0.080 ± 0.005
	IND	$(3.7 \pm 0.2) \times 10^{-1}$	4.97 ± 0.06	$(2.3 \pm 0.1) \times 10^{-2}$	4.96 ± 0.03	4.2 ^b	8.2 ± 0.6
	DNZ	$(1.11 \pm 0.09) \times 10^{-1}$	5.01 ± 0.05	$(1.6 \pm 0.2) \times 10^{-4}$	4.96 ± 0.01	---	49 ± 5
Coformers	SAC	105.3 ± 0.5	2.60 ± 0.02	111 ± 1	2.58 ± 0.02	1.6 ^c	0
	4-ABA	80.0 ± 0.9	4.72 ± 0.02	64.4 ± 0.8	4.57 ± 0.04	2.6, 4.8 ^d	0.0021 ± 0.0003
	VAN	64 ± 2	4.99 ± 0.01	54 ± 1	4.94 ± 0.01	7.4 ^e	0.012 ± 0.001
	HBA (H)	96.4 ± 0.6	4.45 ± 0.02	84 ± 2	4.41 ± 0.02	4.48 ^e	0.018 ± 0.001
	SLC	108.2 ± 0.9	3.78 ± 0.03	97 ± 1	3.58 ± 0.06	3.00 ^c	0.043 ± 0.003

(a) from reference 22.

(b) from reference 23.

(c) from reference 24.

(d) from reference 26.

(e) from reference 28.

(f) Calculated from equations (2.25)-(2.27) with pK_a , and solubility values in Table 2.5.

The K_s^T values in Table 2.5 indicate the same trend that was observed with SR_{drug} and $\text{SR}_{\text{coformer}}$ values in Figure 2.8 and Figure 2.9. Highly hydrophobic drugs IND and DNZ have much higher K_s^T values of 8.2 mM^{-1} and 49 mM^{-1} respectively, compared to less hydrophobic drugs PXC and CBZ which had K_s^T values of 0.080 mM^{-1} and 0.054 mM^{-1} , respectively. Coformers had much lower K_s^T values, ranging from 0 mM^{-1} for SAC to 0.043 mM^{-1} for SLC. These solubilization

constants, along with pK_a values reported in the literature, were used to predict cocrystal solubility in FeSSIF, as discussed in a previous section.

Cocrystal solubility measurements at eutectic points

Cocrystals with a solubility much higher than the drug require high $[coformer]_{eu}$ to reach the eutectic point. These coformer concentrations in solution are orders of magnitude above the stoichiometric ratio of the cocrystal. CBZ-SAC, IND-SAC, and PXC-SAC had very high $[SAC]_{eu}$ concentrations in buffer and in FeSSIF (Appendix). $[coformer]_{eu}$ values were as high as six orders of magnitude $[drug]_{eu}$ for the DNZ cocrystals in buffer. In FeSSIF, however, the difference between $[drug]_{eu}$ and $[coformer]_{eu}$ was lowered due to the preferential solubilization of the drug. In FeSSIF, the $[coformer]_{eu}$ was only three orders of magnitude higher than $[drug]_{eu}$ for DNZ cocrystals due to this solubilization effect.

Very high coformer concentrations at the eutectic point can lead to nonideal solution conditions where the assumption that drug interactions with solubilizing agents are unaffected by coformer in solution is no longer justified. These high concentrations in solution can alter drug solubility at the eutectic point and reduce drug solubilization in these conditions. As in the case of CBZ-SAC, this reduced solubilization leads to smaller SR_{drug} and K_s values at the eutectic point compared to those measured and calculated in the absence of coformer. However, for the systems studied, coformer concentrations at the eutectic points did not significantly influence $SR_{cocrystal}$ or cocrystal solubility evaluations. Information regarding drug and cocrystal solubilities and solubilization in FeSSIF at the eutectic point can be found in the Appendix.

Conclusions

This work shows that the behavior of cocrystal solubilization in FeSSIF is different from that of the drug solubilization. A theoretical framework that allows for the simple and

quantitative prediction of cocrystal solubilization ratio from drug solubilization ratio is developed. For a 1:1 cocrystal, the cocrystal solubilization ratio can be obtained from the *square root of the drug solubilization ratio*. $SR_{\text{cocrystal}}$ in solubilizing agents was observed to be orders of magnitude lower than SR_{drug} . Cocrystals of drugs with a wide range of solubilization ratios in FeSSIF were studied. SR_{drug} values range from 720 for DNZ, to 16 for indomethacin, to 2.0 for piroxicam, to 1.8 for CBZ (H). $SR_{\text{cocrystal}}$ values in FeSSIF range from 23 and 24 for DNZ-HBA and DNZ-VAN, to 4 for IND-SAC, to 1.4 for PXC-SAC, and 1.03, 1.3, and 1.5 for CBZ-SAC, CBZ-SLC and CBZ-4ABA (H). The observed $SR_{\text{cocrystal}}$ values were all in excellent agreement with predictions from the simple equations.

The decrease in $SR_{\text{cocrystal}}$ in FeSSIF compared to SR_{drug} ranges from 30 fold for the DNZ cocrystals to about 2 fold or less for the CBZ cocrystals. Large decreases in $SR_{\text{cocrystal}}$ over SR_{drug} for cocrystals of the more hydrophobic drugs is a result of the higher drug solubilization provided by FeSSIF. This finding has important implications for poorly soluble, lipophilic drugs that show large food effect, like DNZ. Cocrystals of drugs like DNZ are solubilized to a lesser extent than the constituent drugs, which can lead to smaller differences between fed and fasted state solubilities. For these drugs, cocrystallization may be a promising approach to diminish food effects. The presented models can be used with drug solubilization descriptors that are measured independently or reported in the literature to predict $SR_{\text{cocrystal}}$ and cocrystal solubility. The hope is that these simple yet realistic models can support cocrystal development by predicting cocrystal characteristics that have not been measured and that influence cocrystal performance.

References

1. Cheney, M. L.; Weyna, D. R.; Shan, N.; Hanna, M.; Wojtas, L.; Zaworotko, M. J. Cofomer Selection in Pharmaceutical Cocrystal Development: a Case Study of a Meloxicam Aspirin Cocrystal That Exhibits Enhanced Solubility and Pharmacokinetics. *Journal of Pharmaceutical Sciences* **2011**, *100*, (6), 2172-2181.
2. Smith, A. J.; Kavuru, P.; Wojtas, L.; Zaworotko, M. J.; Shytle, R. D. Cocrystals of Quercetin with Improved Solubility and Oral Bioavailability. *Molecular Pharmaceutics* **2011**, *8*, (5), 1867-1876.
3. Jung, M. S.; Kim, J. S.; Kim, M. S.; Alhalaweh, A.; Cho, W.; Hwang, S. J.; Velaga, S. P. Bioavailability of indomethacin-saccharin cocrystals. *J. Pharm. Pharmacol.* **2010**, *62*, (11), 1560-1568.
4. Hickey, M. B.; Peterson, M. L.; Scoppettuolo, L. A.; Morrisette, S. L.; Vetter, A.; Guzman, H.; Remenar, J. F.; Zhang, Z.; Tawa, M. D.; Haley, S.; Zaworotko, M. J.; Almarsson, O. Performance comparison of a co-crystal of carbamazepine with marketed product. *Eur. J. Pharm. Biopharm.* **2007**, *67*, (1), 112-119.
5. Bak, A.; Gore, A.; Yanez, E.; Stanton, M.; Tufekcic, S.; Syed, R.; Akrami, A.; Rose, M.; Surapaneni, S.; Bostick, T.; King, A.; Neervannan, S.; Ostovic, D.; Koparkar, A. The co-crystal approach to improve the exposure of a water-insoluble compound: AMG 517 sorbic acid co-crystal characterization and pharmacokinetics. *Journal of Pharmaceutical Sciences* **2008**, *97*, (9), 3942-3956.
6. McNamara, D. P.; Childs, S. L.; Giordano, J.; Iarriccio, A.; Cassidy, J.; Shet, M. S.; Mannion, R.; O'Donnell, E.; Park, A. Use of a glutaric acid cocrystal to improve oral bioavailability of a low solubility API. *Pharm. Res.* **2006**, *23*, (8), 1888-1897.
7. Huang, N.; Rodriguez-Hornedo, N. Engineering Cocrystal Solubility, Stability, and pH(max) by Micellar Solubilization. *Journal of Pharmaceutical Sciences* **2011**, *100*, (12), 5219-5234.
8. Huang, N.; Rodriguez-Hornedo, N. Engineering cocrystal thermodynamic stability and eutectic points by micellar solubilization and ionization. *Crystengcomm* **2011**, *13*, (17), 5409-5422.
9. Huang, N.; Rodriguez-Hornedo, N. Effect of Micellar Solubilization on Cocrystal Solubility and Stability. *Crystal Growth & Design* **2010**, *10*, (5), 2050-2053.
10. Roy, L. Engineering Cocrystal and Cocrystalline Salt Solubility by Modulation of Solution Phase Chemistry. *University of Michigan (Doctoral Dissertation)* **2013**, Retrieved from Deep Blue. (<http://hdl.handle.net/2027.42/98067>).
11. Roy, L.; Rodriguez-Hornedo, N. A Rational Approach for Surfactant Selection to Modulate Cocrystal Solubility and Stability. *Poster presentation at the 2010 AAPS Annual Meeting and Exposition* **2010**, New Orleans, LA, (November 14-18, 2010), Poster R6072.
12. Lipert, M. P.; Rodriguez-Hornedo, N. Cocrystal transition points: Role of cocrystal solubility, drug solubility, and solubilizing agents. *Mol. Pharm.* **2015**, Submitted.
13. Charman, W. N.; Porter, C. J. H.; Mithani, S.; Dressman, J. B. Physicochemical and physiological mechanisms for the effects of food on drug absorption: The role of lipids and pH. *J. Pharm. Sci.* **1997**, *86*, (3), 269-282.
14. Courtney, R.; Wexler, D.; Radwanski, E.; Lim, J.; Laughlin, M. Effect of food on the relative bioavailability of two oral formulations of posaconazole in healthy adults. *British Journal of Clinical Pharmacology* **2004**, *57*, (2), 218-222.

15. Kostewicz, E. S.; Brauns, U.; Becker, R.; Dressman, J. B. Forecasting the oral absorption behavior of poorly soluble weak bases using solubility and dissolution studies in biorelevant media. *Pharm. Res.* **2002**, *19*, (3), 345-349.
16. Schwebel, H. J.; van Hoogevest, P.; Leigh, M. L. S.; Kuentz, M. The apparent solubilizing capacity of simulated intestinal fluids for poorly water-soluble drugs. *Pharm. Dev. Technol.* *16*, (3), 278-286.
17. Mithani, S. D.; Bakatselou, V.; TenHoor, C. N.; Dressman, J. B. Estimation of the increase in solubility of drugs as a function of bile salt concentration. *Pharm. Res.* **1996**, *13*, (1), 163-167.
18. Sunesen, V. H.; Vedelsdal, R.; Kristensen, H. G.; Christrup, L.; Mullertz, A. Effect of liquid volume and food intake on the absolute bioavailability of danazol, a poorly soluble drug. *Eur. J. Pharm. Sci.* **2005**, *24*, (4), 297-303.
19. Charman, W. N.; Rogge, M. C.; Boddy, A. W.; Barr, W. H.; Berger, B. M. Absorption of danazol after administration to different sites of the gastrointestinal-tract and the relationship to single-peak and double-peak phenomena in the plasma profiles. *J. Clin. Pharmacol.* **1993**, *33*, (12), 1207-1213.
20. Childs, S. L.; Kandi, P.; Lingireddy, S. R. Formulation of a Danazol Cocrystal with Controlled Supersaturation Plays an Essential Role in Improving Bioavailability. *Molecular Pharmaceutics* **2013**, *10*, (8), 3112-3127.
21. Winstanley, P. A.; Orme, M. L. E. The effects of food on drug bioavailability. *British Journal of Clinical Pharmacology* **1989**, *28*, (6), 621-628.
22. Bernhard, E.; Zimmermann, F. Contribution to the Understanding of Oxicam Ionization-Constants. *Arzneimittel-Forschung/Drug Research* **1984**, *34-1*, (6), 647-648.
23. Mooney, K. G.; Mintun, M. A.; Himmelstein, K. J.; Stella, V. J. Dissolution Kinetics of Carboxylic-Acids .1. Effect of Ph under Unbuffered Conditions. *J. Pharm. Sci.* **1981**, *70*, (1), 13-22.
24. Newton, D. W.; Kluza, R. B. Pka values of medicinal compounds in pharmacy practice. *Drug Intelligence & Clinical Pharmacy* **1978**, *12*, (9), 546-554.
25. Alhalaweh, A.; Roy, L.; Rodriguez-Hornedo, N.; Velaga, S. P. pH-Dependent Solubility of Indomethacin-Saccharin and Carbamazepine-Saccharin Cocrystals in Aqueous Media. *Molecular Pharmaceutics* **2012**, *9*, (9), 2605-2612.
26. Robinson, R. A.; Biggs, A. I. The ionization constants of para-aminobenzoic acid in aqueous solution at 25-degrees-c. *Aust. J. Chem.* **1957**, *10*, (2), 128-134.
27. Swatloski, R. P.; Visser, A. E.; Huddleston, J. G.; Rogers, R. D. Room temperature ionic liquids as alternatives to organic solvents in liquid/liquid extraction of dilute organic contaminants. *Abstr. Pap. Am. Chem. Soc.* **1999**, *217*, U881-U882.
28. Robinson, R. A.; Kiang, A. K. The ionization constants of vanillin and 2 of its isomers. *Transactions of the Faraday Society* **1955**, *51*, (10), 1398-1402.
29. Lipert, M. P.; Rodriguez-Hornedo, N. Cocrystal Solubilization and Shifting Transition Points in the Presence of Drug Solubilizers. *Poster presentation at the 2014 AAPS Annual Meeting and Exposition* **2014**, San Diego, CA, (November 2-6, 2014), Poster W4108.
30. Lipert, M. P.; Rodriguez-Hornedo, N. Strategies to Predict and Control Cocrystal Solubility and Supersaturation in Surfactant Solutions. *Poster presentation at the 2013 AAPS Annual Meeting and Exposition* **2013**, San Antonio, TX, (November 10-14, 2013), Poster W5148.
31. Roy, L., Lipert, Maya and Rodriguez-Hornedo, Nair, Cocrystal Solubility and Thermodynamic Stability. In *Handbook of Pharmaceutical Salts and Cocrystals*, Submitted,

Quere, J. W. a. L., Ed. Royal Society of Chemistry: London, United Kingdom, 2011; Vol. 16, pp 247-279.

32. Roy, L.; Lipert, M. P.; Huang, N.; Rodriguez-Hornedo, N. Understanding and Predicting Cocrystal Solubility in Biorelevant Media. *Poster presentation at the 2010 AAPS Annual Meeting and Exposition 2010, New Orleans, LA*, (November 14-18, 2010), Poster T3112.

33. Thakuria, R.; Delori, A.; Jones, W.; Lipert, M. P.; Roy, L.; Rodriguez-Hornedo, N. Pharmaceutical cocrystals and poorly soluble drugs. *International Journal of Pharmaceutics* **2013**, *453*, (1), 101-125.

34. Grbic, S.; Parojcic, J.; Djuric, Z.; Ibric, S. Mathematical modeling of pH-surfactant-mediated solubilization of nimesulide. *Drug Dev. Ind. Pharm.* **2009**, *35*, (7), 852-856.

35. Galia, E.; Nicolaidis, E.; Horter, D.; Lobenberg, R.; Reppas, C.; Dressman, J. B. Evaluation of various dissolution media for predicting in vivo performance of class I and II drugs. *Pharm. Res.* **1998**, *15*, (5), 698-705.

36. Rodriguez-Hornedo, N.; Nehru, S. J.; Seefeldt, K. F.; Pagan-Torres, Y.; Falkiewicz, C. J. Reaction crystallization of pharmaceutical molecular complexes. *Molecular Pharmaceutics* **2006**, *3*, (3), 362-367.

37. Good, D. J.; Rodriguez-Hornedo, N. Solubility Advantage of Pharmaceutical Cocrystals. *Crystal Growth & Design* **2009**, *9*, (5), 2252-2264.

38. Good, D. J.; Rodriguez-Hornedo, N. Cocrystal Eutectic Constants and Prediction of Solubility Behavior. *Crystal Growth & Design* **2010**, *10*, (3), 1028-1032.

39. Bethune, S. J.; Huang, N.; Jayasankar, A.; Rodriguez-Hornedo, N. Understanding and Predicting the Effect of Cocrystal Components and pH on Cocrystal Solubility. *Crystal Growth & Design* **2009**, *9*, (9), 3976-3988.

40. Bethune, S. J. Thermodynamic and Kinetic Parameters that Explain Crystallization and Solubility of Pharmaceutical Cocrystals. University of Michigan, Ann Arbor, MI, 2009.

41. Alvarez-Nunez, F. A.; Yalkowsky, S. H. Relationship between Polysorbate 80 solubilization descriptors and octanol-water partition coefficients of drugs. *Int. J. Pharm.* **2000**, *200*, (2), 217-222.

42. Kleberg, K.; Jacobsen, J.; Mullertz, A. Characterising the behaviour of poorly water soluble drugs in the intestine: application of biorelevant media for solubility, dissolution and transport studies. *J. Pharm. Pharmacol.* **62**, (11), 1656-1668.

43. Caron, J. C.; Shroot, B. Determination of partition-coefficients of glucocorticosteroids by high-performance liquid-chromatography. *J. Pharm. Sci.* **1984**, *73*, (12), 1703-1706.

44. Palagiano, F.; Arenare, L.; Barbato, F.; LaRotonda, M. I.; Quaglia, F.; Bonina, F. P.; Montenegro, L.; deCaprariis, P. In vitro and in vivo evaluation of terpenoid esters of indomethacin as dermal prodrugs. *Int. J. Pharm.* **1997**, *149*, (2), 171-182.

45. Machatha, S. G.; Yalkowsky, S. H. Comparison of the octanol/water partition coefficients calculated by ClogP((R)), ACDlogP and KowWin((R)) to experimentally determined values. *Int. J. Pharm.* **2005**, *294*, (1-2), 185-192.

46. Tsai, R.-S.; Carrupt, P.-A.; Tayar, N. E.; Giroud, Y.; Andrade, P.; Testa, B.; Brée, F.; Tillement, J.-P. Physicochemical and Structural Properties of Non-Steroidal Anti-inflammatory Oxicams. *Helvetica Chimica Acta* **1993**, *76*, (2), 842-854.

47. Hansch, C.; Rockwell, S. D.; Jow, P. Y. C.; Leo, A.; Steller, E. E. Substituent constants for correlation analysis. *J. Med. Chem.* **1977**, *20*, (2), 304-306.

48. Leo, A.; Jow, P. Y. C.; Silipo, C.; Hansch, C. Calculation of hydrophobic constant (log p) from pi and f constants. *J. Med. Chem.* **1975**, *18*, (9), 865-868.

Appendix

Cocrystal and drug solubility at the eutectic point

Table 2.6 shows the measured cocrystal solubilities at the eutectic point in FeSSIF and buffer.

Table 2.6. Measured eutectic concentrations and calculated stoichiometric solubility in FeSSIF and buffer.

Media	Cocrystal	[drug] _{eu} (mM)	[coformer] _{eu} (mM)	S _{cocrystal} (mM) ^a	pH (eutectic)
buffer	DNZ-HBA	(2.0±0.4)×10 ⁻⁴	79±4	(1.2±0.1)×10 ⁻¹	4.47±0.04
	DNZ-VAN	(2.1±0.1)×10 ⁻⁴	16±3	(5.7±0.2)×10 ⁻²	4.96±0.01
	IND-SAC	(6.0±0.3)×10 ⁻³	104±20	(7.9±0.3)×10 ⁻²	3.66 ± 0.02
	PXC-SAC	(3.64±0.01)×10 ⁻²	94±2	1.85±0.03	3.64 ±0.02
	CBZ-SAC	(7.8±0.5)×10 ⁻¹	124±3	9.8±0.3	3.08 ± 0.03
	CBZ-SLC	(5.1±0.2)×10 ⁻¹	49.8±0.9	5.1±0.1	4.37 ± 0.02
	CBZ-4ABA (H)	(4.4±0.2)×10 ⁻¹	13.1±0.4	1.73±0.06	4.84 ± 0.03
FeSSIF	PXC-SAC	(6.80±0.06)×10 ⁻²	97±1	2.60±0.03	3.79 ±0.02
	DNZ-HBA	(9.9±0.8)×10 ⁻²	78±1	2.8±0.1	4.46±0.06
	IND-SAC	(1.50±0.2)×10 ⁻¹	87±4	3.6±0.2	3.65 ± 0.05
	DNZ-VAN	(1.0±0.2)×10 ⁻¹	19.4±0.8	1.39±0.03	5.00±0.01

CBZ-SAC	1.07±0.03	95.9±0.3	10.1±0.1	3.11 ± 0.02
CBZ-SLC	(9.1±0.2)×10 ⁻¹	49.9±0.6	6.71±0.09	4.29 ± 0.02
CBZ-4ABA (H)	(7.4±0.3)×10 ⁻¹	15.6±0.4	2.57±0.05	4.94 ± 0.02

(a) Calculated using equation (2.28) for 1:1 cocrystals and equation (2.29) for 2:1 cocrystals from experimentally measured eutectic concentrations as described in the text.

Highly soluble cocrystals require high [coformer]_{eu} to reach the eutectic point. CBZ-SAC, IND-SAC, and PXC-SAC had very high [SAC]_{eu} concentrations in buffer and in FeSSIF.

[coformer]_{eu} values were as much as six orders of magnitude higher than the [drug]_{eu} as in the case of the DNZ cocrystals in buffer. In FeSSIF, however, the difference in [drug]_{eu} and [coformer]_{eu} was muted due to the preferential solubilization of the drug. In FeSSIF, the [coformer]_{eu} was only three orders of magnitude higher than [drug]_{eu} for DNZ cocrystals due to this solubilization effect. Extremely high coformer concentrations at the eutectic point can create nonideal solution conditions where the assumption that drug interactions with solubilizing agents are unaffected by coformer in solution is no longer justified. This will be discussed in a subsequent section.

Cocrystals that have much higher solubilities than their constituent drugs require excess coformer to reach the equilibrium solubility. Solubility of these highly soluble cocrystals is measured at the eutectic point, where two solid phases (cocrystal and drug) are in equilibrium with solution³⁷. At the eutectic point, cocrystal dissolution leads to high concentrations of coformer in solution. The drug concentration at the eutectic point also serves as a measure of the equilibrium solubility of the drug in the presence of coformer in solution since the solution is saturated with drug as well as cocrystal phases. Table 2.7 shows the comparison of drug

solubility measured in the absence of cofomer (independently measured) to the solubility measured at the eutectic point in the presence of cofomer. To analyze the impact of cofomer on drug solubilization, K_s^T values were calculated and compared from both the independently measured and eutectic point solubility values.

Table 2.7 Comparison of drug solubilities in FeSSIF buffer measured in the absence of and in the presence of cofomer and calculated K_s^T values.

Component	S_{FeSSIF} (mM) drug	$\text{pH}_{\text{FeSSIF}}$	S_{buffer} (M) drug	$\text{pH}_{\text{buffer}}$	$K_{s,T}$ (M^{-1}) drug ^a
CBZ (H)	0.75±0.02	4.86±0.05	0.42±0.02	4.95±0.01	0.054±0.003
CBZ-SLC	0.91±0.02	4.29±0.02	0.51±0.02	4.37±0.02	0.052±0.004
CBZ-4ABA (H)	0.74±0.03	4.94±0.02	0.44±0.02	4.84±0.03	0.045±0.003
CBZ-SAC	1.07±0.03	3.11±0.02	0.78±0.05	3.08±0.03	0.025±0.002
PXC (H)	$(6.0\pm 0.3)\times 10^{-2}$	5.03±0.02	$(3.1\pm 0.1)\times 10^{-2}$	4.98±0.01	0.080±0.005
PXC-SAC	$(6.80\pm 0.06)\times 10^{-2}$	3.79±0.02	$(3.64\pm 0.01)\times 10^{-2}$	3.64±0.02	0.057±0.004
IND	$(3.7\pm 0.2)\times 10^{-1}$	4.97±0.06	$(2.3\pm 0.1)\times 10^{-3}$	4.96±0.03	8.2±0.6
IND-SAC	$(1.5\pm 0.2)\times 10^{-1}$	3.65±0.05	$(6.0\pm 0.3)\times 10^{-3}$	3.66±0.02	1.6±0.2
DNZ	$(1.11\pm 0.09)\times 10^{-1}$	5.01±0.05	$(1.6\pm 0.2)\times 10^{-4}$	4.96±0.01	49±5
DNZ-HBA	$(9.9\pm 0.8)\times 10^{-2}$	4.46±0.06	$(2.0\pm 0.4)\times 10^{-4}$	4.47±0.04	34±4
DNZ-VAN	$(1.0\pm 0.2)\times 10^{-1}$	5.00±0.01	$(2.1\pm 0.1)\times 10^{-4}$	4.96±0.01	33±3

(a) Calculated as described by equations (2.25)-(2.27).

Solubility and K_s^T values for drugs can be influenced by both the cofomer concentration at the eutectic point and the pH differences between the solubility measurements in the absence

and the presence of cofomer. The presence of excess cofomer in solution at the eutectic point can alter the pH of the media when cofomers are ionizable, which is the case for most of the systems studied in this work. The impact of these differences in K_s^T on cocystal solubility prediction will be examined in the next section.

Table 2.8 shows the experimentally determined and the predicted solubility values in FeSSIF using both independently measured and eutectic point measured K_s^T values and equations in Table 2.2. The solubility predictions in buffer do not change between the two methods because there is no solubilization and therefore no K_s^T .

Table 2.8. Comparison of experimentally measured cocystal solubility and predicted solubility from K_s^T determined independently and at the eutectic point.

(a)

Cocrystal	S_{cocystal} FeSSIF (mM)			Eutectic pH	S_{cocystal} buffer (mM)		Eutectic pH
	Pred, K_s^T indep ^a	Pred, K_s^T eu ^b	Exp ^c		Pred ^d	Exp ^c	
	CBZ-SAC	7.7	6.7		10.1±0.1	3.11 ± 0.02	
CBZ-SLC	6.6	6.5	6.71±0.09	4.29 ± 0.02	5.2	5.1±0.1	4.37 ± 0.02
PXC-SAC	4.2	4.5	2.60±0.03	3.79 ± 0.02	2.8	1.85±0.03	3.64 ± 0.02
DNZ-HBA	4.2	3.5	2.8±0.1	4.46±0.06	0.15	0.12±0.01	4.47±0.04
IND-SAC	4.4	1.9	3.6±0.2	3.65 ± 0.05	0.42	0.79±0.03	3.66 ± 0.02
CBZ-4ABA (H)	2.7	2.5	2.57±0.05	4.94 ± 0.02	0.17	1.73±0.06	4.84 ± 0.03
DNZ-VAN	1.7	1.5	1.39±0.03	5.00 ± 0.01	5.9×10^{-2}	$(5.7 \pm 0.2) \times 10^{-2}$	4.96 ± 0.01

(b) Predicted using equations in Table 2.2, K_{sp} values in Table 2.3, and pK_a and K_s^T values in Table 2.5.

- (c) Predicted using equations in Table 2.2, K_{sp} values in Table 2.3, pK_a values in Table 2.5, and K_s^T values measured at the eutectic point in Table 2.7.
- (d) Calculated using equation (2.28) for 1:1 cocrystals and equation (2.29) for 2:1 cocrystals from experimentally measured eutectic concentrations.
- (e) Predicted using equations in Table 2.2, K_{sp} values in Table 2.3, and pK_a values in Table 2.5.

For all cocrystals, predicted solubility values in FeSSIF are within a factor of two of the experimentally measured value regardless of which K_s^T value is used. Since K_s^T values measured in the absence of coformer do an equally good job of predicting cocrystal solubility compared to K_s^T values measured at the eutectic point, it is clear that cocrystal solubility can be quantitatively predicted without performing the cocrystal eutectic measurements in FeSSIF for these systems.

Derivation of K_s^T equations

Explanation of terms:

Subscript aq – aqueous

Subscript m – micellar

Subscript T – total (aqueous + micellar)

ABH – amphoteric coformer (nonionized)

-ABH+ - zwitterionic drug (neutral)

M – micellar surfactant (total surfactant concentration – critical micellar concentration)

K_a – acid dissociation constant

K_s – micellar solubilization constant

S – solubility

For a monoprotic weakly acidic constituent:

$$S_T^{HA} = S_{aq}^{HA} \left(1 + 10^{pH-pK_{a,acid}} + \underbrace{\left(K_s^{HA} + 10^{pH-pK_{a,acid}} K_s^{A^-} \right)}_{K_s^{A,T}} [M] \right) \quad (2.30)$$

or

$$S_T^{HA} = S_{aq}^{HA} \left(1 + 10^{\text{pH}-\text{pKa,acid}} + K_s^{A,T} [M] \right) \quad (2.31)$$

Solving for $K_s^{A,T}$:

$$K_s^{A,T} = \frac{\frac{S_T^{HA}}{S_{aq}^{HA}} - 1 - 10^{\text{pH}-\text{pKa,acid}}}{[M]} \quad (2.32)$$

For an amphoteric constituent:

$$S_T^{ABH} = S_{aq}^{ABH} \left(1 + 10^{\text{pH}-\text{pKa1,amphoteric}} + 10^{\text{pKa2,amphoteric}-\text{pH}} \underbrace{\left(K_s^{ABH} + 10^{\text{pH}-\text{pKa1,amphoteric}} K_s^{-AB} + 10^{\text{pKa2,amphoteric}-\text{pH}} K_s^{HABH^+} \right)}_{K_s^{ABH,T}} [M] \right) \quad (2.33)$$

or:

$$S_T^{ABH} = S_{aq}^{ABH} \left(1 + 10^{\text{pH}-\text{pKa1,amphoteric}} + 10^{\text{pKa2,amphoteric}-\text{pH}} + K_s^{ABH,T} [M] \right) \quad (2.34)$$

solving for K_s^T :

$$K_s^{ABH,T} = \frac{\frac{S_T^{ABH}}{S_{aq}^{ABH}} - 1 - 10^{\text{pH}-\text{pKa1,amphoteric}} - 10^{\text{pKa2,amphoteric}-\text{pH}}}{[M]} \quad (2.35)$$

For a zwitterionic constituent:

$$S_T^{-ABH^+} = S_{aq}^{-ABH^+} \left(1 + 10^{\text{pH}-\text{pKa1,zwitterionic}} + 10^{\text{pKa2,zwitterionic}-\text{pH}} \underbrace{\left(K_s^{-ABH^+} + 10^{\text{pH}-\text{pKa1,zwitterionic}} K_s^{-AB} + 10^{\text{pKa2,zwitterionic}-\text{pH}} K_s^{HABH^+} \right)}_{K_s^{-ABH^+,T}} [M] \right) \quad (2.36)$$

Or:

$$S_T^{-ABH^+} = S_{aq}^{-ABH^+} \left(1 + 10^{\text{pH}-\text{pKa1,zwitterionic}} + 10^{\text{pKa2,zwitterionic}-\text{pH}} + K_s^{-ABH^+,T} [M] \right) \quad (2.37)$$

Solving for K_s^T :

$$K_s^{-ABH^+,T} = \frac{S_T^{-ABH^+} - 1 \cdot 10^{\text{pH}-\text{pKa}_{1,\text{zwitterionic}}} - 10^{\text{pKa}_{2,\text{zwitterionic}}-\text{pH}}}{S_{\text{aq}}^{-ABH^+} [M]} \quad (2.38)$$

Solubility derivations

Explanation of terms:

Subscript aq – aqueous

Subscript m – micellar

Subscript T – total (aqueous + micellar)

R – nonionizable drug

HA – monoprotic weakly acidic coformer (nonionized)

ABH – amphoteric coformer (nonionized)

-ABH+ - zwitterionic drug (neutral)

M – micellar surfactant (total surfactant concentration – critical micellar concentration)

K_{sp} – cocrystal solubility product

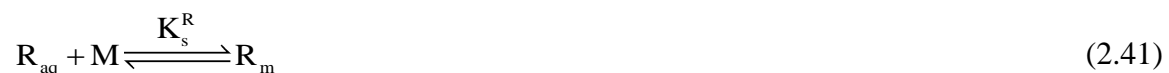
K_a – acid dissociation constant

K_s – micellar solubilization constant

S – solubility

RHA (1:1 nonionizable drug R, monoprotic weakly acidic coformer HA)

Relevant equilibria:





Associated equilibrium constants are given by:

$$K_{\text{sp}} = [R]_{\text{aq}} [HA]_{\text{aq}} \quad (2.44)$$

$$K_{\text{a}} = \frac{[A^-]_{\text{aq}} [H^+]_{\text{aq}}}{[HA]_{\text{aq}}} \quad (2.45)$$

$$K_s^{\text{R}} = \frac{[R]_{\text{m}}}{[R]_{\text{aq}} [M]} \quad (2.46)$$

$$K_s^{\text{HA}} = \frac{[HA]_{\text{m}}}{[HA]_{\text{aq}} [M]} \quad (2.47)$$

$$K_s^{A^-} = \frac{[A^-]_{\text{m}}}{[A^-]_{\text{aq}} [M]} \quad (2.48)$$

Cocrystal RHA total solubility in solubilizing agents

Mass balance on R is given by:

$$[R]_{\text{T}} = [R]_{\text{aq}} + [R]_{\text{m}} \quad (2.49)$$

Substituting equilibrium constants gives:

$$[R]_{\text{T}} = \frac{K_{\text{sp}}}{[HA]_{\text{aq}}} (1 + K_s^{\text{R}} [M]) \quad (2.50)$$

Mass balance on A is given by:

$$[A]_{\text{T}} = [HA]_{\text{aq}} + [A^-]_{\text{aq}} + [HA]_{\text{m}} + [A^-]_{\text{m}} \quad (2.51)$$

Substituting equilibrium constants into (2.51) gives

$$[A]_{\text{T}} = [HA]_{\text{aq}} \left(1 + 10^{\text{pH} - \text{pK}_{\text{a,coformer}}} + K_s^{\text{HA}} [M] + 10^{\text{pH} - \text{pK}_{\text{a,coformer}}} K_s^{A^-} [M] \right) \quad (2.52)$$

Combining (2.50) and (2.52) gives:

$$[\text{R}]_{\text{T}} = \frac{K_{\text{sp}}}{[\text{A}]_{\text{T}}} \left(1 + K_{\text{s}}^{\text{R}} [\text{M}]\right) \left(1 + 10^{\text{pH}-\text{pK}_{\text{a,coformer}}} + K_{\text{s}}^{\text{HA}} [\text{M}] + 10^{\text{pH}-\text{pK}_{\text{a,coformer}}} K_{\text{s}}^{\text{A}^{-}} [\text{M}]\right) \quad (2.53)$$

Cocrystal solubility in stoichiometric conditions:

$$S_{\text{RHA,T}} = [\text{R}]_{\text{T}} = [\text{A}]_{\text{T}} \quad (2.54)$$

Substituting (2.54) into (2.53),

$$S_{\text{RHA,T}} = \sqrt{K_{\text{sp}} \left(1 + K_{\text{s}}^{\text{R}} [\text{M}]\right) \left(1 + 10^{\text{pH}-\text{pK}_{\text{a,coformer}}} + K_{\text{s}}^{\text{HA}} [\text{M}] + 10^{\text{pH}-\text{pK}_{\text{a,coformer}}} K_{\text{s}}^{\text{A}^{-}} [\text{M}]\right)} \quad (2.55)$$

Substituting the total solubilization constant K_{s}^{T} :

$$S_{\text{RHA,T}} = \sqrt{K_{\text{sp}} \left(1 + K_{\text{s}}^{\text{R}} [\text{M}]\right) \left(1 + 10^{\text{pH}-\text{pK}_{\text{a,coformer}}} + K_{\text{s}}^{\text{HA,T}} [\text{M}]\right)} \quad (2.56)$$

HDHA (1:1 monoprotic weakly acidic drug HD, monoprotic weakly acidic coformer HA)

Relevant equilibria are given by:



Associated equilibrium constants are given by:

$$K_{sp} = [\text{HD}]_{\text{aq}} [\text{HA}]_{\text{aq}} \quad (2.64)$$

$$K_a^{\text{HD}} = \frac{[\text{D}^-]_{\text{aq}} [\text{H}^+]_{\text{aq}}}{[\text{HD}]_{\text{aq}}} \quad (2.65)$$

$$K_a^{\text{HA}} = \frac{[\text{A}^-]_{\text{aq}} [\text{H}^+]_{\text{aq}}}{[\text{HA}]_{\text{aq}}} \quad (2.66)$$

$$K_s^{\text{HD}} = \frac{[\text{HD}]_{\text{m}}}{[\text{HD}]_{\text{aq}} [\text{M}]} \quad (2.67)$$

$$K_s^{\text{HA}} = \frac{[\text{HA}]_{\text{m}}}{[\text{HA}]_{\text{aq}} [\text{M}]} \quad (2.68)$$

$$K_s^{\text{D}^-} = \frac{[\text{D}^-]_{\text{m}}}{[\text{D}^-]_{\text{aq}} [\text{M}]} \quad (2.69)$$

$$K_s^{\text{A}^-} = \frac{[\text{A}^-]_{\text{m}}}{[\text{A}^-]_{\text{aq}} [\text{M}]} \quad (2.70)$$

Cocrystal HDHA total solubility in solubilizing agents

Mass balance on D is given by:

$$[\text{D}]_{\text{T}} = [\text{HD}]_{\text{aq}} + [\text{D}^-]_{\text{aq}} + [\text{HD}]_{\text{m}} + [\text{D}^-]_{\text{m}} \quad (2.71)$$

Substituting (2.64), (2.65), (2.67), and (2.69) into (2.71) gives:

$$[\text{D}]_{\text{T}} = \frac{K_{sp}}{[\text{HA}]_{\text{aq}}} \left(1 + 10^{\text{pH}-\text{pKa,drug}} + K_s^{\text{HD}} [\text{M}] + 10^{\text{pH}-\text{pKa,drug}} K_s^{\text{D}^-} [\text{M}] \right) \quad (2.72)$$

Mass balance on A is given by:

$$[\text{A}]_{\text{T}} = [\text{HA}]_{\text{aq}} + [\text{A}^-]_{\text{aq}} + [\text{HA}]_{\text{m}} + [\text{A}^-]_{\text{m}} \quad (2.73)$$

Substituting (2.66), (2.68), and (2.70) into (2.73) gives:

$$[\text{A}]_{\text{T}} = [\text{HA}]_{\text{aq}} \left(1 + 10^{\text{pH}-\text{pKa,coformer}} + K_s^{\text{HA}} [\text{M}] + 10^{\text{pH}-\text{pKa,coformer}} K_s^{\text{A}^-} [\text{M}] \right) \quad (2.74)$$

Combining (2.72) and (2.74) gives:

$$[D]_T = \frac{K_{sp}}{[A]_T} \left(1 + 10^{\text{pH}-\text{pKa,drug}} + K_s^{\text{DX}} [M] + 10^{\text{pH}-\text{pKa,drug}} K_s^{\text{D}^-} [M] \right) \quad (2.75)$$

$$\left(1 + 10^{\text{pH}-\text{pKa,coformer}} + K_s^{\text{HA}} [M] + 10^{\text{pH}-\text{pKa,coformer}} K_s^{\text{A}^-} [M] \right)$$

Cocrystal solubility in stoichiometric solutions is given by:

$$S_{\text{HDHA,T}} = [D]_T = [A]_T \quad (2.76)$$

Substituting (2.75) into (2.76),

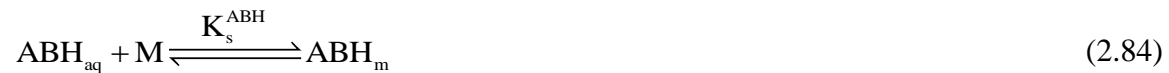
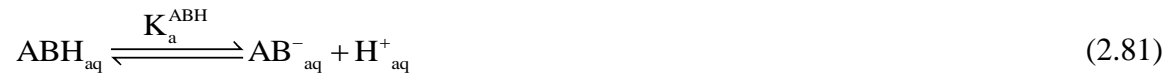
$$S_{\text{HDHA,T}} = \sqrt{K_{sp} \left(1 + 10^{\text{pH}-\text{pKa,drug}} + K_s^{\text{HD}} [M] + 10^{\text{pH}-\text{pKa,drug}} K_s^{\text{D}^-} [M] \right) \left(1 + 10^{\text{pH}-\text{pKa,coformer}} + K_s^{\text{HA}} [M] + 10^{\text{pH}-\text{pKa,coformer}} K_s^{\text{A}^-} [M] \right)} \quad (2.77)$$

Substituting K_s^T values for HD and HA:

$$S_T^{\text{HDHA}} = \sqrt{K_{sp}^{\text{HDHA}} \left(1 + 10^{\text{pH}-\text{pKa,drug}} + K_s^{\text{HD,T}} [M] \right) \left(1 + 10^{\text{pH}-\text{pKa,coformer}} + K_s^{\text{HA,T}} [M] \right)} \quad (2.78)$$

R₂HAB (2:1 monoprotic weakly basic drug R, amphoteric coformer ABH)

Relevant equilibria are given by:



Associated equilibrium constants are given by:

$$K_{sp} = [R]_{aq}^2 [ABH]_{aq} \quad (2.86)$$

$$K_a^{ABH_2^+} = \frac{[ABH]_{aq} [H^+]_{aq}}{[ABH_2^+]_{aq}} \quad (2.87)$$

$$K_a^{ABH} = \frac{[AB^-]_{aq} [H^+]_{aq}}{[ABH]_{aq}} \quad (2.88)$$

$$K_s^R = \frac{[R]_m}{[R]_{aq} [M]} \quad (2.89)$$

$$K_s^{ABH_2^+} = \frac{[ABH_2^+]_m}{[ABH_2^+]_{aq} [M]} \quad (2.90)$$

$$K_s^{ABH} = \frac{[ABH]_m}{[ABH]_{aq} [M]} \quad (2.91)$$

$$K_s^{AB^-} = \frac{[AB^-]_m}{[AB^-]_{aq} [M]} \quad (2.92)$$

Cocrystal R₂HAB total solubility in solubilizing agents

Mass balance on R is given by:

$$[R]_T = [R]_{aq} + [R]_m \quad (2.93)$$

Substituting (2.86) and (2.89) into (2.93) gives:

$$[R]_T^2 = \frac{K_{sp}}{[ABH]_{aq}} (1 + K_s^R [M])^2 \quad (2.94)$$

Mass balance on AB is given by:

$$[AB]_T = [ABH]_{aq} + [ABH_2^+]_{aq} + [AB^-]_{aq} + [ABH]_m + [ABH_2^+]_m + [AB^-]_m \quad (2.95)$$

Substituting (2.87), (2.88), and (2.90)-(2.92) into (2.95) gives:

$$[AB]_T = [ABH]_{aq} \left(\frac{1 + 10^{pH-pK_{a1,amphoteric}} + 10^{pK_{a2,amphoteric}-pH} + K_s^{ABH} [M] + 10^{pK_{a2,amphoteric}-pH} K_s^{ABH_2^+} [M]}{+10^{pH-pK_{a1,amphoteric}} K_s^{AB^-} [M]} \right) \quad (2.96)$$

Combining (2.94) and (2.96) gives

$$[R]_T^2 = \frac{K_{sp}}{[AB]_T} (1 + K_s^R [M])^2 \left(\frac{1 + 10^{pH-pK_{a1,amphoteric}} + 10^{pK_{a2,amphoteric}-pH} + K_s^{ABH} [M] + 10^{pK_{a2,amphoteric}-pH} K_s^{ABH_2^+} [M]}{+10^{pH-pK_{a1,amphoteric}} K_s^{AB^-} [M]} \right) \quad (2.97)$$

Cocrystal solubility in stoichiometric solutions of cocrystal constituents is given by:

$$S_{R_2ABH,T} = \frac{1}{2} [R]_T = [A]_T \quad (2.98)$$

Substituting equilibrium constants in terms of molar concentrations of drug:

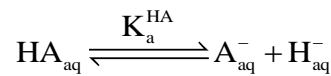
$$S_{R_2ABH,T} = 2 \sqrt[3]{\frac{K_{sp}}{4} (1 + K_s^R [M])^2 \left(\frac{1 + 10^{pH-pK_{a1,amphoteric}} + 10^{pK_{a2,amphoteric}-pH} + K_s^{ABH} [M]}{+10^{pK_{a2,amphoteric}-pH} K_s^{ABH_2^+} [M] + 10^{pH-pK_{a1,amphoteric}} K_s^{AB^-} [M]} \right)} \quad (2.99)$$

In terms of total solubilization constant K_s^T :

$$S_{R_2ABH,T} = 2 \sqrt[3]{\frac{K_{sp}^{R_2ABH}}{4} (1 + K_s^{R,T} [M])^2 (1 + 10^{pH-pK_{a1,amphoteric}} + 10^{pK_{a2,amphoteric}-pH} + K_s^{ABH,T} [M])} \quad (2.100)$$

$^-ABH^+HA$ (1:1 zwitterionic drug $^-ABH^+$, monoprotic weakly acidic cofomer HA)

Relevant equilibria are given by:





$$K_s^{\text{HA}} = \frac{[\text{HA}]_{\text{m}}}{[\text{HA}]_{\text{aq}}[\text{M}]} \quad (2.107)$$

$$K_s^{\text{A}^-} = \frac{[\text{A}^-]_{\text{m}}}{[\text{A}^-]_{\text{aq}}[\text{M}]} \quad (2.108)$$

Mass balance on ${}^{-}\text{ABH}^+$ is given by:

$$[{}^{-}\text{ABH}^+]_{\text{T}} = [{}^{-}\text{ABH}^+]_{\text{aq}} + [\text{ABH}_2^+]_{\text{aq}} + [{}^{-}\text{AB}]_{\text{aq}} + [{}^{-}\text{ABH}^+]_{\text{m}} + [\text{ABH}_2^+]_{\text{m}} + [{}^{-}\text{AB}]_{\text{m}} \quad (2.109)$$

Substituting (2.87), (2.88), and (2.90)-(2.92) into (2.95) gives:

$$[{}^{-}\text{ABH}^+]_{\text{T}} = [{}^{-}\text{ABH}^+]_{\text{aq}} \left(\frac{1 + 10^{\text{pH}-\text{pKa}_{1,\text{zwitterionic}}} + 10^{\text{pKa}_{2,\text{zwitterionic}}-\text{pH}} + K_s^{-}\text{ABH}^+ [\text{M}] + 10^{\text{pKa}_{2,\text{zwitterionic}}-\text{pH}} K_s^{\text{ABH}_2^+} [\text{M}]}{+ 10^{\text{pH}-\text{pKa}_{1,\text{zwitterionic}}} K_s^{\text{AB}^-} [\text{M}]} \right) \quad (2.110)$$

Mass balance on A is given by:

$$[\text{A}]_{\text{T}} = [\text{HA}]_{\text{aq}} + [\text{A}^-]_{\text{aq}} + [\text{HA}]_{\text{m}} + [\text{A}^-]_{\text{m}} \quad (2.111)$$

Substituting (2.66), (2.68), and (2.70) into (2.73) gives:

$$[\text{A}]_{\text{T}} = [\text{HA}]_{\text{aq}} \left(1 + 10^{\text{pH}-\text{pKa}_{\text{acid}}} + K_s^{\text{HA}} [\text{M}] + 10^{\text{pH}-\text{pKa}_{\text{acid}}} K_s^{\text{A}^-} [\text{M}] \right) \quad (2.112)$$

Combining equations:

$$[{}^{-}\text{ABH}^+]_{\text{T}} = \frac{K_{\text{sp}}}{[\text{A}]_{\text{T}}} \left(\frac{\left(1 + 10^{\text{pH}-\text{pKa}_{1,\text{zwitterionic}}} + 10^{\text{pKa}_{2,\text{zwitterionic}}-\text{pH}} + K_s^{-}\text{ABH}^+ [\text{M}] + 10^{\text{pKa}_{2,\text{zwitterionic}}-\text{pH}} K_s^{\text{ABH}_2^+} [\text{M}] \right)}{+ 10^{\text{pH}-\text{pKa}_{1,\text{zwitterionic}}} K_s^{\text{AB}^-} [\text{M}]} \right) \left(1 + 10^{\text{pH}-\text{pKa}_{\text{acid}}} + K_s^{\text{HA}} [\text{M}] + 10^{\text{pH}-\text{pKa}_{\text{acid}}} K_s^{\text{A}^-} [\text{M}] \right) \quad (2.113)$$

Cocrystal solubility in stoichiometric solutions of constituents is given by:

$$S_{-}\text{ABH}^+\text{HA,T} = [{}^{-}\text{ABH}^+]_{\text{T}} = [\text{A}]_{\text{T}} \quad (2.114)$$

Substituting X into X and substituting KsT values gives:

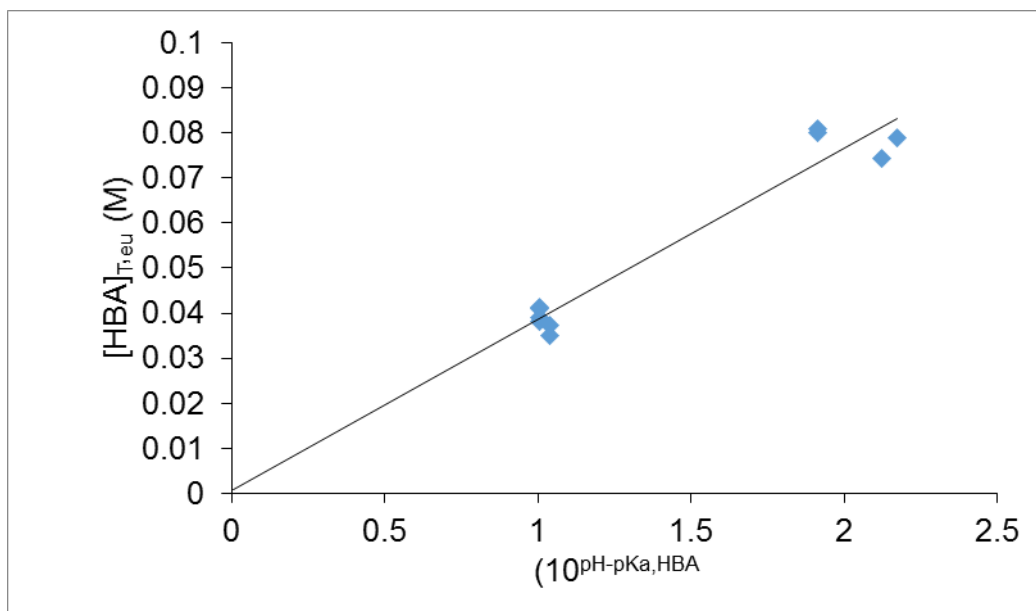
$$S_T^{-ABH^+HA} = \sqrt{K_{sp}^{-ABH^+HA} \left(1 + 10^{\text{pH}-\text{pKa}_{1,\text{zwitterionic}}} + 10^{\text{pKa}_{2,\text{zwitterionic}}-\text{pH}} + K_s^{-ABH^+,T} [\text{M}]\right) \left(1 + 10^{\text{pH}-\text{pKa}_{\text{acid}}} + K_s^{\text{HA},T} [\text{M}]\right)} \quad (2.115)$$

K_{sp} Measurements

DNZ-HBA

DNZ-HBA K_{sp} was determined by linear regression analysis of cocrystal eutectic point concentrations measured in pH 2 (10 mM phosphate) buffer, pH 5 (12 mM acetate) buffer, and unbuffered aqueous solution (water) according to the following equation:

$$[\text{HBA}]_{\text{eu}} = \frac{K_{sp}}{[\text{DNZ}]_{\text{eu}}} \left(1 + 10^{\text{pH}-\text{pKa}_{\text{HBA}}}\right) \quad (2.116)$$



Regression parameters:

	<i>Coefficients</i>	<i>Standard Error</i>	<i>t Stat</i>	<i>P-value</i>
Intercept	5.307E-04	4.915E-03	0.108	9.167E-01
X Variable 1	3.806E-02	3.259E-03	11.678	2.637E-06

<i>Regression Statistics</i>	
Multiple R	0.972
R Square	0.945
Adjusted R Square	0.938
Standard Error	5.182E-03
Observations	10

Table 2.9 shows the comparison between K_{sp} obtained by linear regression of all data points and those calculated at each specific pH measurement according to:

$$K_{sp} = [\text{DNZ}]_{eu} [\text{HBA}]_{0,eu} \quad (2.117)$$

Where

$$[\text{HBA}]_{0,eu} = \frac{[\text{HBA}]_{T,eu}}{1 + 10^{\text{pH} - \text{p}K_{a,\text{HBA}}}} \quad (2.118)$$

Table 2.9. Comparison of K_{sp} values obtained by linear regression and single point calculations for DNZ-HBA.

pH	K_{sp} (mM ²)
4.47±0.04	8.56 x 10 ⁻³
3.07±0.04	1.50 x 10 ⁻²
2.12±0.03	1.43 x 10 ⁻²
Regression (all points)	(1.1±0.4) x 10 ⁻²

DNZ-VAN

DNZ-VAN K_{sp} was determined by eutectic point measurements in pH 2 (10 mM phosphate) buffer, and pH 5 (12 mM acetate) buffer. The K_{sp} value reported is the average of the K_{sp} values determined by the two sets of eutectic point measurements:

Table 2.10. Eutectic concentrations of DNZ and VAN used to calculate K_{sp} of DNZ-VAN.

pH	$[\text{DNZ}]_{eu}$ (mM)	error	$[\text{VAN}]_{T,eu}$ (mM)	error	$[\text{VAN}]_{0,eu}$ (mM)	K_{sp} (mM ²)
4.96	1.95 x 10 ⁻⁴	3.66x10 ⁻⁶	16.1	2.66x10 ⁻²	16.0	3.13Ex10 ⁻³

4.96	2.03×10^{-4}	3.90×10^{-5}	18.5	0.226	18.5	3.75×10^{-3}
4.95	2.16×10^{-4}	3.04×10^{-5}	16.3	0.137	16.2	3.51×10^{-3}
2.15	1.96×10^{-4}	1.46×10^{-5}	21.0	2.77×10^{-2}	21.0	4.11×10^{-3}
2.18	2.19×10^{-4}	8.73×10^{-5}	20.0	5.97×10^{-2}	20.0	4.39×10^{-3}
AVERAGE						3.5×10^{-3}
STDEV						5.0×10^{-4}

PXC-SAC

PXC-SAC K_{sp} was determined by a single point eutectic measurement in pH 5 acetate buffer

Table 2.11. Eutectic concentrations of PXC and SAC used to calculate the K_{sp} of PXC-SAC.

	pH	[PXC] _{T,eu} (mM)	[PXC] _{eu0} (mM)	[SAC] _{T,eu} (mM)	[SAC] _{eu0} (mM)	K_{sp} (mM ²)
	3.64	3.55×10^{-2}	3.45×10^{-2}	93.1	2.09	7.18×10^{-2}
	3.63	3.68×10^{-2}	3.57×10^{-2}	93.4	2.14	7.63×10^{-2}
	3.64	3.61×10^{-2}	3.49×10^{-2}	97.3	2.18	7.61×10^{-2}
	3.63	3.89×10^{-2}	3.77×10^{-2}	92.6	2.12	8.00×10^{-2}
	3.63	3.56×10^{-2}	3.45×10^{-2}	94.1	2.16	7.45×10^{-2}
	3.62	3.68×10^{-2}	3.57×10^{-2}	95.4	2.23	7.97×10^{-2}
	3.64	3.53×10^{-2}	3.42×10^{-2}	94.0	2.11	7.21×10^{-2}
AVERAGE	3.632857	3.64×10^{-2}	3.53×10^{-2}	94.3	2.15	7.58×10^{-2}
STDEV	0.007559	1.24×10^{-3}	1.20×10^{-3}	1.59	5.01E-02	3.27×10^{-3}

CHAPTER 3

COCRYSTAL SUPERSATURATION DURING DISSOLUTION IN PHYSIOLOGICALLY RELEVANT SURFACTANTS

Introduction

Cocrystallization with hydrophilic cofomers has been reported to improve the solubility, dissolution, and ultimately oral absorption and bioavailability of poorly soluble hydrophobic drugs¹⁻⁶. Cocrystals that are more soluble than the drug are prone to solution-mediated phase transformation to the less soluble drug during dissolution in aqueous environments, negating any solubility enhancement benefit. Recently, synthetic formulation surfactants have been shown to impart thermodynamic stability to cocrystals of carbamazepine and indomethacin that were otherwise unstable in aqueous solution⁷⁻⁹. Cocrystal solubility increases with the concentration of solubilizing agent in solution, while the cocrystal solubility advantage over drug ($S_{\text{cocrystal}}/S_{\text{drug}}$) decreases⁷⁻⁹. This behavior is explained by the preferential solubilization of the constituent drug by the solubilizing agent compared to the cofomer. When drug is preferentially solubilized by solubilizing agents, $S_{\text{cocrystal}}/S_{\text{drug}}$ decreases, and solubilizing agent concentration can be selected to target a particular level of supersaturation⁷⁻¹¹.

Mathematical models have been derived to predict cocrystal solubility, and $S_{\text{cocrystal}}/S_{\text{drug}}$ based on the solution equilibria for cocrystal dissociation, and constituent ionization and micellar solubilization and the models confirmed by experimental data for several cocrystals in the presence of solubilizing agents. Preliminary powder dissolution studies of the indomethacin-

saccharin cocrystal in the presence of Tween 80 have explored the connection between $S_{\text{cocrystal}}/S_{\text{drug}}$ and kinetic cocrystal dissolution behavior. When $S_{\text{cocrystal}}/S_{\text{drug}}$ was reduced from 26 in aqueous solution to 6 by addition of 0.01% Tween 80, the cocrystal exhibited slowed conversion kinetics and maintained supersaturated indomethacin concentrations longer than in aqueous buffer¹⁰. There are no other reported studies to our knowledge that explore the impact of $S_{\text{cocrystal}}/S_{\text{drug}}$ reduction due to preferential solubilization on kinetic dissolution behavior of cocrystals to our knowledge. Furthermore, cocrystal dissolution is routinely evaluated in biorelevant media containing physiologically relevant solubilizing agents without any knowledge of the drug concentrations and supersaturations to anticipate.

The aim of this work was to evaluate the relationship between $S_{\text{cocrystal}}/S_{\text{drug}}$ and cocrystal powder dissolution behavior. In particular, the impact of $S_{\text{cocrystal}}/S_{\text{drug}}$ reduction due to preferential solubilization on cocrystal dissolution was explored in the physiologically relevant surfactant fed-state simulated intestinal fluid (FeSSIF). FeSSIF is routinely used in dissolution testing and it contains relatively high concentrations of sodium taurocholate and lecithin which are known to form mixed micelles in aqueous solution and solubilize hydrophobic drugs. It is hypothesized that the preferential solubilization of constituent drugs by FeSSIF will result in lower peak supersaturations, sustained supersaturated drug concentrations, and slowed or prevented transformation to drug during powder dissolution. The cocrystals studied include: 1:1 carbamazepine-saccharin (CBZ-SAC), 1:1 carbamazepine-salicylic acid (CBZ-SLC), 2:1 carbamazepine 4-aminobenzoic acid hydrate, (CBZ-4ABA-HYD), 1:1 piroxicam-saccharin (PXC-SAC), 1:1 indomethacin-saccharin (IND-SAC), 1:1 danazol-hydroxybenzoic acid (DNZ-HBA), and 1:1 danazol-vanillin (DNZ-VAN). The selected cocrystals include both 1:1 and 2:1 cocrystal stoichiometries and cover a range of ionization behaviors for both drug and coformers.

PXC is a zwitterionic drug with pKa values of 1.86 and 5.46¹², and IND is a monoprotic weakly acidic drug with a pKa of 4.2¹³. SAC is a monoprotic weak acid with pKa values reported between 1.6-2.2¹⁴, SLC is a monoprotic weak acid with a reported pKa value of 3.0¹⁴, 4ABA is amphoteric with pKa values 2.6 and 4.8¹⁵, HBA is a monoprotic weak acid with a reported pKa value of 4.48¹⁶ and VAN is a monoprotic weak acid with a pKa of 7.4¹⁶.

Theoretical

Calculation of cocrystal solubility and thermodynamic stability from eutectic point measurements

The stoichiometric solubility of the cocrystals (cocrystal at equilibrium with solution concentrations of constituents equal to their molar ratio) is calculated total eutectic concentrations by the following equations for 1:1 and 2:1 cocrystals¹⁷:

$$S_T^{1:1 \text{ cocrystal}} = \sqrt{[\text{drug}]_{T,\text{eu}} [\text{coformer}]_{T,\text{eu}}} \quad (3.1)$$

$$S_T^{2:1 \text{ cocrystal}} = 2 \left(\sqrt[3]{\frac{[\text{drug}]_{T,\text{eu}}^2 [\text{coformer}]_{T,\text{eu}}}{4}} \right) \quad (3.2)$$

$[\text{constituent}]_{T,\text{eu}}$ is defined as the sum of the concentrations of all species dissolved at the eutectic point ($[\text{constituent}]_{T,\text{eu}} = [\text{constituent}]_{\text{aq,eu}} + [\text{constituent}]_{\text{m,eu}}$) in the presence of a solubilizing agent. $[\text{constituent}]_{\text{aq,eu}}$ represents the total aqueous concentration at a particular pH in the absence of solubilizing agent ($[\text{constituent}]_{\text{aq,eu}} = [\text{constituent}]_{\text{nonionized,aq,eu}} + [\text{constituent}]_{\text{ionized,aq,eu}}$) and is the sum of the nonionized and ionized contributions to the eutectic concentration. $[\text{constituent}]_{\text{m,eu}}$ represents the cocrystal solubilized by solubilizing agents ($[\text{constituent}]_{\text{m,eu}} = [\text{constituent}]_{\text{nonionized,m,eu}} + [\text{constituent}]_{\text{ionized,s,eu}}$) and contributions from the

ionized species as appropriate. These methods of accessing cocrystal equilibrium solubility in nonstoichiometric conditions are well established in the literature^{7-9, 17, 18}.

The cocrystal thermodynamic stability can be calculated from the drug and coformer eutectic concentrations by calculating the eutectic constant, K_{eu} . K_{eu} is a directly measurable parameter calculated according to¹⁹:

$$K_{eu} = \frac{[\text{coformer}]_{T,eu}}{[\text{drug}]_{T,eu}} \quad (3.3)$$

The eutectic constant is related to the cocrystal thermodynamic stability, also called the cocrystal solubility advantage ($S_{\text{cocrystal}}/S_{\text{drug}}$). For cocrystal A_xB_y , where A and B are the cocrystal constituents, drug and coformer respectively; and x and y are the stoichiometric coefficients or molar ratios, K_{eu} is a function of $S_{\text{cocrystal}}/S_{\text{drug}}$ as follows^{17, 19}:

$$K_{eu} = \frac{[\text{coformer}]_{T,eu}}{[\text{drug}]_{T,eu}} = xy^{\frac{x}{y}} \left(\frac{S_{\text{cocrystal}}}{S_{\text{drug}}} \right)^{\frac{(x+y)}{y}} \quad (3.4)$$

This relationship is valid in both aqueous and solubilizing agent solutions as it relies on the total measured eutectic concentrations of drug and coformer in the conditions of interest.

$S_{\text{cocrystal}}/S_{\text{drug}}$ in the presence of a solubilizing agent can be predicted using the full cocrystal and drug solubility equations¹⁰. For a 1:1 cocrystal of a nonionizable drug R with a monoprotic weakly acidic coformer HA:

$$\left(\frac{S_{\text{cocrystal}}}{S_{\text{drug}}} \right)^{\text{RHA}} = \frac{\sqrt{K_{sp}^{\text{RHA}} \left(1 + K_{s,T}^{\text{R}} [\text{M}] \right) \left(1 + \frac{K_a^{\text{HA}}}{[\text{H}^+]} + K_{s,T}^{\text{HA}} [\text{M}] \right)}}{S_{\text{aq}}^{\text{R}} \left(1 + K_{s,T}^{\text{R}} [\text{M}] \right)} \quad (3.5)$$

For a 1:1 cocrystal of a monoprotic weakly acidic drug HD with a monoprotic weakly acidic coformer HA:

$$\left(\frac{S_{\text{cocrystal}}}{S_{\text{drug}}}\right)^{\text{HDHA}} = \frac{\sqrt{K_{\text{sp}}^{\text{HDHA}} \left(1 + \frac{K_{\text{a}}^{\text{HD}}}{[\text{H}^+]} + K_{\text{s,T}}^{\text{HD}}[\text{M}]\right) \left(1 + \frac{K_{\text{a}}^{\text{HA}}}{[\text{H}^+]} + K_{\text{s,T}}^{\text{HA}}[\text{M}]\right)}}{S_{\text{aq}}^{\text{HD}} \left(1 + \frac{K_{\text{a}}^{\text{HD}}}{[\text{H}^+]} + K_{\text{s,T}}^{\text{HD}}[\text{M}]\right)} \quad (3.6)$$

For a 1:1 cocrystal of a zwitterionic drug $^-\text{ABH}^+$ with a monoprotic weakly acidic coformer HA:

$$\left(\frac{S_{\text{cocrystal}}}{S_{\text{drug}}}\right)^{-\text{ABH}^+\text{HA}} = \frac{\sqrt{K_{\text{sp}}^{-\text{ABH}^+\text{HA}} \left(1 + \frac{K_{\text{a1}}^{-\text{ABH}^+}}{[\text{H}^+]} + \frac{[\text{H}^+]}{K_{\text{a2}}^{-\text{ABH}^+}} + K_{\text{s}}^{-\text{ABH}^+,\text{T}}[\text{M}]\right) \left(1 + \frac{K_{\text{a}}^{\text{HA}}}{[\text{H}^+]} + K_{\text{s}}^{\text{HA},\text{T}}[\text{M}]\right)}}{S_{\text{aq}}^{-\text{ABH}^+} \left(1 + \frac{K_{\text{a1}}^{-\text{ABH}^+}}{[\text{H}^+]} + \frac{[\text{H}^+]}{K_{\text{a2}}^{-\text{ABH}^+}} + K_{\text{s}}^{-\text{ABH}^+,\text{T}}[\text{M}]\right)} \quad (3.7)$$

For a 2:1 cocrystal of a nonionizable drug with an amphoteric coformer:

$$\left(\frac{S_{\text{cocrystal}}}{S_{\text{drug}}}\right)^{\text{R}_2\text{ABH}} = \frac{2\sqrt[3]{\frac{K_{\text{sp}}^{\text{R}_2\text{ABH}}}{4} \left(1 + K_{\text{s}}^{\text{R},\text{T}}[\text{M}]\right)^2 \left(1 + \frac{K_{\text{a1}}^{\text{ABH}}}{[\text{H}^+]} + \frac{[\text{H}^+]}{K_{\text{a2}}^{\text{ABH}}} + K_{\text{s}}^{\text{ABH},\text{T}}[\text{M}]\right)}}{S_{\text{aq}}^{\text{R}} \left(1 + K_{\text{s},\text{T}}^{\text{R}}[\text{M}]\right)} \quad (3.8)$$

Equations (3.5)-(3.8) take into account the total solubilization of ionizable components, as indicated by total solubilization constants at a defined pH, or K_{s}^{T} . K_{s}^{T} definitions and derivations can be found in the Appendix of Chapter 2.

$S_{\text{cocrystal}}/S_{\text{drug}}$ in FeSSIF and in buffer can be experimentally determined by two methods.

Method 1: $S_{\text{cocrystal}}/S_{\text{drug}}$ can be calculated from the experimentally determined K_{eu} as described by equation (3.4) from measured eutectic point drug and coformer concentration measurements.

Method 2: $S_{\text{cocrystal}}/S_{\text{drug}}$ can be calculated from $S_{\text{cocrystal}}$ measured at the eutectic point as described by equations (3.1) and (3.2) and from S_{drug} measured in the absence of coformer (drug

solid phase only), but corrected for pH to be at the pH of the cocrystal solubility measurement (pH_{eu}). This ensures that the $S_{\text{cocrystal}}$ and S_{drug} pH conditions to be equivalent. The main difference between these two methods is that in Method 1, the drug solubility is measured in the presence of coformer at the eutectic point. At the eutectic point, drug solid phase and cocrystal solid phase are in equilibrium with the solution, so high coformer concentrations in solution are possible. In Method 2, the drug solubility is measured in equilibrium with solid phase only, and in the absence of coformer in solution. If the presence of coformer affects the drug solubility, the $S_{\text{cocrystal}}/S_{\text{drug}}$ values obtained by these two methods will vary. Under stoichiometric conditions, the concentration of coformer in solution will be less than the coformer concentration present at the eutectic point (Method 1), but higher than no coformer at all (Method 2). Comparison of the $S_{\text{cocrystal}}/S_{\text{drug}}$ obtained by these two methods will show of the range of $S_{\text{cocrystal}}/S_{\text{drug}}$ values that can be anticipated for the cocrystals studied and reveal the possible sources of error in their calculation.

$S_{\text{cocrystal}}/S_{\text{drug}}$ in FeSSIF and in buffer can also be predicted from the reported or experimentally determined equilibrium constants (K_{sp} , $\text{p}K_{\text{a}}$, K_{s}^{T} , $S_{\text{aq}}^{\text{drug}}$) as well as the solution conditions of interest (pH, [M]) as described by equations (3.6)-(3.8). These models are useful to predict $S_{\text{cocrystal}}/S_{\text{drug}}$ in conditions that the cocrystal and/or drug solubility have not yet been measured.

Materials and Methods

Materials

Cocrystal constituents

Anhydrous carbamazepine form III (CBZ), anhydrous indomethacin form γ (IND) were purchased from Sigma Chemical Company (St. Louis, MO) and used as received. Anhydrous

piroxicam form I was received as a gift from Pfizer (Groton, CT) and used as received.

Anhydrous danazol was received as a gift from Renovo Research (Atlanta, GA) and used as received.

Anhydrous saccharin (SAC), 4- aminobenzoic acid (4ABA), and salicylic acid (SLC), were purchased from Sigma Chemical Company (St. Louis, MO) and used as received.

Anhydrous hydroxybenzoic acid was purchased from Acros Organics (Pittsburgh, PA) and used as received. Anhydrous vanillin was purchased from Fisher Scientific (Fair Lawn, NJ) and used as received. Carbamazepine dihydrate (CBZ (H)), piroxicam monohydrate (PXC (H)), and hydroxybenzoic acid monohydrate (HBA (H)) were prepared by slurring CBZ, PXC, and HBA in deionized water for at least 24 hours. All crystalline drugs and cofomers were characterized by X-ray power diffraction (XRPD) and differential scanning calorimetry (DSC) before carrying out experiments.

Solvents and buffer components

Ethyl acetate and ethanol were purchased from Acros Organics (Pittsburgh, PA) and used as received, and HPLC grade methanol and acetonitrile were purchased from Fisher Scientific (Pittsburgh, PA). Trifluoroacetic acid spectrophometric grade 99% was purchased from Aldrich Company (Milwaukee, WI) and phosphoric acid ACS reagent 85% was purchased from Sigma Chemical Company (St. Louis, MO). Water used in this study was filtered through a double deionized purification system (Milli Q Plus Water System) from Millipore Co. (Bedford, MA).

FeSSIF and acetate buffer were prepared using sodium taurocholate (NaTC) purchased from Sigma Chemical Company (St. Louis, MO), lecithin purchased from Fisher Scientific (Pittsburgh, PA), sodium hydroxide pellets (NaOH) purchased from J.T. Baker (Philipsburg, NJ), and acetic acid and potassium chloride (KCl) purchased from Acros Organics (Pittsburgh, PA).

Methods

FeSSIF and acetate buffer preparation

FeSSIF and acetate buffer were prepared according to the protocol of Galia and coworkers²⁰. Acetate buffer was prepared as a stock solution at room temperature by dissolving 8.08 g NaOH (pellets), 17.3 g glacial acetic acid and 23.748 g NaCl in 2 L of purified water. The pH was adjusted to 5.00 with 1 N NaOH and 1N HCl. FeSSIF was prepared by dissolving 0.41 g sodium taurocholate in 12.5 mL of pH 5 acetate buffer. 0.148 g lecithin was added with magnetic stirring at 37 °C until dissolved. The volume was adjusted to exactly 50 mL with acetate buffer.

Cocrystal synthesis

Cocrystals were prepared by the reaction crystallization method²¹ at 25°C. The 1:1 indomethacin-saccharin cocrystal (IND-SAC) was synthesized by adding stoichiometric amounts of cocrystal components (IND and SAC) to nearly saturated SAC solution in ethyl acetate. The 1:1 carbamazepine saccharin cocrystal (CBZ-SAC) was prepared by adding stoichiometric amounts of cocrystal components (CBZ and SAC) to nearly saturated SAC solution in ethanol. The 1:1 carbamazepine-salicylic acid cocrystal (CBZ-SLC) was prepared by adding stoichiometric amounts of cocrystal components (CBZ and SLC) to nearly saturated SLC solution in acetonitrile. The 2:1 carbamazepine-4-aminobenzoic acid monohydrate cocrystal (CBZ-4ABA (H)) was prepared by suspending stoichiometric amounts of cocrystal components (CBZ and 4ABA) in a 0.01M 4ABA aqueous solution at pH 3.9. The 1:1 piroxicam-saccharin cocrystal (PXC-SAC) was prepared by adding stoichiometric amounts of cocrystal components (PXC and SAC) to nearly saturated SAC in acetonitrile. The 1:1 danazol-hydroxybenzoic acid cocrystal (DNZ-HBA) was prepared by adding stoichiometric amounts of cocrystal components (DNZ and HBA) to nearly saturated HBA solution in ethyl acetate. The 1:1 danazol-vanillin

cocrystal (DNZ-VAN) was prepared by adding stoichiometric amounts of cocrystal components (DNZ and VAN) to nearly saturated VAN solution in ethyl acetate. Prior to carrying out any solubility experiments, solid phases were characterized by XRPD and DSC and stoichiometry verified by HPLC. Full conversion to cocrystal was observed in 24 hours.

Solubility measurements of cocrystal constituents

Cocrystal constituent solubilities were measured in FeSSIF and pH 5.00 acetate buffer (FeSSIF without NaTC and lecithin). Solubilities of cocrystal constituents were determined by adding excess solid (drug or coformer) to 3 mL of media (FeSSIF or buffer). Solutions were magnetically stirred and maintained at $25 \pm 0.1^\circ\text{C}$ using a water bath for up to 96 h. At 24 hr intervals, 0.30 mL of samples were collected, pH of solutions measured, and filtered through a $0.45 \mu\text{m}$ pore membrane. After dilution with mobile phase, solution concentrations of drug or coformer were analyzed by HPLC. The equilibrium solid phases were characterized by XRPD and DSC.

Cocrystal solubility measurements

Cocrystal equilibrium solubilities were measured in FeSSIF and pH 5.00 acetate buffer (FeSSIF without NaTC and lecithin) at the eutectic point, where drug and cocrystal solid phases are in equilibrium with solution. The eutectic point between cocrystal and drug was approached by cocrystal dissolution (suspending solid cocrystal (~100 mg) and drug (~50 mg) in 3 mL of media (FeSSIF or buffer)) and by cocrystal precipitation (suspending solid cocrystal (~50 mg) and drug (~100 mg) in 3 mL of media (FeSSIF or buffer) nearly saturated with coformer). Solutions were magnetically stirred and maintained at $25 \pm 0.1^\circ\text{C}$ using a water bath for up to 96 h. At 24 hr intervals, 0.30 mL aliquots of suspension were collected, pH was measured, before filtration through a $0.45 \mu\text{m}$ pore membrane. Solid phases were also collected at 24 hr intervals

to ensure the sample was at the eutectic point (confirmed by presence of both drug and cocrystal solid phases and constant [coformer] and [drug] solution concentrations). After dilution of filtered solutions with mobile phase, drug and coformer concentrations were analyzed by HPLC. The equilibrium solid phases were characterized by XRPD and DSC.

Calculation of $S_{\text{cocrystal}}/S_{\text{drug}}$

$S_{\text{cocrystal}}/S_{\text{drug}}$ in FeSSIF and in buffer was experimentally determined by two methods.

Method 1: $S_{\text{cocrystal}}/S_{\text{drug}}$ was calculated from the experimentally determined K_{eu} as described by equation (3.4) from measured eutectic point drug and coformer concentration measurements.

This is described in more detail in the theoretical section. Method 2: $S_{\text{cocrystal}}/S_{\text{drug}}$ was calculated from $S_{\text{cocrystal}}$ measured at the eutectic point as described by equations (3.1) and (3.2) and from S_{drug} measured in the absence of coformer (drug solid phase only), but corrected for pH to be at the pH of the cocrystal solubility measurement (pH_{eu}).

$S_{\text{cocrystal}}/S_{\text{drug}}$ in FeSSIF and in buffer was also predicted from the reported or experimentally determined equilibrium constants (K_{sp} , pK_{a} , K_{s}^{T} , $S_{\text{aq}}^{\text{drug}}$) as well as the solution conditions of interest (pH, [M]) as described by equations (3.6)-(3.8) in the theoretical section.

Cocrystal dissolution studies

250 mg of sieved cocrystal (45-106 μm) was suspended in 30 mL of FeSSIF or acetate buffer at $25 \pm 0.1^\circ\text{C}$. The resulting slurry was stirred at 150 rpm using an overhead impeller stirrer. Aliquots were withdrawn at predetermined time points and filtered through a 0.45 μm PVDF syringe filter. Solution concentrations were analyzed by HPLC. Final solid phases after 4 hours were characterized by XRPD and DSC.

X-ray powder diffraction

X-ray powder diffraction diffractograms of solid phases were collected on a benchtop Rigaku Miniflex X-ray diffractometer (Rigaku, Danverse, MA) using Cu K α radiation ($\lambda=1.54\text{\AA}$), a tube voltage of 30 kV, and a tube current of 15 mA. Data were collected from 5 to 40° at a continuous scan rate of 2.5°/min.

Thermal analysis

Solid phases collected from the slurry studies were dried at room temperature and analyzed by differential scanning calorimetry (DSC) using a TA instrument (Newark, DE) 2910MDSC system equipped with a refrigerated cooling unit. DSC experiments were performed by heating the samples at a rate of 10 °C/min under a dry nitrogen atmosphere. A high purity indium standard was used for temperature and enthalpy calibration. Standard aluminum sample pans were used for all measurements.

High performance liquid chromatography

Solution concentrations were analyzed by a Waters HPLC (Milford, MA) equipped with an ultraviolet-visible spectrometer detector. For the IND-SAC and CBZ-SAC, CBZ-SLC, CBZ-4ABA-HYD cocrystals and their components, a C18 Thermo Electron Corporation (Quebec, Canada) column (5 μm , 250 x 4.6 mm) at ambient temperature was used. For the IND-SAC cocrystal, the injection volume was 20 μl and analysis conducted using an isocratic method with a mobile phase composed of 70% acetonitrile and 30% water with 0.1% trifluoroacetic acid and a flow rate of 1 ml/min. Absorbance of IND and SAC were monitored at 265 nm. For the CBZ cocrystals, the injection volume was 20 μl and analysis conducted using an isocratic method with a mobile phase composed of 55% methanol and 45% water with 0.1% trifluoroacetic acid and a flow rate of 1 mL/min. Absorbance was monitored as follows:

CBZ and 4ABA at 284 nm, SAC at 265 nm, and SLC at 303 nm. For the PXC-SAC, DNZ-HBA, and DNZ-VAN cocrystals and their components, a C18 Waters Atlantis (Milford, MA) column (5 μ M 250 x 6 mm) at ambient temperature was used. For PXC-SAC, the injection volume was 20 μ L and analysis was conducted using an isocratic method with a mobile phase composed of 70% methanol and 30% water with 0.3% phosphoric acid and a flow rate of 1 mL/min. Absorbance of PXC was monitored at 340 nm and SAC at 240 nm. For the DNZ cocrystals, the injection volume was 20 μ L in FeSSIF experiments, and 100 μ L in buffer experiments due to the extremely low solubility of DNZ in aqueous solutions. Analysis was conducted using an isocratic method composed of 80% methanol and 20% water with 0.1% trifluoroacetic acid and a flow rate of 1 mL/min. Absorbance of DNZ was monitored at 285 nm, HBA at 242 nm, and VAN at 300 nm. For all cocrystals, the Waters' operation software Empower 2 was used to collect and process data.

Results

Drug solubility

Comparison of drug solubility measured at the eutectic point and drug solubility measured in the absence of coformer, or in equilibrium with drug solid phase only is presented in the Appendix of Chapter 2. For the purpose of comparing deviations in $S_{\text{cocrystal}}/S_{\text{drug}}$ values obtained from Methods 1 and 2, drug solubility values measured in the presence of coformer at the eutectic point (for Method 1), measured in the absence of coformer, and in the absence of coformer at the pH of the eutectic point measurement (Method 2) are presented in Table 3.1.

Table 3.1. Comparison of drug solubility values measured at the eutectic point (in the presence of coformer in solution) and in the absence of coformer.

Media	Cocrystal	$S_{\text{drug,eu}}^a$	pH_{eu}	S_{drug}^b	pH	$S_{\text{drug at pH}_{\text{eu}}}^c$
buffer	CBZ-SAC	0.78±0.05	3.08±0.03	0.42±0.02	4.95±0.01	0.42±0.02
	CBZ-SLC	0.51±0.02	4.37±0.02	0.42±0.02	4.95±0.01	0.42±0.02
	CBZ-4ABA- HYD	0.44±0.02	4.84±0.03	0.42±0.02	4.95±0.01	0.42±0.02
	PXC-SAC	(3.64±0.01)×10 ⁻²	3.64±0.02	(3.1±0.1)×10 ⁻²	4.98±0.01	(2.4±0.1)×10 ⁻²
	IND-SAC	(6.0±0.3)×10 ⁻³	3.66±0.02	(2.3±0.1)×10 ⁻³	4.96±0.03	(4.3±0.2)×10 ⁻³
	DNZ-HBA	(2.0 ±0.4)×10 ⁻⁴	4.47±0.04	(1.6±0.2)×10 ⁻⁴	4.96±0.01	(1.6±0.2)×10 ⁻⁴
	DNZ-VAN	(2.1±0.1)×10 ⁻⁴	4.96±0.01	(1.6±0.2)×10 ⁻⁴	4.96±0.01	(1.6±0.2)×10 ⁻⁴
FeSSIF	CBZ-SAC	1.07±0.03	3.11±0.02	0.75±0.02	4.86±0.05	0.75±0.02
	CBZ-SLC	0.91±0.02	4.29±0.02	0.75±0.02	4.86±0.05	0.75±0.02
	CBZ-4ABA- HYD	0.74±0.03	4.94±0.02	0.75±0.02	4.86±0.05	0.75±0.02
	PXC-SAC	(6.80±0.06)×10 ⁻²	3.79±0.02	(6.0±0.3)×10 ⁻²	5.03±0.02	(5.0±0.3)×10 ⁻²
	IND-SAC	(1.5±0.2)×10 ⁻¹	3.65±0.05	(3.7±0.2)×10 ⁻¹	4.97±0.06	(7.3 ±0.2)×10 ⁻²
	DNZ-HBA	(9.9±0.8) ×10 ⁻²	4.46±0.06	(1.11±0.09) ×10 ⁻¹	5.01±0.05	1.11±0.09) ×10 ⁻¹
	DNZ-VAN	(1.0±0.2)×10 ⁻¹	5.00±0.01	(1.11±0.09) ×10 ⁻¹	5.01±0.05	1.11±0.09) ×10 ⁻¹

(a) Measured at the eutectic point in the presence of cocrystal and drug solid phases and in equilibrium with solution.

(b) Measured independently in the presence of only drug solid phase in equilibrium with solution.

(c) Calculated from the drug solubility values measured independently to be at the pH_{eu} .

Drug solubility can be influenced by both the coformer concentration at the eutectic point and the pH differences between the solubility measurements in the absence and the presence of coformer. The presence of excess coformer in solution at the eutectic point can alter the pH of the media when coformers are ionizable, which is the case for most of the systems studied in this work.

CBZ solubility is unaffected by pH differences (as it is nonionizable) and is not affected significantly by the presence of coformer except for the case of SAC. The extremely high SAC concentration at the eutectic point Table 3.1 actually increases the solubility of CBZ in aqueous buffer. The CBZ solubility at the eutectic point was 0.78 mM in presence of SAC, which is nearly double the CBZ solubility measured independently in pH 5 aqueous buffer (0.42 mM). This was confirmed by an independent solubility experiment where CBZ solubility (0.75 mM) was measured in a high SAC concentration without the presence of cocrystal.

For IND, the difference between the independently measured and eutectic point solubility is partially due to a pH difference between the two experimental conditions. IND is a weak acid with a pK_a of 4.2. The eutectic pH values are around 3.65 while the pH of the independent solubility measurement is around 5.00. Therefore, IND concentrations in FeSSIF at $pH < pK_a$ are two fold lower than at $pH > pK_a$ (0.15 mM at pH 3.65 vs. 0.37 mM at pH 4.97). In buffer, however, this pH effect is overshadowed by supersaturated IND concentrations. In buffer, IND-SAC is 132 times more soluble than IND, and it is likely that the eutectic point measurement had supersaturated IND concentrations due to this large solubility advantage. The growth of a higher energy (and solubility) form of IND from supersaturated solutions has been shown to increase IND solubility by as much as 3 fold from highly supersaturated solutions⁴⁹.

PXC and DNZ do not have large differences in the drug solubility in the absence or in the presence of coformer. The drug solubility values measured independently and at the eutectic point are in good agreement. For DNZ, there is not a large solubility difference between the values measured at the eutectic point versus those measured in the absence of coformer as shown in Table 3.1; however, DNZ has a very low solubility in aqueous buffer (on the order of 10^{-4} mM), and even small changes in S_{buffer} lead to moderate differences in $S_{\text{cocystal}}/S_{\text{drug}}$. The impact of these differences in $S_{\text{cocystal}}/S_{\text{drug}}$ will be examined in a subsequent section.

Cocystal solubility

A comprehensive discussion of cocystal solubility and solubility prediction in the presence of physiologically relevant surfactants has been presented in Chapter 2 of this dissertation. The solubility of a cocystal is the highest theoretical concentration that can be attained during cocystal dissolution assuming the dose of the cocystal is sufficient to reach the solubility. The solubility may not be reached during dissolution if the dose is too low, if cocystal undergoes solution-mediated transformation to a more stable and less soluble solid form, and if the time-frame of the dissolution study is too short to reach equilibrium. Nevertheless, knowledge of cocystal solubility under dissolution conditions is useful to anticipate the concentrations that may be achieved during cocystal dissolution in stoichiometric conditions. From eutectic measurements in FeSSIF and buffer, the stoichiometric cocystal solubility can be calculated from the experimentally drug and coformer eutectic concentrations using equation (3.1) and (3.2). All the cofomers studied in this work have ionizable acidic groups, and excess coformer in solution at the eutectic point leads to a reduction in pH compared to the pH under stoichiometric conditions and/or the starting pH. During dissolution in stoichiometric conditions, the bulk solution pH will likely remain close to the initial starting pH

of the dissolution media, so the cocrystal solubility at pH 5.00 was predicted and compared to the measured solubility at the eutectic point in Table 3.2.

Table 3.2. Cocrystal constituent eutectic concentrations and stoichiometric solubility at the eutectic point compared to solubility at pH 5.00.

Media	Cocrystal	[drug] _{eu} (mM)	[coformer] _{eu} (mM)	S _{cocrystal} (mM) ^a	pH _{eu}	S _{cocrystal} at pH 5.00 ^b (mM)
buffer	DNZ-VAN	(2.1±0.1)x10 ⁻⁴	16±3	(5.7±0.2)x10 ⁻²	4.96±0.01	5.9x10 ⁻²
	DNZ-HBA	(2.0±0.4)x10 ⁻⁴	79±4	(1.2±0.1)x10 ⁻¹	4.47±0.04	0.22
	CBZ-4ABA (H)	(4.4±0.2)x10 ⁻¹	13.1±0.4	1.73±0.06	4.84 ± 0.03	1.8
	IND-SAC	(6.0±0.3)x10 ⁻²	104±20	(7.9±0.3)x10 ⁻²	3.66 ± 0.02	5.0
	CBZ-SLC	(5.1±0.2)x10 ⁻¹	49.8±0.9	5.1±0.1	4.37 ± 0.02	11
	PXC-SAC	(3.64±0.01)x10 ⁻²	94±2	1.85±0.03	3.64 ±0.02	16
	CBZ-SAC	(7.8±0.5)x10 ⁻¹	124±3	9.8±0.3	3.08 ± 0.03	50
FeSSIF	DNZ-VAN	(1.0±0.2)x10 ⁻¹	19.4±0.8	1.39±0.03	5.00±0.01	1.7
	DNZ-HBA	(9.9±0.8)x10 ⁻²	78±1	2.8±0.1	4.46±0.06	6.0
	CBZ-4ABA (H)	(7.4±0.3)x10 ⁻¹	15.6±0.4	2.57±0.05	4.94 ± 0.02	2.9
	IND-SAC	(1.50±0.2)x10 ⁻¹	87±4	3.6±0.2	3.65 ± 0.05	21
	CBZ-SLC	(9.1±0.2)x10 ⁻¹	49.9±0.6	6.71±0.09	4.29 ± 0.02	14
	PXC-SAC	(6.80±0.06)x10 ⁻²	97±1	2.60±0.03	3.79 ±0.02	22
	CBZ-SAC	1.07±0.03	95.9±0.3	10.1±0.1	3.11 0.02	67

(a) Calculated from measured constituent eutectic concentrations using equation (3.1) for 1:1 cocrystals and (3.2) for 2:1 cocrystals.

(b) Calculated using the equations in Table 2.2, K_{sp} values in Table 2.3, and pK_a and K_s^T values in Table 2.5.

All measured cocrystal solubilities (Table 3.2) are higher in FeSSIF compared to buffer due to micellar solubilization except for CBZ-SAC, which was not solubilized. Cocrystal solubility increased by as much as 24 fold as for the case of DNZ-VAN, where the solubility increased from 0.057 mM to 1.39 mM in FeSSIF. At pH 5.00, cocrystal solubilities are predicted to exhibit similar increases due to micellar solubilization compared to those observed at the eutectic point, so higher concentrations of drug are anticipated during cocrystal dissolution in FeSSIF compared to aqueous buffer. If solubilities measured at the eutectic point are compared to those predicted at pH 5.00, it is clear that solubility increases as pH increases for all the cocrystals studied due to the ionization of acidic components. SAC cocrystals, in particular, exhibited large solubility increases due to the ionization of SAC. PXC-SAC solubility is predicted to increase by an order of magnitude between the eutectic pH values of 3.64-3.79 and 5.00. This large increase in cocrystal solubility at pH 5.00 compared to the eutectic point indicates that the cocrystal solubility advantage ($S_{\text{cocrystal}}/S_{\text{drug}}$) may be higher in dissolution conditions than those measured at the eutectic point. This increase in solubility advantage due to ionization can lead to the cocrystal being more unstable in dissolution conditions due to a larger thermodynamic driving force for conversion to the constituent drug. $S_{\text{cocrystal}}/S_{\text{drug}}$ and implications for dissolution of cocrystals will be discussed in a subsequent section.

Cocrystal thermodynamic stability

As described in the theoretical section, the K_{eu} is related to $S_{\text{cocrystal}}/S_{\text{drug}}$ and is a directly measurable parameter that can inform cocrystal dissolution studies. $S_{\text{cocrystal}}/S_{\text{drug}}$ is the maximum theoretical supersaturation achievable during cocrystal dissolution so knowledge of K_{eu} (and thus $S_{\text{cocrystal}}/S_{\text{drug}}$) is useful to predict this supersaturation. Figure 3.1 shows the K_{eu} for 1:1 cocrystals calculated from directly measured eutectic concentrations (Method 1) plotted

against $S_{\text{cococrystal}}/S_{\text{drug}}$ predicted using the full equations (3.5)-(3.8) under the eutectic conditions (pH, [M]) and measured or reported equilibrium constants.

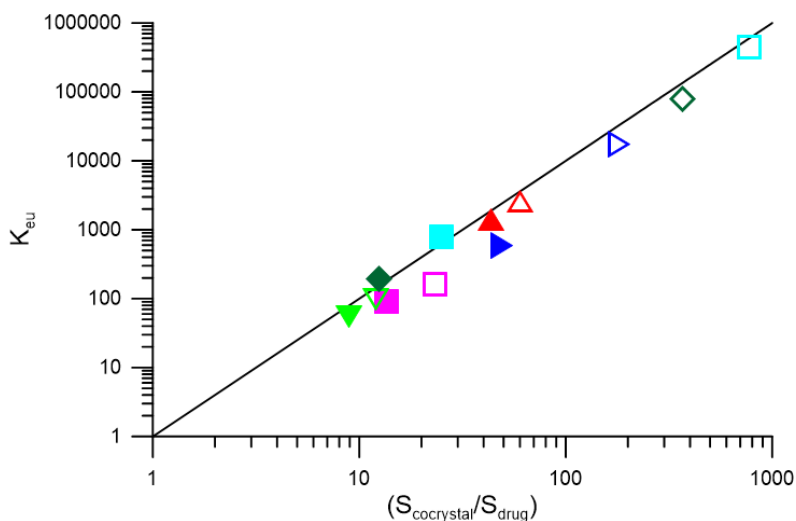


Figure 3.1. K_{eu} dependence on cococrystal solubility advantage ($S_{\text{cococrystal}}/S_{\text{drug}}$) in FeSSIF (filled symbols) and buffer (open symbols) at 25°C for 1:1 cococrystals IND-SAC (▶), CBZ-SAC (■), CBZ-SLC (▼), PXC-SAC (▲), DNZ-HBA (■), and DNZ-VAN (◆). Experimental errors fit within the size of each symbol. The line represents $K_{\text{eu}} = (S_{\text{cococrystal}}/S_{\text{drug}})^2$. K_{eu} values are experimentally determined at the eutectic point according to equation (3.3) (Method 1) and $S_{\text{cococrystal}}/S_{\text{drug}}$ values are predicted using equations (3.5)-(3.7).

Since K_{eu} and $S_{\text{cococrystal}}/S_{\text{drug}}$ values span several orders of magnitude for this set of cococrystals, results are presented in a log-log plot. The line in Figure 3.1 represents the theoretical relationship between K_{eu} and $S_{\text{cococrystal}}/S_{\text{drug}}$:

$$K_{\text{eu}} = \left(\frac{S_{\text{cococrystal}}}{S_{\text{drug}}} \right)^2 \quad (3.9)$$

Figure 3.1 shows that the experimentally measured K_{eu} values correlate with the $S_{\text{cococrystal}}/S_{\text{drug}}$ as predicted by equations (3.5)-(3.7). The relationship between K_{eu} and $S_{\text{cococrystal}}/S_{\text{drug}}$ for these 1:1 cococrystals is predicted by equation (3.9) which is represented by the line in the plot. There are slight deviations for some cococrystals, particularly where the

$S_{\text{cocystal}}/S_{\text{drug}}$ is larger than that predicted by the K_{eu} , which will be addressed in the subsequent section. Overall, $S_{\text{cocystal}}/S_{\text{drug}}$ can be reasonably estimated by calculating the K_{eu} from measured constituent eutectic concentrations.

For a 2:1 cocystal, the relationship between K_{eu} and $S_{\text{cocystal}}/S_{\text{drug}}$ is given by¹⁹:

$$K_{\text{eu}} = 4 \left(\frac{S_{\text{cocystal}}}{S_{\text{drug}}} \right)^3 \quad (3.10)$$

Where the cocystal solubility is in terms of molarity (moles of drug/L of solvent) which means the solubility of a 2:1 cocystal is in terms of drug concentration. Table 3.3 shows the comparison between the calculated $S_{\text{cocystal}}/S_{\text{drug}}$ calculated from the measured K_{eu} (Method 1), the calculated $S_{\text{cocystal}}/S_{\text{drug}}$ from cocystal solubility measured at the eutectic point and drug solubility measured in the absence of cofomer (Method 2), and those predicted from the full equations (3.5)-(3.8) at the pH of the eutectic point from reported or measured equilibrium constants.

Table 3.3. Experimentally determined K_{eu} and $S_{cocrystal}/S_{drug}$ calculated from Methods 1 and 2 compared to predicted $S_{cocrystal}/S_{drug}$ using equations (3.5)-(3.8) at the eutectic point pH.

Cocrystal	Media	K_{eu}^a	$S_{cocrystal}/S_{drug} \text{ exp}^b$	$S_{cocrystal}/S_{drug} \text{ exp}^c$	$S_{cocrystal}/S_{drug}$	pH
			Method 1	Method 2	pred ^d	
DNZ-HBA	Buffer	440000±70000	660±50	770±90	770	4.47±0.04
	FeSSIF	790±60	28±1	25±3	25	4.46±0.06
DNZ-VAN	Buffer	80000±4000	280±20	370±70	360	4.96±0.01
	FeSSIF	200±10	14±1	13±1	13	5.00±0.01
IND-SAC	Buffer	17000±900	132±4	181±3	180	3.66±0.02
	FeSSIF	600±50	24±1	49±1	38	3.65±0.05
PXC-SAC	Buffer	2600±100	51±1	78±3	60	3.64±0.04
	FeSSIF	1400±100	37±1	52±2	43	3.79±0.02
CBZ-SAC	Buffer	160±10	12.6±0.4	23±2	13.8	3.08±0.03
	FeSSIF	90±2	9.5±0.1	13.5±0.5	13.5	3.11±0.02
CBZ-SLC	Buffer	97±3	9.9±0.2	12±1	12	4.37±0.02
	FeSSIF	54±1	7.4±0.1	9.0±0.3	8.9	4.29±0.02
CBZ-4ABA-	Buffer	30±2	3.9±0.07	4.1±0.3	4.1	4.84±0.03
HYD	FeSSIF	21±1	3.5±0.1	3.4±0.1	3.4	4.94±0.02

(a) Calculated from experimentally measured constituent eutectic concentrations in Table 3.2 according to equation (3.3).

(b) Calculated using Method 1 from K_{eu} according to equation (3.9) for 1:1 cocrystals and (3.10) for 2:1 cocrystals.

(c) Calculated using Method 2 from $S_{cocrystal}$ measured at the eutectic point according to equation (3.1) for 1:1 cocrystals and equation (3.2) for 2:1 cocrystals and S_{drug} calculated at pH_{eu} from Table 3.1.

- (d) Calculated using K_{sp} values from Table 2.3, pK_a values and K_s^T values from Table 2.5 according to equations (3.5)-(3.8).

Results in Table 3.3 show the utility of K_{eu} for determining the $S_{cocrystal}/S_{drug}$ of cocrystals measured at the eutectic point. The measured $S_{cocrystal}/S_{drug}$ values calculated using Methods 1 and 2 under eutectic conditions are in reasonable agreement. Significant deviations do occur for DNZ-HBA, DNZ-VAN, IND-SAC, PXC-SAC, and CBZ-SAC due to the differences in drug solubility measured at the eutectic point to that measured independently at pH_{eu} as shown in Table 3.1. CBZ-4ABA-HYD and CBZ-SLC are well predicted as CBZ solubility did not vary significantly in the presence and absence of coformer in solution. The cocrystals studied range from 660 times more soluble than drug for DNZ-HBA to 3.9 times more soluble in aqueous buffer, and 37 times more soluble than drug for PXC-SAC to 3.5 times more soluble in FeSSIF as determined using Method 1.

Significant differences between measured $S_{cocrystal}/S_{drug}$ calculated by Method 1 and the values predicted from equilibrium constants using equations (3.5)-(3.8) do exist for some cocrystals, particularly CBZ-SAC, IND-SAC, DNZ-HBA, and DNZ-VAN. The presence of SAC at the eutectic point has been observed to decrease CBZ solubilization (described in detail in Chapter 2) which explains the discrepancy in $S_{cocrystal}/S_{drug}$ in Table 3.3 for CBZ-SAC in FeSSIF. For IND-SAC, the disagreement in $S_{cocrystal}/S_{drug}$ is likely due to the difference in S_{drug} at the eutectic point compared to that predicted by equation (3.6). As described in Chapter 2, IND solubility at the eutectic point is much higher than IND solubility in a single saturated solution in the absence of coformer. This is due to supersaturation with respect to IND (IND dissolving from cocrystal rather than from solid drug), which results in a higher S_{drug} and a lower $S_{cocrystal}/S_{drug}$ compared to that predicted by equation (3.6). DNZ-VAN deviations likely occur due to this difference in DNZ solubility at the eutectic point versus solubility in the absence of

coformer. As described, in Chapter 2, DNZ solubility measured at the eutectic point is nearly twice that measured independently, and this difference likely caused large discrepancy in $S_{\text{cococrystal}}/S_{\text{drug}}$ calculated using Method 1 and predicted using equations (3.5)-(3.8) in Table 3.3.

Equations (3.5)-(3.8) require $S_{\text{drug}}^{\text{aq}}$ values that are measured in the absence of coformer in solution as an input. The $S_{\text{cococrystal}}/S_{\text{drug}}$ values calculated by Method 2 and the predicted values using equations (3.5)-(3.8) are in good agreement for this reason.

Values in Table 3.3 reveal that $S_{\text{cococrystal}}/S_{\text{drug}}$ decreases in FeSSIF compared to aqueous buffer for many of the cococrystals studied. Figure 3.2 shows the measured $(S_{\text{cococrystal}}/S_{\text{drug}})_{\text{aq}}$ and $(S_{\text{cococrystal}}/S_{\text{drug}})_{\text{FeSSIF}}$ calculated by Method 1 for the cococrystals studied.

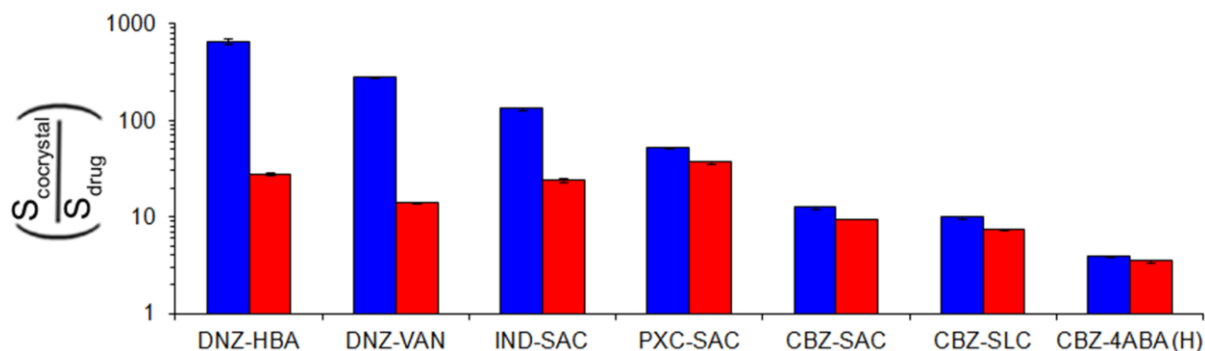


Figure 3.2. $S_{\text{cococrystal}}/S_{\text{drug}}$ values measured at pH_{eu} at 25°C in FeSSIF (■) and buffer (■). Values were calculated by Method 1 as described in the Theoretical and Methods sections using equation (3.9) for 1:1 cococrystals and equation (3.10) for 2:1 cococrystals. pH values for each measurement are in Table 3.2.

All cococrystals retain a solubility advantage over drug in both FeSSIF and buffer ($S_{\text{cococrystal}}/S_{\text{drug}} > 1$). For cococrystals of highly solubilized drugs such as DNZ and IND, the $S_{\text{cococrystal}}/S_{\text{drug}}$ is reduced dramatically in FeSSIF compared to buffer due to preferential solubilization of the drug over coformer, whereas for less solubilized drugs such as PXC and CBZ, this large reduction is not observed.

Table 3.4 shows the log P, K_s^{drug} values and $S_{\text{cococrystal}}/S_{\text{drug}}$ in buffer relative to $S_{\text{cococrystal}}/S_{\text{drug}}$ in FeSSIF calculated using Method 1.

Table 3.4. Log P, K_s^{drug} and $S_{\text{cococrystal}}/S_{\text{drug}}$ decrease in FeSSIF compared to buffer calculated using Method 1.

Cococrystal	Log P drug	K_s^{drug} (mM^{-1}) ^e	$(S_{\text{cococrystal}}/S_{\text{drug}})_{\text{buffer}} / (S_{\text{cococrystal}}/S_{\text{drug}})_{\text{FeSSIF}}$ ^f
DNZ-HBA	4.53 ^a	49±5	23
DNZ-VAN	4.53 ^a	49±5	20
IND-SAC	4.27 ^b	8.2±0.6	5.5
PXC-SAC	1.8 ^c	0.080±0.005	1.4
CBZ-SAC	2.32 ^d	0.054±0.003	1.3
CBZ-SLC	2.32 ^d	0.054±0.003	1.3
CBZ-4ABA-HYD	2.32 ^d	54±3	1.1

(a) From reference ²².

(b) From reference ²³.

(c) From reference ²⁴.

(d) From reference ²⁵.

(e) Calculated from measured drug solubilities in FeSSIF and buffer in Table 2.5 using equations (2.25)-(2.27).

(f) Calculated using Method 1 from measured K_{eu} values according to equation (3.9) for 1:1 cococrystals and (3.10) for 2:1 cococrystals.

DNZ, a very hydrophobic (log P = 4.53) and highly solubilized drug ($K_s = 4.9 \text{ mM}^{-1}$) exhibits the largest reduction in $S_{\text{cococrystal}}/S_{\text{drug}}$ in FeSSIF compared to buffer. DNZ-HBA's solubility advantage over DNZ was 23 fold lower in FeSSIF compared to buffer, while DNZ-

VAN's advantage was reduced by a factor of 20. IND, another hydrophobic ($\log P = 4.27$) and highly solubilized ($K_s = 8.2 \text{ mM}^{-1}$) drug had a large reduction in $S_{\text{cocrystal}}/S_{\text{drug}}$ in FeSSIF compared to buffer of 5.5 as well. Less hydrophobic, less solubilized drugs CBZ and PXC had lower reductions in $S_{\text{cocrystal}}/S_{\text{drug}}$ in FeSSIF for the cocrystal systems studied. $S_{\text{cocrystal}}/S_{\text{drug}}$ is the thermodynamic limit of the cocrystal solubility advantage and is a measure of the maximum supersaturation possible during cocrystal dissolution. $S_{\text{cocrystal}}/S_{\text{drug}}$ values also indicate the thermodynamic driving force for conversion from a metastable highly soluble cocrystal back to the poorly soluble, stable drug form. The large reduction in $S_{\text{cocrystal}}/S_{\text{drug}}$ in FeSSIF compared to buffer for DNZ and IND cocrystals, therefore indicate a lower driving force for conversion during dissolution in FeSSIF compared to buffer may slow or prevent transformation in these media.

As described earlier, there can be large pH differences between the eutectic point conditions and the initial pH of 5.00 of FeSSIF and blank aqueous buffer. Knowledge of $S_{\text{cocrystal}}/S_{\text{drug}}$ at pH 5.00 is essential to anticipate supersaturation values during dissolution studies in these media where the bulk pH is unlikely to vary much from initial pH. Table 3.5 shows the measured $S_{\text{cocrystal}}/S_{\text{drug}}$ in buffer and FeSSIF at the eutectic point and the calculated $S_{\text{cocrystal}}/S_{\text{drug}}$ at pH 5.00 using equations (3.5)-(3.8).

Table 3.5. $S_{\text{cocystal}}/S_{\text{drug}}$ calculated using Method 1 at the eutectic pH compared to $S_{\text{cocystal}}/S_{\text{drug}}$ predicted at pH 5.00.

Cocrystal	$S_{\text{cocystal}}/S_{\text{drug}}$ pH eu ^a			$(S_{\text{cocystal}}/S_{\text{drug}})_{\text{buffer}} / (S_{\text{cocystal}}/S_{\text{drug}})_{\text{FeSSIF}}$	$S_{\text{cocystal}}/S_{\text{drug}}$ pH 5.00 ^b			$(S_{\text{cocystal}}/S_{\text{drug}})_{\text{buffer}} / (S_{\text{cocystal}}/S_{\text{drug}})_{\text{FeSSIF}}$
	Buffer	FeSSIF	pH exp		Buffer	FeSSIF		
	DNZ-HBA	660±50	28±1		4.46±0.06	23	1400±100	
DNZ-VAN	280±6	14±1	5.00±0.01	20	380±40	16±2	25	
IND-SAC	132 ± 4	24 ± 1	3.65±0.05	5.5	220±40	57±7	7	
PXC-SAC	52± 1	37 ± 1	3.79±0.02	1.4	520±60	370±40	1.5	
CBZ-SAC	12.6 ± 0.4	9.5 ± 0.1	3.11±0.02	1.3	120±10	89±2	1.3	
CBZ-SLC	9.9 ± 0.2	7.4 ± 0.1	4.29±0.02	1.3	25±1	19±1	1.3	
CBZ-4ABA HYD	3.9 ± 0.1	3.5 ± 0.1	4.94±0.04	1.1	4.4±0.1	3.8±0.1	1.2	

(a) Calculated using Method 1 from measured eutectic drug and coformer concentrations using equations (3.9) for 1:1 cocrystals and (3.10) for 2:1 cocrystals

(b) Predicted using equations (3.5)-(3.8), K_{sp} values from Table 2.3 and pK_a and K_s^T values from Table 2.5.

Table 3.5 shows that the solubility advantage of these cocrystals increases as pH increases due to the ionization of acidic cocrystal components. $S_{\text{cocystal}}/S_{\text{drug}}$ for all cocrystals studied were higher at pH 5.00 compared to the experimental pH at the eutectic point. Though the $S_{\text{cocystal}}/S_{\text{drug}}$ changed by as much as an order of magnitude between the eutectic pH and pH 5.00, as in the case of PXC-SAC, the decrease of $S_{\text{cocystal}}/S_{\text{drug}}$ in FeSSIF compared to buffer was similar at pH 5.00 compared to the eutectic point for the cocrystals studied. Similar to $S_{\text{cocystal}}/S_{\text{drug}}$ values at the eutectic pH, highly solubilized, hydrophobic drugs like DNZ and IND

exhibited larger decreases in solubility advantage at pH 5.00 compared to PXC and CBZ. IND-SAC and PXC-SAC were selected for powder dissolution testing in FeSSIF and buffer to assess the impact that a reduced $S_{\text{cocrystal}}/S_{\text{drug}}$ in FeSSIF compared to buffer has on the dissolution profile and transformation kinetics.

Cocrystal dissolution and supersaturation

IND-SAC and PXC-SAC were selected for powder dissolution testing to examine the impact of $S_{\text{cocrystal}}/S_{\text{drug}}$ reduction due to preferential micellar solubilization on the powder dissolution profile, supersaturation generated during dissolution, and transformation kinetics. Since IND-SAC exhibited a relatively large decrease in $S_{\text{cocrystal}}/S_{\text{drug}}$ in FeSSIF compared to buffer (5.5 fold lower at eutectic and 7 fold lower at pH 5.00), it is predicted that the driving force for transformation will be reduced in FeSSIF compared to buffer, leading to a slower transformation to parent drug. On the other hand, PXC-SAC, which had a relatively small decrease in $S_{\text{cocrystal}}/S_{\text{drug}}$ in FeSSIF compared to buffer (1.4 fold lower at eutectic, 1.5 fold at pH 5.00), is not predicted to have a large difference in dissolution profile in FeSSIF compared to aqueous buffer because the driving force for transformation is relatively unchanged.

Figure 3.3a shows the powder dissolution profile of IND-SAC in FeSSIF and buffer.

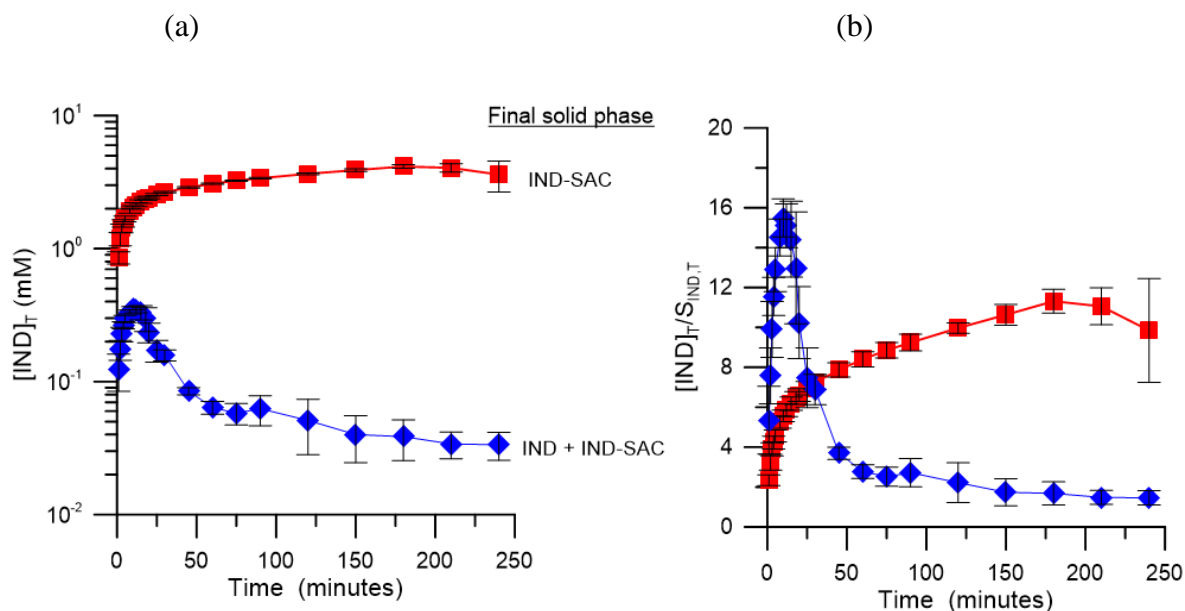


Figure 3.3. IND-SAC dissolution in FeSSIF (■) and buffer (◆) at 25°C. (a) $[IND]_T$ vs time profile for dissolution and (b) supersaturation generated by IND-SAC during dissolution ($[IND]_T/S_T^{IND}$).

As predicted by solubility values in Table 3.2, IND-SAC obtains and maintains a higher drug solution concentration in FeSSIF compared to buffer (Figure 3.3a). IND-SAC achieves a maximum concentration of 4.1 mM in FeSSIF which remains relatively constant for the duration of the experiment. This is less than the predicted solubility of 21 mM in Table 3.2, but it is unlikely that the cocrystal reached equilibrium during the four hour experiment. The solid phase at the end of the experiment was observed to be pure IND-SAC, indicating no solution-mediated transformation occurred. Additionally, the pH of FeSSIF was monitored and remained relatively constant between 5.00-4.95 for the duration of the experiment as shown in Figure 3.4a.

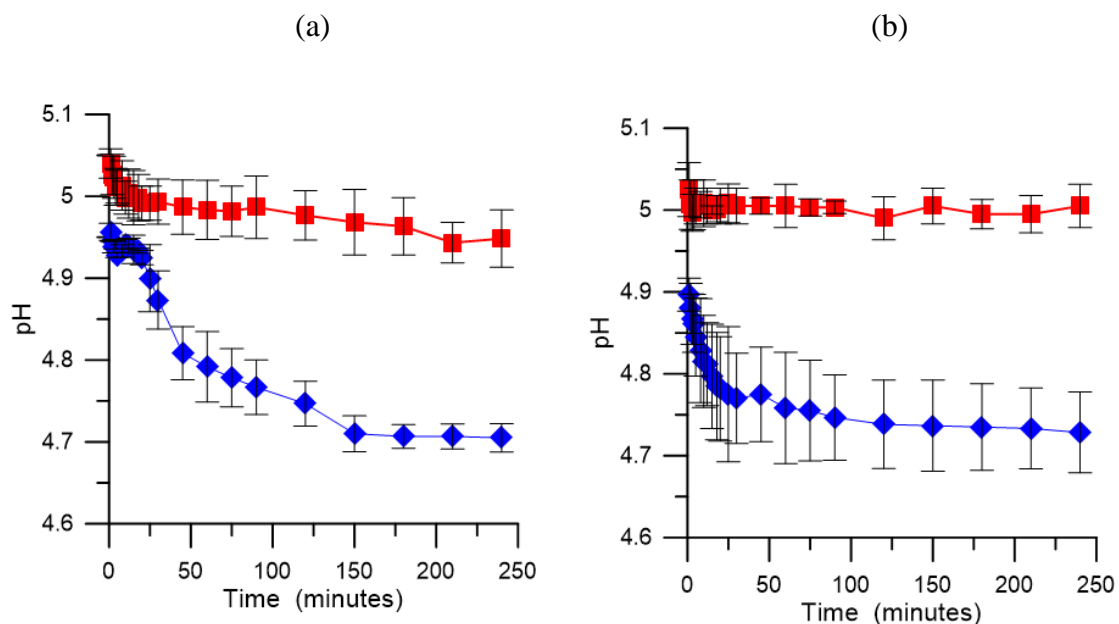


Figure 3.4. pH during cocystal dissolution for (a) IND-SAC and (b) PXC-SAC in (■) FeSSIF and (◆) buffer at 25°C.

If conversion to IND were to occur, a large decrease in pH would be expected as the SAC concentration in solution increased. Additionally, no excess SAC was measured in solution, as shown in Figure 3.5b, further evidence that the cocystal did not transform in FeSSIF during the time course of the experiment.

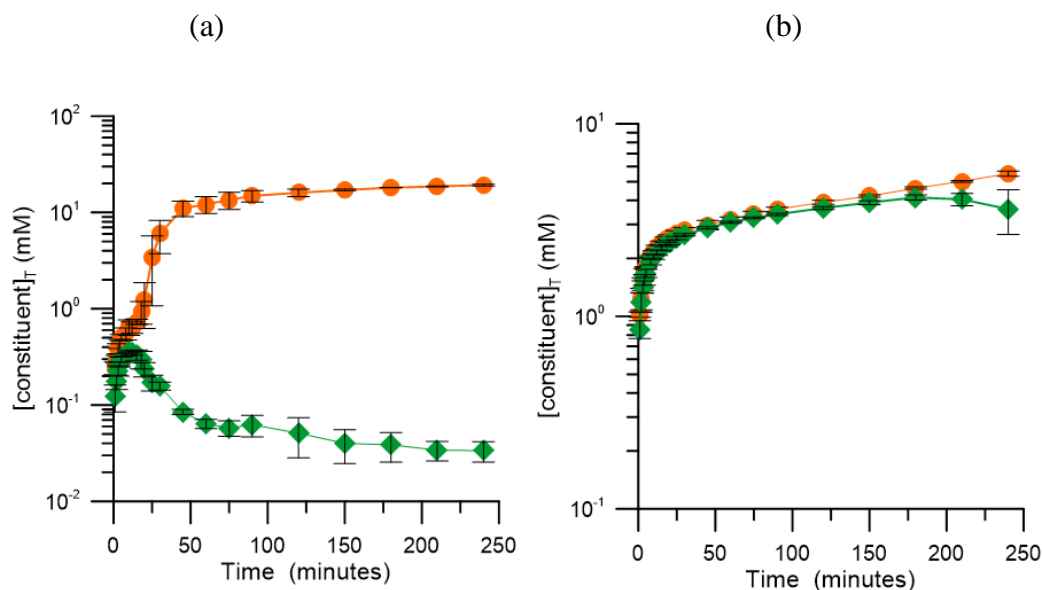


Figure 3.5. Concentration-time profile for [IND]_T (◆) and [SAC]_T (●) during dissolution of IND-SAC in (a) buffer and (b) FeSSIF.

Figure 3.5b shows that only at later time points (210 and 240 minutes), do the SAC concentrations start to increase while IND decrease, indicating that solution-mediated transformation may be beginning to occur. If the time course of the experiment was extended, it is likely that the transformation would have been detected by solid phase analysis and accompanied by a solution pH decrease.

In buffer, the cocrystal achieves a peak concentration of 0.36 mM at around 10 minutes, but this rapidly decreases by orders of magnitude, and by the end of the experiment, the concentration of IND is 0.034 mM which is very close to the solubility of IND in the aqueous buffer (0.023 mM). This is much less than the IND-SAC predicted solubility in buffer of 5.00 mM in Table 3.2, indicated solution-mediated transformation occurred. The solid phase at the end of the experiment was observed to be a mixture of IND-SAC and IND, the pH of the solution was 4.71 as shown in Figure 3.4a, and a 600 fold excess of SAC was measured in solution (Figure 3.5a), verifying that transformation to drug had occurred.

The supersaturation values in Figure 3.3b indicate that as hypothesized, the 5.5 fold decrease in $S_{\text{cocystal}}/S_{\text{drug}}$ in FeSSIF compared to buffer led to a reduced but sustained supersaturation and slower transformation to drug. In buffer, IND-SAC reached a peak supersaturation of 15.5 which rapidly decreased to 1.5 as it converted to IND. In FeSSIF, a supersaturation of 11 was achieved and maintained for the duration of the experiment. The 5.5 fold reduction in $S_{\text{cocystal}}/S_{\text{drug}}$ in FeSSIF led to a lower but sustained supersaturation as well as higher IND concentrations due to the solubilization of IND by FeSSIF.

Figure 3.6a shows the powder dissolution profile of PXC-SAC in FeSSIF and buffer.

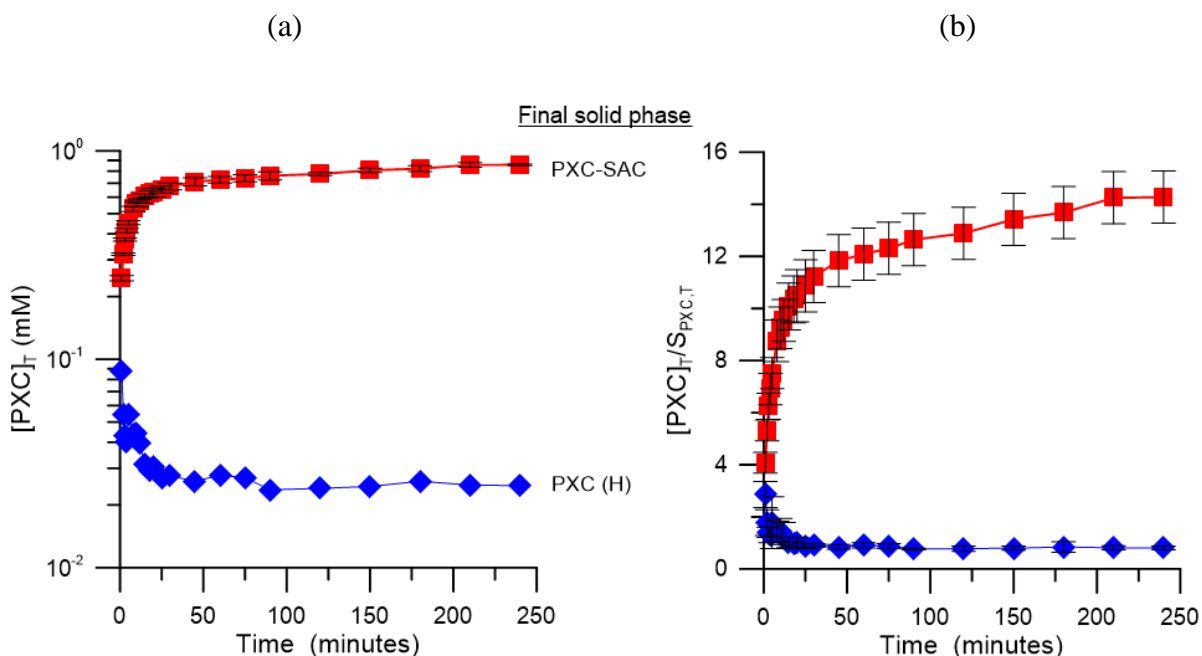


Figure 3.6. PXC-SAC dissolution in FeSSIF (■) and buffer (◆) at 25°C. (a) $[PXC]_T$ vs time profile for dissolution from neat cocrystal and (b) supersaturation generated by PXC-SAC during dissolution ($[PXC]_T/S_{PXC,T}$).

PXC-SAC obtains and maintains a higher drug solution concentration in FeSSIF compared to buffer (Figure 3.6a). PXC-SAC achieves a maximum concentration of 0.86 mM in FeSSIF which remains relatively constant for the duration of the experiment. The solid phase at the end

of the experiment was observed to be pure PXC-SAC, indicating no solution-mediated transformation occurred. Additionally, the pH of FeSSIF was monitored and remained constant around 5.00 for the duration of the experiment as shown in Figure 3.4b, and no excess SAC was measured in solution as shown in Figure 3.7b, further evidence that the cocrystal did not transform.

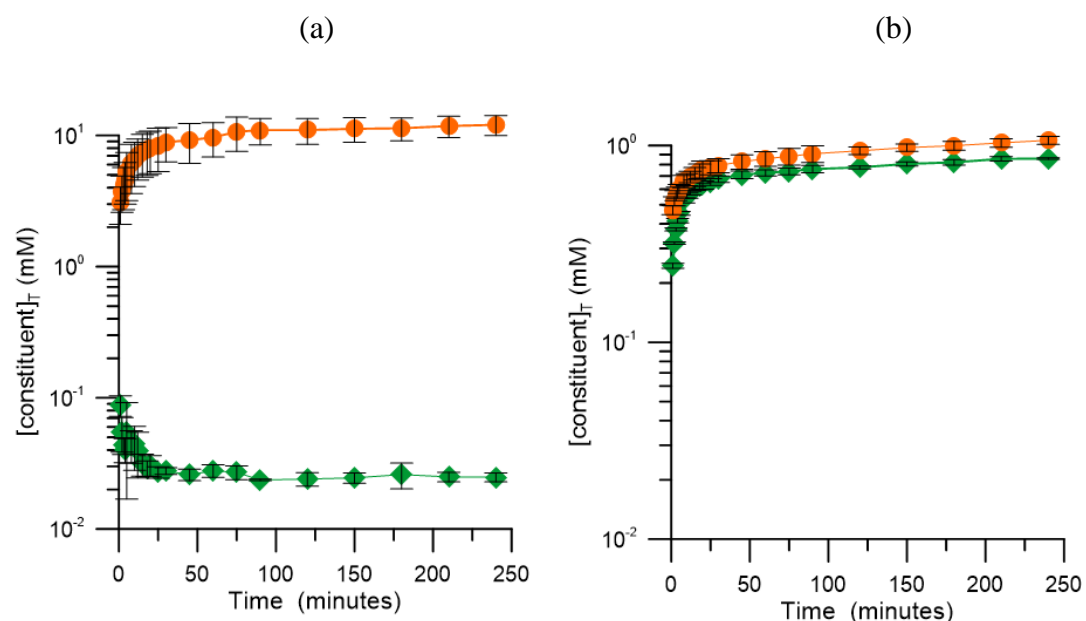


Figure 3.7. Concentration-time profile for [PXC]_T (◆) and [SAC]_T (●) during dissolution of PXC-SAC in (a) buffer and (b) FeSSIF.

In buffer, the cocrystal achieves a peak concentration of 0.088 mM at the first time point at 1 minute, and this decreases until the end of the experiment where the concentration of PXC is 0.025 mM which is approximately the solubility of PXC (H) in the aqueous buffer (0.03 mM). This is much less than the PXC-SAC predicted solubility in buffer of 16 mM in Table 3.2, indicating solution-mediated transformation occurred. The solid phase at the end of the experiment was observed to be pure PXC (H), the pH of the solution was 4.73 as shown in Figure 3.4b, and a 500 fold excess of SAC (Figure 3.7a) was measured in solution and a verifying that transformation to drug had occurred.

Since the PXC-SAC reduction in $S_{\text{cocrystral}}/S_{\text{drug}}$ in FeSSIF compared to buffer was only 1.4, it was not hypothesized that a slower transformation to drug would occur since the driving force for conversion is relatively unchanged. However, PXC-SAC did not undergo solution-mediated transformation to drug in FeSSIF, while it did in aqueous buffer. As seen in Figure 3.6b, the peak supersaturation of 3 of PXC is observed at 1 minute in buffer, but this rapidly decreases as the cocrystral converts to drug. In FeSSIF, however, a supersaturation of 14 is observed and maintained for the duration of the experiment. PXC-SAC achieved a higher drug concentration, sustained supersaturation, and no conversion to drug in FeSSIF compared to buffer even though the driving force for conversion was still high in this media. This could possibly be due to kinetic phenomena where components in the FeSSIF media inhibit the nucleation or growth of PXC crystals, resulting in a huge difference in dissolution profile in FeSSIF compared to buffer.

Conclusions

In this work, reported mathematical models describing cocrystral solubility advantage ($S_{\text{cocrystal}}/S_{\text{drug}}$) were used to analyze cocrystals in FeSSIF and buffer. All cocrystals exhibited lower solubility advantages in FeSSIF compared to aqueous buffer due to preferential solubilization of the drug constituent, with cocrystals of more hydrophobic and highly solubilized drugs exhibiting the largest decreases in $S_{\text{cocrystal}}/S_{\text{drug}}$. The reported models were in good agreement with the experimentally measured $S_{\text{cocrystal}}/S_{\text{drug}}$ values. Up to a 23 fold decrease in $S_{\text{cocrystal}}/S_{\text{drug}}$ was observed for the DNZ-HBA cocrystal of the highly solubilized drug DNZ ($\log P = 4.53$).

The effect of $S_{\text{cocrystal}}/S_{\text{drug}}$ reduction due to preferential solubilization by FeSSIF on cocrystal powder dissolution profile was examined for IND-SAC and PXC-SAC. IND-SAC and

PXC-SAC achieved higher concentrations during dissolution in FeSSIF compared to buffer due to the solubilization of IND and PXC. The $S_{\text{cocrystral}}/S_{\text{drug}}$ values measured at the eutectic point in FeSSIF and buffer were good indicators of the dissolution behavior for these systems. The decreased $S_{\text{cocrystral}}/S_{\text{drug}}$ resulted in sustained supersaturated drug concentrations and slower transformation to drug in FeSSIF compared to aqueous buffer. During the course of the four hour dissolution experiment, both IND-SAC and PXC-SAC readily converted to drug in aqueous buffer but this transformation did not occur in FeSSIF due to the reduced driving force for transformation. $S_{\text{cocrystral}}/S_{\text{drug}}$ can be predicted from mechanism-based models presented here, and these values can be used to anticipate cocrystral dissolution and transformation behavior in a variety of surfactant solutions as long as the drug solubility and the cocrystral K_{sp} , and drug and cofomer K_{a} and K_{s}^{T} values are known.

References

1. Cheney, M. L.; Weyna, D. R.; Shan, N.; Hanna, M.; Wojtas, L.; Zaworotko, M. J. Cofomer Selection in Pharmaceutical Cocrystral Development: a Case Study of a Meloxicam Aspirin Cocrystral That Exhibits Enhanced Solubility and Pharmacokinetics. *J. Pharm. Sci.* **2011**, *100*, (6), 2172-2181.
2. Smith, A. J.; Kavuru, P.; Wojtas, L.; Zaworotko, M. J.; Shytle, R. D. Cocrystrals of Quercetin with Improved Solubility and Oral Bioavailability. *Mol. Pharm.* **2011**, *8*, (5), 1867-1876.
3. Childs, S. L.; Kandi, P.; Lingireddy, S. R. Formulation of a Danazol Cocrystral with Controlled Supersaturation Plays an Essential Role in Improving Bioavailability. *Mol. Pharm.* **2013**, *10*, (8), 3112-3127.
4. McNamara, D. P.; Childs, S. L.; Giordano, J.; Iarriccio, A.; Cassidy, J.; Shet, M. S.; Mannion, R.; O'Donnell, E.; Park, A. Use of a glutaric acid cocrystral to improve oral bioavailability of a low solubility API. *Pharm. Res.* **2006**, *23*, (8), 1888-1897.
5. Bak, A.; Gore, A.; Yanez, E.; Stanton, M.; Tufekcic, S.; Syed, R.; Akrami, A.; Rose, M.; Surapaneni, S.; Bostick, T.; King, A.; Neervannan, S.; Ostovic, D.; Koparkar, A. The co-crystal approach to improve the exposure of a water-insoluble compound: AMG 517 sorbic acid cocrystral characterization and pharmacokinetics. *J. Pharm. Sci.* **2008**, *97*, (9), 3942-3956.
6. Jung, M. S.; Kim, J. S.; Kim, M. S.; Alhalaweh, A.; Cho, W.; Hwang, S. J.; Velaga, S. P. Bioavailability of indomethacin-saccharin cocrystrals. *J. Pharm. Pharmacol.* **2010**, *62*, (11), 1560-1568.
7. Huang, N.; Rodriguez-Hornedo, N. Engineering Cocrystral Solubility, Stability, and pH(max) by Micellar Solubilization. *J. Pharm. Sci.* **2011**, *100*, (12), 5219-5234.

8. Huang, N.; Rodriguez-Hornedo, N. Engineering cocrystal thermodynamic stability and eutectic points by micellar solubilization and ionization. *Crystengcomm* **2011**, *13*, (17), 5409-5422.
9. Huang, N.; Rodriguez-Hornedo, N. Effect of Micellar Solubilization on Cocrystal Solubility and Stability. *Cryst. Growth Des.* **2010**, *10*, (5), 2050-2053.
10. Roy, L. Engineering Cocrystal and Cocrystalline Salt Solubility by Modulation of Solution Phase Chemistry. *University of Michigan (Doctoral Dissertation)* **2013**, Retrieved from Deep Blue. (<http://hdl.handle.net/2027.42/98067>).
11. Roy, L.; Rodriguez-Hornedo, N. A Rational Approach for Surfactant Selection to Modulate Cocrystal Solubility and Stability. *Poster presentation at the 2010 AAPS Annual Meeting and Exposition* **2010**, New Orleans, LA, (November 14-18, 2010), Poster R6072.
12. Bernhard, E.; Zimmermann, F. Contribution to the Understanding of Oxicam Ionization-Constants. *Arzneimittel-Forschung/Drug Research* **1984**, *34-1*, (6), 647-648.
13. Mooney, K. G.; Mintun, M. A.; Himmelstein, K. J.; Stella, V. J. Dissolution Kinetics of Carboxylic-Acids .1. Effect of Ph under Unbuffered Conditions. *J. Pharm. Sci.* **1981**, *70*, (1), 13-22.
14. Newton, D. W.; Kluza, R. B. Pka values of medicinal compounds in pharmacy practice. *Drug Intelligence & Clinical Pharmacy* **1978**, *12*, (9), 546-554.
15. Robinson, R. A.; Biggs, A. I. The ionization constants of para-aminobenzoic acid in aqueous solution at 25-degrees-c. *Aust. J. Chem.* **1957**, *10*, (2), 128-134.
16. Robinson, R. A.; Kiang, A. K. The ionization constants of vanillin and 2 of its isomers. *Transactions of the Faraday Society* **1955**, *51*, (10), 1398-1402.
17. Good, D. J.; Rodriguez-Hornedo, N. Solubility Advantage of Pharmaceutical Cocrystals. *Cryst. Growth Des.* **2009**, *9*, (5), 2252-2264.
18. Bethune, S. J.; Huang, N.; Jayasankar, A.; Rodriguez-Hornedo, N. Understanding and Predicting the Effect of Cocrystal Components and pH on Cocrystal Solubility. *Cryst. Growth Des.* **2009**, *9*, (9), 3976-3988.
19. Good, D. J.; Rodriguez-Hornedo, N. Cocrystal Eutectic Constants and Prediction of Solubility Behavior. *Cryst. Growth Des.* **2010**, *10*, (3), 1028-1032.
20. Galia, E.; Nicolaidis, E.; Horter, D.; Lobenberg, R.; Reppas, C.; Dressman, J. B. Evaluation of various dissolution media for predicting in vivo performance of class I and II drugs. *Pharm. Res.* **1998**, *15*, (5), 698-705.
21. Rodriguez-Hornedo, N.; Nehru, S. J.; Seefeldt, K. F.; Pagan-Torres, Y.; Falkiewicz, C. J. Reaction crystallization of pharmaceutical molecular complexes. *Mol. Pharm.* **2006**, *3*, (3), 362-367.
22. Caron, J. C.; Shroot, B. Determination of partition-coefficients of glucocorticosteroids by high-performance liquid-chromatography. *J. Pharm. Sci.* **1984**, *73*, (12), 1703-1706.
23. Palagiano, F.; Arenare, L.; Barbato, F.; LaRotonda, M. I.; Quaglia, F.; Bonina, F. P.; Montenegro, L.; deCaprariis, P. In vitro and in vivo evaluation of terpenoid esters of indomethacin as dermal prodrugs. *Int. J. Pharm.* **1997**, *149*, (2), 171-182.
24. Tsai, R. S.; Carrupt, P. A.; Eltayar, N.; Giroud, Y.; Andrade, P.; Testa, B.; Bree, F.; Tillement, J. P. Physicochemical and Structural-Properties of Nonsteroidal Antiinflammatory Oxicams. *Helvetica Chimica Acta* **1993**, *76*, (2), 842-854.
25. Machatha, S. G.; Yalkowsky, S. H. Comparison of the octanol/water partition coefficients calculated by ClogP((R)), ACDlogP and KowWin((R)) to experimentally determined values. *Int. J. Pharm.* **2005**, *294*, (1-2), 185-192.

CHAPTER 4

UNDERSTANDING THE RELATIONSHIP BETWEEN COCRYSTAL SOLUBILIZATION RATIO AND DRUG HYDROPHOBICITY

Introduction

The solubilization of drugs by solubilizing agents such as physiologically relevant surfactants has been shown to be correlated to their hydrophobicity¹⁻³. Specifically, the increase in solubility as a function of solubilizing agent can be predicted from the drug octanol-water partition coefficient (log P) and aqueous solubility of the drug. Drugs with higher log P values are solubilized to a greater extent than less hydrophobic (lower log P) drugs. Numerous studies have confirmed this relationship between the solubilization ratio (SR) of nonionizable drugs in the presence of physiologically relevant bile salts and the log P of the drug^{3,4}.

In ionizing conditions, log P is not a good predictor of drug solubilization². Ionized drugs interact differently than nonionized drugs and the log D (octanol-water distribution coefficient) at the pH of interest is a key parameter correlated with solubilization. Log D takes into account the extent of ionization in media of interest and is calculated by many commonly used software packages based on drug structure. In a study of ten drugs of varying ionization properties, log of the solubilization ratio (log SR) in fasted state intestinal fluid (FaSSIF), which has a pH of 6.50 and fed state intestinal fluid (FeSSIF), which has a pH of 5.00 was correlated with measured log P and calculated log D. The R squared value of the linear regression of the

correlation improved from 0.32 to 0.74 when log D was used instead of log P, indicating that log D is a better predictor of log SR in ionizing conditions².

We have previously reported a simple mechanism-based approach to predict SR_{cocystal} from SR_{drug} when coformer solubilization is negligible⁵. This relationship has been confirmed for cocrystals of varying ionization properties in the presence of FeSSIF, in which drugs are highly solubilized and coformers are not. In this work, we develop correlations between the log D (as several of the drugs are ionizable) of the drug and the log SR_{cocystal} in FeSSIF. Additionally, since the relationship between SR_{drug} and SR_{cocystal} is known for these systems, differences between the log SR_{drug} -log D and log SR_{cocystal} -log D correlations are predicted and rationalized. The cocrystals studied include: 1:1 carbamazepine-saccharin (CBZ-SAC), 1:1 carbamazepine-salicylic acid (CBZ-SLC), 2:1 carbamazepine 4-aminobenzoic acid hydrate, (CBZ-4ABA-HYD), 1:1 piroxicam-saccharin (PXC-SAC), 1:1 indomethacin-saccharin (IND-SAC), 1:1 danazol-hydroxybenzoic acid (DNZ-HBA), and 1:1 danazol-vanillin (DNZ-VAN). The selected cocrystals include both 1:1 and 2:1 cocrystal stoichiometries and cover a range of ionization behaviors for both drug and coformers. PXC is a zwitterionic drug with pKa values of 1.86 and 5.46⁶, and IND is a monoprotic weakly acidic drug with a pKa of 4.2⁷. SAC is a monoprotic weak acid with pKa values reported between 1.6-2.2^{8,9}, SLC is a monoprotic weak acid with a reported pKa value of 3.0⁸, 4ABA is amphoteric with pKa values 2.6 and 4.8¹⁰, HBA is a monoprotic weak acid with a reported pKa value of 4.48¹¹ and VAN is a monoprotic weak acid with a pKa of 7.4¹¹.

Theoretical

Estimation of cocrystal solubilization ratio from drug solubilization ratio

The relationship between cocrystal solubilization ratio ($SR_{\text{cocrystal}}$) in drug solubilizing agents and drug solubilization ratio (SR_{drug}) assuming negligible cofomer solubilization has been derived and described in detail in Chapter 2 of this dissertation. To summarize, the general form of the equation for a cocrystal with stoichiometry A_xB_y , where A and B are the cocrystal constituents, drug and cofomer respectively; and x and y are the stoichiometric coefficients or molar ratios, is⁵:

$$SR_{\text{cocrystal}} = \left(SR_{\text{drug}} \right)^{\frac{x}{x+y}} \quad (4.1)$$

where

$$SR = \left(\frac{S_T}{S_{\text{aq}}} \right) \quad (4.2)$$

for either cocrystal or drug. S_T is defined as the sum of the concentrations of all species dissolved ($S_T = S_{\text{aq}} + S_s$). S_{aq} represents the cocrystal aqueous solubility at a particular pH in the absence of solubilizing agent ($S_{\text{aq}} = S_{\text{nonionized, aq}} + S_{\text{ionized, aq}}$) and is the sum of the nonionized and ionized contributions to the aqueous solubility. S_s represents the cocrystal solubilized by solubilizing agents ($S_s = S_{\text{nonionized, s}} + S_{\text{ionized, s}}$) and contributions from the ionized species as appropriate.

From the general form of the relationship between $SR_{\text{cocrystal}}$ and SR_{drug} in equation (4.1) above, the following equations can be derived for cocrystals of 1:1 and 2:1 stoichiometry (systems studied in this work):

For a 1:1 cocrystal:

$$SR_{\text{cocrystal}} = \sqrt{SR_{\text{drug}}} \quad (4.3)$$

For 2:1 cocrystal:

$$SR_{\text{cocrystal}} = SR_{\text{drug}}^{\frac{2}{3}} \quad (4.4)$$

The above relationships are derived from the full solubility equations for drug and cocrystal in solubilizing agents assuming that $K_s^{\text{coformer}} = 0$ and that the pH of the solubilizing agent and buffer for both cocrystal and drug are equal.

Building log SR-log D relationships

It is well established in the literature that the solubilization of drugs by solubilizing agents correlates to their hydrophobicity as described by their log P and/or log D¹⁻³. SR_{drug} increases as log P and/or log D increases and linear regression analysis can be used to correlate log SR_{drug} with log P in nonionizing conditions and log D in ionizing conditions. The purpose of this work is to examine the relationships between $SR_{\text{cocrystal}}$ in FeSSIF and the hydrophobicity of the drug. In order to build log-log relationships between the octanol-water partition coefficient (log P) or distribution constant (log D), log $SR_{\text{cocrystal}}$ must be considered. When a compound contains ionizable components, the log D, which takes ionization into account, is a better predictor of solubilization by solubilizing agents. The octanol-water log D is defined as:

$$\log D = \log \left(\frac{[\text{drug}]_{\text{octanol}}}{[\text{drug}]_{\text{aq,ionized}} + [\text{drug}]_{\text{aq,unionized}}} \right) \quad (4.5)$$

Since several of the drugs studied in this work are ionizable in the conditions of FeSSIF, all further derivations will use log D instead of log P to improve the correlation fit. In order to

derive a log-log relationship between $\log D$ and SR_{cocystal} or SR_{drug} , we must consider how they are related in terms of logs. In terms of logs, equation (4.3) becomes:

$$\log \left(\frac{S_{\text{FeSSIF}}}{S_{\text{buffer}}} \right)_{\text{cocystal}} = \frac{1}{2} \log \left(\frac{S_{\text{FeSSIF}}}{S_{\text{buffer}}} \right)_{\text{drug}} \quad (4.6)$$

For a 2:1 cocystal, the $SR_{\text{cocystal}}-SR_{\text{drug}}$ relationship is:

$$\left(\frac{S_{\text{FeSSIF}}}{S_{\text{buffer}}} \right)_{\text{cocystal}} = \left(\frac{S_{\text{FeSSIF}}}{S_{\text{buffer}}} \right)_{\text{drug}}^{\frac{2}{3}} \quad (4.7)$$

And in terms of logs, equation (4.7) becomes:

$$\log \left(\frac{S_{\text{FeSSIF}}}{S_{\text{buffer}}} \right)_{\text{cocystal}} = \frac{2}{3} \log \left(\frac{S_{\text{FeSSIF}}}{S_{\text{buffer}}} \right)_{\text{drug}} \quad (4.8)$$

These relationships are useful for applying $\log SR_{\text{drug}}-\log D$ correlations to cocystals of these drugs. That is, by correlating measured $\log SR_{\text{drug}}$ and $\log D$ in a solubilizing agent, one can anticipate what $\log SR_{\text{cocystal}}$ would be for a cocystal of a drug with a particular $\log D$. For example, if the linear regression relationship between experimentally determined SR_{drug} values and $\log D$ is determined, an equation of the following form is obtained:

$$\log \left(\frac{S_{\text{FeSSIF}}}{S_{\text{buffer}}} \right)_{\text{drug}} = m_{\text{drug}} \log D_{\text{drug}} + b_{\text{drug}} \quad (4.9)$$

By relating the $\log SR_{\text{drug}}$ to $\log SR_{\text{cocystal}}$ using equations (4.6) and (4.8), one can determine how SR_{cocystal} will relate to drug $\log D$. For the case of 1:1 cocystals, $\log SR_{\text{cocystal}} = (1/2)\log SR_{\text{drug}}$ as shown by equation (4.3). Therefore, a $\log SR_{\text{cocystal}}-\log D$ linear regression for 1:1 cocystals such as:

$$\log\left(\frac{S_{\text{FeSSIF}}}{S_{\text{buffer}}}\right)_{\text{cocystal}} = m_{\text{cocystal}} \log D_{\text{drug}} + b_{\text{cocystal}} \quad (4.10)$$

can be predicted from simply knowing how the slope (m) and intercept (b) of a cocystal linear regression equation are theoretically related to the experimentally determined drug linear regression equation. For a 1:1 cocystal,

$$m_{\text{cocystal}} = \frac{m_{\text{drug}}}{2} \quad (4.11)$$

and

$$b_{\text{cocystal}} = \frac{b_{\text{drug}}}{2} \quad (4.12)$$

By substituting, the linear regression equation for 1:1 cocystals in terms of the experimentally determined drug regression equation is:

$$\log\left(\frac{S_{\text{FeSSIF}}}{S_{\text{buffer}}}\right)_{\text{cocystal}} = \left(\frac{m_{\text{drug}}}{2}\right) \log D_{\text{drug}} + \left(\frac{b_{\text{drug}}}{2}\right) \quad (4.13)$$

Similarly, for a 2:1 cocystal using equation (4.8) to substitute:

$$\log\left(\frac{S_{\text{FeSSIF}}}{S_{\text{buffer}}}\right)_{\text{cocystal}} = \frac{2}{3}(m_{\text{drug}}) \log D_{\text{drug}} + \frac{2}{3}(b_{\text{drug}}) \quad (4.14)$$

These equations are useful for estimating $\log SR_{\text{cocystal}}$ where the drug $\log P/\log D$ is known without experimentally measuring the SR_{cocystal} value. SR_{drug} and $\log P$ and/or $\log D$ values in solubilizing agents are often available in the literature, and using equations (4.13) and

(4.14) the prediction of $SR_{\text{cocrystal}}$ in these conditions is possible from sole knowledge of drug hydrophobicity.

Materials and Methods

Materials

Cocrystal constituents

Anhydrous carbamazepine form III (CBZ), anhydrous indomethacin form γ (IND) were purchased from Sigma Chemical Company (St. Louis, MO) and used as received. Anhydrous piroxicam form I was received as a gift from Pfizer (Groton, CT) and used as received. Anhydrous danazol was received as a gift from Renovo Research (Atlanta, GA) and used as received.

Anhydrous saccharin (SAC), 4- aminobenzoic acid (4ABA), and salicylic acid (SLC), were purchased from Sigma Chemical Company (St. Louis, MO) and used as received. Anhydrous hydroxybenzoic acid was purchased from Acros Organics (Pittsburgh, PA) and used as received. Anhydrous vanillin was purchased from Fisher Scientific (Fair Lawn, NJ) and used as received. Carbamazepine dihydrate (CBZ (H)), piroxicam monohydrate (PXC (H)), and hydroxybenzoic acid monohydrate (HBA (H)) were prepared by slurring CBZ, PXC, and HBA in deionized water for at least 24 hours. All crystalline drugs and cofomers were characterized by X-ray power diffraction (XRPD) and differential scanning calorimetry (DSC) before carrying out experiments.

Solvents and buffer components

Ethyl acetate and ethanol were purchased from Acros Organics (Pittsburgh, PA) and used as received, and HPLC grade methanol and acetonitrile were purchased from Fisher Scientific (Pittsburgh, PA). Trifluoroacetic acid spectrophometric grade 99% was purchased from Aldrich

Company (Milwaukee, WI) and phosphoric acid ACS reagent 85% was purchased from Sigma Chemical Company (St. Louis, MO). Water used in this study was filtered through a double deionized purification system (Milli Q Plus Water System) from Millipore Co. (Bedford, MA).

FeSSIF and acetate buffer were prepared using sodium taurocholate (NaTC) purchased from Sigma Chemical Company (St. Louis, MO), lecithin purchased from Fisher Scientific (Pittsburgh, PA), sodium hydroxide pellets (NaOH) purchased from J.T. Baker (Philipsburg, NJ), and acetic acid and potassium chloride (KCl) purchased from Acros Organics (Pittsburgh, PA).

Methods

FeSSIF and acetate buffer preparation

FeSSIF and acetate buffer were prepared according to the protocol of Galia and coworkers¹². Acetate buffer was prepared as a stock solution at room temperature by dissolving 8.08 g NaOH (pellets), 17.3 g glacial acetic acid and 23.748 g NaCl in 2 L of purified water. The pH was adjusted to 5.00 with 1 N NaOH and 1N HCl. FeSSIF was prepared by dissolving 0.41 g sodium taurocholate in 12.5 mL of pH 5.00 acetate buffer. 0.148 g lecithin was added with magnetic stirring at 37 °C until dissolved. The volume was adjusted to exactly 50 mL with acetate buffer.

Cocrystal synthesis

Cocrystals were prepared by the reaction crystallization method¹³ at 25°C. The 1:1 indomethacin-saccharin cocrystal (IND-SAC) was synthesized by adding stoichiometric amounts of cocrystal constituents (IND and SAC) to nearly saturated SAC solution in ethyl acetate. The 1:1 carbamazepine saccharin cocrystal (CBZ-SAC) was prepared by adding stoichiometric amounts of cocrystal constituents (CBZ and SAC) to nearly saturated SAC solution in ethanol. The 1:1 carbamazepine-salicylic acid cocrystal (CBZ-SLC) was prepared by adding

stoichiometric amounts of cocrystal constituents (CBZ and SLC) to nearly saturated SLC solution in acetonitrile. The 2:1 carbamazepine-4-aminobenzoic acid monohydrate cocrystal (CBZ-4ABA (H)) was prepared by suspending stoichiometric amounts of cocrystal constituents (CBZ and 4ABA) in a 0.01M 4ABA aqueous solution at pH 3.9. The 1:1 piroxicam-saccharin cocrystal (PXC-SAC) was prepared by adding stoichiometric amounts of cocrystal constituents (PXC and SAC) to nearly saturated SAC in acetonitrile. The 1:1 danazol-hydroxybenzoic acid cocrystal (DNZ-HBA) was prepared by adding stoichiometric amounts of cocrystal constituents (DNZ and HBA) to nearly saturated HBA solution in ethyl acetate. The 1:1 danazol-vanillin cocrystal (DNZ-VAN) was prepared by adding stoichiometric amounts of cocrystal constituents (DNZ and VAN) to nearly saturated VAN solution in ethyl acetate. Prior to carrying out any solubility experiments, solid phases were characterized by XRPD and DSC and stoichiometry verified by HPLC. Full conversion to cocrystal was observed in 24 hours.

Solubility measurements of cocrystal constituents

Cocrystal constituent solubilities were measured in FeSSIF and pH 5.00 acetate buffer (FeSSIF without NaTC and lecithin). Solubilities of cocrystal constituents were determined by adding excess solid (drug or coformer) to 3 mL of media (FeSSIF or buffer). Solutions were magnetically stirred and maintained at $25 \pm 0.1^\circ\text{C}$ using a water bath for up to 96 h. At 24 hr intervals, 0.30 mL of samples were collected, pH of solutions measured, and filtered through a $0.45 \mu\text{m}$ pore membrane. After dilution with mobile phase, solution concentrations of drug or coformer were analyzed by HPLC. The equilibrium solid phases were characterized by XRPD and DSC.

Cocrystal solubility measurements

Cocrystal equilibrium solubilities were measured in FeSSIF and pH 5.00 acetate buffer (FeSSIF without NaTC and lecithin) at the eutectic point, where drug and cocrystal solid phases are in equilibrium with solution^{37,38}. The eutectic point between cocrystal and drug was approached by cocrystal dissolution (suspending solid cocrystal (~100 mg) and drug (~50 mg) in 3 mL of media (FeSSIF or buffer)) and by cocrystal precipitation (suspending solid cocrystal (~50 mg) and drug (~100 mg) in 3 mL of media (FeSSIF or buffer) nearly saturated with coformer). Solutions were magnetically stirred and maintained at $25 \pm 0.1^\circ\text{C}$ using a water bath for up to 96 h. At 24 hr intervals, 0.30 mL aliquots of suspension were collected, pH was measured, before filtration through a $0.45 \mu\text{m}$ pore membrane. Solid phases were also collected at 24 hr intervals to ensure the sample was at the eutectic point (confirmed by presence of both drug and cocrystal solid phases and constant [coformer] and [drug] solution concentrations). After dilution of filtered solutions with mobile phase, drug and coformer concentrations were analyzed by HPLC. The equilibrium solid phases were characterized by XRPD and DSC.

The cocrystal stoichiometric solubility was calculated from measured total eutectic concentrations of drug and coformer ($[\text{drug}]_{\text{T,eu}}$ and $[\text{coformer}]_{\text{T,eu}}$) according to the following equations for 1:1 and 2:1 cocrystals³⁷:

$$S_{\text{T}}^{1:1 \text{ cocrystal}} = \sqrt{[\text{drug}]_{\text{T,eu}} [\text{coformer}]_{\text{T,eu}}} \quad (4.15)$$

$$S_{\text{T}}^{2:1 \text{ cocrystal}} = 2 \left(\sqrt[3]{\frac{[\text{drug}]_{\text{T,eu}}^2 [\text{coformer}]_{\text{T,eu}}}{4}} \right) \quad (4.16)$$

This method of calculating the stoichiometric solubility of cocrystals from equilibrium solubility measurements in nonstoichiometric conditions is well established in the literature^{7-10, 37-39}.

X-ray powder diffraction

X-ray powder diffraction diffractograms of solid phases were collected on a benchtop Rigaku Miniflex X-ray diffractometer (Rigaku, Danverse, MA) using Cu K α radiation ($\lambda=1.54\text{\AA}$), a tube voltage of 30 kV, and a tube current of 15 mA. Data were collected from 5 to 40° at a continuous scan rate of 2.5°/min.

Thermal analysis

Solid phases collected from the slurry studies were dried at room temperature and analyzed by differential scanning calorimetry (DSC) using a TA instrument (Newark, DE) 2910MDSC system equipped with a refrigerated cooling unit. DSC experiments were performed by heating the samples at a rate of 10 °C/min under a dry nitrogen atmosphere. A high purity indium standard was used for temperature and enthalpy calibration. Standard aluminum sample pans were used for all measurements.

High performance liquid chromatography

Solution concentrations were analyzed by a Waters HPLC (Milford, MA) equipped with an ultraviolet-visible spectrometer detector. For the IND-SAC and CBZ-SAC, CBZ-SLC, CBZ-4ABA-HYD cocrystals and their components, a C18 Thermo Electron Corporation (Quebec, Canada) column (5 μm , 250 x 4.6 mm) at ambient temperature was used. For the IND-SAC cocrystal, the injection volume was 20 μl and analysis conducted using an isocratic method with a mobile phase composed of 70% acetonitrile and 30% water with 0.1% trifluoroacetic acid and a flow rate of 1 ml/min. Absorbance of IND and SAC were monitored at 265 nm. For the CBZ cocrystals, the injection volume was 20 μl and analysis conducted using an isocratic method with

a mobile phase composed of 55% methanol and 45% water with 0.1% trifluoroacetic acid and a flow rate of 1 mL/min. Absorbance was monitored as follows:

CBZ and 4ABA at 284 nm, SAC at 265 nm, and SLC at 303 nm. For the PXC-SAC, DNZ-HBA, and DNZ-VAN cocrystals and their components, a C18 Waters Atlantis (Milford, MA) column (5 μ M 250 x 6 mm) at ambient temperature was used. For PXC-SAC, the injection volume was 20 μ L and analysis was conducted using an isocratic method with a mobile phase composed of 70% methanol and 30% water with 0.3% phosphoric acid and a flow rate of 1 mL/min. Absorbance of PXC was monitored at 340 nm and SAC at 240 nm. For the DNZ cocrystals, the injection volume was 20 μ L in FeSSIF experiments, and 100 μ L in buffer experiments due to the extremely low solubility of DNZ in aqueous solutions. Analysis was conducted using an isocratic method composed of 80% methanol and 20% water with 0.1% trifluoroacetic acid and a flow rate of 1 mL/min. Absorbance of DNZ was monitored at 285 nm, HBA at 242 nm, and VAN at 300 nm. For all cocrystals, the Waters' operation software Empower 2 was used to collect and process data.

Results

Log D is a better predictor of SR than log P for ionizable drugs

Figure 4.1 shows the correlation of $\log SR_{\text{drug}}$ with $\log P$ and $\log D$. $\log D$ is a better predictor of $\log SR_{\text{drug}}$ compared to $\log P$ due to the ionization of IND, an acid ($pK_a = 4.2^7$), and PXC, a zwitterion ($pK_a = 1.86$ and 5.46^6).

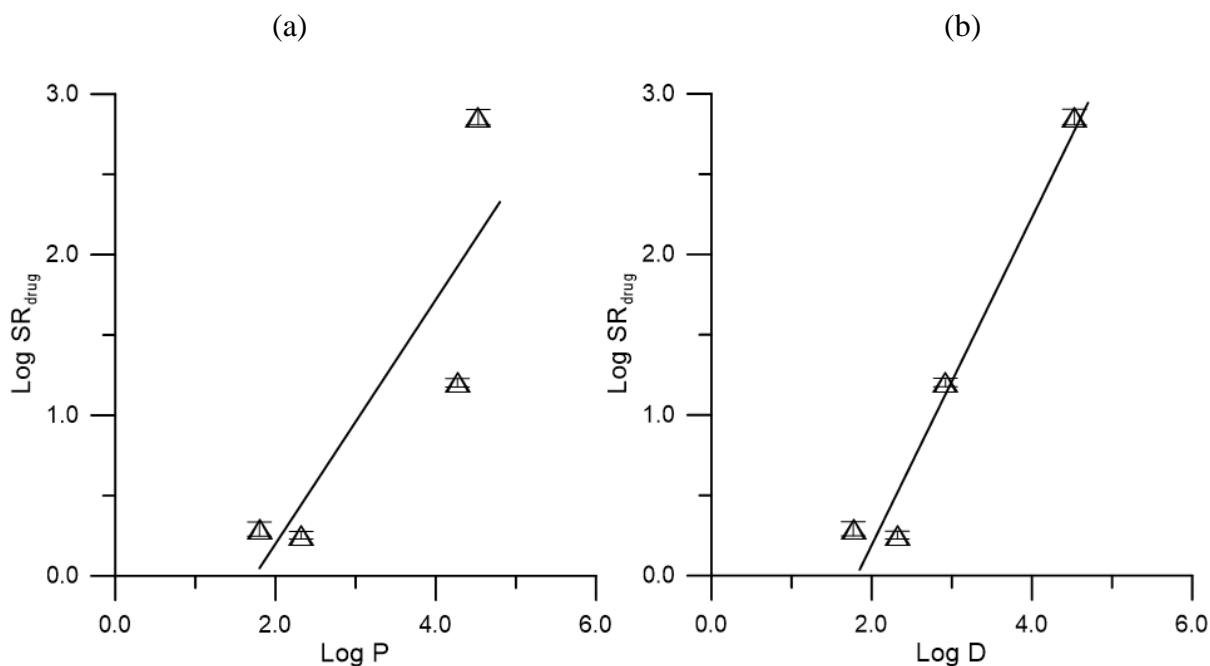


Figure 4.1. Log SR_{drug} correlation with (a) log P and (b) log D. Symbols (\triangle) represent experimentally measured data and the lines are a result of linear regression of the data (a) $y = (0.76 \pm 0.08)x - 1.3 \pm 0.3$ and (b) $y = (1.02 \pm 0.09)x - 1.9 \pm 0.3$ where errors on regression parameters represent the 95% confidence interval. Log P values are from the literature and log D values calculated at experimentally measured pH values in Table 4.1 using the ADMET Predictor Module in Gastro-Plus. For nonionizable drugs DNZ and CBZ (H), the measured log P was used in lieu of a calculated log D since the log D is not predicted to change with pH.

The linear regression fit improves from an R^2 value of 0.74 to 0.94 when log D is substituted for log P. Table 4.1 shows the experimentally measured SR values (from Chapter 2) as well as the log P and log D values used for the fitted log SR_{drug}-log P and log SR_{drug}-log D correlations. The pH of the solubility measurements in FeSSIF and in buffer used to calculate SR were very close to 5.00, the initial pH of FeSSIF and blank aqueous buffer. The log D values were calculated at the pH of the solubility measurements indicated in Table 4.1.

Table 4.1. Log P, log D, and SR values used to correlate log SR_{drug} with drug hydrophobicity.

Drug	log P ^a	log D ^b	pH _{sol}	SR _{drug}	log (SR _{drug})
DNZ	4.53	4.53	4.98±0.03	720 ± 80	2.86±0.05
IND	4.27	2.92	4.97±0.01	16 ± 1	1.20±0.03
CBZ (H)	2.32	2.32	4.90±0.07	1.8 ± 0.1	0.25±0.02
PXC (H)	1.80	1.77	5.00±0.03	2.0 ± 0.2	0.29±0.04

(a) Values from references¹⁴⁻¹⁷.

(b) Calculated using the ADMET predictor module in Gastro-Plus for IND and PXC (H). For nonionizable drugs DNZ and CBZ (H), the measured log P was used in lieu of a calculated log D since the log D is not predicted to change with pH.

Though the sample set is small (4 drugs), it is clear that log SR_{drug} correlates with the log D of these drugs. This is in good agreement with previously reported log SR_{drug} – log P and log D correlations for several of the drugs studied in this work in FeSSIF and other physiologically relevant surfactants containing sodium taurocholate (NaTC)^{2,3}. In those studies, R² values ranged from 0.74-0.99, though the particular regression parameters (slope and intercept) were different from those reported here. These differences in fitted regression relationships are mainly due to the slight variation in solubilizing agent concentration between the literature and this work.

Next, the log SR_{cocrystal} correlation with the log P and log D of the drug is considered. From measured coformer solubilities in FeSSIF and buffer reported in Chapter 2, it was determined that the SR_{coformer} values for the cocrystal systems studied were negligible. Therefore, SR_{cocrystal} should correlate with the hydrophobicity of the drug, since the assumption that coformers are not solubilized is justified for the systems studied. As predicted by equations (4.13) and (4.14), the SR_{cocrystal}-log P and/or log D relationship depend on the stoichiometry of

the cocrystal. Only one 2:1 cocrystal (CBZ-4ABA-HYD) was studied in this work, so linear regression analysis was not performed on $SR_{\text{cocrystal}}-\log D$ data for 2:1 cocrystals. Figure 4.2 shows the correlation of $\log SR_{\text{cocrystal}}$ for 1:1 cocrystals with $\log P$ and $\log D$ of the constituent drug.

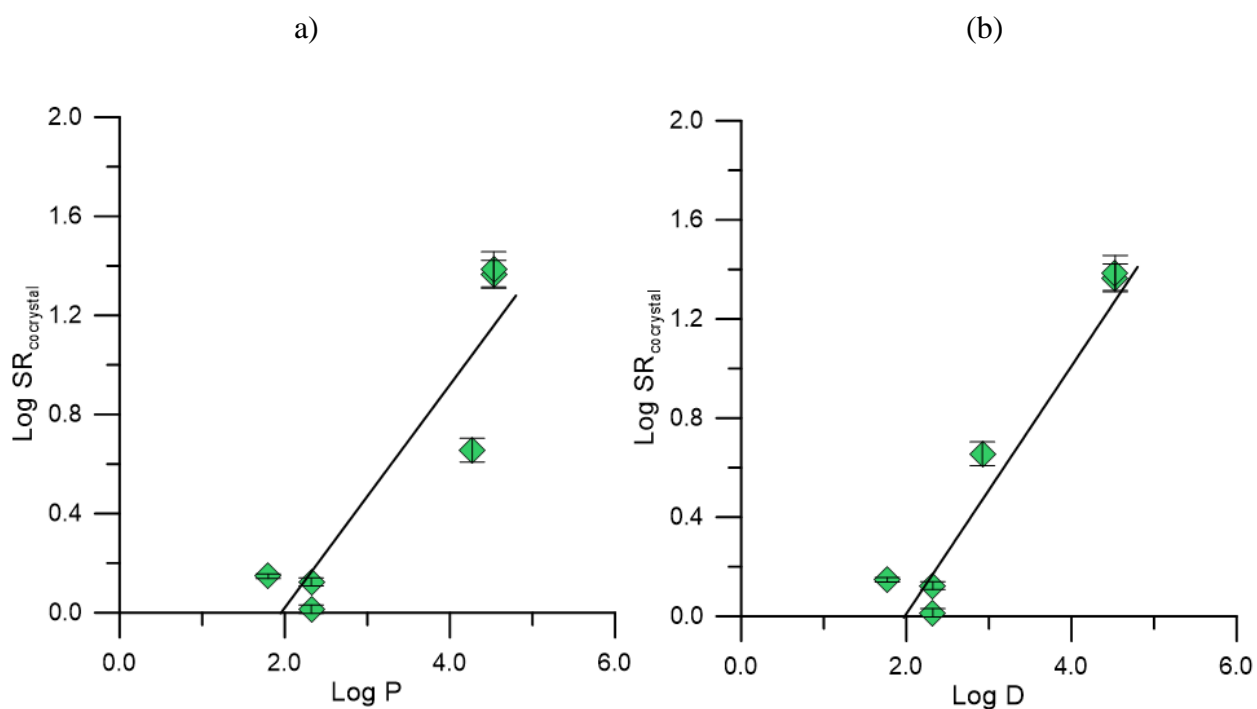


Figure 4.2. $\log SR_{\text{cocrystal}}$ correlation with (a) $\log P$ and (b) $\log D$. Symbols (\blacklozenge) represent experimentally measured data and the lines are a result of linear regression of the data (a) $y = (0.45 \pm 0.07)x - 0.9 \pm 0.3$ and (b) $y = (0.50 \pm 0.05)x - 1.0 \pm 0.2$ where errors on regression parameters represent the 95% confidence interval. $\log P$ values are from literature and $\log D$ values calculated using the ADMET Predictor Module in Gastro-Plus. For nonionizable drugs DNZ and CBZ (H), the measured $\log P$ was used in lieu of a calculated $\log D$ since the $\log D$ is not predicted to change with pH.

$\log D$ is a better predictor of $\log SR_{\text{cocrystal}}$ than $\log P$ due to the ionization of IND and PXC as was observed in the $\log SR_{\text{drug}}-\log D$ correlation. The R^2 value increases from 0.84 to 0.92 for the linear regression fits of the experimentally measured SR data when $\log D$ is used instead of $\log P$. $SR_{\text{cocrystal}}$ values are calculated from measured cocrystal solubilities in FeSSIF

and buffer at the eutectic point. Since many of the cocrystals studied have weakly acidic components, the eutectic point pH values were lower than the initial pH of 5.00 of FeSSIF and blank aqueous buffer. For the ionizable drugs IND and PXC, it is necessary to calculate the log D at the pH of the experimental conditions of the solubility measurements. The log D values calculated for the correlation in Figure 4.3b were calculated at the eutectic point pHs shown in Table 4.2 since these are the conditions under which SR values were measured.

Table 4.2 shows the measured $SR_{\text{cocrystal}}$ at the eutectic point and the log P and log D values used in the $\log SR_{\text{cocrystal}} - \log P$ and $\log SR_{\text{cocrystal}} - \log D$ correlations for 1:1 cocrystals.

Table 4.2. Log P, log D, and SR values used to correlate $\log SR_{\text{cocrystal}}$ of 1:1 cocrystals with drug hydrophobicity.

Cocrystal	$\log P^a$ drug	$\log D^b$ drug	pH_{eu}	pH_{eu}	$SR_{\text{cocrystal}}$	$\log SR_{\text{cocrystal}}$
DNZ-VAN	4.53	4.53	4.98±0.03		24±4	1.39±0.07
DNZ-HBA	4.53	4.53	4.46±0.06		23±3	1.36±0.06
IND-SAC	4.27	3.71	3.65 ± 0.05		4.5±0.3	0.66±0.05
CBZ-SLC	2.32	2.32	4.29 ± 0.02		1.33±0.05	0.12±0.02
CBZ-SAC	2.32	2.32	3.11 ± 0.02		1.03±0.04	0.023±0.007
PXC-SAC	1.80	1.79	3.79 ± 0.02		1.40±0.03	0.15±0.01

(a) From references 14-17.

(b) Calculated using the ADMET predictor module in Gastro-Plus for IND and PXC (H). For nonionizable drugs DNZ and CBZ (H), the measured log P was used in lieu of a calculated log D since the log D is not predicted to change with pH.

The $\log SR_{\text{cocrystal}}$ values correlate well with drug log D. The pH of the eutectic point is significantly lower than pH 5.00 due to the presence of excess coformer in solution, especially in the case of the SAC cocrystals. CBZ-SAC, IND-SAC, and PXC-SAC had pH values ranging

from 3.11-3.79. The $SR_{\text{cococrystal}}$ values are different at pH 5.00 compared to the eutectic pH values since all cococrystals have ionizable drugs and/or cofomers. However, solubility measurements with a final pH equal to the initial pH of 5.00 of FeSSIF and blank aqueous buffer was impossible because all the cococrystals studied were unstable in aqueous solution and the only method of accessing the equilibrium solubility was at the eutectic point, with in the presence of excess cofomer. Since log SR-log D correlations were better fits for both SR_{drug} and $SR_{\text{cococrystal}}$, only log D correlations will be considered for the remaining analysis in this work. However, for systems without ionizable components, log P would be a good descriptor of drug hydrophobicity to correlate with drug and cococrystal solubilization.

Predicting log $SR_{\text{cococrystal}}$ from log SR_{drug} -log D correlations

The fitted linear regression data in Figure 4.1 and Figure 4.2 indicate that log $SR_{\text{cococrystal}}$ for 1:1 cococrystals has a weaker dependence on log D compared to log SR_{drug} . Figure 4.3 compares the experimentally determined log SR-log D correlations for drug and 1:1 cococrystals.

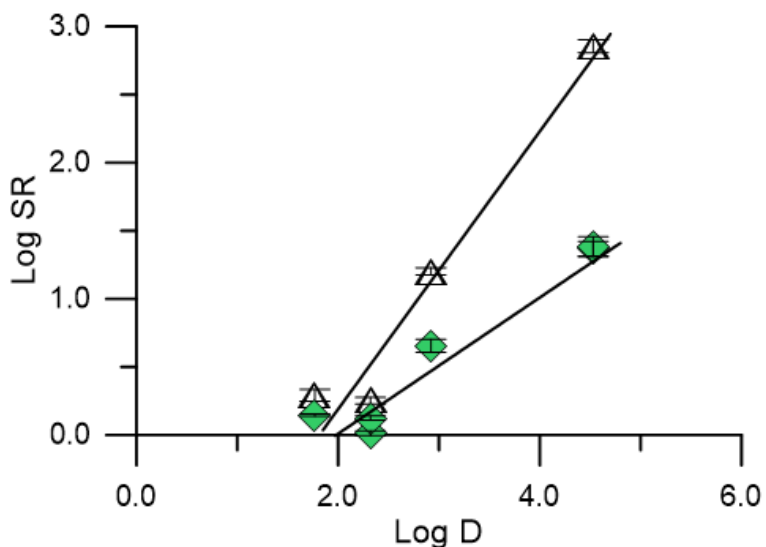


Figure 4.3. Log $SR_{\text{cococrystal}}$ -log D for 1:1 cococrystals and log SR_{drug} -log D correlations. Symbols for drugs (\triangle) and cococrystals (\blacklozenge) represent experimentally measured data and the lines are a result of linear regression of the data ($y = (1.02 \pm 0.09)x - 1.9 \pm 0.3$) for drugs and ($y =$

$(0.50 \pm 0.05)x - 1.0 \pm 0.2$) for cocrystals. Errors on regression parameters indicate the 95% confidence interval. $\log D$ values calculated using the ADMET Predictor Module in Gastro-Plus. For nonionizable drugs DNZ and CBZ (H), the measured $\log P$ was used in lieu of a calculated $\log D$ since the $\log D$ is not predicted to change with pH.

The slope and intercept of the 1:1 cocrystal $\log SR$ - $\log D$ correlation are significantly smaller than that of the drug. Equations (4.6) and (4.8), indicate how $\log SR_{\text{cocrystal}}$ is expected to relate to $\log SR_{\text{drug}}$ of the constituent drug as long as SR_{coformer} is negligible. As described in the theoretical section, the slope (m) and intercept (b) of cocrystal linear regression equations are expected to be smaller than that of the drug. For a 1:1 cocrystal,

$$m_{\text{cocrystal}} = \frac{m_{\text{drug}}}{2} \quad (4.17)$$

and

$$b_{\text{cocrystal}} = \frac{b_{\text{drug}}}{2} \quad (4.18)$$

It is possible to use these relationships to predict $\log SR_{\text{cocrystal}}$ simply from knowledge of drug $\log D$ based on an experimentally determined $\log SR_{\text{drug}}$ - $\log D$ correlation. After a $\log SR_{\text{drug}}$ - $\log D$ linear regression equation has been obtained from fitted data, equations (4.17) and (4.18) indicate how the slope and intercept of a 1:1 cocrystal linear regression equation should relate to the experimentally determined slope and intercept of the drug linear regression equation.

Table 4.3 compares the fitted linear regression equation of experimentally measured $\log SR_{\text{cocrystal}}$ - $\log D$ (Figure 4.2b) for 1:1 cocrystals to the predicted linear equation. The predicted linear equation is calculated from equations (4.13) and the linear regression equation of the fitted experimentally measured $\log SR_{\text{drug}}$ - $\log D$ ($y = (1.02 \pm 0.09)x - 1.9 \pm 0.3$) in Figure 4.2b.

Table 4.3. Comparison of fitted and predicted linear relationships between $\log \text{SR}_{\text{cococrystal}}$ of 1:1 cococrystals and $\log D$ of the constituent drug.

	Equation	Slope (m) ^a	Intercept (b) ^a
Fitted	$y = (0.50 \pm 0.05) \log D - 1.0 \pm 0.2$	0.50 ± 0.05	-1.0 ± 0.2
Predicted	$y = 0.51(\log D) - 1.03$	0.51	1.03

(a) Errors on regression parameters represent the 95% confidence interval.

There is excellent agreement between the equations for the linear regression of the experimentally determined $\log \text{SR}_{\text{cococrystal}} - \log D$ and the line predicted by equation (4.13). Theoretically, the slope and intercept of the cococrystal linear regression equation should be half that of the constituent drugs as predicted by equation (4.13). The measured regression slope of 0.50 for cococrystals is half that of the drug regression slope of 1.02 ($m_{\text{cococrystal}}/m_{\text{drug}} = 1/2$) and the measured regression intercept of -1.0 is half that of the drug regression intercept of -1.9 ($b_{\text{cococrystal}}/b_{\text{drug}} = 1/2$).

Even though the $\text{SR}_{\text{cococrystal}}$ was only measured for one 2:1 cococrystal (and therefore no linear regression equation fitted to the data), the $\log \text{SR}_{\text{cococrystal}} - \log D$ relationship can be predicted from the linear regression equation for the $\log \text{SR}_{\text{drug}} - \log D$ ($y = (1.02 \pm 0.09)x - 1.9 \pm 0.3$) similar to the case for the 1:1 cococrystals. As indicated by equation (4.14), the slope and intercept should be 2/3 those of the drug equation. Table 4.4 shows the predicted linear regression equations for 1:1 and 2:1 cococrystals based on the experimentally determined $\log \text{SR}_{\text{drug}} - \log D$ equation.

Table 4.4. Predicted $\log SR_{\text{cocystal}} - \log D$ linear regression equations for 1:1 and 2:1 cocrystals.

Stoichiometry	Predicted Linear Regression Equation ^a
1:1 cocrystals	$y = 0.51(\log D) - 1.03$
2:1 cocrystals	$y = 0.68(\log D) - 1.38$

(a) Predicted from equations (4.13) and (4.14) based on the experimentally determined drug linear regression equation of $y = (1.02 \pm 0.09)x - 1.9 \pm 0.3$.

The equations in Table 4.4 are plotted against the experimentally determined $\log SR_{\text{cocystal}}$ and calculated $\log D$ values in Figure 4.4.

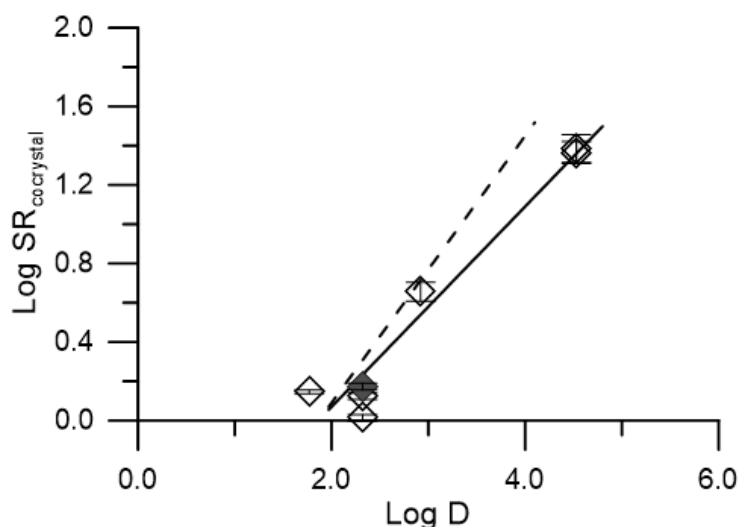


Figure 4.4. $\log SR_{\text{cocystal}}$ correlation with $\log D$. Symbols represent experimentally measured values for 1:1 cocrystals (◇) and 2:1 (◆) cocrystals. The lines represent predicted linear regression equations in Table X, $y = 0.51(\log D) - 1.03$ for 1:1 cocrystals and $y = 0.68(\log D) - 1.38$ for 2:1 cocrystals. $\log D$ values are calculated using the ADMET Predictor Module in Gastro-Plus. For nonionizable drugs DNZ and CBZ (H), the measured $\log P$ was used in lieu of a calculated $\log D$ since the $\log D$ is not predicted to change with pH.

The predicted linear regression equations are in good agreement with the experimentally measured SR_{cocystal} values. Table 4.5 shows the predicted and measured SR_{cocystal} values.

Table 4.5. Comparison of predicted and measured $\log SR_{\text{cococrystal}}$ for 1:1 and 2:1 cococrystals.

Cococrystal	$\log D$ drug ^a	pH_{eu}	$\log SR_{\text{cococrystal exp}}$	$\log SR_{\text{cococrystal pred}}^b$
DNZ-VAN (1:1)	4.53	4.46±0.06	1.39±0.07	1.28
DNZ-HBA(1:1)	4.53	4.46±0.06	1.36±0.06	1.28
IND-SAC (1:1)	3.71	3.65 ± 0.05	0.66±0.05	0.86
CBZ-4ABA-HYD (2:1)	2.32	4.94 ± 0.02	0.17±0.02	0.20
CBZ-SLC (1:1)	2.32	4.29 ± 0.02	0.12±0.02	0.15
CBZ-SAC (1:1)	2.32	3.11 ±0.02	0.023±0.007	0.15
PXC-SAC (1:1)	1.79	3.79 ± 0.02	0.15±0.01	0.03

(a) Log D values are calculated at pH_{eu} using the ADMET Predictor Module in Gastro-Plus.

(b) Predicted using $y = 0.51(\log D) - 1.03$ for 1:1 cococrystals and $y = 0.68(\log D) - 1.38$ for 2:1 cococrystals.

The predicted $\log SR_{\text{cococrystal}}$ values are in reasonable agreement with the experimentally measured values using the linear regression equations. There are some deviations for cococrystals of less solubilized drugs, particularly for the CBZ-SAC and PXC-SAC cococrystals. For CBZ-SAC, the predicted log SR is much higher than the experimentally measured value. High SAC concentrations at the eutectic point were observed to lower CBZ solubilization as described in Chapter 2, which causes the low measured $SR_{\text{cococrystal}}$ value for CBZ-SAC. The deviation for PXC-SAC is likely due to the log D value used for prediction. Log D values for PXC calculated^{15, 18-20} using different software packages can differ by as much as 2 fold depending on the pH conditions of interest. For the best prediction, a measured log D in the experimental conditions of interest would be optimal.

Considering that the predicted values are calculated from a log SR_{drug} -log D correlation of only 4 drugs, the fit for the majority of the cocrystals is reasonable. A more robust log SR_{drug} -log D correlation of more drugs of varying log D would lead to better log $SR_{\text{cocrystal}}$ predictions, and this work provides the theoretical framework to make these predictions.

Conclusions

In this work we develop mathematical models that describe the relationship between log $SR_{\text{cocrystal}}$ and log SR_{drug} for the purpose of comparing the correlation between log SR and drug hydrophobicity (as described by log P or log D) for drugs and cocrystals. Ionizable drugs are considered and log D was determined to be a better drug hydrophobicity descriptor than log P for these drugs and cocrystals. The log $SR_{\text{cocrystal}}$ exhibits a weaker dependence on drug log D for compared to log SR_{drug} , which is predicted from mathematical models presented here. The presented models can be used to predict log $SR_{\text{cocrystal}}$ simply from knowledge of drug log D if a robust log SR_{drug} -log D linear regression correlation is calculated from experimentally measured SR_{drug} values. These models are valuable since SR_{drug} and log P and/or log D are commonly measured and reported drug properties. From the proposed models, $SR_{\text{cocrystal}}$ of a cocrystal of a given drug can be predicted before a cocrystal has even been synthesized. These predictions can guide solid form selection decisions since the solubilization of a cocrystal of a given drug can be anticipated as long as the stoichiometry of that cocrystal is known.

References

1. Alvarez-Nunez, F. A.; Yalkowsky, S. H. Relationship between Polysorbate 80 solubilization descriptors and octanol-water partition coefficients of drugs. *Int. J. Pharm.* **2000**, *200*, (2), 217-222.
2. Fagerberg, J. H.; Tsinman, O.; Sun, N.; Tsinman, K.; Avdeef, A.; Bergstrom, C. A. S. Dissolution Rate and Apparent Solubility of Poorly Soluble Drugs in Biorelevant Dissolution Media. *Mol. Pharm.* **2010**, *7*, (5), 1419-1430.

3. Mithani, S. D.; Bakatselou, V.; TenHoor, C. N.; Dressman, J. B. Estimation of the increase in solubility of drugs as a function of bile salt concentration. *Pharm. Res.* **1996**, *13*, (1), 163-167.
4. Charman, W. N.; Porter, C. J. H.; Mithani, S.; Dressman, J. B. Physicochemical and physiological mechanisms for the effects of food on drug absorption: The role of lipids and pH. *J. Pharm. Sci.* **1997**, *86*, (3), 269-282.
5. Huang, N.; Rodriguez-Hornedo, N. Engineering Cocrystal Solubility, Stability, and pH(max) by Micellar Solubilization. *J. Pharm. Sci.* **2011**, *100*, (12), 5219-5234.
6. Bernhard, E.; Zimmermann, F. Contribution to the Understanding of Oxicam Ionization-Constants. *Arzneimittel-Forschung/Drug Research* **1984**, *34-1*, (6), 647-648.
7. Mooney, K. G.; Mintun, M. A.; Himmelstein, K. J.; Stella, V. J. Dissolution Kinetics of Carboxylic-Acids .1. Effect of Ph under Unbuffered Conditions. *J. Pharm. Sci.* **1981**, *70*, (1), 13-22.
8. Newton, D. W.; Kluza, R. B. Pka values of medicinal compounds in pharmacy practice. *Drug Intelligence & Clinical Pharmacy* **1978**, *12*, (9), 546-554.
9. Alhalaweh, A.; Roy, L.; Rodriguez-Hornedo, N.; Velaga, S. P. pH-Dependent Solubility of Indomethacin-Saccharin and Carbamazepine-Saccharin Cocrystals in Aqueous Media. *Mol. Pharm.* **2012**, *9*, (9), 2605-2612.
10. Robinson, R. A.; Biggs, A. I. The ionization constants of para-aminobenzoic acid in aqueous solution at 25-degrees-c. *Aust. J. Chem.* **1957**, *10*, (2), 128-134.
11. Robinson, R. A.; Kiang, A. K. The ionization constants of vanillin and 2 of its isomers. *Transactions of the Faraday Society* **1955**, *51*, (10), 1398-1402.
12. Galia, E.; Nicolaidis, E.; Horter, D.; Lobenberg, R.; Reppas, C.; Dressman, J. B. Evaluation of various dissolution media for predicting in vivo performance of class I and II drugs. *Pharm. Res.* **1998**, *15*, (5), 698-705.
13. Rodriguez-Hornedo, N.; Nehru, S. J.; Seefeldt, K. F.; Pagan-Torres, Y.; Falkiewicz, C. J. Reaction crystallization of pharmaceutical molecular complexes. *Mol. Pharm.* **2006**, *3*, (3), 362-367.
14. Caron, J. C.; Shroot, B. Determination of partition-coefficients of glucocorticosteroids by high-performance liquid-chromatography. *J. Pharm. Sci.* **1984**, *73*, (12), 1703-1706.
15. Tsai, R. S.; Carrupt, P. A.; Eltayar, N.; Giroud, Y.; Andrade, P.; Testa, B.; Bree, F.; Tillement, J. P. Physicochemical and Structural-Properties of Nonsteroidal Antiinflammatory Oxicams. *Helvetica Chimica Acta* **1993**, *76*, (2), 842-854.
16. Palagiano, F.; Arenare, L.; Barbato, F.; LaRotonda, M. I.; Quaglia, F.; Bonina, F. P.; Montenegro, L.; deCaprariis, P. In vitro and in vivo evaluation of terpenoid esters of indomethacin as dermal prodrugs. *Int. J. Pharm.* **1997**, *149*, (2), 171-182.
17. Machatha, S. G.; Yalkowsky, S. H. Comparison of the octanol/water partition coefficients calculated by ClogP((R)), ACDlogP and KowWin((R)) to experimentally determined values. *Int. J. Pharm.* **2005**, *294*, (1-2), 185-192.
18. Acuna, J. A.; Delafuente, C.; Vazquez, M. D.; Tascon, M. L.; Sanchezbatanero, P. Voltammetric Determination of Piroxicam in Micellar Media by Using Conventional and Surfactant Chemically-Modified Carbon-Paste Electrodes. *Talanta* **1993**, *40*, (11), 1637-1642.
19. Jinno, J.; Oh, D. M.; Crison, J. R.; Amidon, G. L. Dissolution of ionizable water-insoluble drugs: The combined effect of pH and surfactant. *J. Pharm. Sci.* **2000**, *89*, (2), 268-274.

20. Vrečer, F.; Vrbinc, M.; Meden, A. Characterization of piroxicam crystal modifications. *Int. J. Pharm.* **2003**, *256*, (1-2), 3-15.

CHAPTER 5

COCRYSTAL SOLUBILIZATION IN THE PRESENCE OF MULTIPLE SOLUBILIZING AGENTS

Introduction

Cocrystal solubility is profoundly affected by the presence of solubilizing agents in solution¹⁻⁵. Differential solubilization of cocrystal constituents can lead to a reduction in the solubility advantage of the cocrystal over the drug ($S_{\text{cocrystal}}/S_{\text{drug}}$) when the drug constituent is solubilized and the coformer is not¹⁻⁵. Mathematical models that consider relevant solution equilibria have been derived to describe and predict the influence of single solubilizing agents on cocrystal solubility and thermodynamic stability. The solubility values predicted by these models have been shown to be in good agreement with experimentally measured solubilities for cocrystals of carbamazepine and indomethacin in the presence of several synthetic surfactants¹⁻⁵. In the presence of these additives, cocrystal solubility relative to the drug solubility was switched, and this behavior predicted using the reported models.

It is likely that the solubility of a formulated cocrystal drug product would be affected by several additives simultaneously. The cocrystal would encounter synthetic solubilizing agents in the formulation as well as endogenous surfactants *in vivo*. A mechanistic understanding of the combined effect of several solubilizing agents on cocrystal solution behavior is yet to be established. It has been reported that the *in vitro* dissolution profile of the danazol-vanillin cocrystal was improved drastically when formulated with a vitamin E-TPGS solubilizing agent

and hydroxypropylcellulose precipitation inhibitor in the presence of fasted state simulated intestinal fluid (FaSSIF)⁶. The combined effect of the additives resulted in a 10 fold increase in area under the curve (AUC) of the plasma drug concentration- time profile in an *in vivo* study in rats compared to a 1.7 fold increase for the unformulated cocrystal⁶. Could this behavior have been predicted from knowledge of the solubilization mechanisms of cocrystals in the presence of these solubilizing agents? Does solubilization by multiple solubilizing agents have an additive effect on cocrystal solubility and stability? How does the decrease in $S_{\text{cocrystal}}/S_{\text{drug}}$ observed in a single solubilizing agent compared to the decrease in multiple solubilizing agents?

The aim of this work is to develop models to predict cocrystal solubility and $S_{\text{cocrystal}}/S_{\text{drug}}$ in the presence of multiple solubilizing agents. As a first approximation, solubility in the presence of two ideally mixing solubilizing agents will be considered. This treatment of the solubilizing agents assumes that solubilization by each solubilizing agent is unaffected by the presence of the other solubilizing agent. Two 1:1 cocrystals of the poorly solubility drug danazol (DNZ) were chosen for study: the danazol-hydroxybenzoic acid cocrystal (DNZ-HBA) and danazol-vanillin (DNZ-VAN). DNZ is a nonionizable, hydrophobic drug ($\log P = 4.53^7$) that has been shown to be highly solubilized by solubilizing agents^{6, 8-11}. Hydroxybenzoic acid (HBA) is a weakly acidic ($\text{pKa} = 4.48^{12}$) hydrophilic ($\log P = 1.60^{13, 14}$) cofomer, and vanillin is a weakly acidic ($\text{pKa} = 7.4^{12}$), hydrophilic ($\log P = 1.26^{13, 14}$) cofomer. These cocrystals were chosen based on literature reports that their solubility is highly affected by multiple solubilizing agents⁶ and their high aqueous solubility and $S_{\text{cocrystal}}/S_{\text{drug}}$. Solubilizing agents were selected to mimic a cocrystal in the presence of one synthetic formulation additive (Tween 80) and one physiologically relevant surfactant (fed state simulated intestinal fluid (FeSSIF)). Solubilizing agents were selected based on their high solubilizing capacity of DNZ.

Theoretical

Cocrystal solubility in multiple surfactants

Cocrystal solubility and thermodynamic stability in the presence of multiple solubilizing agents is determined by the equilibria between the cocrystal and drug solid phases and the drug and coformer constituents in the solution phase. The effect of micellar solubilization of cocrystal constituents by multiple solubilizing agents can be mathematically modeled by examining the relevant solution equilibria and expanding upon previously reported models that consider a single solubilizing agents. In this analysis, two micellar surfactants will be considered.

The relevant equilibria for a 1:1 cocrystal RHA, where R represents a nonionizable drug, HA represents a monoprotic weakly acidic coformer, M_A represents micellar surfactant A, and M_B represents micellar surfactant B, are:





And the associated equilibrium constants are:

The cocrystal solubility product K_{sp} :

$$K_{sp} = [R]_{aq} [HA]_{aq} \quad (5.9)$$

The ionization constant K_a for the monoprotic weakly acidic coformer HA:

$$K_a = \frac{[A^-]_{aq} [H^+]_{aq}}{[HA]_{aq}} \quad (5.10)$$

The micellar solubilization constants $K_{s,A}^R$ and $K_{s,B}^R$ for drug R in surfactants A and B:

$$K_{s,A}^R = \frac{[R]_{mA}}{[R]_{aq} [M]_A} \quad (5.11)$$

$$K_{s,B}^R = \frac{[R]_{mB}}{[R]_{aq} [M]_B} \quad (5.12)$$

The micellar solubilization constants $K_{s,A}^{HA}$ and $K_{s,B}^{HA}$ for unionized coformer HA in surfactants A and B:

$$K_{s,A}^{HA} = \frac{[HA]_{mA}}{[HA]_{aq} [M]_A} \quad (5.13)$$

$$K_{s,B}^{HA} = \frac{[HA]_{mB}}{[HA]_{aq} [M]_B} \quad (5.14)$$

The micellar solubilization constants $K_{s,A}^{A^-}$ and $K_{s,B}^{A^-}$ for ionized coformer A^- in surfactants A and B:

$$K_{s,A}^{A^-} = \frac{[A^-]_{mA}}{[A^-]_{aq}[M]_A} \quad (5.15)$$

$$K_{s,B}^{A^-} = \frac{[A^-]_{mB}}{[A^-]_{aq}[M]_B} \quad (5.16)$$

The subscript aq refers to the aqueous phase while m refers to the micellar phase. This way of defining the micellar solubilization constants utilizes the mass action model of solubilization and assumes that surfactants A and B mix ideally. That is, that solubilization by either A or B is independent of solubilization by the other surfactant. Assuming ideally mixing surfactants allows the solubilization contributions of each surfactant to the total cocrystal solubility to be treated additively. Activities are replaced by concentrations assuming dilute solution conditions.

The total solubility of RHA, $S_{RHA,T}$, is derived by considering the mass balances on R and HA:

$$[R]_T = [R]_{aq} + [R]_{mA} + [R]_{mB} \quad (5.17)$$

and

$$[A]_T = [HA]_{aq} + [HA]_{mA} + [HA]_{mB} + [A^-]_{aq} + [A^-]_{mA} + [A^-]_{mB} \quad (5.18)$$

and substituting the above equilibrium constants to give

$$S_{RHA,T} = \sqrt{K_{sp} \left(1 + K_{s,A}^R [M]_A + K_{s,B}^R [M]_B \right) \left(1 + 10^{pH-pK_a} + K_{s,A}^{HA} [M]_A + K_{s,B}^{HA} [M]_B + K_{s,A}^{A^-} [M]_A 10^{pH-pK_a} + K_{s,B}^{A^-} [M]_B 10^{pH-pK_a} \right)} \quad (5.19)$$

in terms of the stoichiometric cocrystal solubility, which are equimolar drug and cofomer in the case of this 1:1 cocrystal.

To simplify equation (5.19), total solubilization constants in specified pH conditions (K_s^T) can be substituted. For nonionizable drug R, $K_s^{R,T}$ is simply the solubilization constant for the nonionized component (K_s^R) and the calculation of a total solubilization constant is not necessary. For ionizable components, the total solubilization constant takes into account the equilibrium solubilization constants in a given media for both the ionized and unionized species. For example, for weakly acidic component HA, the total solubility in a surfactant as a function of intrinsic aqueous solubility S_{aq} , ionization constant K_a , and micellar solubilization is given by:

$$S_T^{HA} = S_{aq}^{HA} \left(1 + 10^{pH-pK_{a,acid}} + \underbrace{\left(K_s^{HA} + 10^{pH-pK_{a,acid}} K_s^{A^-} \right)}_{K_s^{A,T}} [M] \right) \quad (5.20)$$

In order to take into account the solubilization of both unionized and ionized components, the solubilization constants can be grouped into $K_s^{HA,T}$ which indicates the total solubilization of HA at a given pH in a particular surfactant.

$$S_T^{HA} = S_{aq}^{HA} \left(1 + 10^{pH-pK_{a,acid}} + K_s^{HA,T} [M] \right) \quad (5.21)$$

The simplified equation for the solubility of 1:1 cocystal RHA in two surfactants then becomes:

$$S_{RHA,T} = \sqrt{K_{sp} \left(1 + K_s^R_{A,T} [M_A] + K_s^R_{B,T} [M_B] \right) \left(1 + 10^{pH-pK_a} + K_s^{HA}_{A,T} [M_A] + K_s^{HA}_{B,T} [M_B] \right)} \quad (5.22)$$

The micellar surfactant concentrations $[M_A]$ and $[M_B]$ are the total surfactant concentrations minus the critical micellar concentration (CMC) of each surfactant. This assumes the CMC of each surfactant is unaffected by the presence of the other surfactant and is constant in the range of concentrations and solubilizations considered here.

This equation can serve as an approximation of cocrystal solubility in *in vivo* conditions where the cocrystal may be in the presence of a formulation surfactant as well as endogenous surfactants. K_s^T and K_a values of cocrystal components are often available in the literature and the prediction only requires a measure of cocrystal K_{sp} and knowledge of the solution conditions (pH, [M]) of interest. This can be useful knowledge to design appropriate dissolution experiments and choose formulations that target a specific cocrystal solubility *in vivo*.

The stoichiometric solubility of the cocrystals (cocrystal at equilibrium with solution concentrations of constituents equal to their molar ratio) is calculated from experimentally measured total eutectic concentrations in the presence of surfactants by the following equation for 1:1 cocrystals^{15, 16}:

$$S_T^{1:1 \text{ cocrystal}} = \sqrt{[\text{drug}]_{T,eu} [\text{coformer}]_{T,eu}} \quad (5.23)$$

This method of accessing cocrystal equilibrium solubility in nonstoichiometric conditions is well established in the literature^{4, 5, 15-18}.

Cocrystal solution stability in multiple surfactants

$S_{\text{cocrystal}}/S_{\text{drug}}$, the ratio of the cocrystal solubility to the drug solubility, is a measure of the cocrystal thermodynamic stability in solution. It has been previously reported in this dissertation and elsewhere that $S_{\text{cocrystal}}/S_{\text{drug}}$ of a 1:1 cocrystal RHA of nonionizable drug R and monoprotic weakly acidic coformer HA in the presence of a surfactant is⁴:

$$\left(\frac{S_{\text{cocrystal}}}{S_{\text{drug}}} \right)^{\text{RHA}} = \frac{\sqrt{K_{sp}^{\text{RHA}} (1 + K_{s,T}^R [M]) (1 + 10^{\text{pH} - \text{pKa}} + K_{s,T}^{\text{HA}} [M])}}{S_{R, \text{aq}}^0 (1 + K_{s,T}^R [M])} \quad (5.24)$$

In the presence of two ideally mixing surfactants A and B, the solubilization by each surfactant is additive, and equation (5.24) becomes

$$\left(\frac{S_{\text{cocystal}}}{S_{\text{drug}}}\right)^{\text{RHA}} = \frac{\sqrt{K_{\text{sp}} \left(1 + K_{\text{s,A,T}}^{\text{R}} [\text{M}_\text{A}] + K_{\text{s,B,T}}^{\text{R}} [\text{M}_\text{B}]\right) \left(1 + 10^{\text{pH}-\text{pK}_\text{a}} + K_{\text{s,A,T}}^{\text{HA}} [\text{M}_\text{A}] + K_{\text{s,B,T}}^{\text{HA}} [\text{M}_\text{B}]\right)}}{S_{\text{R,aq}}^0 \left(1 + K_{\text{s,A}}^{\text{R}} [\text{M}_\text{A}] + K_{\text{s,B}}^{\text{R}} [\text{M}_\text{B}]\right)} \quad (5.25)$$

The above equation allows for the prediction of $S_{\text{cocystal}}/S_{\text{drug}}$ in two surfactants from knowledge of cocystal K_{sp} , drug and cofomer K_{s}^{T} values in each surfactant, and drug intrinsic aqueous solubility ($S_{\text{drug,aq}}^0$). This is helpful to predict if a cocystal will be stabilized ($S_{\text{cocystal}}/S_{\text{drug}} = 1$) in a given formulation or to target a theoretical supersaturation.

Figure 5.1 shows the theoretical $S_{\text{cocystal}}/S_{\text{drug}}$ for two 1:1 cocystals RHA (of the same drug R) in the presence of one or two surfactants. The cocystals are modeled as formulated cocystals with one surfactant representing a physiologically relevant (endogenous) surfactant at the concentration of FeSSIF, and the other a synthetic formulation surfactant at varying concentrations. The impact of different aqueous solubility advantages ($S_{\text{cocystal}}/S_{\text{drug}})_{\text{aq}}$ on the ability of these cocystals to be stabilized by the formulation surfactant is examined. Cofomer solubilization was assumed to be negligible and the cocystals to be in nonionizing conditions. $K_{\text{s}}^{\text{drug,T}}$ values were selected from common range for hydrophobic drug solubilization in physiologically relevant and synthetic formulation surfactants.

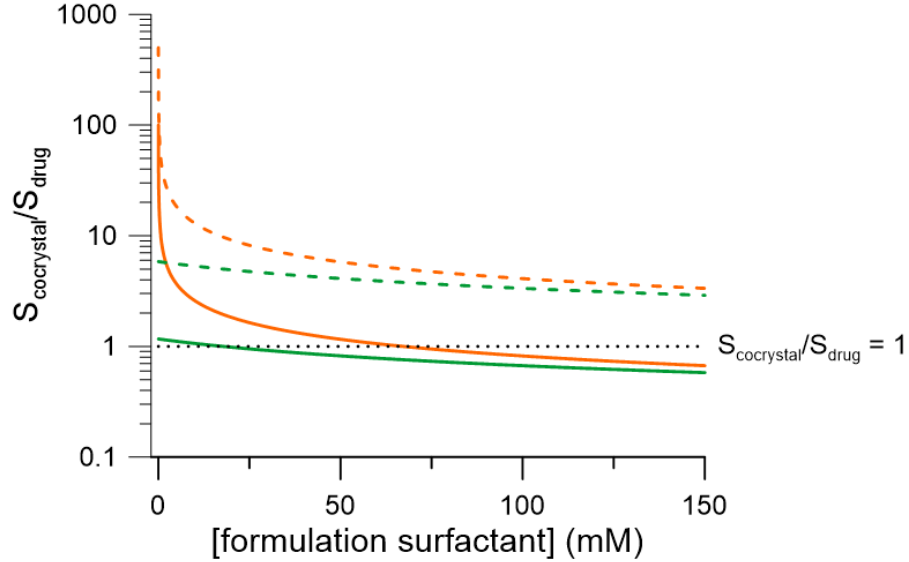


Figure 5.1. $S_{\text{cocrystal}}/S_{\text{drug}}$ for two 1:1 cocrystals predicted from equation (5.24) for 1 surfactant (formulation only) and (5.25) for 2 surfactants (formulation + physiologically relevant) in increasing concentrations of a formulation surfactant. Dotted lines represent cocrystal A with $(S_{\text{cocrystal}}/S_{\text{drug}})_{\text{aq}} = 500$ and solid lines represent cocrystal B with $(S_{\text{cocrystal}}/S_{\text{drug}})_{\text{aq}} = 100$. Conditions with only one solubilizing agent (formulation) are shown in orange and those with two solubilizing agents (formulation + physiologically relevant) are shown in green. Values used for predictions are: $K_{\text{sp}} = 2.5 \text{ mM}^2$ for cocrystal A and 62.5 mM^2 for cocrystal B, $S_{\text{drug, aq}}^0 = 0.5 \text{ mM}$, $K_{\text{s, formulation surfactant}} = 150 \text{ mM}^{-1}$, $K_{\text{s, physiologically relevant}} = 50 \text{ mM}^{-1}$, $[\text{M}]$ of the physiologically relevant surfactant = 147 mM (that of FeSSIF).

When $(S_{\text{cocrystal}}/S_{\text{drug}})_{\text{aq}} = 100$, cocrystal RHA is stabilized ($(S_{\text{cocrystal}}/S_{\text{drug}})_{\text{T}} = 1$) in both the formulation surfactant alone and in a physiologically relevant surfactant in addition to a formulation surfactant. The presence of two surfactants allows the cocrystal to be stabilized at a lower concentration of formulation surfactant. In the presence of the physiologically relevant surfactant, only 18 mM of formulation surfactant is needed to stabilize the cocrystal, while in the absence, around 70 mM is necessary. This highlights the large reduction in $S_{\text{cocrystal}}/S_{\text{drug}}$ that is possible in the presence of multiple surfactants.

$(S_{\text{cocrystal}}/S_{\text{drug}})_{\text{aq}}$ has a large impact on the ability of a cocrystal to be stabilized in a formulation. When $(S_{\text{cocrystal}}/S_{\text{drug}})_{\text{aq}} = 500$, the cocrystal cannot be stabilized in a reasonable

concentration of the formulation surfactant even when a physiologically relevant surfactant is present. The lowest $S_{\text{cocrystral}}/S_{\text{drug}}$ achievable is 5 at 150 mM of formulation surfactant in the presence physiologically relevant surfactant. Even though very highly soluble cocrystals may not be able to be stabilized in multiple surfactants, it is clear that the $S_{\text{cocrystal}}/S_{\text{drug}}$ can be decreased by orders of magnitude by selection of solubilizing agents with appropriate $K_s^{\text{drug,T}}$ values. When more than one surfactant is present, the $S_{\text{cocrystal}}/S_{\text{drug}}$ can be reduced effectively with a lower concentration of one of the surfactants since the stabilizing power of the surfactants is additive. Selection of formulation surfactants to dial-in a target $S_{\text{cocrystal}}/S_{\text{drug}}$ can optimize cocrystal dissolution profile to achieve higher drug concentrations and sustained supersaturations.

Experimentally, $S_{\text{cocrystal}}/S_{\text{drug}}$ is assessed from the drug and coformer eutectic concentrations by calculating the eutectic constant, $K_{\text{eu}}^{15, 16}$. K_{eu} is a directly measurable parameter calculated according to:

$$K_{\text{eu}} = \frac{[\text{coformer}]_{\text{eu}}}{[\text{drug}]_{\text{eu}}} \quad (5.26)$$

The eutectic constant is related to the cocrystal thermodynamic stability, also called the cocrystal solubility advantage $S_{\text{cocrystal}}/S_{\text{drug}}$. For cocrystal A_xB_y , where A and B are the cocrystal constituents, drug and coformer respectively; and x and y are the stoichiometric coefficients or molar ratios, $S_{\text{cocrystal}}/S_{\text{drug}}$ is a function of K_{eu} as follows^{15, 16}:

$$K_{\text{eu}} = \frac{[\text{coformer}]_{\text{T,eu}}}{[\text{drug}]_{\text{T,eu}}} = xy^{\frac{x}{y}} \left(\frac{S_{\text{cocrystal}}}{S_{\text{drug}}} \right)^{\frac{(x+y)}{y}} \quad (5.27)$$

This relationship is valid in both aqueous and solubilizing agent solutions as it relies on the total measured eutectic concentrations of drug and coformer in the conditions of interest. For a 1:1 cocrystal, equation (5.27) becomes

$$K_{eu} = \frac{[\text{coformer}]_{eu}}{[\text{drug}]_{eu}} = \left(\frac{S_{\text{cocrystal}}}{S_{\text{drug}}} \right)^2 \quad (5.28)$$

And

$$\left(\frac{S_{\text{cocrystal}}}{S_{\text{drug}}} \right) = \sqrt{\frac{[\text{coformer}]_{eu}}{[\text{drug}]_{eu}}} \quad (5.29)$$

Materials and Methods

Materials

Cocrystal constituents

Anhydrous danazol was received as a gift from Renovo Research (Atlanta, GA) and used as received. Anhydrous hydroxybenzoic acid was purchased from Acros Organics (Pittsburgh, PA) and used as received. Anhydrous vanillin was purchased from Fisher Scientific (Fair Lawn, NJ) and used as received. Hydroxybenzoic acid monohydrate (HBA (H)) was prepared by slurring HBA in deionized water for at least 24 hours. All crystalline drugs and coformers were characterized by X-ray power diffraction (XRPD) and differential scanning calorimetry (DSC) before carrying out experiments.

Solvents and buffer components

Ethyl acetate was purchased from Acros Organics (Pittsburgh, PA) and used as received, and HPLC grade methanol was purchased from Fisher Scientific (Pittsburgh, PA). Trifluoroacetic acid spectrophotometric grade 99% was purchased from Aldrich Company

(Milwaukee, WI). Water used in this study was filtered through a double deionized purification system (Milli Q Plus Water System) from Millipore Co. (Bedford, MA).

Tween 80 solutions, FeSSIF, and acetate buffer were prepared using Tween 80 purchased from Sigma Chemical Company (St. Louis, MO), sodium taurocholate (NaTC) purchased from Sigma Chemical Company (St. Louis, MO), lecithin purchased from Fisher Scientific (Pittsburgh, PA), sodium hydroxide pellets (NaOH) purchased from J.T. Baker (Philipsburg, NJ), and acetic acid and potassium chloride (KCl) purchased from Acros Organics (Pittsburgh, PA).

Methods

FeSSIF, acetate buffer, and Tween 80 solution preparation

FeSSIF and acetate buffer were prepared according to the protocol of Galia and coworkers¹⁹. Acetate buffer was prepared as a stock solution at room temperature by dissolving 8.08 g NaOH (pellets), 17.3 g glacial acetic acid and 23.748 g NaCl in 2 L of purified water. The pH was adjusted to 5.00 with 1 N NaOH and 1N HCl. FeSSIF was prepared by dissolving 0.41 g sodium taurocholate in 12.5 mL of pH 5.00 acetate buffer. 0.148 g lecithin was added with magnetic stirring at 37 °C until dissolved. The volume was adjusted to exactly 50 mL with acetate buffer. Tween 80 solutions were prepared by dissolving an appropriate amount (25 mM, 50 mM, 150 mM) of Tween 80 in pH 5.00 acetate buffer.

Cocrystal synthesis

Cocrystals were prepared by the reaction crystallization method²⁰ at 25°C. The 1:1 danazol-hydroxybenzoic acid cocrystal (DNZ-HBA) was prepared by adding stoichiometric amounts of cocrystal components (DNZ and HBA) to nearly saturated HBA solution in ethyl acetate. The 1:1 danazol-vanillin cocrystal (DNZ-VAN) was prepared by adding stoichiometric amounts of cocrystal components (DNZ and VAN) to nearly saturated VAN solution in ethyl

acetate. Prior to carrying out any solubility experiments, solid phases were characterized by XRPD and DSC and stoichiometry verified by HPLC. Full conversion to cocrystal was observed in 24 hours.

Solubility measurements of cocrystal constituents

Cocrystal constituent solubilities were measured in FeSSIF, Tween 80, and pH 5.00 acetate buffer (FeSSIF without NaTC and lecithin or Tween 80). The solubilities of the cocrystal components were determined by adding excess solid to 3 mL of media (FeSSIF, Tween 80, or buffer). Solutions were magnetically stirred and maintained at $25 \pm 0.1^\circ\text{C}$ using a water bath for up to 96 h. In 24 hr intervals, 0.30 mL of samples were collected, pH of solutions measured, and filtered through a 0.45 μm pore membrane. After dilution with mobile phase, solution concentrations of drug or coformer were analyzed by HPLC. The final solid phases were characterized by XRPD and DSC.

Cocrystal solubility measurements

Cocrystal equilibrium solubilities were measured in FeSSIF, Tween 80, and pH 5.00 acetate buffer (FeSSIF without NaTC and lecithin) at the eutectic point, where drug and cocrystal solid phases are in equilibrium with solution. The eutectic point between cocrystal and drug was approached by cocrystal dissolution (suspending solid cocrystal (~100 mg) and drug (~50 mg) in 3 mL of media (FeSSIF or buffer)) and by cocrystal precipitation (suspending solid cocrystal (~50 mg) and drug (~100 mg) in 3 mL of media (FeSSIF or buffer) nearly saturated with coformer). Solutions were magnetically stirred and maintained at $25 \pm 0.1^\circ\text{C}$ using a water bath for up to 96 h. At 24 hr intervals, 0.30 mL aliquots of suspension were collected, pH was measured, before filtration through a 0.45 μm pore membrane. Solid phases were also collected at 24 hr intervals to ensure the sample was at the eutectic point (confirmed by presence of both

drug and cocrystal solid phases and constant [coformer] and [drug] solution concentrations). After dilution of filtered solutions with mobile phase, drug and coformer concentrations were analyzed by HPLC. The equilibrium solid phases were characterized by XRPD and DSC.

The stoichiometric solubility of the cocrystals (cocrystal equilibrium solubility in the absence of excess coformer) is calculated by the following equations for 1:1 cocrystals¹⁵:

$$S_T^{1:1 \text{ cocrystal}} = \sqrt{[\text{drug}]_{T,\text{eu}} [\text{coformer}]_{T,\text{eu}}} \quad (5.30)$$

X-ray powder diffraction

X-ray powder diffraction diffractograms of solid phases were collected on a benchtop Rigaku Miniflex X-ray diffractometer (Rigaku, Danverse, MA) using Cu K α radiation ($\lambda=1.54\text{\AA}$), a tube voltage of 30 kV, and a tube current of 15 mA. Data were collected from 5 to 40° at a continuous scan rate of 2.5°/min.

Thermal analysis

Solid phases collected from the slurry studies were dried at room temperature and analyzed by differential scanning calorimetry (DSC) using a TA instrument (Newark, DE) 2910MDSC system equipped with a refrigerated cooling unit. DSC experiments were performed by heating the samples at a rate of 10 °C/min under a dry nitrogen atmosphere. A high purity indium standard was used for temperature and enthalpy calibration. Standard aluminum sample pans were used for all measurements.

High performance liquid chromatography

Solution concentrations were analyzed by a Waters HPLC (Milford, MA) equipped with an ultraviolet-visible spectrometer detector. For the DNZ-HBA and DNZ-VAN cocrystals and their components, a C18 Waters Atlantis (Milford, MA) column (5 μM 250 x 6 mm) at ambient

temperature was used. The injection volume was 20 μL in FeSSIF and Tween 80 experiments, and 100 μL in buffer experiments due to the extremely low solubility of DNZ in aqueous solutions. Analysis was conducted using an isocratic method composed of 80% methanol and 20% water with 0.1% trifluoroacetic acid and a flow rate of 1 mL/min. Absorbance of DNZ was monitored at 285 nm, HBA at 242 nm, and VAN at 300 nm. For all cocrystals, the Waters' operation software Empower 2 was used to collect and process data.

Results

Cocrystal component solubilization in multiple surfactants

To determine if Tween 80 and FeSSIF mix ideally, the solubilization of cocrystal constituents by Tween 80 in pH 5.00 blank aqueous buffer was compared to their solubilization by Tween 80 in the presence of FeSSIF. Drug and coformer solubilities were measured in increasing concentrations of Tween 80 either in buffer with Tween 80 or in Tween 80 + FeSSIF. Figure 5.2 and Table 5.1 show the measured DNZ solubility in 25, 50 and 150 mM Tween 80 in buffer and FeSSIF.

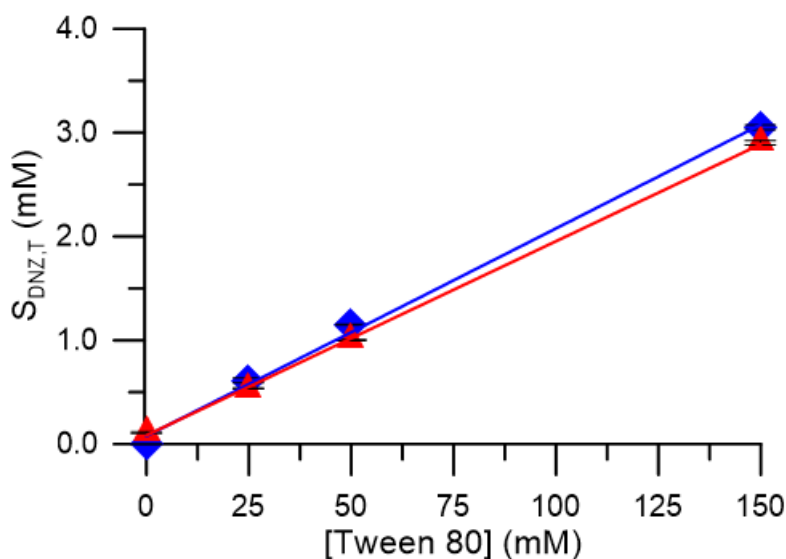


Figure 5.2. Influence of Tween 80 on the solubility of DNZ in pH 5.00 buffer and in FeSSIF. Symbols represent experimentally measured solubility values in Tween 80 in pH 5.00 buffer (◆) and in Tween 80 + FeSSIF (▲). Lines are drawn according to equations obtained from linear regression of the data: $y = (2.00 \pm 0.03)x + 0.008 \pm 0.003$ for Tween 80 in buffer (blue) and $y = (1.87 \pm 0.01)x + 0.008 \pm 0.001$ for Tween 80 + FeSSIF (red). Errors on regression parameters represent the 95% confidence interval.

Table 5.1. Influence of Tween 80 on the solubility of DNZ in pH 5.00 buffer and FeSSIF.

Media	[Tween 80] (mM)	S _{DNZ} (mM)	pH
Buffer	0	$(1.6 \pm 0.2) \times 10^{-4}$	4.96 ± 0.01
	25	0.61 ± 0.02	4.97 ± 0.02
	50	1.15 ± 0.06	4.99 ± 0.01
	150	3.05 ± 0.02	5.02 ± 0.01
FeSSIF	0	0.11 ± 0.01	5.01 ± 0.05
	25	0.54 ± 0.04	5.04 ± 0.01
	50	1.00 ± 0.05	5.06 ± 0.01
	150	2.90 ± 0.02	5.07 ± 0.02

DNZ solubilization by Tween 80 is not significantly affected by the presence of FeSSIF. The linear regression parameters for the measured DNZ solubility in buffer + Tween 80 are not significantly different from the data in FeSSIF + Tween 80. In buffer, the linear regression equation is $y = (2.00 \pm 0.03)x + 0.008 \pm 0.003$ and in FeSSIF, the equation is $y = (1.87 \pm 0.01)x +$

0.008±0.001). Similar behavior is seen for the solubilization of coformers HBA and VAN by Tween 80 in buffer and FeSSIF as shown in Figure 5.3 and Table 5.2.

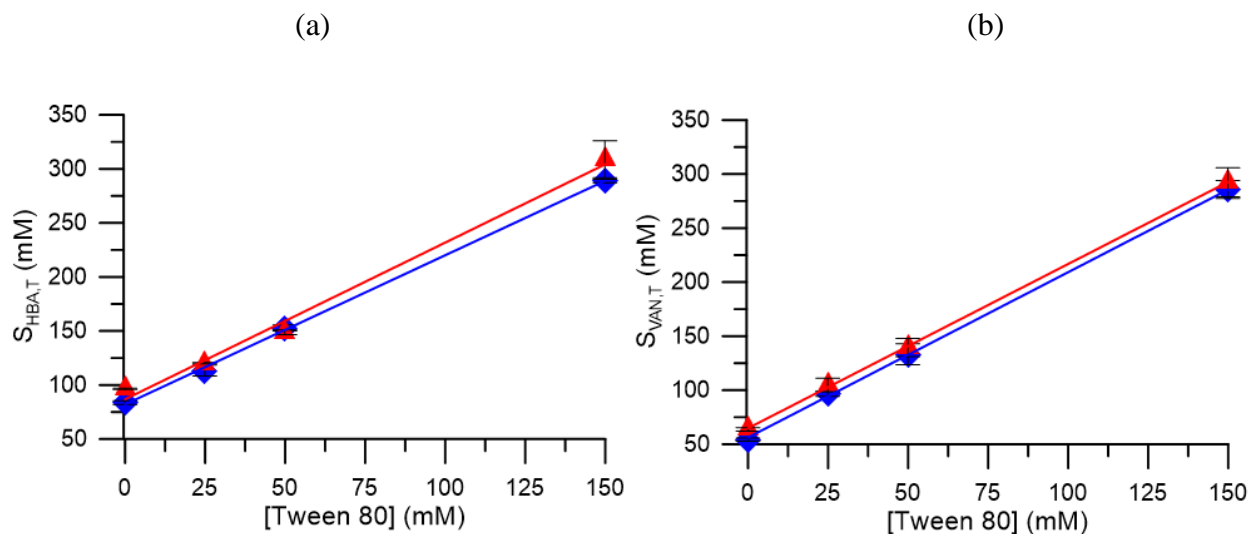


Figure 5.3. Influence of Tween 80 on the solubility of HBA (H) (a) and VAN (b) in pH 5.00 buffer and in FeSSIF. Symbols represent experimentally measured solubility values in Tween 80 in pH 5.00 buffer (◆) and Tween 80 + FeSSIF (▲). Lines are drawn according to equations obtained from linear regression of the data: for (a) $y = (1.38 \pm 0.02)x + 82 \pm 2$ for Tween 80 in buffer (blue) and $y = (1.45 \pm 0.06)x + 87 \pm 5$ for Tween 80 + FeSSIF (red), for (b) $y = (1.53 \pm 0.03)x + 57 \pm 2$ in Tween 80 in buffer (blue) and $y = (1.52 \pm 0.03)x + 55 \pm 3$ in Tween 80 in FeSSIF (red). Errors on regression parameters represent the 95% confidence interval. HBA (H) represents the monohydrate form of HBA which is the stable form in aqueous solution.

Table 5.2. Influence of Tween 80 on the solubility of HBA (H) and VAN in pH 5.00 buffer and FeSSIF.

Media	[Tween 80] (mM)	$S_{\text{HBA (H)}} \text{ (mM)}$	Final pH	$S_{\text{VAN}} \text{ (mM)}$	Final pH
Buffer	0	84±2	4.41±0.04	54.3±0.1	4.94±0.01
	25	113±5	4.40±0.01	96.6±0.2	4.98±0.01
	50	153±3	4.39±0.01	130±10	4.98±0.01
	150	289±2	4.34±0.01	286±8	5.02±0.01
FeSSIF	0	96.4±0.6	4.45±0.02	63.7±0.2	4.99±0.01
	25	120±4	4.42±0.01	105±6	5.06±0.02
	50	149±2	4.43±0.02	139±8	5.07±0.01
	150	310±20	4.39±0.03	290±10	5.08±0.02

As was observed for DNZ, HBA (H) and VAN solubilization by Tween 80 were similar in buffer and in FeSSIF. The linear regression equations for the solubility of each coformer in Tween 80 are very similar in FeSSIF and buffer. For HBA (H), $y = (1.38 \pm 0.02)x + 82 \pm 2$ in buffer and $y = (1.45 \pm 0.06)x + 87 \pm 5$ in FeSSIF. For VAN, $y = (1.53 \pm 0.03)x + 57 \pm 2$ in buffer and $y = (1.52 \pm 0.03)x + 55 \pm 3$ in FeSSIF. From the linear regression equations for DNZ, HBA (H), and VAN, solubilization constants (K_s^{drug} and K_s^{coformer}) can be calculated to further assess the solubilization of each component by Tween 80 in buffer and by Tween 80 in FeSSIF.

For nonionizable drug DNZ, the linear regression equation takes the form

$$S_T = S_0 (1 + K_s [M]) \quad (5.31)$$

where the slope is equal to K_s/S_0 . For monoprotic weakly acidic cofomers HBA and VAN,

$$S_T = S_0 (1 + 10^{\text{pH}-\text{pKa}} + K_s^T [M]) \quad (5.32)$$

where the slope is equal to K_s^T/S_0 . S_0 is equal to the measured intrinsic (nonionized) solubility in blank aqueous buffer or FeSSIF. The K_s and K_s^T values for DNZ, HBA (H) and VAN obtained from linear regression are shown in Figure 5.1.

Table 5.3. K_s^T in Tween 80 calculated from linear regression analysis of measured solubility values of DNZ, HBA (H), and VAN in increasing concentrations of Tween 80 in buffer and FeSSIF

Media	DNZ		HBA (H)		VAN	
	Slope	K_s^T (mM ⁻¹) ^a	Slope	K_s^T (mM ⁻¹) ^b	Slope	K_s^T (mM ⁻¹) ^c
Tween 80 pH 5.00 buffer	2.00±0.03	125±16	1.38±0.02	0.031±0.001	1.53±0.03	0.028±0.001
Tween 80 + FeSSIF	1.87±0.01	121±14	1.45±0.06	0.032±0.001	1.52±0.03	0.028±0.001

(a) Calculated using equation (5.31), $S_0 = (1.6±0.2) \times 10^{-4}$ mM and CMC of Tween 80 = 0.01 mM⁻¹ from reference ²¹.

(b) Calculated using equation (5.32) and $S_0 = 45±2$ mM and CMC of Tween 80 = 0.01 mM⁻¹ (reference ²¹).

(c) Calculated using equation (5.32) and $S_0 = 54±1$ mM and CMC of Tween 80 = 0.01 mM⁻¹ (reference ²¹).

DNZ is highly solubilized by Tween 80 as shown by K_s^T values of 125 and 121 mM⁻¹. This is not surprising as DNZ is a very hydrophobic drug with a log P of 4.53 and micellar solubilization of drugs has been shown to correlate with log P^{7, 22, 23}. Comparatively, the hydrophilic cofomers HBA (H) (log P = 1.60¹³) and VAN (log P = 1.26¹³) are not solubilized significantly, with K_s^T values in the range of 0.028-0.032 mM⁻¹.

Cocrystal constituent solubilization by Tween 80 is very similar in buffer compared to FeSSIF. The similarity of the K_s^T values for Tween 80 determined from linear regression analysis in buffer and FeSSIF indicates that Tween 80 and FeSSIF can be treated as ideally mixing surfactants. That is, solubilization by Tween 80 is unaffected by the presence of FeSSIF. This means that the K_s^T values of cocrystal components measured independently (separately) in Tween 80 and FeSSIF can be used to predict cocrystal solubility using equation (5.22).

Assuming ideally mixing surfactants in this way reduces the number of experiments that need to

be done because the K_s^T values of compounds only need to be measured in separate single surfactants and not in surfactant mixtures.

Cocrystal solubility prediction in multiple surfactants

Equation (5.22) can be used to predict the solubility of DNZ-HBA and DNZ-VAN in the presence of two surfactants as a function of K_{sp} , K_a , and measured K_s^T values along with knowledge of the pH of [M] values of the media of interest. Table 5.4 shows the measured K_{sp} and reported pK_a of the cofomers for DNZ-HBA and DNZ-VAN.

Table 5.4. Cocrystal K_{sp} and cofomer pK_a values at 25°C.

Cocrystal	K_{sp} (mM ²) ^a	Cofomer pK_a ^b
DNZ-HBA	$(1.1 \pm 0.4) \times 10^{-2}$ mM ²	4.48
DNZ-VAN	$(3.5 \pm 0.5) \times 10^{-3}$ mM ²	7.4

(a) K_{sp} was experimentally determined from cocrystal eutectic point measurements as described in the Appendix in Chapter 2.

(b) pK_a values reported in reference ¹².

The K_s^T values calculated from measured cocrystal component solubilities in aqueous buffer, FeSSIF, and various concentrations of Tween 80 are shown in Table 5.5.

Table 5.5. K_s^T values for DNZ, HBA, and VAN in FeSSIF and Tween 80.

Component	K_s^T FeSSIF (mM ⁻¹) ^a	K_s^T Tween 80 (mM ⁻¹) ^b
DNZ	49±5	125±16
HBA	0.018±0.001	0.031±0.001
VAN	0.012±0.001	0.028±0.001

(a) Calculated from single solubility measurements in FeSSIF and buffer in Table 2.5 as described in Chapter 2.

(b) Calculated from linear regression analysis shown in Figure 5.2, Figure 5.3, and Table 5.3 and described in the text.

The thermodynamic equilibrium constants in Table 5.4 and Table 5.5 can be used to predict DNZ cocrystal solubility in aqueous, single surfactant, and two surfactant solutions. The derivation for DNZ cocrystal solubility in the presence of two surfactants is shown in the theoretical section and is given by equation (5.22). The equations to predict cocrystal solubility as a function of pH in aqueous solutions and in a single micellar surfactant have been previously reported and are

$$S_{\text{cocrystal, aq}} = \sqrt{K_{\text{sp}} \left(1 + 10^{\text{pH} - \text{pKa, coformer}}\right)} \quad (5.33)$$

in aqueous buffer¹⁸ and

$$S_{\text{cocrystal, T}} = \sqrt{K_{\text{sp}} \left(1 + K_{\text{s}}^{\text{R}} [\text{M}]\right) \left(1 + 10^{\text{pH} - \text{pKa, coformer}} + K_{\text{s}}^{\text{coformer}} [\text{M}]\right)} \quad (5.34)$$

in a single micellar surfactant¹ for a 1:1 cocrystal RHA such as DNZ-HBA and DNZ-VAN.

Table 5.6 shows the experimentally measured and predicted stoichiometric cocrystal solubilities in buffer, Tween 80, and FeSSIF.

Table 5.6. Comparison between predicted and experimentally measured cocrystal solubility values.

Cocrystal	[Tween 80] (mM)	$S_{\text{cocrystal FeSSIF}}$ (mM)			$S_{\text{cocrystal buffer (mM)}}$		
		Pred ^a	Exp ^b	pH ^c	Pred ^a	Exp ^b	pH ^c
DNZ-HBA	0	4.2	2.8±0.1	4.46±0.06	0.15	0.12±0.01	4.47±0.04
	25	11	9.1±0.3	4.46±0.02	9.6	8.8±0.2	4.45±0.01
	50	17	13.5±0.4	4.43±0.01	16	14.2±0.2	4.43±0.01
	150	38	35.5±0.5	4.41±0.02	37	31.7±0.5	4.42±0.01
DNZ-VAN	0	1.7	1.39±0.03	5.00 ± 0.01	0.059	0.057±0.02	4.96 ± 0.01
	25	5.0	4.2±0.2	5.04 ± 0.01	4.4	N/A	N/A
	50	7.9	6.6±0.1	5.06 ± 0.01	7.4	N/A	N/A
	150	20	16.3±0.3	5.08 ± 0.01	19	17.2±0.2	5.02±0.01

(a) Predicted from equation (5.33) in aqueous buffer, (5.34) in a single surfactant, and (5.22) in two surfactants.

(b) Calculated from experimentally measured eutectic concentrations using equation (5.30).

(c) Experimentally measured eutectic point pH values.

To compare to stoichiometric cocrystal solubilities calculated from experimentally measured eutectic concentrations, solubilities were predicted at the eutectic pHs indicated in Table 5.6 rather than that of the initial FeSSIF and buffer (pH 5.00). However, the pH values only deviated from 5.00 slightly for these cocrystals because the pK_a of HBA is 4.48 and the pK_a of VAN is 7.4. Solubilities in buffer and a particular Tween 80 concentration did not differ significantly from solubility in FeSSIF + that particular Tween 80 concentration. In other words, the solubilizing effect of Tween 80 on cocrystal solubility and stability greatly outweighed that of FeSSIF. While there were significant differences between solubility in blank aqueous buffer and FeSSIF, once Tween 80 was added at any concentration, the solubilities were similar in

FeSSIF and buffer. For example, DNZ-HBA solubility in 25 mM Tween 80 in buffer is 88 mM and is 91 mM in 25 mM Tween 80 + FeSSIF. For this reason, DNZ-VAN solubilities at the eutectic point were not measured in 25 mM or 50 mM Tween 80 + buffer. DNZ-HBA and DNZ-VAN solubilities in buffer, FeSSIF, and Tween 80 separately, and Tween 80 + FeSSIF are predicted within a factor of two. Figure 5.4 shows the good agreement between the predicted and experimentally measured values.

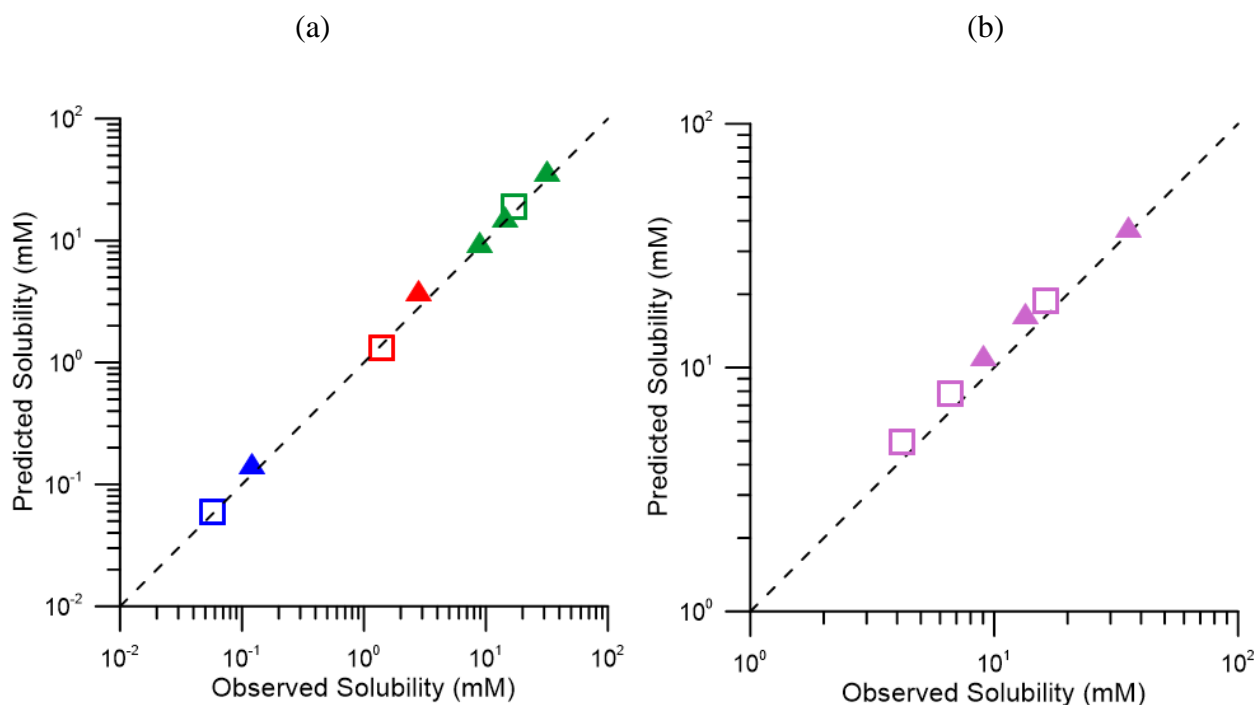


Figure 5.4. Comparison of predicted and observed DNZ-HBA (▲) and DNZ-VAN (□) in (a) buffer (blue symbols), FeSSIF (red symbols), and Tween 80 (green symbols) separately and (b) Tween 80 and FeSSIF (purple symbols) at 25°C. Predictions were made using equation (5.33) in aqueous buffer, (5.34) in a single surfactant, and (5.22) in two surfactants. Line indicates the function $y=x$, where the predicted and observed solubilities are equivalent. Experimental errors fit within the size of each symbol.

DNZ-HBA and DNZ-VAN solubility can be predicted over orders of magnitude in buffer, FeSSIF, Tween 80, and in Tween 80 + FeSSIF using equations (5.33), (5.34), and (5.22). This to our knowledge the first time that cocrystal solubility has been predicted in the presence of two

surfactants using mechanism-based models. When surfactants can be assumed to mix ideally, cocrystal solubility are predicted in two surfactants based on knowledge of the cocrystal K_{sp} , as well as the K_a and K_s^T values of the drug and coformer in each surfactant of interest. When the surfactants or solubilizing agents of interest do not mix ideally, interaction or nonideality terms must be included, which is beyond the scope of this work.

The stoichiometric solubility of the cocrystals was calculated from measured total eutectic concentrations of drug and coformer ($[drug]_{eu}$ and $[coformer]_{eu}$) according to the following equations for a 1:1 cocrystal:

$$S_T^{1:1 \text{ cocrystal}} = \sqrt{[drug]_{T,eu} [coformer]_{T,eu}} \quad (5.35)$$

Table 5.7 shows the measured DNZ-HBA solubilities at the eutectic point in increasing concentrations of Tween 80 in FeSSIF and buffer.

Table 5.7. Measured DNZ and HBA eutectic concentrations used to calculate stoichiometric cocrystal solubility ($S_{\text{cocrystal}}$), K_{eu} , and $S_{\text{cocrystal}}/S_{\text{drug}}$.

	[Tween 80] (mM)	pH	[DNZ] _{eu} (mM)	[HBA] _{eu} (mM)	$S_{\text{cocrystal}}$ (mM) ^a	$S_{\text{cocrystal}}/S_{\text{drug}}$ ^b	$S_{\text{cocrystal}}/S_{\text{drug}}$ ^c	K_{eu} ^d
Buffer	0	4.47±0.04	(2.0±0.4)×10 ⁻⁴	79±4	0.12±0.01	770±90	660±50	440,000±67,000
	25	4.45±0.01	0.75±0.02	103±2	88±2	14.3±0.6	11.7±0.1	138±8
	50	4.43±0.01	1.49±0.04	136±1	142±2	12.4±0.2	9.6±0.2	92±3
	150	4.42±0.01	4.25±0.06	236±6	317±5	10.4±0.2	7.5±0.1	56±2
FeSSIF	0	4.46±0.06	(9.9±0.8)×10 ⁻²	78±1	28±1	25±3	28±4	790±60
	25	4.46±0.02	0.71±0.07	113±5	91±3	17.0±0.5	12±1	160±30
	50	4.43±0.01	1.26±0.06	144±2	135±4	13.5±0.4	10.7±0.2	115±4
	150	4.41±0.02	4.6±0.2	273±5	355±5	12.2±0.2	7.7±0.2	59±3

(a) Calculated from equation (5.35) as described in the text.

(b) Calculated from $S_{\text{cocrystal}}$ measured at the eutectic point in Table 5.7 and S_{drug} measured in the absence of cofomer in Table 5.9.

(c) Calculated from K_{eu} using equation (5.27).

(d) Calculated from ratio of $[HBA]_{\text{eu}}/[DNZ]_{\text{eu}}$.

Highly soluble cocrystals require high $[\text{coformer}]_{\text{eu}}$ to reach the eutectic point. $[HBA]_{\text{eu}}$ values were orders of magnitude larger than $[DNZ]_{\text{eu}}$ values at all surfactant concentrations, indicating that the cocrystal maintained a solubility advantage over the drug in all conditions. At high Tween 80 concentrations (150 mM), however, the difference between $[HBA]_{\text{eu}}$ and $[DNZ]_{\text{eu}}$ was dampened due to preferential solubilization of DNZ. This corresponded to a dramatic reduction in $S_{\text{cocrystal}}/S_{\text{drug}}$ calculated from K_{eu} from 660 in buffer to 7.7 in 150 mM Tween 80.

As described in the theoretical section, $(S_{\text{cocrystal}}/S_{\text{drug}})_{\text{aq}}$ greatly impacts the ability of a cocrystal to be stabilized in surfactants. Since $(S_{\text{cocrystal}}/S_{\text{drug}})_{\text{aq}}$ is 660 in the pH conditions

studied, DNZ-HBA was not stabilized at any Tween 80 concentration, regardless if FeSSIF was present or not. $S_{\text{cocrystal}}/S_{\text{drug}}$ was also calculated from the measured $S_{\text{cocrystal}}$ and S_{drug} measured in the absence of coformer (not at the eutectic point). Differences between $S_{\text{cocrystal}}/S_{\text{drug}}$ calculated from measured eutectic concentrations and $S_{\text{cocrystal}}/S_{\text{drug}}$ calculated using S_{drug} measured in the absence of coformer are due to differences in S_{drug} in these conditions. Comparison of S_{drug} in the presence of and in the absence of coformer will be discussed in more detail in a subsequent section. In general, S_{drug} was slightly higher in the presence of coformer which lead to lower $S_{\text{cocrystal}}/S_{\text{drug}}$ values calculated from the measured eutectic concentrations compared to those values calculated using S_{drug} measured in the absence of coformer. This was observed at all surfactant concentrations except for pure FeSSIF.

DNZ-VAN solubility behavior in Tween 80 and FeSSIF was similar to DNZ-HBA. Table 5.8 shows the measured DNZ-VAN solubilities at the eutectic point in increasing concentrations of Tween 80 in FeSSIF and buffer.

Table 5.8. Measured DNZ and VAN eutectic concentrations used to calculate stoichiometric cocrystal solubility ($S_{\text{cocrystal}}$), K_{eu} , and $S_{\text{cocrystal}}/S_{\text{drug}}$.

	[Tween 80] (mM)	pH	[DNZ] _{eu} (mM)	[VAN] _{eu} (mM)	$S_{\text{cocrystal}}$ (mM) ^a	$S_{\text{cocrystal}}/S_{\text{drug}}$ ^b	$S_{\text{cocrystal}}/S_{\text{drug}}$ ^c	K_{eu} ^d
Buffer	0	4.96±0.01	(2.1±0.1)×10 ⁻⁴	16±3	(5.7±0.2)×10 ⁻²	370±70	280±6	78,000±4.000
	25	----	----	----	----	----	----	----
	50	-----	---	----	----	----	-----	----
	150	5.02±0.01	3.27±0.03	90±2	17.2±0.2	5.6±0.1	5.3±0.1	27±1
FeSSIF	0	5.00±0.01	0.10±0.02	19.4±0.8	1.39±0.03	13±1	14.0±0.3	195±9
	25	5.04±0.01	0.52±0.03	34±4	4.2±0.2	7.8±0.3	8.0±0.7	64±11
	50	5.06±0.01	1.0±0.2	43±1	6.6±0.1	6.6±0.1	6.5±0.1	43±2
	150	5.08±0.01	3.05±0.04	87±2	16.3±0.3	5.6±0.1	5.3±0.1	29±1

(a) Calculated from equation (5.35) as described in the text.

(b) Calculated from $S_{\text{cocrystal}}$ measured at the eutectic point in Table 5.7 and S_{drug} measured in the absence of coformer in Table 5.9.

(c) Calculated from K_{eu} using equation (5.27).

(d) Calculated from ratio of $[VAN]_{\text{eu}}/[DNZ]_{\text{eu}}$.

$[VAN]_{\text{eu}}$ values were orders of magnitude larger than $[DNZ]_{\text{eu}}$ values at 0-25 mM Tween 80; however, at 50 mM and 150 mM Tween 80, $[VAN]_{\text{eu}}$ was only one order of magnitude larger than $[DNZ]_{\text{eu}}$ due to preferential solubilization of DNZ. This corresponded to a dramatic reduction in $S_{\text{cocrystal}}/S_{\text{drug}}$ calculated from K_{eu} from 280 in buffer to 5.3 in 150 mM Tween 80. $S_{\text{cocrystal}}/S_{\text{drug}}$ of DNZ-VAN was reduced more than DNZ-HBA since $(S_{\text{cocrystal}}/S_{\text{drug}})_{\text{aq}}$ is 280, or about half that of DNZ-HBA (660). As described earlier, due to the overpowering solubilizing power of Tween 80, DNZ-HBA and DNZ-VAN did not show large differences in $S_{\text{cocrystal}}$, K_{eu} , or $S_{\text{cocrystal}}/S_{\text{drug}}$ in buffer or FeSSIF at a particular Tween 80 concentration.

As for DNZ-HBA, $S_{\text{cocrystal}}/S_{\text{drug}}$ was also calculated from the measured $S_{\text{cocrystal}}$ and S_{drug} measured in the absence of coformer (not at the eutectic point). Similar to the trend observed for DNZ-HBA, S_{drug} was slightly higher in the presence of coformer which led to lower $S_{\text{cocrystal}}/S_{\text{drug}}$ values; however, this was only observed for measurements in the presence of Tween 80 only, and the difference in $S_{\text{cocrystal}}/S_{\text{drug}}$ by the two methods in the presence of FeSSIF and Tween 80 was not significant.

Drug solubility in the presence of and in the absence of coformer

The drug concentration at the eutectic point also serves as a measure of the equilibrium solubility of the drug in the presence of coformer in solution since the solution is saturated with drug as well as cocrystal phases. Table 5.9 shows the comparison of DNZ solubility measured in the absence of coformer (independently measured) to the solubility measured at the eutectic point in the presence of coformer (either HBA or VAN).

Table 5.9. Comparison of DNZ solubilities in increasing concentrations of Tween 80 in buffer or FeSSIF measured in the absence of and in the presence of coformer at the eutectic point (either DNZ-HBA or DNZ-VAN eutectic point).

Media	[Tween 80] (mM)	S _{DNZ} (mM) ^a	pH	S _{DNZ HBA eutectic} (mM) ^b	pH	S _{DNZ VAN eutectic} (mM) ^b	pH
Buffer	0	(1.6±0.2)×10 ⁻⁴	4.96±0.01	(2.0±0.4)×10 ⁻⁴	4.47±0.04	(2.1±0.1)×10 ⁻⁴	4.96±0.01
	25	0.61±0.02	4.97±0.02	0.75±0.02	4.45±0.01	----	----
	50	1.15±0.06	4.99±0.01	1.49±0.04	4.43±0.01	---	-----
	150	3.05±0.02	5.02±0.01	4.25±0.06	4.42±0.01	3.27±0.03	5.02±0.01
FeSSIF	0	0.11±0.01	5.01±0.05	(9.9±0.8)×10 ⁻²	4.46±0.06	0.10±0.02	5.00±0.01
	25	0.54±0.04	5.04±0.01	0.71±0.07	4.46±0.02	0.52±0.03	5.04±0.01
	50	1.00±0.05	5.06±0.01	1.26±0.06	4.43±0.01	1.0±0.2	5.06±0.01
	150	2.90±0.02	5.07±0.02	4.6±0.2	4.41±0.02	3.05±0.04	5.08±0.01

(a) Measured with only drug solid phase in equilibrium with solution.

(b) Measured at the eutectic point with drug and cocrystal solid phases in equilibrium with solution.

DNZ solubility values are consistently slightly higher at the eutectic point compared to those values measured in the absence of coformer in solution. This is likely due to supersaturation caused by cocrystal dissolution (and subsequent drug precipitation to reach the eutectic point). While the eutectic point was approached from both cocrystal dissolution and cocrystal precipitation (to avoid supersaturated drug values), the very high cocrystal solubilities of DNZ-HBA and DNZ-VAN compared to drug likely resulted in supersaturated drug concentrations. These higher drug values could also be due to solution complexation between DNZ and the coformers, but the difference between DNZ solubility measured independently and the values measured at the eutectic point did not increase as coformer concentrations increased, so this is probably not the case.

$S_{\text{cococrystal}}/S_{\text{drug}}$ and cococrystal dissolution in the presence of multiple surfactants

Figure 5.5 shows $S_{\text{cococrystal}}/S_{\text{drug}}$ calculated from K_{eu} for DNZ-HBA and DNZ-VAN in buffer and FeSSIF as a function of Tween 80 concentration.

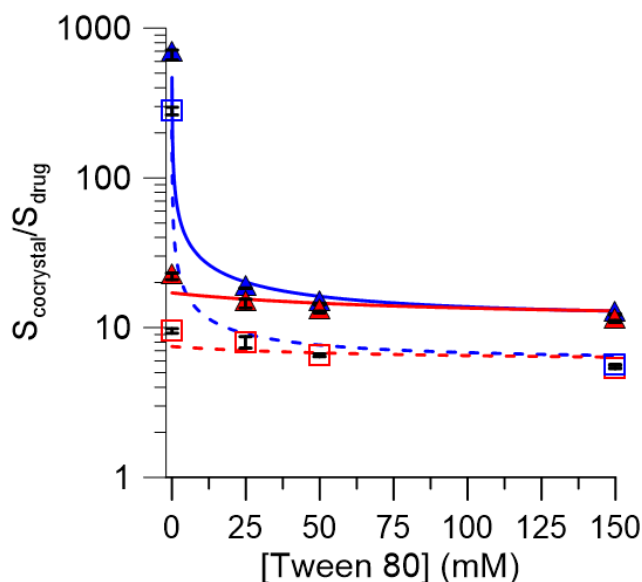


Figure 5.5. $S_{\text{cococrystal}}/S_{\text{drug}}$ for DNZ-HBA (—) and DNZ-VAN (----) predicted using equation (5.24) for increasing concentrations of Tween 80 in pH 5.00 buffer (blue lines) and equation (5.25) for increasing concentrations of Tween 80 in FeSSIF (red lines). Values used for predictions are K_{sp} values from Table 5.4, K_{s}^{T} and pK_{a} values from Table 2.5, and measured value of $S_{\text{DNZ, aq}}^0 = 1.6 \times 10^{-4}$ mM. Symbols represent experimentally measured values for DNZ-HBA in buffer (\blacktriangle) DNZ-HBA in FeSSIF (\blacktriangle), DNZ-VAN in buffer (\square) and DNZ-VAN in FeSSIF (\square) at 0, 25, 50, and 150 mM Tween 80.

$S_{\text{cococrystal}}/S_{\text{drug}}$ decreases dramatically in the presence of Tween 80. However, the ability of Tween 80 to decrease the solubility advantage is dampened in the presence of FeSSIF. In buffer, $S_{\text{cococrystal}}/S_{\text{drug}}$ of DNZ-HBA drops by orders of magnitude from 660 to 7.5 from 0 to 150 mM Tween 80. In FeSSIF, this decrease is only from 28 to 7.7 from 0 to 150 mM Tween 80. Similar behavior is seen for DNZ-VAN in buffer and FeSSIF at increasing concentrations of Tween 80. Since the $(S_{\text{cococrystal}}/S_{\text{drug}})_{\text{aq}}$ of DNZ-HBA and DNZ-VAN are relatively high (660 and 280 at the eutectic point pH), neither cococrystal is stabilized in FeSSIF + 150 mM Tween 80. DNZ-VAN

exhibited the lowest $S_{\text{cocrystal}}/S_{\text{drug}}$ of 5.3 in FeSSIF + 150 mM Tween 80, so these conditions were selected for a preliminary powder dissolution study of DNZ-VAN to assess the impact of the decrease in $S_{\text{cocrystal}}/S_{\text{drug}}$ in two surfactants on the cocrystal dissolution profile.

Figure 5.6 shows the powder dissolution profile of DNZ-VAN in FeSSIF and FeSSIF + 150 mM Tween 80.

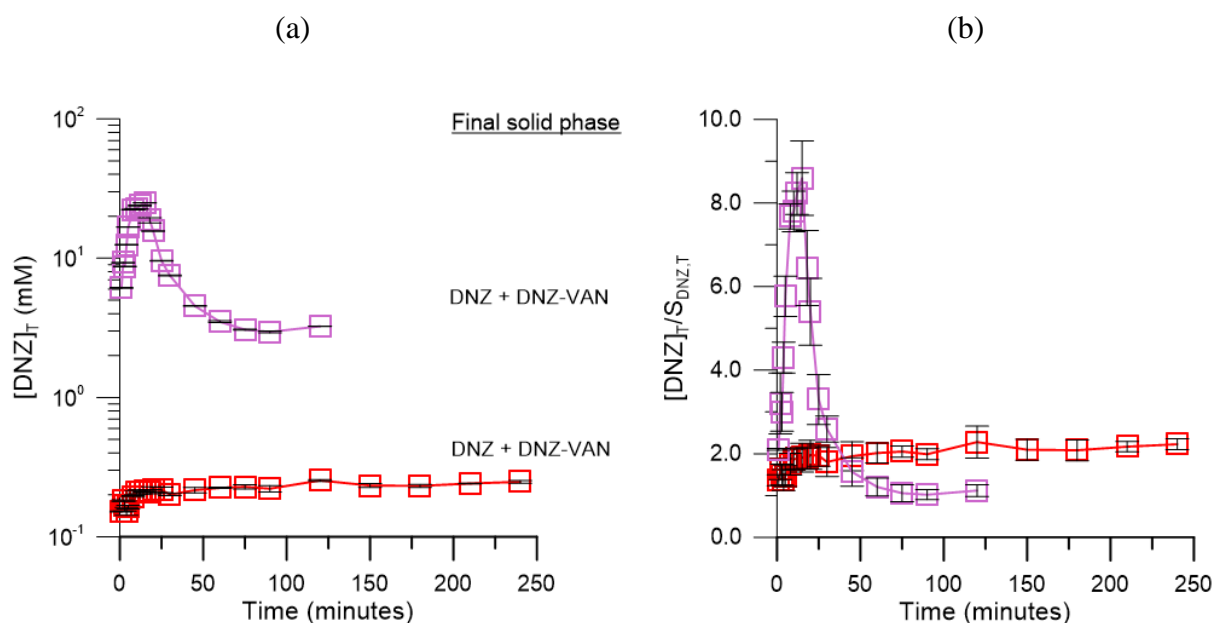


Figure 5.6. DNZ-VAN dissolution in FeSSIF (□) and FeSSIF + 150 mM Tween 80 (□) at 25°C. (a) $[DNZ]_T$ vs time profile and (b) supersaturation generated by DNZ-VAN during dissolution ($[DNZ]_T/S_{DNZ,T}$). The pH of both media had an initial and final pH of 5.00.

DNZ-VAN achieves a higher peak concentration in the presence of 150 mM Tween 80 + FeSSIF compared to FeSSIF. In the presence of 150 mM Tween 80, DNZ-VAN achieves a peak concentration of 24 ± 3 mM and a peak supersaturation of 8.6 ± 0.9 at 15 minutes, which are slightly higher than the measured solubility of 16.3 ± 0.3 mM and measured $S_{\text{cocrystal}}/S_{\text{drug}}$ of 5.3 ± 0.1 . The disagreement between the equilibrium studies and dissolution conditions may be due to underestimation of DNZ-VAN by eutectic point measurement or the preliminary nature of

this dissolution experiment. Only one repetition of the study was completed and error values on concentrations represent the error due to sampling by HPLC (different injections). Further repetitions of this experiment would elucidate if the disagreement is due to large variability in solution concentration during dissolution or if the solubility measurement method needs to be examined. After 15 minutes, solution-mediated transformation to DNZ occurs. $[\text{DNZ}]_T$ decreases rapidly to the solubility of DNZ and supersaturation decreases to 1.1 ± 0.1 which is maintained from 50 minutes for the remainder of the experiment.

The solid phase at the end of the experiment is a mixed phase of DNZ and DNZ-VAN, confirming that conversion occurred. This conversion is further confirmed by the high concentration of VAN, which is shown in Figure 5.7b for FeSSIF + 150 mM Tween 80.

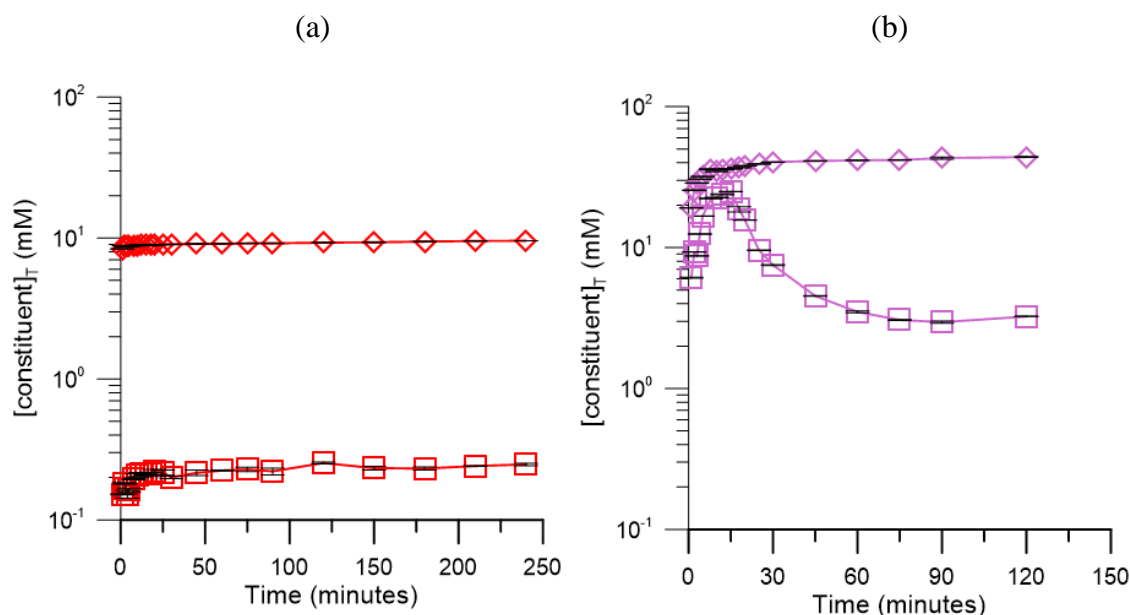


Figure 5.7. Concentrations of DNZ (\square) and VAN (\diamond) during DNZ-VAN dissolution in FeSSIF (a) and FeSSIF + 150 mM Tween 80 (b) at 25°C. The pH of both media had an initial and final pH of 5.00.

As shown in Figure 5.7b, VAN concentrations continue to increase as DNZ concentrations decrease during solution-transformation to drug. The pH of the dissolution media does not

change significantly despite these high VAN concentrations because the pK_a of VAN is 7.4 while the dissolution media is 5.00 so no large decrease in pH is observed. The supersaturation behavior in Figure 5.6b is similar to the reported supersaturation behavior of DNZ-VAN observed when the cocrystal is formulated with the solubilizing agent TPGS and the precipitation inhibitor HPMC⁶. In that study, a peak supersaturation of 5.6 was observed at around 15 minutes during powder dissolution of the formulated cocrystal in FaSSIF followed by conversion to DNZ.

In FeSSIF, a DNZ concentration of 0.24 mM is obtained and maintained for the duration of the experiment, which is less than the measured solubility of 1.39 mM. The final solid phase was a mixed phase of DNZ and DNZ-VAN, indicating that solution-mediated transformation to drug had occurred. Results in Figure 5.7a confirm the instantaneous conversion of the cocrystal to drug based on the high VAN concentrations compared to DNZ concentrations for the duration of the experiment. However, the cocrystal maintained a supersaturated state with $[DNZ]_T/S_{T,DNZ}$ of around 2.4 for the duration of the 240 minute experiment, which is similar to what others have reported for DNZ-VAN dissolution in FaSSIF⁶. FaSSIF and FeSSIF contain the same solubilizing agents (sodium taurocholate and lecithin), though FeSSIF has a five-fold higher concentration of them compared to FaSSIF. Based on the literature and observed dissolution behavior of DNZ-VAN in FeSSIF in Figure 5.6, in the presence of these solubilizing agents and VAN, DNZ is able to maintain a moderately supersaturated concentration for hours. Despite this supersaturated state, the reduction in $S_{cocrystal}/S_{drug}$ from 14.0 in FeSSIF to 5.3 in FeSSIF + 150 Tween 80 resulted in a higher peak supersaturation for the formulated cocrystal.

Conclusions

Theoretical relationships that describe cocrystal solubility and thermodynamic stability in the presence of multiple surfactants are derived in this work for the first time. These equations are useful to predict the solution behavior of cocrystals as formulated products, where they may encounter solubilizing agents in the formulation and/or endogenous surfactants *in vivo*.

Surfactants are assumed to mix ideally, which is a valid assumption for the Tween 80 and FeSSIF concentrations studied in this work. Experimentally measured cocrystal solubilities are in excellent agreement with the proposed models. The solubility of DNZ-HBA and DNZ-VAN in the presence Tween 80 and FeSSIF is quantitatively predicted from cocrystal K_{sp} (measured in aqueous solution) and cocrystal component K_a values reported in the literature and K_s^T values determined from drug and coformer solubility measurements in Tween 80 and FeSSIF independently.

DNZ is significantly solubilized by FeSSIF and Tween 80 while the hydrophilic cofomers HBA and VAN are not. This preferential solubilization of DNZ leads to a dramatic decrease in $S_{cocrystal}/S_{drug}$ as Tween 80 concentration increases, but this effect is dampened in the presence of FeSSIF, particularly at low Tween 80 concentrations. Decreased $S_{cocrystal}/S_{drug}$ for DNZ-VAN in FeSSIF + 150 mM Tween 80 results in higher drug concentrations and high supersaturations during dissolution compared to FeSSIF alone.

References

1. Huang, N.; Rodriguez-Hornedo, N. Engineering Cocrystal Solubility, Stability, and pH(max) by Micellar Solubilization. *J. Pharm. Sci.* **2011**, *100*, (12), 5219-5234.
2. Huang, N.; Rodriguez-Hornedo, N. Engineering cocrystal thermodynamic stability and eutectic points by micellar solubilization and ionization. *Crystengcomm* **2011**, *13*, (17), 5409-5422.
3. Huang, N.; Rodriguez-Hornedo, N. Effect of Micelliar Solubilization on Cocrystal Solubility and Stability. *Cryst. Growth Des.* **2010**, *10*, (5), 2050-2053.

4. Roy, L. Engineering Cocrystal and Cocrystalline Salt Solubility by Modulation of Solution Phase Chemistry. *University of Michigan (Doctoral Dissertation)* **2013**, Retrieved from Deep Blue. (<http://hdl.handle.net/2027.42/98067>).
5. Roy, L.; Rodriguez-Hornedo, N. A Rational Approach for Surfactant Selection to Modulate Cocrystal Solubility and Stability. *Poster presentation at the 2010 AAPS Annual Meeting and Exposition* **2010**, New Orleans, LA, (November 14-18, 2010), Poster R6072.
6. Childs, S. L.; Kandi, P.; Lingireddy, S. R. Formulation of a Danazol Cocrystal with Controlled Supersaturation Plays an Essential Role in Improving Bioavailability. *Mol. Pharm.* **2013**, *10*, (8), 3112-3127.
7. Caron, J. C.; Shroot, B. Determination of partition-coefficients of glucocorticosteroids by high-performance liquid-chromatography. *J. Pharm. Sci.* **1984**, *73*, (12), 1703-1706.
8. Bakatselou, V.; Oppenheim, R. C.; Dressman, J. B. Solubilization and Wetting Effects of Bile-Salts on the Dissolution of Steroids. *Pharm. Res.* **1991**, *8*, (12), 1461-1469.
9. Charman, W. N.; Rogge, M. C.; Boddy, A. W.; Barr, W. H.; Berger, B. M. Absorption of danazol after administration to different sites of the gastrointestinal-tract and the relationship to single-peak and double-peak phenomena in the plasma profiles. *J. Clin. Pharmacol.* **1993**, *33*, (12), 1207-1213.
10. Naylor, L. J.; Bakatselou, V.; RodriguezHornedo, N.; Weiner, N. D.; Dressman, J. B. Dissolution of steroids in bile salt solutions is modified by the presence of lecithin. *Eur. J. Pharm. Biopharm.* **1995**, *41*, (6), 346-353.
11. Sunesen, V. H.; Vedelsdal, R.; Kristensen, H. G.; Christrup, L.; Mullertz, A. Effect of liquid volume and food intake on the absolute bioavailability of danazol, a poorly soluble drug. *Eur. J. Pharm. Sci.* **2005**, *24*, (4), 297-303.
12. Robinson, R. A.; Kiang, A. K. The ionization constants of vanillin and 2 of its isomers. *Transactions of the Faraday Society* **1955**, *51*, (10), 1398-1402.
13. Hansch, C.; Rockwell, S. D.; Jow, P. Y. C.; Leo, A.; Steller, E. E. Substituent constants for correlation analysis. *J. Med. Chem.* **1977**, *20*, (2), 304-306.
14. Leo, A.; Jow, P. Y. C.; Silipo, C.; Hansch, C. Calculation of hydrophobic constant (log p) from pi and f constants. *J. Med. Chem.* **1975**, *18*, (9), 865-868.
15. Good, D. J.; Rodriguez-Hornedo, N. Solubility Advantage of Pharmaceutical Cocrystals. *Cryst. Growth Des.* **2009**, *9*, (5), 2252-2264.
16. Good, D. J.; Rodriguez-Hornedo, N. Cocrystal Eutectic Constants and Prediction of Solubility Behavior. *Cryst. Growth Des.* **2010**, *10*, (3), 1028-1032.
17. Alhalaweh, A.; Roy, L.; Rodriguez-Hornedo, N.; Velaga, S. P. pH-Dependent Solubility of Indomethacin-Saccharin and Carbamazepine-Saccharin Cocrystals in Aqueous Media. *Mol. Pharm.* **2012**, *9*, (9), 2605-2612.
18. Bethune, S. J.; Huang, N.; Jayasankar, A.; Rodriguez-Hornedo, N. Understanding and Predicting the Effect of Cocrystal Components and pH on Cocrystal Solubility. *Cryst. Growth Des.* **2009**, *9*, (9), 3976-3988.
19. Galia, E.; Nicolaidis, E.; Horter, D.; Lobenberg, R.; Reppas, C.; Dressman, J. B. Evaluation of various dissolution media for predicting in vivo performance of class I and II drugs. *Pharm. Res.* **1998**, *15*, (5), 698-705.
20. Rodriguez-Hornedo, N.; Nehru, S. J.; Seefeldt, K. F.; Pagan-Torres, Y.; Falkiewicz, C. J. Reaction crystallization of pharmaceutical molecular complexes. *Mol. Pharm.* **2006**, *3*, (3), 362-367.

21. Chatterjee, A.; Moulik, S. P.; Sanyal, S. K.; Mishra, B. K.; Puri, P. M. Thermodynamics of micelle formation of ionic surfactants: A critical assessment for sodium dodecyl sulfate, cetyl pyridinium chloride and dioctyl sulfosuccinate (Na salt) by microcalorimetric, conductometric, and tensiometric measurements. *Journal of Physical Chemistry B* **2001**, *105*, (51), 12823-12831.
22. Alvarez-Nunez, F. A.; Yalkowsky, S. H. Relationship between Polysorbate 80 solubilization descriptors and octanol-water partition coefficients of drugs. *Int. J. Pharm.* **2000**, *200*, (2), 217-222.
23. Mithani, S. D.; Bakatselou, V.; TenHoor, C. N.; Dressman, J. B. Estimation of the increase in solubility of drugs as a function of bile salt concentration. *Pharm. Res.* **1996**, *13*, (1), 163-167.

CHAPTER 6

COCRYSTAL TRANSITION POINTS: ROLE OF COCRYSTAL SOLUBILITY, DRUG SOLUBILITY, AND SOLUBILIZING AGENTS

Introduction

Cocrystals are playing an important role in solving many of the challenges related to the bioavailability of poorly-water soluble drugs¹⁻⁸. One of the vital properties of cocrystals is their tunable solubility^{2, 4, 9-17} offering dramatic benefits to drug absorption and bioavailability. Chemical interactions between cocrystal constituents and dissolution media additives are critically important for cocrystals to achieve a wide range of solubility and thermodynamic stability behaviors.

We recently discovered that the same cocrystal can display higher, equal, or lower solubility than the constituent drug, depending on the concentration of drug solubilizing agents¹⁰⁻¹². As a result of this phenomenon, cocrystals can exhibit transition points at which the cocrystal solubility advantage over the parent drug is switched by the presence of drug solubilizing agents. The indomethacin-saccharin cocrystal, for example, has a solubility 26 times higher than indomethacin in pH 2 buffer¹⁶. This solubility advantage is however eliminated in the presence of drug solubilizing agents and the cocrystal becomes less soluble than indomethacin in solutions with SLS or Brij, or Tween 80 among others^{18, 19}. The underlying mechanism for this behavior was determined to be the solubilizing agent preferential solubilization for the drug, and its indifference for coformer solubilization. Coformers are much

more hydrophilic than the constituent drugs and therefore such selective drug solubilization is generally observed with solubilizing agents in aqueous media.

The solubilizing agent concentration at the transition point is referred to as the CSC or critical stabilization concentration¹⁰⁻¹². Studies on carbamazepine and indomethacin cocrystals led to the recognition of the transition point and established the factors that determine the value of the CSC^{10-12, 18, 19}. CSC was found to decrease with increasing drug solubilization and drug selectivity by the additive, and with decreasing cocrystal aqueous solubility (in the absence of solubilizing agents). CSC values for CBZ cocrystals in solutions of sodium lauryl sulfate were in the range of 23 to 187 mM¹⁰⁻¹², which can be encountered in formulation, processing, and dissolution media.

Cocrystal transition points are not only dependent on the effectiveness of the drug solubilizing agent but also on the extent of ionization and solubilization of cocrystal components, i.e., drug and coformer^{10-12, 18, 19}. These findings have challenged the traditional notion of cocrystal solubility and thermodynamic stability, since not only do cocrystals exhibit transition points, but the CSC at the transition points shift with the nature and concentration of solubilizing agents.

When selecting a cocrystal, designing a pharmaceutical product, and developing meaningful characterization methods, it is essential to know how the cocrystal transition point is affected. While the variation of cocrystal transition points with surfactant properties can be predicted using theoretical models with the associated equilibrium constants, we wished to develop a simplified version of the more rigorous theoretical models and evaluate their predictive power for a broad range of cocrystals and drug solubilizing agents.

During these studies we derived simple relationships to quantitatively predict cocrystal solubilization by drug solubilizing agents from knowledge of drug solubilization. We have also discovered that (1) the cocrystal transition points are defined by a solubility value (S^*) and a CSC, and (2) that S^* is independent of solubilizing agents as long as coformer solubilization is negligible. An important property of S^* is that it is only dependent on cocrystal and drug aqueous solubilities in the absence of solubilizing agents. This means that once cocrystal and drug solubilities in aqueous media are known at a particular temperature and pH, then S^* can be estimated from the equations derived in this work. Knowledge of S^* for a given cocrystal will guide the selection and concentrations of solubilizing agents since S^* has associated CSCs.

The selection criterion for cocrystals and solubilizing agents in this work was that cocrystal and drug solubilities be measured under equilibrium conditions. We included cocrystals studied in our laboratory as well as reported in the literature. Solubilities and transition points for cocrystals of carbamazepine, indomethacin, danazol, piroxicam, and pterostilbene in the presence of a range of drug solubilizing agents comprising surfactants and lipid-based systems were analyzed in light of the simple equations and concepts presented here.

Theoretical

Calculation of cocrystal solubilization from drug solubilization

A simplified model that can be used to establish the influence of drug solubilizing agents on cocrystal solubility is important to guide cocrystal formulation. We have found a simple mathematical relationship that allows for calculation of cocrystal solubilization ratio ($SR_{\text{cocrystal}}$) from knowledge of a common descriptor of drug solubilization, the drug solubilization ratio (SR_{drug}). For a 1:1 cocrystal, the solubilization ratio is given by

$$SR_{\text{cocystal}} = \sqrt{SR_{\text{drug}}} \quad (6.1)$$

or

$$\left(\frac{S_T}{S_{\text{aq}}}\right)_{\text{cocystal}} = \sqrt{\left(\frac{S_T}{S_{\text{aq}}}\right)_{\text{drug}}}$$

under the condition that cofomer solubilization by the additive is negligible. This relationship is of practical importance since drug solubilizing agents such as surfactants, lipids, and complexing agents among others are often included or encountered in cocystal formulations as well as in dissolution media.

At a specific pH and solubilizing agent concentration, SR is defined as the ratio of the total solubility (S_T) to the aqueous solubility (S_{aq})

$$SR_{\text{cocystal}} = \left(\frac{S_T}{S_{\text{aq}}}\right)_{\text{cocystal}} \quad (6.2)$$

S_T is defined as the sum of the concentrations of all species dissolved ($S_T = S_{\text{aq}} + S_s$). S_{aq} represents the cocystal aqueous solubility at a particular pH in the absence of solubilizing agent ($S_{\text{aq}} = S_{\text{nonionized, aq}} + S_{\text{ionized, aq}}$) and is the sum of the nonionized and ionized contributions to the aqueous solubility. S_s represents the cocystal solubilized by solubilizing agents ($S_s = S_{\text{nonionized, s}} + S_{\text{ionized, s}}$) and contributions from the ionized species as appropriate.

Without getting into a lot of detail, the relationship between cocystal and drug solubilization ratios (equation (6.1)) can be found from the equation that describes cocystal total solubility as a function of pH and solubilizing agent¹⁰⁻¹², by replacing the equilibrium constants

for ionization and solubilization with drug and cocrystal solubility terms. For a 1:1 cocrystal of a nonionizable drug and an ionizable (monoprotic) acidic coformer, the cocrystal solubility is

$$S_{\text{cocrystal,T}} = \sqrt{K_{\text{sp}} \left(1 + K_{\text{s}}^{\text{drug}}[\text{M}]\right) \left(1 + 10^{\text{pH} - \text{pK}_{\text{a,coformer}}} + K_{\text{s}}^{\text{coformer}}[\text{M}]\right)} \quad (6.3)$$

where K_{sp} is the cocrystal solubility product, K_{s} stands for solubilization constants of cocrystal constituents, and the term in brackets is the concentration of solubilizing agent, which for a micellar surfactant is $[\text{M}]$. K_{a} represents the dissociation constant of a monoprotic acidic coformer. When solubilizing agents enhance drug solubility and not coformer solubility ($K_{\text{s}}^{\text{coformer}} = 0$), the cocrystal solubility equation becomes

$$S_{\text{cocrystal,T}} = \sqrt{K_{\text{sp}} \left(1 + K_{\text{s}}^{\text{drug}}[\text{M}]\right) \left(1 + 10^{\text{pH} - \text{pK}_{\text{a,coformer}}}\right)} \quad (6.4)$$

This equation can be expressed in terms of cocrystal and drug solubilities by considering that the cocrystal aqueous solubility (nonionized + ionized species) as a function of pH is

$$S_{\text{cocrystal,aq}} = \sqrt{K_{\text{sp}} \left(1 + 10^{\text{pH} - \text{pK}_{\text{a,coformer}}}\right)} \quad (6.5)$$

and the drug solubilization ratio is

$$\left(\frac{S_{\text{T}}}{S_{\text{aq}}}\right)_{\text{drug}} = \left(1 + K_{\text{s}}^{\text{drug}}[\text{M}]\right) \quad (6.6)$$

Substituting equations (6.4) and (6.5) in equation (6.2) gives the relationship between cocrystal solubilization ratio and drug solubilization ratio presented in equation (6.1).

For the case of a 2:1 cocrystal (drug:coformer) the relationship becomes

$$SR_{\text{cocrystal}} = (SR_{\text{drug}})^{\frac{2}{3}} \quad (6.7)$$

or

$$\left(\frac{S_T}{S_{\text{aq}}} \right)_{\text{cocrystal}} = \left(\frac{S_T}{S_{\text{aq}}} \right)_{\text{drug}}^{\frac{2}{3}}$$

The general form of the equation for a cocrystal with stoichiometry A_xB_y , where A and B are the cocrystal constituents, drug and coformer respectively; and x and y are the stoichiometric coefficients or molar ratios, is

$$SR_{\text{cocrystal}} = (SR_{\text{drug}})^{\frac{x}{x+y}} \quad (6.8)$$

or

$$\left(\frac{S_T}{S_{\text{aq}}} \right)_{\text{cocrystal}} = \left(\frac{S_T}{S_{\text{aq}}} \right)_{\text{drug}}^{\frac{x}{x+y}}$$

Solubilizing agents in aqueous media may favor interactions with drugs over coformers, since the drug constituents of cocrystals generally are quite hydrophobic whereas coformers are hydrophilic. We have confirmed such behavior for cocrystals of hydrophobic drugs, carbamazepine, indomethacin, and danazol with hydrophilic coformers in solutions of synthetic and biorelevant solubilizing agents^{10-12, 18-23}.

The shape of the $SR_{\text{cocrystal}}$ versus SR_{drug} curves (Figure 6.1) reflects the impact of different cocrystal stoichiometries on $SR_{\text{cocrystal}}$. The curvature of the plots is due to preferential solubilization of drug over coformer. $SR_{\text{cocrystal}}$ is predicted to be much lower than SR_{drug} with a

1:1 cocrystal being lower than the 2:1. The plot shows that drug solubilizing agents with SR_{drug} values of 100 and 1000 will result in $SR_{cocrystal}$ values of 10 and 31.6 for 1:1 cocrystals. SR_{drug} can reach values in the order of 10^6 with some solubilizing agents, and therefore one would expect cocrystals of these drugs to have solubilization ratios that are orders of magnitude lower than the drug. These predictions will be compared with experimental observations for several cocrystals and solubilizing agents in the results section.

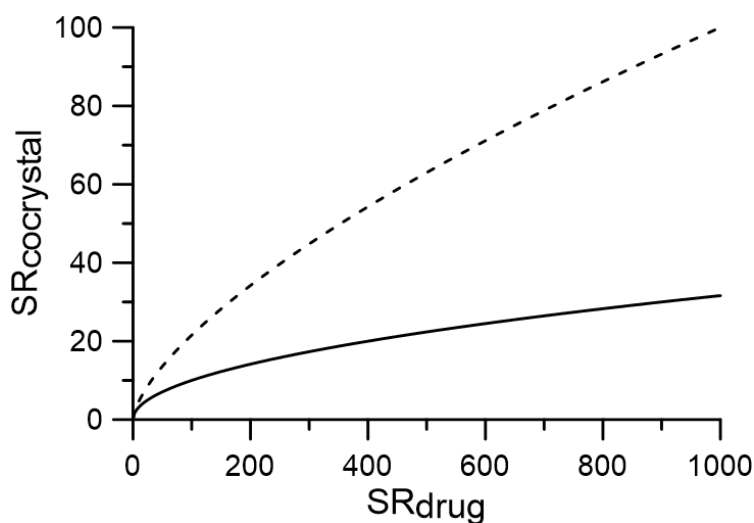


Figure 6.1. Dependence of $SR_{cocrystal}$ on SR_{drug} for cocrystal stoichiometries 1:1 (—) and 2:1 (----) predicted from equations (6.1) and (6.7) using a typical range of SR_{drug} values.

Cocrystal transition points

Drug solubilizing agents have been shown to switch the cocrystal solubility advantage^{10-12, 18, 19}. That is, a cocrystal that is more soluble than the drug in aqueous solution can become less soluble than the drug depending on the nature and concentration of the solubilizing agent.

Cocrystals were shown to possess transition points in the presence of solubilizing agents that have selective affinity for the drug. This behavior was mathematically explained by a drug solubility that is *linearly* dependent on solubilizing agent concentration,

$$S_{\text{drug,T}} = S_{\text{drug,aq}}^0 (1 + K_s^{\text{drug}} [\text{M}]) \quad (6.9)$$

and a cocrystal solubility that exhibits *nonlinear* dependence. $S_{\text{drug,aq}}^0$ represents the nonionized drug aqueous solubility (which for simplicity will be denoted as $S_{\text{drug,aq}}^0$). Cocrystal solubility exhibits a *square root* dependence on solubilizing agent concentration (equation (6.4)) for 1:1 cocrystals when coformer solubilization is negligible. For the case of 2:1 cocrystals, the solubility exhibits a *2/3 power* dependence. Theoretical predictions were recently reported to be in excellent agreement with experimental observations for carbamazepine and indomethacin cocrystals in the presence of several solubilizing agents^{10-12, 18, 19, 21, 23}.

Figure 6.2 illustrates the concept of cocrystal transition points, indicated by the intersection of the cocrystal and drug solubility curves. The position of the transition point is defined by a solubility (S^*) and a solubilizing agent concentration (CSC or critical stabilization concentration). Since the transition point that we are referring to is that between cocrystal and drug crystalline phases, the solubilities of the drug and the cocrystal are equal at this point.

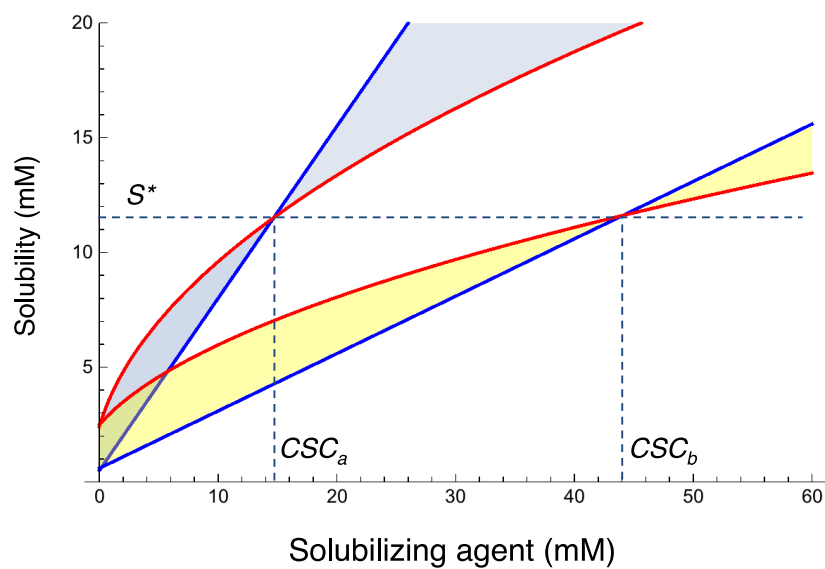


Figure 6.2. Transition points (S^* and CSC) for a cocystal (—) and its constituent drug (—) in two different solubilizing agents, a and b . S^* is constant and CSC varies with the extent of drug solubilization by the solubilizing agent. Drug is solubilized to a greater extent by a than by b and thus $CSC_a < CSC_b$. The curves were generated from equations (6.4) and (6.9) under nonionizing conditions and the parameter values $S^0_{\text{drug, aq}} = 0.5 \text{ mM}$, $S^0_{\text{cocystal, aq}} = 2.4 \text{ mM}$ ($K_{\text{sp}} = 5.76 \text{ mM}^2$), $K_s^{\text{drug}} = 1.5 \text{ mM}$ and 0.5 mM^{-1} for solubilizing agents a and b , respectively.

The position of the transition point for a given cocystal and its drug, (depicted in Figure 6.2) varies with solubilizing agent or with the degree to which the drug is solubilized (K_s^{drug}). For a given cocystal and a drug, the transition points exhibit a constant S^* but a variable CSC . A lower CSC is obtained with a stronger drug solubilizing agent ($K_s = 1.5 \text{ mM}^{-1}$) than with a weaker one ($K_s = 0.5 \text{ mM}^{-1}$). In other words, a lower concentration of solubilizing agent is required to reach the transition point with a stronger solubilizing agent.

In contrast to the CSC , whose values differ for both solubilizing agents, the value of S^* is constant. This property of S^* is found by examining the mathematical models that describe cocystal and drug solubilization as follows. At the transition point, the solubilities of cocystal and drug are equal

$$S_{\text{cocystal,T}} = S_{\text{drug,T}} = S^* \quad (6.10)$$

The solubilization ratio equations of cocystal and drug at the transition point can be written in terms of S^* , which for a 1:1 cocystal (from equation ((6.1)) is

$$\left(\frac{S^*}{S_{\text{aq}}}\right)_{\text{cocystal}} = \sqrt{\left(\frac{S^*}{S_{\text{aq}}}\right)_{\text{drug}}} \quad (6.11)$$

and solving for S^* gives

$$S^* = \frac{(S_{\text{cocystal,aq}})^2}{S_{\text{drug,aq}}} \quad (6.12)$$

This equation shows that the solubility value at the transition point is governed by two fundamental parameters, the *aqueous solubilities of cocystal and of drug*. S_{aq} refers to the (unionized + ionized) aqueous solubilities of cocystal and of drug and therefore equation (6.12) applies to a range of ionizing conditions (pH and appropriate solubility values).

S^* for a 2:1 cocystal is found by a similar approach and is

$$S^* = \frac{(S_{\text{cocystal,aq}})^3}{(S_{\text{drug,aq}})^2} \quad (6.13)$$

A plot of equation (6.12) in Figure 6.3 provides some insight about the dependence of S^* on the corresponding aqueous solubilities, $S_{\text{cocystal,aq}}$ and $S_{\text{drug,aq}}$ for a 1:1 cocystal. Typical values for drug and cocystal solubilities have been used in this example. S^* is shown to increase with increasing $S_{\text{cocystal,aq}}$, and the increase in S^* is greater at lower $S_{\text{drug,aq}}$.

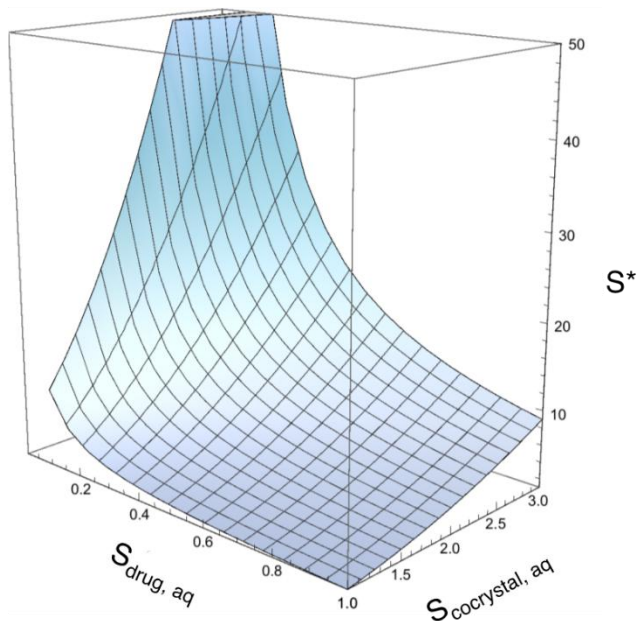


Figure 6.3. Graphical representation of S^* as a function of cocrystal and drug aqueous solubilities for a 1:1 cocrystal, according to equation (6.12). S^* is reached at the cocrystal/drug transition point.

For the case of a drug with $S_{\text{drug, aq}} = 0.3$ mM and its (1:1) cocrystal with $S_{\text{cococrystal, aq}} = 3.0$ mM, the transition solubility for this system is then $S^* = 30$ mM. This means that a cocrystal will not maintain its solubility advantage over the drug above 30 mM (under the conditions of this example) since cocrystal is less soluble than drug at S values above S^* . Another factor that influences the value of S^* is the solution pH. For the case of cocrystals with ionizable components, pH will determine the drug and cofomer ionization and change the aqueous solubilities of drug and cocrystal, thereby altering the position the value of S^* . It is therefore possible to calculate the influence of pH on the cocrystal transition point.

Another useful expression of S^* is in terms of the cocrystal solubility advantage (SA) given by

$$S^* = S_{\text{cocystal, aq}} \left(\frac{S_{\text{cocystal}}}{S_{\text{drug}}} \right)_{\text{aq}} \quad (6.14)$$

or

$$S^* = S_{\text{cocystal, aq}} (SA_{\text{aq}})$$

where

$$SA_{\text{aq}} = \left(\frac{S_{\text{cocystal}}}{S_{\text{drug}}} \right)_{\text{aq}} \quad (6.15)$$

For a 2:1 cocystal, the S^* expression in terms of solubility advantage becomes:

$$S^* = S_{\text{cocystal, aq}} (SA_{\text{aq}})^2 \quad (6.16)$$

Cocrystals with low SA_{aq} will possess low S^* values, which means that lower concentrations of drug solubilizing agents are required to reach S^* .

*Implications of cofomer solubilization on SR_{cocystal} and S^**

The equations presented above assume that cofomer solubilization is negligible ($K_s^{\text{coformer}} = 0$). Under some conditions this assumption is not justified ($K_s^{\text{coformer}} > 0$) and relevant terms need to be included in the SR_{cocystal} and S^* equations to account for the deviations due to cofomer solubilization.

The contribution of cofomer solubilization is included in the following equations as a factor by which the simpler equations are multiplied. The cocystal solubilization ratio of a 1:1 cocystal of a nonionizable drug and a monoprotic acidic cofomer is

$$\left(\frac{S_T}{S_{aq}}\right)_{\text{cocrystal}} = \sqrt{\varepsilon \left(\frac{S_T}{S_{aq}}\right)_{\text{drug}}} \quad (6.17)$$

where

$$\varepsilon = \frac{(1+10^{\text{pH-pKa,coformer}} + K_s^{\text{cof}} [M])}{(1+10^{\text{pH-pKa,coformer}})} \quad (6.18)$$

It can be seen that when $K_s^{\text{coformer}} = 0$, $\varepsilon = 1$ and the equation is equal to the simple equation (6.1)

. When $K_s^{\text{coformer}} > 0$, $\varepsilon > 1$ and the coformer solubilization, as well as solubilizing agent concentration and coformer ionization must be considered.

The expression for S^* is given by

$$S^* = \varepsilon \frac{(S_{\text{cocrystal, aq}})^2}{S_{\text{drug, aq}}} \quad (6.19)$$

S^* equations can also be expressed in terms of cocrystal K_{sp} . In terms of the unionized cocrystal (solubility product) and drug aqueous solubilities, when $K_s^{\text{coformer}} = 0$,

$$S^* = \frac{K_{sp} (1+10^{\text{pH-pKa,coformer}})}{S_{\text{drug, aq}}^0} \quad (6.20)$$

When $K_s^{\text{coformer}} > 0$, S^* is given by:

$$S^* = \frac{K_{sp} (1+10^{\text{pH-pKa,coformer}} + K_s^{\text{coformer}} [M])}{S_{\text{drug, aq}}^0} \quad (6.21)$$

based on the full solubility equations of cocrystal and drug, (equations (6.3) and (6.9)) and nonionized cocrystal and drug solubilities.

Materials and Methods

Materials

Cocrystal components

Anhydrous carbamazepine form III (CBZ), anhydrous indomethacin form γ (IND) were purchased from Sigma Chemical Company (St. Louis, MO) and used as received. Anhydrous piroxicam form I (PXC) was received as a gift from Pfizer (Groton, CT) and used as received. Anhydrous danazol was received as a gift from Renovo Research (Atlanta, GA) and used as received.

Anhydrous saccharin (SAC), 4- aminobenzoic acid (4ABA), and salicylic acid (SLC), were purchased from Sigma Chemical Company (St. Louis, MO) and used as received. Anhydrous hydroxybenzoic acid was purchased from Acros Organics (Pittsburgh, PA) and used as received. Anhydrous vanillin was purchased from Fisher Scientific (Fair Lawn, NJ) and used as received. Carbamazepine dihydrate (CBZD) piroxicam monohydrate (PXCH), and hydroxybenzoic acid monohydrate (HBAH) were prepared by slurring CBZ, PXC, and HBA in deionized water for at least 24 hours. All crystalline drugs and cofomers were characterized by X-ray power diffraction (XRPD) and differential scanning calorimetry (DSC) before carrying out experiments.

Solvents and buffer components

Ethyl acetate and ethanol were purchased from Acros Organics (Pittsburgh, PA) and used as received, and HPLC grade methanol and acetonitrile were purchased from Fisher Scientific

(Pittsburgh, PA). Trifluoroacetic acid spectrophometric grade 99% was purchased from Aldrich Company (Milwaukee, WI) and phosphoric acid ACS reagent 85% was purchased from Sigma Chemical Company (St. Louis, MO). Water used in this study was filtered through a double deionized purification system (Milli Q Plus Water System) from Millipore Co. (Bedford, MA).

Tween 80 solutions, FeSSIF, and acetate buffer were prepared using Tween 80 purchased from Sigma Chemical Company (St. Louis, MO), sodium taurocholate (NaTC) purchased from Sigma Chemical Company (St. Louis, MO), lecithin purchased from Fisher Scientific (Pittsburgh, PA), sodium hydroxide pellets (NaOH) purchased from J.T. Baker (Philipsburg, NJ), and acetic acid and potassium chloride (KCl) purchased from Acros Organics (Pittsburgh, PA).

Methods

FeSSIF, acetate buffer, and Tween 80 solution preparation

FeSSIF and acetate buffer were prepared according to the protocol of Galia and coworkers²⁴. Acetate buffer was prepared as a stock solution at room temperature by dissolving 8.08 g NaOH (pellets), 17.3 g glacial acetic acid and 23.748 g NaCl in 2 L of purified water. The pH was adjusted to 5.00 with 1 N NaOH and 1 N HCl.

FeSSIF was prepared by dissolving 0.41 g sodium taurocholate in 12.5 mL of pH 5 acetate buffer. 0.148 g lecithin was added with magnetic stirring at 37 °C until dissolved. The volume was adjusted to exactly 50 mL with acetate buffer. Tween 80 solutions were prepared by dissolving an appropriate amount (25 mM, 50 mM, and 150 mM) of Tween 80 in pH 5 acetate buffer.

Cocrystal synthesis

Cocrystals were prepared by the reaction crystallization method²⁵ at 25°C. The 1:1 indomethacin-saccharin cocrystal (IND-SAC) was synthesized by adding stoichiometric amounts of cocrystal components (IND and SAC) to nearly saturated SAC solution in ethyl acetate. The 1:1 carbamazepine saccharin cocrystal (CBZ-SAC) was prepared by adding stoichiometric amounts of cocrystal components (CBZ and SAC) to nearly saturated SAC solution in ethanol. The 1:1 carbamazepine-salicylic acid cocrystal (CBZ-SLC) was prepared by adding stoichiometric amounts of cocrystal components (CBZ and SLC) to nearly saturated SLC solution in acetonitrile. The 2:1 carbamazepine-4-aminobenzoic acid monohydrate cocrystal (CBZ-4ABA-HYD) was prepared by suspending stoichiometric amounts of cocrystal components (CBZ and 4ABA) in a 0.01 M 4ABA aqueous solution at pH 3.9. The 1:1 piroxicam-saccharin cocrystal (PXC-SAC) was prepared by adding stoichiometric amounts of cocrystal components (PXC and SAC) to nearly saturated SAC in acetonitrile. The 1:1 danazol-hydroxybenzoic acid cocrystal (DNZ-HBA) was prepared by adding stoichiometric amounts of cocrystal components (DNZ and HBA) to nearly saturated HBA solution in ethyl acetate. The 1:1 danazol-vanillin cocrystal (DNZ-VAN) was prepared by adding stoichiometric amounts of cocrystal components (DNZ and VAN) to nearly saturated VAN solution in ethyl acetate. Prior to carrying out any solubility experiments, solid phases were characterized by XRPD and DSC and stoichiometry verified by HPLC. Full conversion to cocrystal was observed in 24 hours.

Drug solubility measurements

Drug solubilities were either reported in the literature or experimentally determined in this work. When reported values at a specific surfactant concentration were not available, drug solubility values at the surfactant concentration of the cocrystal solubility measurements were

interpolated from data at other at other surfactant concentrations. Drug solubility values in sodium lauryl sulfate (SLS), Myrj 52, Brij 99, Tween 80 (IND only), and a lipid formulation were obtained from the literature^{12, 19, 26-28}. Drug solubilities were measured in FeSSIF, Tween 80, and pH 5 acetate buffer (FeSSIF without NaTC and lecithin or Tween 80). The solubilities of the drugs were determined by adding excess solid to 3 mL of media (FeSSIF, Tween 80, or buffer). Solutions were magnetically stirred and maintained at $25 \pm 0.1^\circ\text{C}$ using a water bath for up to 96 hours. In 24 hour intervals, 0.30 mL of samples were collected, pH of solutions measured, and filtered through a $0.45 \mu\text{m}$ pore membrane. After dilution with mobile phase, drug solution concentrations were analyzed by HPLC. The final solid phases were characterized by XRPD and DSC.

Cocrystal solubility measurements

Cocrystal equilibrium solubilities were either reported in the literature or experimentally determined in this work. Literature cocrystal solubility values were taken from experimentally determined values at specific reported surfactant concentrations. Cocrystal solubility values in sodium lauryl sulfate (SLS), Myrj 52, Brij 99, Tween 80 (IND-SAC only), and a lipid formulation were obtained from the literature^{12, 19, 26-28}. Cocrystal equilibrium solubilities were measured in FeSSIF, Tween 80, and pH 5 acetate buffer (FeSSIF without NaTC and lecithin) at the eutectic point, where drug and cocrystal solid phases are in equilibrium with solution. The eutectic point between cocrystal and drug was approached by cocrystal dissolution (suspending solid cocrystal (~100 mg) and drug (~50 mg) in 3 mL of media (FeSSIF or buffer)) and by cocrystal precipitation (suspending solid cocrystal (~50 mg) and drug (~100 mg) in 3 mL of media (FeSSIF or buffer) nearly saturated with cofomer). Solutions were magnetically stirred and maintained at $25 \pm 0.1^\circ\text{C}$ using a water bath for up to 96 hours. In 24 hour intervals, 0.30 mL

of samples were collected, pH of solutions measured, and filtered through a 0.45 μm pore membrane. Solid phases were also collected in 24 hour intervals to ensure the sample was at the eutectic (confirmed by presence of both drug and cocrystal solid phases). After dilution with mobile phase, drug and coformer solution concentrations were analyzed by HPLC. The final solid phases were characterized by XRPD and DSC.

X-ray powder diffraction

X-ray powder diffraction diffractograms of solid phases were collected on a benchtop Rigaku Miniflex X-ray diffractometer (Rigaku, Wilmington, MA) using Cu K α radiation ($\lambda=1.54\text{\AA}$), a tube voltage of 30 kV, and a tube current of 15 mA. Data were collected from 5 to 40° at a continuous scan rate of 2.5°/min.

Thermal analysis

Solid phases collected from the slurry studies were dried at room temperature and analyzed by differential scanning calorimetry (DSC) using a TA instrument (Newark, DE) 2910MDSC system equipped with a refrigerated cooling unit. DSC experiments were performed by heating the samples at a rate of 10 °C/min under a dry nitrogen atmosphere. A high purity indium standard was used for temperature and enthalpy calibration. Standard aluminum sample pans were used for all measurements.

High performance liquid chromatography

Solution concentrations were analyzed by a Waters HPLC (Milford, MA) equipped with an ultraviolet-visible spectrometer detector. For the IND-SAC and CBZ-SAC, CBZ-SLC, CBZ-4ABA-HYD cocrystals and their components, a C18 Thermo Electron Corporation (Quebec, Canada) column (5 μm , 250 x 4.6 mm) at ambient temperature was used. For the IND-SAC cocrystal, the injection volume was 20 μl and analysis conducted using an isocratic method with

a mobile phase composed of 70% acetonitrile and 30% water with 0.1% trifluoroacetic acid and a flow rate of 1 ml/min. Absorbance of IND and SAC were monitored at 265 nm. For the CBZ cocrystals, the injection volume was 20 μ l and analysis conducted using an isocratic method with a mobile phase composed of 55% methanol and 45% water with 0.1% trifluoroacetic acid and a flow rate of 1 mL/min. Absorbance was monitored as follows: CBZ and 4ABA at 284 nm, SAC at 265 nm, and SLC at 303 nm. For the PXC-SAC, DNZ-HBA, and DNZ-VAN cocrystals and their components, a C18 Waters Atlantis (Milford, MA) column (5 μ M 250 x 6 mm) at ambient temperature was used. For PXC-SAC, the injection volume was 20 μ L and analysis was conducted using an isocratic method with a mobile phase composed of 70% methanol and 30% water with 0.3% phosphoric acid and a flow rate of 1 mL/min. Absorbance of PXC was monitored at 340 nm and SAC at 240 nm. For the DNZ cocrystals, the injection volume was 20 μ L in FeSSIF experiments, and 100 μ L in buffer experiments due to the extremely low solubility of DNZ in aqueous solutions. Analysis was conducted using an isocratic method composed of 80% methanol and 20% water with 0.1% trifluoroacetic acid and a flow rate of 1 mL/min. Absorbance of DNZ was monitored at 285 nm, HBA at 242 nm, and VAN at 300 nm. For all cocrystals, the Waters' operation software Empower 2 was used to collect and process data.

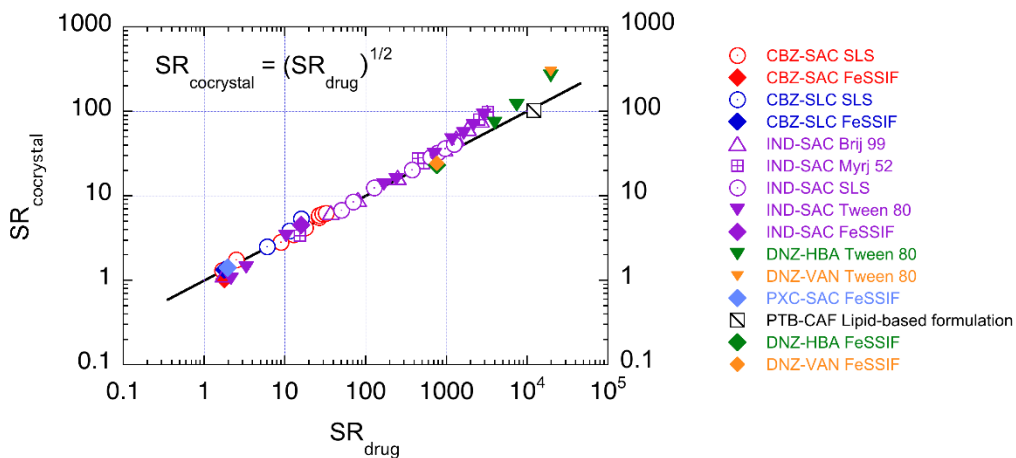
Results

Solubilization ratios of cocrystals and drugs

Figure 6.4 shows the observed and predicted dependence of cocrystal solubilization ratio ($SR_{\text{cocrystal}}$) on drug solubilization ratio (SR_{drug}) for cocrystals of carbamazepine (CBZ), piroxicam (PXC), indomethacin (IND), danazol (DNZ) and pterostilbene (PTB) in different solubilizing agents. Solubilizing agents included: anionic surfactants (SLS, FeSSIF), nonionic

surfactants (Tween 80, Myrj 52, and Brij 99), and a lipid formulation (Captex 355/Capmul MCM (1/3): Cremophor EL (3:7)).

a



b

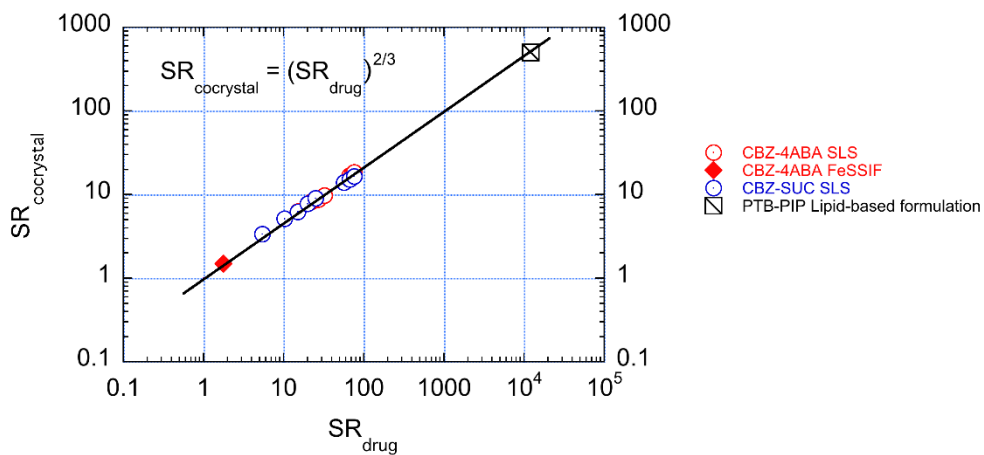


Figure 6.4. $SR_{\text{cocrystal}}$ dependence on SR_{drug} for (a) 1:1 cocrystals and (b) 2:1 cocrystals. Lines represent theoretical relationships between $SR_{\text{cocrystal}}$ and SR_{drug} according to equation (6.1) for 1:1 cocrystals and (6.7) for 2:1 cocrystals. 1:1 cocrystals have a slope of $1/2$. 2:1 cocrystals have a slope of $2/3$. Symbols represent experimentally determined SR values in equilibrium conditions.

Logarithmic plots are presented since values range across 6 orders of magnitude for SR_{drug} and 4 orders of magnitude for SR_{cocystal} . The cocystal solubilization ratio for a 1:1 cocystal is equal to square root of the drug solubilization ratio

$$\left(\frac{S_T}{S_{\text{aq}}}\right)_{\text{cocystal}} = \sqrt{\left(\frac{S_T}{S_{\text{aq}}}\right)_{\text{drug}}}$$

which in logarithmic form becomes

$$\text{Log}\left(\frac{S_T}{S_{\text{aq}}}\right)_{\text{cocystal}} = \frac{1}{2} \text{Log}\left(\frac{S_T}{S_{\text{aq}}}\right)_{\text{drug}} \quad (6.22)$$

The line in Figure 6.4a has a slope of 1/2.

Figure 6.4b shows 2:1 cocystals according to the logarithmic form of

$$\left(\frac{S_T}{S_{\text{aq}}}\right)_{\text{cocystal}} = \left(\frac{S_T}{S_{\text{aq}}}\right)_{\text{drug}}^{\frac{2}{3}}$$

which is

$$\text{Log}\left(\frac{S_T}{S_{\text{aq}}}\right)_{\text{cocystal}} = \frac{2}{3} \text{Log}\left(\frac{S_T}{S_{\text{aq}}}\right)_{\text{drug}} \quad (6.23)$$

The line in Figure 6.4b has a slope of 2/3.

These plots reveal that (1) SR_{cocystal} is well approximated by SR_{drug} over a wide range of values for different drugs, cocystals, and drug solubilizing agents assuming cofomer solubilization is negligible, and that (2) 1:1 cocystals are solubilized to a lesser extent than the 2:1 cocystals for the same value of SR_{drug} .

Drug solubilizing agents with SR_{drug} values as high as 12,000 (PTB) and 20,000 (DNZ) resulted in SR_{cocystal} of 102 (1:1 PTB-CAF in lipids), 300 (1:1 DNZ-HBA and DNZ-VAN in Tween 80), and 530 (2:1 cocystal PTB-PIP). Solubilization ratios of 2:1 cocystals are well predicted for the systems studied, CBZ-SUC and CBZ-4ABA-HYD in SLS, and PTB-PIP in lipid-based media (Figure 6.4b). The positive deviations observed for several 1:1 cocystals at high values of SR_{drug} appear to be a result of cofomer solubilization under the conditions studied, which will be examined in a later section.

These results indicate that if drug solubilization is known then cocystal solubilization can be calculated (under the same experimental conditions). Although small changes in cofomer solubilization by the additive can result in deviations from predictions, these relationships are very important to guide additive selection for cocystal formulations and dissolution methods.

Prediction of cocystal solubility ($S_{\text{cocystal},T}$) in the presence of drug solubilizing agents

From the results of cocystal and drug SR relationships presented above one can anticipate the impact that formulating poorly soluble drugs with very effective solubilizing agents may have on cocystal solubility. An example of this analysis is applied to understanding the solubilization of PTB cocystals in lipid-based solubilizers^{26, 28} (Table 6.1).

PTB is poorly water-soluble. Two cocystals with caffeine (CAF) and piperazine (PIP) were shown to increase its aqueous solubility by orders of magnitude^{26, 27}. However, this cocystal solubility advantage was eliminated when cocystals were formulated in a lipid system²⁸. In fact, the cocystals became less soluble than PTB in the presence of these lipids. A key question to ask is whether this observation could have been predicted from the simple relationships presented here.

Table 6.1. Comparison of experimental and predicted PTB cocrystal solubilities in lipid-based formulations.

Solid phase	Aqueous	Experimental	Predicted
	solubility ^a	Total solubility in lipid ^b	Total solubility in
	S _{aq} (mM)	S _T (mM)	lipid ^c S _T (mM)
PTB	0.0819	1002	----
PTB-CAF (1:1)	2.19	222	242
PTB-PIP (2:1)	0.492	246	262

a) From references 24 and 25.

b) From reference 26.

c) Calculated from equations (6.24) and (6.25) for 1:1 and 2:1 cocrystals as described in the text.

Cocrystal solubility in media containing drug solubilizing agents such as lipid-based systems can be obtained by simply solving for S_{cocrystal,T} in equations (6.1) and (6.7), which for a 1:1 cocrystal becomes

$$S_{\text{cocrystal,T}} = S_{\text{cocrystal,aq}} \sqrt{\left(\frac{S_T}{S_{\text{aq}}}\right)_{\text{drug}}} \quad (6.24)$$

and for a 2:1 cocrystal, gives

$$S_{\text{cocrystal,T}} = S_{\text{cocrystal,aq}} \left(\frac{S_T}{S_{\text{aq}}}\right)_{\text{drug}}^{\frac{2}{3}} \quad (6.25)$$

Once the cocrystal aqueous solubility and drug solubilization ratio are known then the cocrystal solubility in the media containing the solubilizing agents can be readily calculated.

For PTB-CAF (1:1 cocrystal) the solubility in the lipid formulation, $S_{\text{cocrystal,T}}$ is

$$S_{\text{cocrystal,T}} = S_{\text{cocrystal,aq}} \sqrt{\left(\frac{S_{\text{T}}}{S_{\text{aq}}}\right)_{\text{drug}}} = 2.19\sqrt{1.22 \times 10^4} = 242 \text{ mM}$$

For PTB-PIP (2:1 cocrystal), $S_{\text{cocrystal,T}}$ is

$$S_{\text{cocrystal,T}} = S_{\text{cocrystal,aq}} \left(\frac{S_{\text{T}}}{S_{\text{aq}}}\right)_{\text{drug}}^{\frac{2}{3}} = 4.92 \times 10^{-1} (1.22 \times 10^4)^{\frac{2}{3}} = 262 \text{ mM}$$

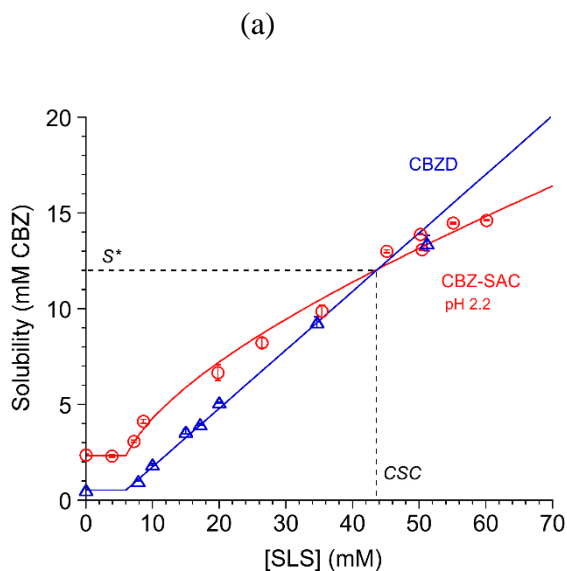
The predicted cocrystal solubilities in the lipid formulation are in very good agreement with the measured values (222 and 246 mM) shown in Table 6.1. These simple relationships provide quantitative information about cocrystal solubility without the need of more rigorous equations (equation (6.3) for example) that require knowledge of equilibrium constants associated with the solution processes. The full equations are however valuable when the assumptions underlying the simple relationships are no longer warranted.

The PTB cocrystal formulation in lipid-based systems also teaches us about the ability of strong drug solubilizing agents to reverse the cocrystal solubility advantage over drug. The particular combination and concentration of lipids/surfactants in this formulation induced this reversal. Lower concentrations of these lipids/surfactants would have decreased the cocrystal solubility advantage without reversing it. This switch of cocrystal solubility over drug solubility has been shown for other cocrystals with solubilizing agents and indicates the existence of a cocrystal transition point.

Cocrystal transition points

Figure 6.5 and Figure 6.6 show the transition points for several CBZ cocrystals in aqueous solutions of SLS. It is noted that two parameters characterize the transition point: (1) solubility at which both drug and cocrystal exhibit the same solubility (S^*) and (2) solubilizing agent concentration (CSC). Our previous work focused on the CSC^{10-12, 18, 19}, here we will focus on S^* . One important observation that emerged from the present study is that aqueous solubility is a key indicator of the transition point. In fact, S^* as described in the theoretical section, is independent of the solubilizing agent, and is only determined by the drug and cocrystal aqueous solubilities.

S^* values in the following analysis were obtained by a graphical method from experimentally measured cocrystal and drug solubility dependence on solubilizing agent concentrations (Figure 6.5 and Figure 6.6). These experimentally determined S^* values were then compared with those predicted by simple equations based on knowledge of drug and cocrystal aqueous solubilities.



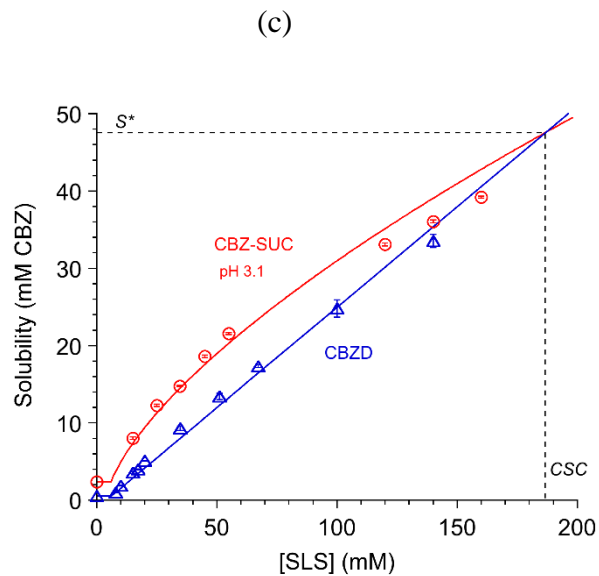
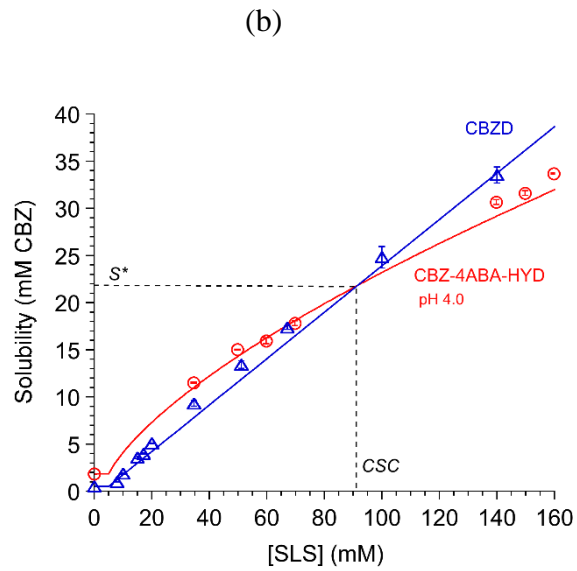


Figure 6.5. Transition points for CBZ cocrystals induced by solubilizing CBZ with SLS for (a) CBZ-SAC, (b) CBZ-4ABA-HYD, and (c) (CBZ-SUC) from reference 13. Transition points are characterized by a solubility (S^*) and a solubilizing agent concentration (CSC). Both S^* and CSC vary with cocrystal aqueous solubility and stoichiometry. Symbols represent experimentally measured cocrystal (\circ) and drug (\triangle) solubility values¹².

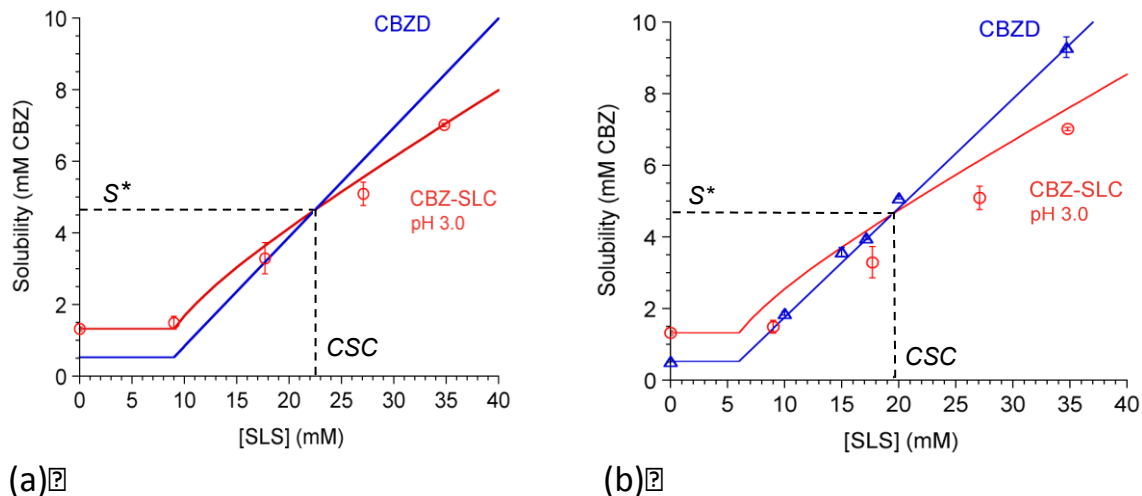


Figure 6.6. Transition points for CBZ and CBZ-SLC induced by solubilizing CBZ with SLS from reference 13. Transition points are characterized by a solubility (S^*) and a solubilizing agent concentration (CSC). Both S^* and CSC vary with cocrystal aqueous solubility and stoichiometry. SLC was found to influence the CMC of SLS, raising it from 6 mM (a) to 9 mM, (b) which had a minor impact on the CSC (20-23 mM) and no impact on S^* . Symbols represent experimentally measured cocrystal (\circ) and drug (\triangle) solubility values¹².

S^* values determined graphically from the intersection of solubility vs solubilizing agent curves for drug and cocrystal (Figure 6.5 and Figure 6.6) are presented in Table 6.2. S^* is observed to increase with cocrystal aqueous solubility and with the molar content of drug in the cocrystal. For this small series of cocrystals the range of S^* is 4.6 to 47.6 mM. S^* can play an important role in cocrystal selection as it establishes the upper solubility limit at which a cocrystal has an advantage over drug in solutions with solubilizing agents.

S^* values were also predicted with the simplified equations under the assumption that $K_s^{\text{coformer}} = 0$ according to

$$S^* = \frac{(S_{\text{cocrystal, aq}})^2}{S_{\text{drug, aq}}}$$

for 1:1 cocrystals, and

$$S^* = \frac{(S_{\text{cocystal,aq}})^3}{(S_{\text{drug,aq}})^2}$$

for 2:1 cocrystals at a particular solution pH.

$S_{\text{cocystal,aq}}$ and $S_{\text{drug,aq}}$ were measured in aqueous solutions without solubilizing agents at a particular pH (as described in the methods section). $S_{\text{drug,aq}}$ stands for the CBZ dihydrate (CBZD) solubility since this is the thermodynamically stable form of CBZ under the experimental conditions studied.

Results in Table 6.2 indicate that there is excellent agreement between predicted and observed S^* values. The largest deviation was observed for the SLC cocrystal, where coformer solubilization leads to a positive deviation in predicted S^* . Deviations in S^* due to coformer solubilization are examined in a subsequent section.

Table 6.2. Predicted and observed S^* values for CBZ cocrystals in aqueous solutions of SLS.

Cocrystal	pH	$S_{\text{cocystal,aq}}^a$ (mM)	$S^*_{\text{pred}}^b$ (mM)	$S^*_{\text{exp}}^c$ (mM)
CBZ-SLC (1:1)	3.0	1.32 ± 0.06	3.3	4.6
CBZ-SAC (1:1)	2.2	2.36 ± 0.05	10.5	12.0
CBZ-4ABA-HYD (2:1)	4.0	1.83 ± 0.02	21.8	22.0
CBZ-SUC (2:1)	3.1	2.38 ± 0.02	48.0	47.6

a) Solubility values at 25°C from reference 13, in terms of CBZ mM.

b) Predicted from equations (6.12) and (6.13) for 1:1 and 2:1 cocrystals with $S_{\text{CBZD,aq}} = 0.53$ mM.

c) Determined from the intersection of $S_{\text{cocystal,T}}$ and $S_{\text{drug,T}}$ curves in Figure 6.5 and Figure 6.6.

It is instructive to apply this analysis to estimate the S^* values of PTB cocrystals.

S^* values of 59 mM (PTB-CAF) and 18 mM (PTB-PIP) were predicted, from equations (6.12) and (6.13) with values for the aqueous solubilities of drug and cocrystals presented in Table 6.1. Comparing the predicted S^* values with the PTB solubility in lipid-based media (1 M) reveals that the lipid mixture concentration used in the reported study was above the transition point for each cocrystal. This is also consistent with the observed cocrystal solubilities (222 mM and 246 mM) being lower than the PTB solubility (1 M) in the lipid formulation.

Comparing the S^* values for the CBZ and PTB cocrystals reveals that S^* increases with cocrystal solubility for the 1:1 and 2:1 cocrystals studied. S^* values are within the range of 4.6 to 57 mM for both CBZ and PTB cocrystals even though the aqueous solubility of CBZD is about 700 times higher than the solubility of PTB. S^* is inversely related to $S_{\text{drug,aq}}$ and proportional to $S_{\text{cocrystal,aq}}$ squared or cubed. PTB cocrystals have aqueous solubilities higher than the CBZ cocrystals considered here, and compensate for the low aqueous solubility of PTB.

Solubilization ratio and cocrystal transition points

The relationships between cocrystal and drug solubilization ratios presented in equations (6.1) and (6.7) and Figure 6.4 are useful to predict the $SR_{\text{cocrystal}}$ from knowledge of SR_{drug} but do not provide information about the cocrystal transition point and particularly S^* . The question is how to establish where a cocrystal stands with respect to its transition point in a given formulation or in the presence of solubilizing agents from knowledge of SR_{drug} and without having to measure $SR_{\text{cocrystal}}$.

The relationship between solubilization ratio and cocrystal transition point or S^* can be easily found by rewriting equation (6.1) for 1: 1 cocrystals as

$$\left(\frac{S_{\text{cocrystal}}}{S_{\text{drug}}}\right)_{\text{aq}} = \left(\frac{S_{\text{cocrystal}}}{S_{\text{drug}}}\right)_{\text{T}} \sqrt{\left(\frac{S_{\text{T}}}{S_{\text{aq}}}\right)_{\text{drug}}} \quad (6.26)$$

The criterion for the cocrystal transition point is that $S_{\text{cocrystal,T}} = S_{\text{drug,T}}$, therefore

$$\left(\frac{S_{\text{cocrystal}}}{S_{\text{drug}}}\right)_{\text{T}} = 1 \quad (6.27)$$

and equation (6.26) becomes.

$$\left(\frac{S_{\text{cocrystal}}}{S_{\text{drug}}}\right)_{\text{aq}} = \sqrt{\left(\frac{S_{\text{T}}^*}{S_{\text{aq}}}\right)_{\text{drug}}} \quad (6.28)$$

In other words, *at the transition point*

$$SA_{\text{aq}} = \sqrt{SR_{\text{drug}}^*} = SR_{\text{cocrystal}}^* \quad (6.29)$$

and the cocrystal solubility advantage over drug in aqueous media (SA_{aq}) is equal to the square root of the drug solubilization ratio, $(SR_{\text{drug}})^{1/2}$, and to the cocrystal solubilization ratio ($SR_{\text{cocrystal}}$).

Below the cocrystal transition point $S^* > S_{\text{cocrystal,T}} > S_{\text{drug,T}}$ which means that

$$\left(\frac{S_{\text{cocrystal}}}{S_{\text{drug}}}\right)_{\text{T}} > 1 \quad (6.30)$$

Substituting the above equation into equation (6.26) leads to

$$\left(\frac{S_{\text{cocrystal}}}{S_{\text{drug}}}\right)_{\text{aq}} > \sqrt{\left(\frac{S_{\text{T}}}{S_{\text{aq}}}\right)_{\text{drug}}} \quad (6.31)$$

or

$$SA_{\text{aq}} > SR_{\text{cocrystal}}$$

which is indicative of a cocrystal that is below its transition point and thus will possess a higher solubility than the drug in the solubilizing media at the respective SR_{drug} or $SR_{\text{cocrystal}}$ values.

For a 2:1 cocrystal equation (6.7) becomes

$$\left(\frac{S_{\text{cocrystal}}}{S_{\text{drug}}}\right)_{\text{aq}} = \left(\frac{S_{\text{cocrystal}}}{S_{\text{drug}}}\right)_{\text{T}} \left(\frac{S_{\text{T}}}{S_{\text{aq}}}\right)_{\text{drug}}^{\frac{1}{3}} \quad (6.32)$$

Cocrystal is then at the transition point when

$$\left(\frac{S_{\text{cocrystal}}}{S_{\text{drug}}}\right)_{\text{aq}} = \left(\frac{S_{\text{T}}^*}{S_{\text{aq}}}\right)_{\text{drug}}^{\frac{1}{3}} \quad (6.33)$$

Cocrystal is below the transition point when

$$\left(\frac{S_{\text{cocrystal}}}{S_{\text{drug}}}\right)_{\text{aq}} > \left(\frac{S_{\text{T}}}{S_{\text{aq}}}\right)_{\text{drug}}^{\frac{1}{3}} \quad (6.34)$$

or

$$SA_{\text{aq}} > \sqrt{SR_{\text{cocrystal}}} \quad (6.35)$$

Applying this analysis to DNZ cocrystals in Tween 80 and PTB cocrystals in lipid-based media (Figure 6.7) demonstrates the important role of cocrystal solubility advantage ($SA_{aq} = (S_{cocrystal}/S_{drug})_{aq}$) in determining the position of the cocrystal solubility with respect to the transition point and S^* . For instance, it can be seen that both DNZ cocrystals meet the criteria for being below the transition point in 150 mM Tween 80 since $(SA)_{aq} > SR_{cocrystal}$. SA_{aq} values for the two DNZ cocrystals (770 and 370) are greater than their SR values (264 and 300), indicating that the DNZ cocrystals are below the transition point (at this concentration of Tween 80). PTB cocrystals are however above the transition point in the lipid mixture²⁸ since $(SA)_{aq} < SR_{cocrystal}$ for the 1:1 cocrystal ($26 < 111$) and $(SA)_{aq}^2 < SR_{cocrystal}^{1/2}$ for the 2:1 cocrystal ($6 < 23$). The effect of drug solubilizing agent findings are in excellent agreement with the observed cocrystal and drug solubilities with respect to the transition point.

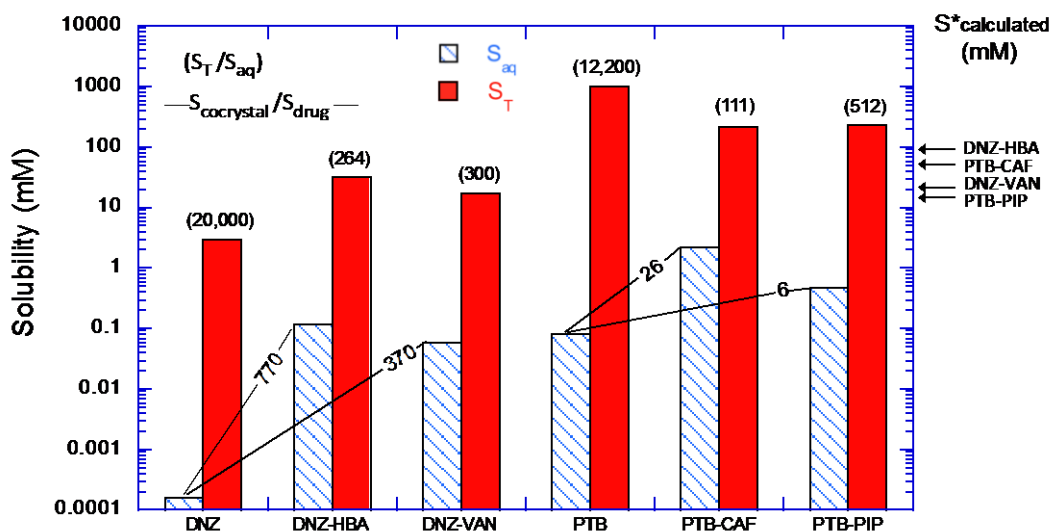


Figure 6.7. Measured solubilities for DNZ and PTB and their cocrystals in solubilizing agents: Tween 80 aqueous solution (150 mM, pH 5.0) for DNZ and lipid mixture for PTB. How to determine where a cocrystal stands with respect to its transition point in a given formulation or in the presence of solubilizing agents from knowledge of SR_{drug} and without having to measure $SR_{cocrystal}$ is described in the text. Numbers in parentheses represent SR values, and numbers within the lines represent SA_{aq} . Transition point solubilities, S^* , were calculated from equations (6.12) and (6.13) for 1:1 DNZ and PTB cocrystals and the 2:1 PTB-PIP cocrystal with the

measured values of $S_{\text{drug,aq}}$ and $S_{\text{cocystal,aq}}$ presented in the plot. PTB data obtained from references²⁶⁻²⁸.

S^* values were also calculated for the DNZ and PTB cocystals according to equations (6.12) and (6.13). Whether a cocystal is above or below the transition point in a given formulation can be determined by comparing the S^* values with the cocystal solubilities in the drug solubilizing media. S^* values are between 16 and 94 mM indicating the adjustments that could be made in drug solubilizing agent concentration to move closer to or further away from the transition point.

Influence of cofomer solubilization

Deviations in SR_{cocystal} for a 1:1 cocystal due to cofomer solubilization are accounted for by a factor ε and equation (6.1) for a 1:1 cocystal becomes

$$SR_{\text{cocystal}} = \sqrt{\varepsilon (SR_{\text{drug}})}$$

For a monoprotic weakly acidic cofomer,

$$\varepsilon = \frac{(1 + 10^{\text{pH} - \text{pKa,coformer}} + K_s^{\text{coformer}} [M])}{(1 + 10^{\text{pH} - \text{pKa,coformer}})}$$

When $K_s^{\text{coformer}} = 0$, $\varepsilon = 1$ and SR_{cocystal} can be accurately predicted from SR_{drug} using equation (6.1). However, as shown in Figure 6.4a, the observed SR_{cocystal} values are higher than those predicted from SR_{drug} using equation (6.1) for DNZ-HBA and DNZ-VAN in 150 mM Tween 80, and IND-SAC at increasing concentrations of Tween 80, Brij 99, Myrj 52. In these conditions, $K_s^{\text{coformer}} > 0$ and $\varepsilon > 1$, leading to an underprediction of SR_{cocystal} when ε is ignored.

ε can also be obtained from

$$\sqrt{\varepsilon} = \frac{SR_{\text{cocystal,observed}}}{SR_{\text{cocystal,predicted}}} \quad (6.36)$$

where SR_{cocystal} is predicted from equation (6.1) assuming $K_s^{\text{coformer}} = 0$. Table 6.3 shows the ε values obtained using equations (6.18) and (6.36).

Table 6.3. SR_{cocystal} deviations due to coformer solubilization.

Cocystal	pH	Solubilizing agent	$(K_s^{\text{coformer}})^a$ (mM ⁻¹)	[solubilizing agent] ^b (mM)	$\varepsilon^{1/2}$ pred ^c	$\varepsilon^{1/2}$ exp ^d
DNZ-VAN	5.02	Tween 80	0.0283±0.0009	150	2.28	2.14
DNZ-HBA	4.42	Tween 80	0.031±0.001	150	1.87	1.88
IND-SAC	2.1	Myrj 52	0.083±0.007	100	1.73	1.72
IND-SAC	2.1	Tween 80	0.059±0.003	124	1.66	1.69
IND-SAC	2.1	Brij 99	0.058±0.004	121	1.64	1.70
IND-SAC	2.1	SLS	0.008±0.002	199	1.18	1.17

- a) K_s^{coformer} for HBA, VAN experimentally measured and SAC reported in reference 21.
b) Solubilizing agent concentration is the highest concentration studied for each system.
c) Predicted using equation (6.18) with pKa HBA = 4.48, pKa VAN = 7.4, and pKa SAC = 1.6.
d) Calculated using equation (6.36).

The ε values from the two methods are in excellent agreement. Ignoring ε can lead to underpredicting SR_{cocystal} by as much as 2 fold for solubilizing agents and high concentrations and/or high K_s^{coformer} values.

S^* is influenced by coformer solubilization to a greater extent than SR. While SR has a square root dependence on ε , S^* for a 1:1 cocystal is proportional to ε , as described by:

$$S^* = \varepsilon \frac{(S_{\text{cocystal, aq}})^2}{S_{\text{drug, aq}}}$$

where ε has the same definition as in equation (6.18) for a monoprotic weakly acidic coformer.

ε can also be obtained from

$$\varepsilon = \frac{S^*_{\text{observed}}}{S^*_{\text{predicted}}} \quad (6.37)$$

where S^* is predicted using equation (6.12) assuming $K_s^{\text{coformer}} = 0$. Table 6.4 shows the ε values obtained using equations (6.18) and (6.37).

Table 6.4. S^* deviations due to coformer solubilization for CBZ-SLC and CBZ-SAC.

Cocrystal	pH	$(K_s^{\text{coformer}})^a$ (mM ⁻¹)	[SLS] at CSC ^a (mM)	ε pred ^b	ε exp ^c
CBZ-SLC (1:1)	3.0	0.06	23	1.44	1.40
CBZ-SAC (1:1)	2.2	0.013	44	1.10	1.14

a) Values reported in reference 13.

b) Predicted using equation (6.18) and pKa SLC = 3.0 and pKa SAC = 1.6.

c) Calculated using equation (6.37).

The sensitivity of S^* to ε is shown in Figure 6.8 for CBZ cocrystals.

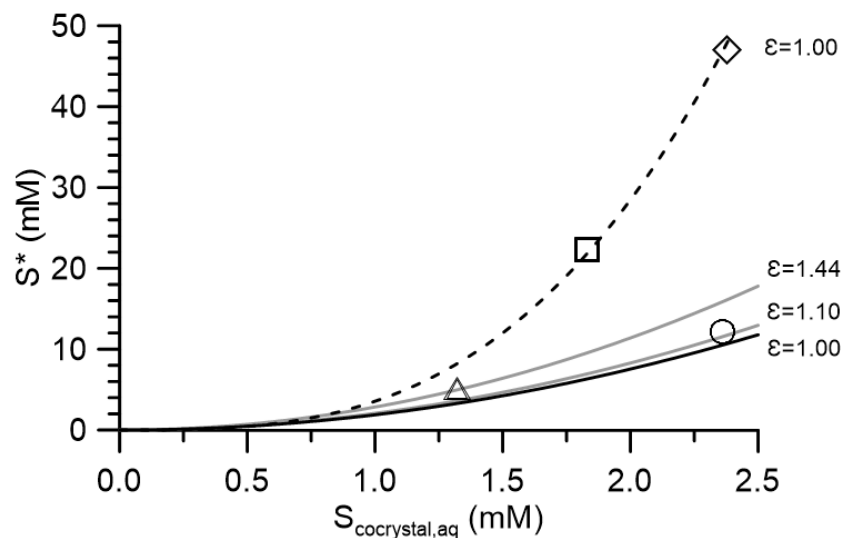


Figure 6.8. The influence of ϵ in SLS on S^* at varying $S_{\text{cocrystal,aq}}$ for CBZ-SLC (Δ), CBZ-SAC (\circ), CBZ-4ABA-HYD (\square), CBZ-SUC (\diamond). S^* is simulated using equation (6.19) for 1:1 (—) and (6.13) for 2:1 (---) cocrystals and $S_{\text{drug,aq}} = 0.53$ mM, solubilizing agent is SLS. ϵ values are 0, 1.10, and 1.44 (calculated values for CBZ-SAC and CBZ-SLC in Table 6.4), and 0 for 2:1 cocrystals since neither SUC or 4ABA were reported to be solubilized in SLS¹².

Figure 6.8 reveals the great influence that $S_{\text{cocrystal,aq}}$ has on S^* for a given drug. For example, for a hypothetical 1:1 cocrystal of CBZ ($S_{\text{drug,aq}} = 0.53$) with a $S_{\text{cocrystal,aq}}$ of 1 mM, the S^* is 1.9 mM. If the $S_{\text{cocrystal,aq}}$ is doubled to 2 mM, the S^* increases by a factor of 4 and is 7.5 mM. For a 2:1 cocrystal, the influence is even greater. For a hypothetical 2:1 cocrystal of CBZ with $S_{\text{cocrystal,aq}}$ of 1 mM, S^* is 3.6 mM. For $S_{\text{cocrystal,aq}}$ of 2 mM, S^* increases by a factor of 8 to 28 mM.

Apart from the dependence of S^* on $S_{\text{cocrystal,aq}}$, Figure 6.8 also shows the influence of ϵ on S^* for CBZ cocrystals. The S^* values for CBZ cocrystals are well predicted when ϵ is taken into account for SAC and SLC which have nonzero K_s^{coformer} values in SLS as shown in Table 6.4.

Conclusions

In this chapter, we present a theoretical framework that allows for the simple and quantitative prediction of cocrystal solubilization ratio from drug solubilization ratio when coformer solubilization is negligible. SR_{drug} values are commonly measured parameters that can help guide cocrystal selection and formulation using the presented equations. While mechanism-based models that predict cocrystal solubility in the presence of solubilizing agents from relevant equilibrium constants have been previously developed, we present here simplified models that allow for the prediction of $S_{\text{cocrystal,T}}$ from only SR_{drug} and $S_{\text{cocrystal,aq}}$.

The concept of a critical transition point solubility S^* is developed, where drug and cocrystal have equal solubilities in the presence of an additive. S^* is only dependent on the aqueous solubilities of the cocrystal and constituent drug and is independent of the nature and concentration of the additive, which to our knowledge has not been presented previously in the literature. S^* represents the maximum cocrystal solubility in any formulation, above which the cocrystal no longer has a solubility advantage over the drug. The relationship between solubilization ratio, aqueous cocrystal solubility advantage, and transition points is described. Whether a cocrystal will be above or below (thermodynamically stable or unstable) in a given formulation can be predicted from simple equations that relate the cocrystal aqueous solubility advantage to the drug solubilization ratio.

Lastly, a method of quantifying the deviation in SR and S^* due to coformer solubilization is derived. A term (ϵ) for is described, which can be incorporated into the simple models for SR and S^* when $K_s^{\text{coformer}} \neq 0$. These findings allow for the facile calculation of important parameters that can guide cocrystal formulation development using simple equations and commonly reported drug solubility descriptors.

References

1. Childs, S. L.; Kandi, P.; Lingireddy, S. R. Formulation of a Danazol Cocrystal with Controlled Supersaturation Plays an Essential Role in Improving Bioavailability. *Molecular Pharmaceutics* **2013**, *10*, (8), 3112-3127.
2. Bak, A.; Gore, A.; Yanez, E.; Stanton, M.; Tufekcic, S.; Syed, R.; Akrami, A.; Rose, M.; Surapaneni, S.; Bostick, T.; King, A.; Neervannan, S.; Ostovic, D.; Koparkar, A. The co-crystal approach to improve the exposure of a water-insoluble compound: AMG 517 sorbic acid co-crystal characterization and pharmacokinetics. *Journal of Pharmaceutical Sciences* **2008**, *97*, (9), 3942-3956.
3. McNamara, D. P.; Childs, S. L.; Giordano, J.; Iarriccio, A.; Cassidy, J.; Shet, M. S.; Mannion, R.; O'Donnell, E.; Park, A. Use of a glutaric acid cocrystal to improve oral bioavailability of a low solubility API. *Pharm. Res.* **2006**, *23*, (8), 1888-1897.
4. Roy, L.; Lipert, M. P.; Rodriguez-Hornedo, N., Co-crystal Solubility and Thermodynamic Stability. In *Pharmaceutical Salts and Co-Crystals*, Wouters, J.; Quere, L., Eds. 2011; pp 247-279.
5. Jung, M. S.; Kim, J. S.; Kim, M. S.; Alhalaweh, A.; Cho, W.; Hwang, S. J.; Velaga, S. P. Bioavailability of indomethacin-saccharin cocrystals. *J. Pharm. Pharmacol.* **2010**, *62*, (11), 1560-1568.
6. Cheney, M. L.; Weyna, D. R.; Shan, N.; Hanna, M.; Wojtas, L.; Zaworotko, M. J. Cofomer Selection in Pharmaceutical Cocrystal Development: a Case Study of a Meloxicam Aspirin Cocrystal That Exhibits Enhanced Solubility and Pharmacokinetics. *Journal of Pharmaceutical Sciences* **2011**, *100*, (6), 2172-2181.
7. Hickey, M. B.; Peterson, M. L.; Scoppettuolo, L. A.; Morrisette, S. L.; Vetter, A.; Guzman, H.; Remenar, J. F.; Zhang, Z.; Tawa, M. D.; Haley, S.; Zaworotko, M. J.; Almarsson, O. Performance comparison of a co-crystal of carbamazepine with marketed product. *Eur. J. Pharm. Biopharm.* **2007**, *67*, (1), 112-119.
8. Smith, A. J.; Kavuru, P.; Wojtas, L.; Zaworotko, M. J.; Shytle, R. D. Cocrystals of Quercetin with Improved Solubility and Oral Bioavailability. *Molecular Pharmaceutics* **2011**, *8*, (5), 1867-1876.
9. Bethune, S. J.; Huang, N.; Jayasankar, A.; Rodriguez-Hornedo, N. Understanding and Predicting the Effect of Cocrystal Components and pH on Cocrystal Solubility. *Crystal Growth & Design* **2009**, *9*, (9), 3976-3988.
10. Huang, N.; Rodriguez-Hornedo, N. Effect of Micellar Solubilization on Cocrystal Solubility and Stability. *Crystal Growth & Design* **2010**, *10*, (5), 2050-2053.
11. Huang, N.; Rodriguez-Hornedo, N. Engineering cocrystal thermodynamic stability and eutectic points by micellar solubilization and ionization. *Crystengcomm* **2011**, *13*, (17), 5409-5422.

12. Huang, N.; Rodriguez-Hornedo, N. Engineering Cocrystal Solubility, Stability, and pH(max) by Micellar Solubilization. *Journal of Pharmaceutical Sciences* **2011**, *100*, (12), 5219-5234.
13. Huang, N.; Rodriguez-Hornedo, N. pH and Micellar Solubilization Effects on Cocrystal Behavior. *Poster presentation at the 2009 AAPS Annual Meeting and Exposition 2009*, Los Angeles, CA, (November 8-12), Poster T3327.
14. Good, D. J.; Rodriguez-Hornedo, N. Solubility Advantage of Pharmaceutical Cocrystals. *Crystal Growth & Design* **2009**, *9*, (5), 2252-2264.
15. Good, D. J.; Rodriguez-Hornedo, N. Cocrystal Eutectic Constants and Prediction of Solubility Behavior. *Crystal Growth & Design* **2010**, *10*, (3), 1028-1032.
16. Alhalaweh, A.; Roy, L.; Rodriguez-Hornedo, N.; Velaga, S. P. pH-Dependent Solubility of Indomethacin-Saccharin and Carbamazepine-Saccharin Cocrystals in Aqueous Media. *Molecular Pharmaceutics* **2012**, *9*, (9), 2605-2612.
17. Thakuria, R.; Delori, A.; Jones, W.; Lipert, M. P.; Roy, L.; Rodriguez-Hornedo, N. Pharmaceutical cocrystals and poorly soluble drugs. *International Journal of Pharmaceutics* **2013**, *453*, (1), 101-125.
18. Roy, L.; Rodriguez-Hornedo, N. A Rational Approach for Surfactant Selection to Modulate Cocrystal Solubility and Stability. *Poster presentation at the 2010 AAPS Annual Meeting and Exposition 2010*, New Orleans, LA, (November 14-18, 2010), Poster R6072.
19. Roy, L. Engineering Cocrystal and Cocrystalline Salt Solubility by Modulation of Solution Phase Chemistry. *University of Michigan (Doctoral Dissertation) 2013*, Retrieved from Deep Blue. (<http://hdl.handle.net/2027.42/98067>).
20. Lipert, M. P.; Roy, L.; Rodriguez-Hornedo, N. Understanding the Thermodynamic Parameters that Control Cocrystal Solubility and Supersaturation during Dissolution in Biorelevant Media. *Poster presentation at the 2012 AAPS Annual Meeting and Exposition 2012*, Chicago, IL, (October 14-18, 2012), Poster T2052.
21. Roy, L.; Lipert, M. P.; Huang, N.; Rodriguez-Hornedo, N. Understanding and Predicting Cocrystal Solubility in Biorelevant Media. *Poster presentation at the 2010 AAPS Annual Meeting and Exposition 2010*, New Orleans, LA, (November 14-18, 2010), Poster T3112.
22. Lipert, M. P.; Rodriguez-Hornedo, N. Cocrystal Solubilization and Shifting Transition Points in the Presence of Drug Solubilizers. *Poster presentation at the 2014 AAPS Annual Meeting and Exposition 2014*, San Diego, CA, (November 2-6, 2014), Poster W4108.
23. Lipert, M. P.; Rodriguez-Hornedo, N. Strategies to Predict and Control Cocrystal Solubility and Supersaturation in Surfactant Solutions. *Poster presentation at the 2013 AAPS Annual Meeting and Exposition 2013*, San Antonio, TX, (November 10-14, 2013), Poster W5148.
24. Galia, E.; Nicolaidis, E.; Horter, D.; Lobenberg, R.; Reppas, C.; Dressman, J. B. Evaluation of various dissolution media for predicting in vivo performance of class I and II drugs. *Pharm. Res.* **1998**, *15*, (5), 698-705.

25. Rodriguez-Hornedo, N.; Nehru, S. J.; Seefeldt, K. F.; Pagan-Torres, Y.; Falkiewicz, C. J. Reaction crystallization of pharmaceutical molecular complexes. *Molecular Pharmaceutics* **2006**, *3*, (3), 362-367.
26. Bethune, S. J.; Schultheiss, N.; Henck, J. O. Improving the Poor Aqueous Solubility of Nutraceutical Compound Pterostilbene through Cocrystal Formation. *Crystal Growth & Design* **2011**, *11*, (7), 2817-2823.
27. Schultheiss, N.; Bethune, S.; Henck, J. O. Nutraceutical cocrystals: utilizing pterostilbene as a cocrystal former. *Crystengcomm* **2010**, *12*, (8), 2436-2442.
28. Singh, S.; Seadeek, C.; Andres, P.; Zhang, H.; Nelson, J. Development of Lipid-Based Drug Delivery System (LBDDS) to Further Enhance Solubility and Stability of Pterostilbene Cocrystals. *Poster presentation at the 2013 AAPS Annual Meeting and Exposition* **2013**, San Antonio, TX, (November 10-14, 2013), Poster W5296.

CHAPTER 7

CONCLUSIONS AND FUTURE WORK

This dissertation has explored the mechanisms of cocrystal solubilization by solubilizing agents and the impact on cocrystal solubility, $S_{\text{cocrystal}}/S_{\text{drug}}$, and transition points. The objectives of this work were to (1) understand the effect of solubilization by physiologically relevant solubilizing agents on cocrystal solubility, $S_{\text{cocrystal}}/S_{\text{drug}}$, and dissolution behavior, (2) develop mathematical models to describe cocrystal solubility and $S_{\text{cocrystal}}/S_{\text{drug}}$ based on cocrystal dissociation and constituent ionization and micellar solubilization solution equilibria, (3) expand these models to consider the combined effect of multiple solubilizing agents, and (4) develop simplified models that allow for the facile estimation of cocrystal solubilization ratio and transition points from commonly reported drug physicochemical and solubility descriptors. Overall, this work pursued enhanced understanding of cocrystal solubilization by drug solubilizing agents based on equilibria that describe cocrystal constituent interactions in solution.

A theoretical framework that results in the simple and quantitative prediction of cocrystal solubilization ratio ($SR_{\text{cocrystal}}$) from drug solubilization ratio (SR_{drug}) when coformer solubilization negligible was derived. $SR_{\text{cocrystal}}$ was up to orders of magnitude lower than SR_{drug} due to preferential solubilization of the drug constituents over the coformer constituents. These models were validated for a set of seven cocrystals comprised of constituents with diverse ionization and micellar solubilization properties in the presence of fed state simulated intestinal fluid (FeSSIF). Additionally, more rigorous models that consider relevant equilibrium constants for the cocrystal, drug and coformer were derived to predict cocrystal solubility in FeSSIF from

cocrystal K_{sp} measured in aqueous buffer, and cocrystal component ionization (K_a) and total micellar solubilization constants at a given pH (K_s^T) for these systems. These models allow for the accurate prediction of $SR_{cocrystal}$ or cocrystal solubility in a solubilizing agent of interest without carrying out the experiment, which can be useful if cocrystal material is sparing.

Cocrystals were discovered to exhibit significantly lower solubility advantages ($S_{cocrystal}/S_{drug}$) in FeSSIF compared to aqueous buffer due to preferential solubilization of the drug constituent, with cocrystals of more hydrophobic and highly solubilized drugs exhibiting the largest decreases in $S_{cocrystal}/S_{drug}$. Mechanism-based mathematical models to predict $S_{cocrystal}/S_{drug}$ were in good agreement with the experimentally measured $S_{cocrystal}/S_{drug}$ values for a diverse series of cocrystals with $S_{cocrystal}/S_{drug}$ ranging from 660 to 3.9 in aqueous buffer. Up to a 23 fold decrease in $S_{cocrystal}/S_{drug}$ was observed for the danazol-hydroxybenzoic acid cocrystal (DNZ-HBA) of the highly solubilized drug danazol (DNZ). The effect of $S_{cocrystal}/S_{drug}$ reduction due to preferential solubilization by FeSSIF on cocrystal powder dissolution profile was examined for indomethacin-saccharin (IND-SAC) and piroxicam-saccharin (PXC-SAC). The decreased $S_{cocrystal}/S_{drug}$ resulted in sustained supersaturated drug concentrations and slower transformation to drug in FeSSIF compared to aqueous buffer for both cocrystals. The $S_{cocrystal}/S_{drug}$ values measured at the eutectic point in FeSSIF and buffer were good indicators of the dissolution behavior for these systems. $S_{cocrystal}/S_{drug}$ can be predicted from the presented models, and these values can be used to anticipate cocrystal dissolution and transformation behavior in a variety of surfactant solutions as long as the drug solubility and the cocrystal K_{sp} , and drug and coformer K_a and K_s^T values are known.

Models that describe the relationship between $\log SR_{cocrystal}$ and $\log SR_{drug}$ in FeSSIF for the purpose of comparing the correlation between $\log SR$ by a solubilizing agent and drug

hydrophobicity (as described by octanol-water distribution coefficient $\log D$) for drugs and cocrystals were derived. The $\log SR_{\text{cocrystal}}$ exhibited a weaker dependence on drug $\log D$ compared to $\log SR_{\text{drug}}$, which was predicted from the derived models. $\log SR_{\text{cocrystal}}$ can be calculated simply from knowledge of drug $\log D$ if a robust $\log SR_{\text{drug}}-\log D$ linear regression correlation is calculated from experimentally measured SR_{drug} values. These models are valuable since SR_{drug} and $\log P$ and/or $\log D$ are commonly measured and reported drug properties.

Theoretical relationships that describe cocrystal solubility and $S_{\text{cocrystal}}/S_{\text{drug}}$ in the presence of multiple surfactants assumed to mix ideally were derived for the first time. The solubility of DNZ-HBA and danazol-vanillin (DNZ-VAN) in the presence Tween 80 and FeSSIF was quantitatively predicted from cocrystal K_{sp} and cocrystal component K_{a} values reported in the literature and K_{s}^{T} values determined from drug and coformer solubility measurements in Tween 80 and FeSSIF independently. Preferential solubilization of DNZ resulted in a dramatic decrease in $S_{\text{cocrystal}}/S_{\text{drug}}$ as Tween 80 concentration increases, but this effect was dampened in the presence of FeSSIF, particularly at low Tween 80 concentrations. Decreased $S_{\text{cocrystal}}/S_{\text{drug}}$ for DNZ-VAN in FeSSIF + 150 mM Tween 80 resulted in higher drug concentrations and metastable high supersaturations during dissolution compared to FeSSIF alone. These models are useful to anticipate the solution behavior of cocrystal drug products, where cocrystalline phases are in the presence of multiple additives in solution.

The concept of a critical transition point solubility S^* was developed, where drug and cocrystal have equal solubilities in the presence of a solubilizing agent. It was demonstrated that S^* is only dependent on the aqueous solubilities of the cocrystal and constituent drug and is independent of the nature and concentration of the additive. The relationship between $SR_{\text{cocrystal}}$, $S_{\text{cocrystal}}/S_{\text{drug}}$, and transition points was investigated. Simple equations that relate the cocrystal

$S_{\text{cocrystal}}/S_{\text{drug}}$ in aqueous solution to SR_{drug} allow for the facile prediction of a cocrystal's position on a phase diagram relative to the transition point. A method of quantifying the deviation in SR and S^* due to coformer solubilization was derived. A term (ϵ) for was described, which can be incorporated into the simple models for SR and S^* when coformer solubilization is not negligible. These findings allow for the calculation of important parameters that can guide cocrystal formulation development using simple equations and commonly reported drug solubility descriptors.

The findings in this work have implications for the development of cocrystals as efficient strategies to enhance the oral delivery of water insoluble drugs. Cocrystal solid and solution chemistry provides precise control over solubility and dissolution properties that can be used to optimize oral drug absorption. Quantitative mathematical relationships established in this work allow for the preliminary prediction of cocrystal solubility in physiologically relevant and synthetic solubilizing agents, but further work is needed to fully realize the potential of cocrystals to enhance oral delivery. Cocrystals are supersaturating drug delivery systems, and methods of optimizing their supersaturation and transformation kinetics are still lacking. Now that mechanism-based models describing cocrystal solution behavior in equilibrium conditions have been established, predictive models for dissolution in physiologically relevant media, where cocrystal may undergo solution-mediated transformation to drug are critical. The influence of cocrystal solution chemistry on drug permeability and absorption also remains to be established, and application of this knowledge will allow accurate *in vivo* absorption and bioavailability predictions to be made.

Experimentally, the equilibrium cocrystal aqueous solubility of highly soluble cocrystals is accessed at the eutectic point in this work. The presence of excess coformer in solution

decreases cocrystal solubility to an experimentally accessible equilibrium point where cocrystal and drug solid phases are in equilibrium in solution, from which the stoichiometric solubility in the absence of excess coformer can be calculated. However, the excess coformer in solution can result in altered pH conditions and solution nonidealities when concentrations are sufficiently high. The stoichiometric solubility of highly soluble cocrystals can also be accessed by measurement in the presence of solubilizing agents. When solubilizing agents are present in concentrations higher than the critical stabilization concentration (CSC), the cocrystal is thermodynamically stable and the solubility can be measured by traditional slurry solubility measurement methods. The stoichiometric solubility in the absence of solubilizing agent can be calculated from knowledge of drug and coformer solubilization properties in the solubilizing agent. Thorough comparison of these two methods of accessing the equilibrium cocrystal solubility of unstable cocrystals is yet to be established. Knowledge of which method is preferable in particular experimental conditions can lead to more accurate cocrystal solubility measurement.